ANNUAL REPORT

NASA GRANT NSG-1288

ANALYSIS OF THE GAS CORE ACTINIDE TRANSMUTATION REACTOR (GCATR)

J. D. Clement and J. H. Rust

NASA Program Manager, F. Hohl

Prepared for the

National Aeronautics and Space Administration

by the

School of Nuclear Engineering
Georgia Institute of Technology
Atlanta, Georgia 30332

February 28, 1977

ACKNOWLEDGMENTS

This work was supported by NASA Grant NSG-1288. The authors wish to express their appreciation to the program manager Dr. Frank Hohl for helpful suggestions during the performance of the research.

The following graduate students, supported by the grant, made significant contributions to the research project: Lyu Kim, Clyde Lightfoot, Frank Rives, Ray Waldo, Pak Tai Wan, and Bruce Byrne.

In addition, the NASA research program was also used as a design project for the Nuclear Engineering design course in the academic curriculum. The following students were of great assistance in the research work:

Patrick Acree
Abderrahnane Belblidia
David Campbell
Benjamin Clark
Stephen Curtis
James Dullea
Robert Forst
Dan Griggs
William Horn
Douglas Moss
Richard Myers
Clyde Norman
John Osterholtz
Harry Patat
Wayne Reitz
Richard P. Saputa
Jeffrey A. Smith
John Snader
James Tahler
Patrick Wattson
Roy Ziering

TABLE OF CONTENTS

LIST OF TABLES

LIST OF TABLES (con'd)

LIST OF ILLUSTRATIONS

SUMMARY

The Georgia Institute of Technology, under the sponsorship of the National Aeronautics and Space Administration, has undertaken a research program entitled "Analysis of the Gas Core Actinide Transmutation Reactor, GCATR." The overall objective of the study is to investigate the feasibility, design, and optimization of the GCATR. This annual report summarizes results from March 1, 1976 to February 28, 1977.

Update of Actinide Cross Sections and Sensitivity Analysis Using the ORIGEN Code

The ORIGEN computer program was implemented on Georgia Tech's Cyber 74 computer system. More recent and accurate values for the actinide cross sections were researched and used to update the ORIGEN cross section library. The latest cross sections were obtained from the Savannah River Laboratory and the Brookhaven National Library. In order to evaluate the effects of uncertainities in the nuclear data, the sensitivity of results based upon variation in the actinide cross sections were analyzed. The results are tabulated in the Report.

Calculations of the Actinide Burnup Potential in the GCATR

Before performing detailed calculations, the potential of the GCATR was explored by making comparative computations of the GCATR with LWR and LMFBR systems.

The comparisons, although based on simplifying assumptions, show that in some respects the GCATR system is superior to LWR and LMFBR transmutation systems. For example, the GCATR services 10 LWR's

in comparison to three for the LMFBR and one for the LWR. Over a 40 year span, the GCATR system provides 520,000 MWe-years in comparison to 192,000 MWe-years for the LMFBR and 40,000 MWe-years for the LWR. The GCATR system burns up 10.239 metric tons of actinides in 40 years as compared to 2.930 for the LMFBR and 0.423 for the LWR. The hazard reduction factor of the GCATR system is 5.85 in comparison to 5.25 for LMFBR and 4.11 for LWR transmutation systems.

Heat Transfer Analysis of Actinide Fuel Rods

A thermal-hydraulic analysis was made of actinide fuel rods in the form of oxides encapulated with a metal cladding. Reasonable design constraints, which limit the actinide rod thermal output, are 590 watts/cm for the linear heat rate and 662°C for the maximum cladding temperature. For the water coolant there will be a constraint on heat flux given by the DNB heat flux. The DNB ratio was not allowed to fall below 1.3.

Heat transfer calculations were made for three possible coolants--sodium, water, and helium. The burnup in the actinide fuel rods was limited to 150,000 MWD/t. These considerations led to maximum fast neutron fluxes in the actinide fuel rods of 4×10^{16} n/cm^2-sec for sodium and 10^{16} n/cm^2-sec for helium. Rod diameters, pitch-to-diameter ratios, and maximum and average volumetric heat generation rates were calculated and tabulated for the three coolants.

GCATR Reactor Design

General criteria for ATR reactor design and particular criteria for the GCATR are formulated and discussed. Calculations were made using

the MACH-1 program for a three-region reactor containing core, actinide, and reflector regions. The core region contained the $^{233}UF_6$ gaseous fuel.

The initial objective of the reactor design analysis was to evaluate characteristics of several modifications of the reactor described and establish the optimal type. MACH-I calculations were performed for a spherical geometry. H_2O and D_2O were each used as the coolant and moderator. By applying a power limit of 2500 MWth to the reactor it was possible to calculate the maximum flux in the actinides. It was clear from these calculations that D_2O was far superior to H_2O in the reactor. Not enough calculations have been performed to determine whether the actinides should be placed in the center or on the outside of the core. A higher flux is obtainable in the center, but more actinides may be placed on the outside. The amount of moderation provided had a significant effect on the results as well. Since the only limit imposed on the flux was on the total number of fissions in the reactor per second, a more thermalized reactor would have a lower flux due to the larger thermal neutron cross fission section for the fuel. However, for a given neutron spectrum the smaller the critical mass the larger the neutron flux.

A major advantage of the GCATR was demonstrated in these calculations, since fluxes several orders of magnitude above those in conventional reactors were achieved. If the flux is to be high and still have a limited power output, the critical mass should be as small as possible. However, if the maximum amount of actinides are to be exposed to a high flux the core should have a large size. This dictates as low a fuel density as possible. Hence, a GCATR is much better suited to this problem than a solid fuel reactor.

Further calculations indicated that a thicker graphite reflector was helpful and that replacing D_2O with graphite had a negligible effect. It was thus concluded that if D_2O were to be used as the coolant for this reactor, its use should be limited to cooling requirements and graphite used exclusively for the reflector.

Further calculations indicated that a sodium coolant would allow a much higher neutron flux than the D_2O coolant from a heat transfer point of view. In addition, a very fast reactor may indeed be preferable to a more thermal one because of the increased fission to capture ratio in the actinides. Future calculations will investigate these possibilities

Overall System Design

The GCATR is designed to transmute by fission the transuranium actinides from ten LWR's. This burnup capability exceeds that of either the LWR or LMFBR. Preliminary drawings are presented. The core is a right circular cylinder with approximate dimensions of a two-meter height and a one-meter diameter. Actinide fuel rods are arranged along the length of the core outside the liner. The fuel assemblies will require a coolant, such as sodium, helium, or high pressure water. The actinide fuel rod coolant will be at a pressure comparable to that of UF_6 so as to reduce the required thickness of the core liner wall. The reactor will need to be enclosed by a thick-walled pressure vessel which could be made of carbon steel with a stainless steel liner.

Because of its high burnup requirements, the GCATR will generate a considerable amount of thermal power which must be converted into electricity in order to economically justify the concept.

Because it was considered undesirable for UF_6 to have the possibility of interacting with water due to failure of a boiler tube, the UF_6 exchanges heat with a molten salt ($NaBF_4$) in an intermediate heat exchanger. $NaBF_4$ was developed as an intermediate coolant for the molten salt breeder reactor and would be inert with UF_6. Another desirable feature of $NaBF_4$ is that the boron present in the salt would eliminate criticality problems with UF_6 in the heat exchanger.

Preliminary calculations with the MACH-I diffusion code indicates that the power generated in the actinide fuel rods ranges from 20-36 percent of the plant output.

Multiple intermediate heat exchangers are employed on the plant so as to keep these heat exchangers compact and also improve upon the reliability and safety by redundancy of equipment. The heat load of these heat exchangers will be of the order of 500 Mw.

The $NaBF_4$ enters the intermediate heat exchanger at 400°C and exits at 510°C. It then enters a boiler where it exchanges heat to produce superheated steam at 100 bar pressure and 480°C. The steam is expanded through high and low pressure turbines to a pressure of 0.07 bar. Steam is extracted at optimal temperatures from three locations in the turbines for use in feedwater heaters. The overall efficiency of the plant is 36 percent.

UF_6 Fuel Reprocessing

The proposed UF_6 reprocessing system is basically the combination of a cold trap process and a fluoride volatility process. Partial removal of fission products from the reactor outlet stream has been devised so that the feed stream to the trap contains fewer fission products than the original reactor outlet stream.

A portion of the GCATR exit fuel stream is fluorinated by inserting F_2 into the fluorinator. For the purpose of analysis it is assumed that all the fission products are in fluoride form through this stage. However, it is important to realize that the assumptions are not correct. Even though fluorine is quite reactive with most materials, the reaction in many instances takes certain times. Some of the fission products are also coated with impurities so that physical contact with fluorine is not allowed for a certain period. Thus, in practical situations it is not possible for certain fission products to form fluoride. In fact, experience with the MSRE has shown that the noble metal fission products (e.g. Mo, Ru, Tc, Rh, Nb, and Pd) are not present in the molten salt as fluorides.

After fluorination the fuel and fission-product fluorides are cooled down to 200°C. In this stage, many fluorides are solidified or exist as liquid slurries. The exit gas stream from this stage (which contains UF_6, gaseous fission products, and volatile fluorides) is fed into a cold trap. The cold trap operates around 56.4°C. Through this trap UF_6 is recovered (as solid) from liquid wastes and volatile gases.

The solid UF_6 is melted and vaporized, and fed into an impurity removal system. The impurity removal system can be a bed of NaF or MgF_2 pellets or a distillation column which selectively absorbs volatile impurities from the UF_6 stream. The purified UF_6 is reheated to an appropriate temperature and sent to the GCATR.

Physical properties of certain fluorides which are not easily available have been estimated. Therefore, the volatility analysis is only approximate, even though the basic principle is sound.

Fission products, such as Mo, Ru, Tc, Rh, Nb, and Pd, may not form

fluorides, but exist as solid particles or plate out inside the reactor. Further study is necessary to make sure that these elements do not create serious complications.

Actinide Partitioning and Reprocessing

An investigation was made to determine the necessary separation factors. The study indicated that separations beyond certain limits may not yield enough to substantiate such separation factors. The separations of 99.9% for uranium, americium and curium, and 99% for neptunium will reduce the hazard potential to about five percent of that for natural uranium. After 99.9% removal of iodine, it will then be the long-lived remaining fission products which control the waste hazard. Higher removal factors for the actinides do not appear to be warranted unless long-lived fission products are also removed, especially Tc-99.

Present proposals for actinide partitioning are based on a sequence of separation processes using solvent extraction, ion exchange, and precipitation. These techniques have not yet been developed. A multistep solvent extraction process combined with other processes, such as cation exchange, may work well in the removal of uranium, neptunium, and plutonium, as well as separation of americium and curium from other wastes.

Tributylphosphate (TBP) may be used as the solvent in the solvent extraction method. As demonstrated in the PUREX process, TBP achieved highly efficient recovery of uranium, plutonium, and neptunium.

As a means of separating americium and curium from the rest of fission products and wastes, two steps of cation exhange is quite promising. The potential here appears to be 99.9 percent or better. In the first step

the lanthanides and actinides are absorbed on a cation exchange resin column and eluted with nitric acid. In the following step the lanthanides and actinides are separated by cation exchange chromatography. Problems to be solved with this process are in converting the spent ion exchange resin to acceptable levels for waste generated in the chromatographic separation.

Precipitation methods combined with ion exchange and/or solvent extraction may be another possible method for partitioning actinides. Even though solid waste handling is unavoidable, ways are now under study for obtaining crude concentrations of plutonium, americium, curium, and fission products. These actinides would then be separated from the lanthanides in further ion exchange or solvent extraction steps. Oak Ridge National Laboratory is studying the use of oxalate precipitation together with ion exchange to isolate the lanthanides and actinides. A removal factor of 0.95 is achieved by precipitation while the remaining is removed in the cation exchange column. Tracer-level studies indicate removal of 0.999 for americium and curium. Almost complete removal has been demonstrated for americium and curium by use of multiple oxalate precipitation stages. Further work in this area is still needed to determine the effect of the handling problems.

Technical feasibility, resultant benefits, and costs of partitioning actinides from high-level wastes are yet to be established. It must be decided if the net benefits will justify the use of partitioning. It must also be kept in mind that the separation schemes do not solve the long-term actinide problem. In order to justify this, the actinides must somehow be transmuted to shorter-lived radionuclides or disposed of from our

environment. These and many more problems still need research and investigation before a feasible actinide-separation-transmutation process can be substantiated.

From research done to date, it is concluded that much research and development is still needed in the area of actinide partitioning. Work being performed at the Oak Ridge National Laboratory may show encouraging results by the end of 1978. Present state-of-the-art methods will not yield the results needed to establish a practical, economically feasible operating partitioning plant. It is believed that research in the area of combined methods of solvent extraction and ion exchange will yield the necessary separations factors.

I. INTRODUCTION

This annual report summarizes results of work performed from March 1, 1976 to February 28, 1977, under NASA Research Grant NSG-1288 entitled "Analysis of the Gas Core Actinide Transmutation Reactor (GCATR)."

The major tasks in the first year were in the following areas:

1. Update of Actinide Cross Sections and Sensitivity Analysis Using the Origen Code
2. Calculations of the Actinide Burnup Potential in the GCATR
3. Heat Transfer Analysis of Actinide Fuel Rods
4. GCATR Reactor Design
5. Reactor Design
6. Overall System Design
7. UF_6 Fuel Reprocessing
8. Actinide Partioning and Reprocessing

These topics are summarized in Chapters I through IX. Chapter X is a discussion of future work to be carried out during the second year of the project.

II. BACKGROUND

The technical background was reviewed in papers included as Appendices A and B. The papers, by Clement, Rust, Schneider and Hohl, were presented at the Third Symposium on Uranium Plasmas at the Princeton University Conference, June 10-12, 1976.

III UPDATE OF ACTINIDE CROSS SECTIONS AND SENSITIVITY ANALYSIS USING THE ORIGEN CODE

Introduction

The value of any calculation depends upon the validity of the data on which it is based and the accuracy of the calculational scheme. In order to be confident of the results of GCATR calculations, a search was made for the most recent and accurate cross section data; then a sensitivity analysis of the ORIGEN results was performed with respect to the possible errors in the cross sections, so that the effect of inaccuracies in the cross section data could be determined.

Implementation of the ORIGEN Code

An integral part of the proposed program was the implementation of the isotope generation and depletion code ORIGEN.[1] The ORIGEN computer code is a collection of programs that: (1) constructs a set of linear, first-order, ordinary differential equations describing the rates of formation and destruction of the nuclides contained in the library; (2) solves the resulting set of equations for a given set of initial conditions and irradiation histories to obtain the isotopic compositions of discharged fuel components as a function of post irradiation time; and (3) uses the isotopic compositions and nuclear properties of individual nuclides to construct tables describing the radioactivities, thermal powers, potential inhalation and ingestion hazards and photon and neutron production rates in the discharged fuels. ORIGEN utilizes a vast library containing information on 813 isotopes whose cross sections were found in various references. This library contained nuclear data pertaining to four different

reactor types — HTGR, LWR, LMFBR, and MSBR. The nuclear data was varied according to the shape of a typical neutron spectrum for each reactor type.

In order to make ORIGEN more directly applicable to the GCATR and contain cross sections equivalent with the most current known today, ORIGEN was modified to allow for easy manipulation of all isotopes from Tl-207 through ES-253. These isotopes were chosen because most discrepancies with cross section values were found among this particular group of cross sections as pointed out by Raman. This option described allows the replacement of particular cross sections by updated values as they became available from the National Laboratories as well as the inclusion of actual spectrum-averaged effective cross sections describing the GCATR into the ORIGEN library. The cross section sensitivity study was greatly facilitated by the cross section manipulation option.

Status of Cross Section Data

A search was made for new cross sections because the ones in the ORIGEN[1] library were outdated. Three papers containing compilations [2][3][4] were investigated. Each listed thermal cross sections and resonance integrals for neutron capture and neutron induced fission. These are listed in Tables III-1 through III-4. Also, a computer tape was obtained from Brookhaven National Laboratory of the Evaluated Nuclear Data File.[5]

The ORIGEN library contains integral cross sections for every actinide isotope in the thermal, resonance, and fast energy ranges for use in LWR calculations. For LMFBR problems, it gives only a complete spectrum-averaged cross section for each type of reaction. Many of these cross

TABLE III-1

THERMAL NEUTRON CAPTURE CROSS SECTIONS

(all units are barns)

ISOTOPE	HALF-LIFE	BNL-325[4]	ORIGEN[1]	BENJAMIN ETAL[2]	BENJAMIN (1975)[3]
Th 228	1.913 yr	123±15	120		
Th 229	7340 yr	54±6	0		
Th 230	7.7×10^4 yr	23.2±0.6	23		
Th 231	25.5 hr		0		
Th 232	1.41×10^{10} yr	7.40±0.08	7.4		
Th 233	22.2 min	1500±100	1500		
Th 234	24.1 d	1.8±0.5	0		
Pa 231	3.25×10^4 yr	210±20	200		210
Pa 232	1.32 d	760±100	0		
Pa 233	27.0 d	41±6	43		41
Pa 234m	1.17 min		0		
Pa 234g	6.67 hr		0		
U 232	72 yr	73.1±1.5	78		73.1
U 233	1.55×10^5 yr	47.7±2.0	49		
U 234	2.47×10^5 yr	100.2±1.5	95		100.2
U 235	7.13×10^8 yr	98.6±1.5	98		
U 236	2.34×10^7 yr	5.2±0.3	6		5.2
U 237	6.75 d	411±138	0		378
U 238	4.51×10^9 yr	2.70±0.02	2.73		
U 239	23.5 min	22±5	0		
U 240	14.1 hr		0		

TABLE III-1 (con't)

ISOTOPE	HALF-LIFE	BNL-325	ORIGEN	BENJAMIN ETAL	BENJAMIN (1975)
Np 234	4.40 d				
Np 235	396 d	1784±204			
Np 236	1.29×10^8 yr		0		
Np 237	2.14×10^6 yr	162±3	170		169
Np 238	2.12 d		0		
Np 239	2.35 d	45±20	60		
Np 240	7.3 min		0		
Np 240g			0		
Pu 236	2.85 yr		0		
Pu 237	45.6 d				
Pu 238	87.8 yr	547±20	500		559
Pu 239	2.44×10^4 yr	268±3	632		
Pu 240	6540 yr	289.5±1.4	366		289.5
Pu 241	15 yr	368±10	550		362
Pu 242	3.87×10^5 yr	18.5±0.4	18.5	18.7	18.5
Pu 243	4.96 hr	60±30	0	87.4	87.4
Pu 244	8.3×10^7 yr	1.7±0.1	1.6		1.7
Pu 245	10.5 hr	150±30	277		
Am 241	433 yr	832±20	925		831.8
Am 242m	152 yr	1400±860	2000		
Am 242g	16 hr		0	0	
Am 243	7.37×10^3 yr	79.3±2.0	105	75.5	77
Am 244m	26 min				
Am 244g	10.1 hr		0		
Cm 242	163 d	16.5	30		20

TABLE III-1 (con't)

ISOTOPE	HALF-LIFE	BNL-325	ORIGEN	BENJAMIN ETAL	BENJAMIN (1975)
Cm 243	28 yr	225±100	200		
Cm 244	17.9 yr	13.9±1.0	10	9.95	10.6
Cm 245	8.5×10^3 yr	345±20	343	371	383
Cm 246	4.76×10^3 yr	1.3±0.3	1.25	1.4	1.44
Cm 247	1.54×10^7 yr	60±30	60	58	58
Cm 248	3.5×10^5 yr	4±1	3.56	2.89	2.89
Cm 249	64 min	1.6±0.8	2.8		
Cm 250	1.7×10^4 yr		2.0		
Bk 249	311 d		1450	1600	1600
Bk 250	3.22 hr		350		
Cf 249	350.6 yr	465±25	450	480	481.4
Cf 250	13.1 yr	2030±200	1900	1701	1701
Cf 251	900 yr	2850±150	2850	2849	2849
Cf 252	2.63 yr	20.4±1.5	19.8	20.4	20.4
Cf 253	17.8 d	17.6±1.8	12.6	12.0	12.0
Cf 254	60.5 d		50		
Es 253	20.47 d	155±20	345	155	155
Es 254m	39.3 hr	1.3			
Es 254g	276 d	<40			

TABLE III-2

NEUTRON CAPTURE RESONANCE INTEGRALS

ISOTOPE		BNL-325 [4]	ORIGEN [1]	BENJAMIN ETAL [2]	BENJAMIN (1975) [3]
Th	228	1013	0		
Th	229	1000±175	0		
Th	230	1010±30	1000		
Th	231		0		
Th	232	85±3	83		
Th	233	400±100	386		
Th	234		0		
Pa	231	1500±100	480		1500
Pa	232		0		
Pa	233	895±30	920		895
Pa	234m		0		
Pa	234g		0		
U	232	280±15	280		280
U	233	140±6	147		
U	234	630±70	665		630
U	235	144±6	130		
U	236	365±20	210		365
U	237	290	0		1200
U	238	275±5	19.9		
U	239		10		
U	240		0		
Np	234		0		
Np	235		0		
Np	236		0		

TABLE III-2 (con't)

ISOTOPE	BNL-325	ORIGEN	BENJAMIN ETAL	BENJAMIN(1975)
Np 237	660±50	756		660
Np 238		0		
Np 239		415		
Np 240m		0		
Np 240g		0		
Pu 236		0		
Pu 237		0		
Pu 238	141±15	150		164
Pu 239	200±20	130		
Pu 240	8013±960	2000		8013
Pu 241	162±8	139		162
Pu 242	1130±30	1280	1280	1275
Pu 243		0	264	264.0
Pu 244	43±4	0		42.5
Pu 245	220±40	0		
Am 241	1477±140	2150		1538
Am 242m	7000±2000	0		
Am 242g		0		
Am 243	1820±70	1500	2159	1927
Am 244m		0		
Am 244g		0		
Cm 242	150±40	0		150
Cm 243	2345±470	500		
Cm 244	650±50	650	585	585
Cm 245	101±8	120	104	104

TABLE III-2 (con't)

ISOTOPE	BNL-325	ORIGEN	BENJAMIN ETAL	BENJAMIN (1975)
Cm 246	121±7	121	119	117.0
Cm 247	800±400	500	500	500
Cm 248	275±75	170	251	251
Cm 249		0		
Cm 250		0		
Bk 249		1240	4000	4000
Bk 250		0		
Cf 249	760±35	1.46	777	625
Cf 250		11,600	11,600	11,500
Cf 251	1600±300	1600	1600	1590
Cf 252	43.5±3.0	44	43.5	43.4
Cf 253		0	12.0	12.1
Cf 254		1650		
Es 253	7300±390	0	7300	7308
Es 254m		0		
Es 254g		0		

TABLE III-3

THERMAL FISSION CROSS SECTIONS

ISOTOPE	BNL-325[4]	ORIGEN[1]	BENJAMIN ETAL[2]	BENJAMIN (1975)[3]
Th 228	<0.3	0		
Th 229	30.5±3.0	32		
Th 230	<0.0012	0		
Th 231		0		
Th 232	0.039±0.004mb			
Th 233	15±2	0		
Th 234	<0.01	0		
Pa 231	.010±.005	0		0.01
Pa 232	700±100	0		
Pa 233	<0.1	0		<1
Pa 234m	<500	0		
Pa 234g	<5000	0		
U 232	75.2±4.7	77		75.2
U 233	531.1±1.3	525		
U 234	<0.65	0		<0.65
U 235	682.2±1.3	520		
U 236		0		
U 237	<0.35	0		<0.35
U 238		0		
U 239	14±3	0		
U 240		0		

TABLE III-3 (con't)

ISOTOPE	BNL-325	ORIGEN	BENJAMIN ETAL	BENJAMIN (1975)
Np 234	900±300	0		
Np 235		0		
Np 236	2500±150	0		
Np 237	.019±.003	0.019		0.019
Np 238	2070±30	1600		2070
Np 239	1	0		
Np 240m		0		
Np 240g		0		
Pu 236	165±20	170		162
Pu 237	2400±300			2200
Pu 238	16.5±0.5	1715		17.3
Pu 239	742.5±3.0	1520		
Pu 240	.030±.045	0		0.030
Pu 241	1009±8	1480		1015
Pu 242	0.2	0.035	0	
Pu 243	196±16	0	180	180
Pu 244		0		
Pu 245		0		
Am 241	3.15±0.10	3.13	3.1	3.14
Am 242m	6600±300	6000	6000	7600
Am 242g	2900±1000	2900	2900	2100
Am 243	<0.07	0.45		
Am 244m	1600±300			
Am 244g	2300±300	2300		

TABLE III- 3(con't)

ISOTOPE	BNL-325	ORIGEN	BENJAMIN ETAL	BENJAMIN (1975)
Cm 242	<5	5		<5
Cm 243	600±50	600		690
Cm 244	1.2±0.1	1.20	1.5	1.1
Cm 245	2020±40	1727	2098	2161
Cm 246	0.17±0.10	0	0.17	0.17
Cm 247	90±10	120	72.3	72.3
Cm 248	0.34±0.07	0	0.11	0.34
Cm 249		50		
Cm 250		0		
Bk 249		0		
Bk 250	960±150	3000		
Cf 249	1660±50	1690		1665
Cf 250	<350	0		
Cf 251	4300±300	3750	4801	4801
Cf 252	32±4	32	32.0	32.0
Cf 253	1300±240	1300	1100	1100
Cf 254		0		
Es 253		0		
Es 254m	1840±80			1840
Es 254g	2900±110			2900

TABLE III-4

FISSION RESONANCE INTEGRALS

ISOTOPE	BNL-325[4]	ORIGEN[1]	BENJAMIN ETAL[2]	BENJAMIN (1975)[3]
Th 228		0		
Th 229	464±70	0		
Th 230		0		
Th 231		0		
Th 232		0		
Th 233		0		
Th 234		0		
Pa 231		0		
Pa 232		0		
Pa 233		0		
Pa 234m		0		
Pa 234g		0		
U 232	320±40	320		320
U 233	764±13	746		
U 234		0		
U 235	275±5	240		
U 236		0		
U 237		0		
U 238		0		
U 239		0		
U 240		0		

TABLE III-4 (con't)

ISOTOPE	BNL-325	ORIGEN	BENJAMIN ETAL	BENJAMIN (1975)
Np 234		0		
Np 235		0		
Np 236		0		
Np 237		0		
Np 238	880±70	0		880
Np 239		0		
Np 240m		0		
Np 240g		0		
Pu 236		0		
Pu 237		0		
Pu 238	24±4	25		25
Pu 239	301±10	300		
Pu 240		0		
Pu 241	570±15	537		570
Pu 242	5	0.6	4.74	4.7
Pu 243		0	541	542
Pu 244		0		
Pu 245		0		
Am 241	21±2	0		21
Am 242m	1570±110	0		1570
Am 242g		0		<300
Am 243		1.5	3.4	3.34
Am 244m		0		
Am 244g		0		

TABLE III-4 (con't)

ISOTOPE	BNL-325	ORIGEN	BENJAMIN ETAL	BENJAMIN (1975)
Cm 242		0		
Cm 243	1860±400	1850		1860
Cm 244	12.5±2.5	12.5	17.1	17.9
Cm 245	750±150	1140	766	766
Cm 246	10±0.4	0	10	9.94
Cm 247	880±100	1060	761	766
Cm 248	13.2±0.8	0	14.7	14.7
Cm 249		0		
Cm 250		0		
Bk 249		0		
Bk 250		0		
Cf 249	2114±70	2920	1863	1610
Cf 250		0		
Cf 251	5900±1000	5400	5400	5380
Cf 252	110±30	110	110	111
Cf 253		0	2000	2000
Cf 254		0		
Es 253		0		
Es 254m		0		
Es 254g	2190±90	0		2200

sections have since become better known. Cross sections that had not been well known when the library was created had been entered as zeros. Much data has since been obtained so that these values can now be assigned.

One of the sources investigated was "A Consistent Set of Transplutonium Multigroup Cross Sections,"[2] by R. W. Benjamin, et al. It lists thermal cross sections and resonance integrals for neutron capture and fission for a number of isotopes. Benjamin also wrote "Status of Measured Neutron Cross Sections of Transactinium Isotopes for Thermal Reactors."[3] In it is listed cross sections for a large number of isotopes and a discussion of the current need for cross section measurement of those isotopes.

The most useful source was "Neutron Cross Sections."[4] This is a very complete compilation of cross section data for every isotope and includes maximum errors for each cross section. These errors were useful as input for the cross section sensitivity analysis because upper and lower limits for each cross section could be substituted for the values in ORIGEN. For these reasons, this source was chosen to update the ORIGEN library.

Differential cross section data was found in "DLC-2D/100G, 100 Group Neutron Cross Section Data Based on ENDF/B."[5] It was obtained from Brookhaven National Laboratory on computer tape and contains ENDF/B3 data with the addition of U-233 and fluorine. This 100 group set was generated from nuclear data in either point by point or parametric representation by the PSR-13/SUPERTOG[6] code. A data retrieval code, DLC2RP,[7] was used to obtain a group by group printout of this data and to prepare it for imput to a reactor physics code. This data was not used in the sensitivity analysis but has been prepared for input into ANISN,[8]

a one-dimensional discrete ordinates transport theory code, which will perform criticality calculations for the GCATR.

Later, Brookhaven National Laboratory will release the Second Volume of "Neutron Cross Sections."[9] This volume will contain graphs of cross sections versus energy for a wide energy range and should become useful as a source of fast cross section data.

Cross Section Update

The cross sections from BNL-325 (shown in Tables III-1 through III-4) were substituted for those in the ORIGEN library for every isotope heavier than, and including, Th-228. These cross sections were more recent and more complete than those in the ORIGEN library. They were also accompanied by the listings of the maximum possible errors in each cross section. These errors were employed in the sensitivity analysis as described in the next section.

Cross Section Sensitivity Analysis

1. Description of Analysis Procedure.

In order to determine the possible effects of uncertainties in the nuclear data, the sensitivity of ORIGEN results to variations in the actinide cross sections was analysed. The specific results analysed were the actinide concentrations in the transmuter core. The general procedure was as follows:

(1) The concentrations (in gram-atoms per metric ton of fresh fuel) of each actinide in the spent fuel of a normal PWR cycle were calculated.

(2) It was assumed that 99.5% of the uranium and plutonium is reprocessed out of the spent fuel at 150 days after discharge from the PWR.

(3) The resulting actinide concentrations were determined at 215 days after reprocessing (365 days after discharge from the PWR).

(4) The concentrations of actinides in a PWR transmuter discharge were calculated, assuming that the actinides from step three are placed in another PWR that is also loaded with one metric ton of fresh fuel. This was chosen as the base case.

(5) Step four was repeated, changing the cross sections for fission or capture of one isotope from the base case. This step was repeated for each isotope studied.

(6) The isotopic concentrations from each run were then compared to those of the base case to determine the difference due to the cross sections. The results are tabulated later in this report.

Steps one, two, and three were done by one ORIGEN calculation. In steps four and five, one ORIGEN run was needed for each case explored. A schematic of the run scheme is shown in Figure III-1.

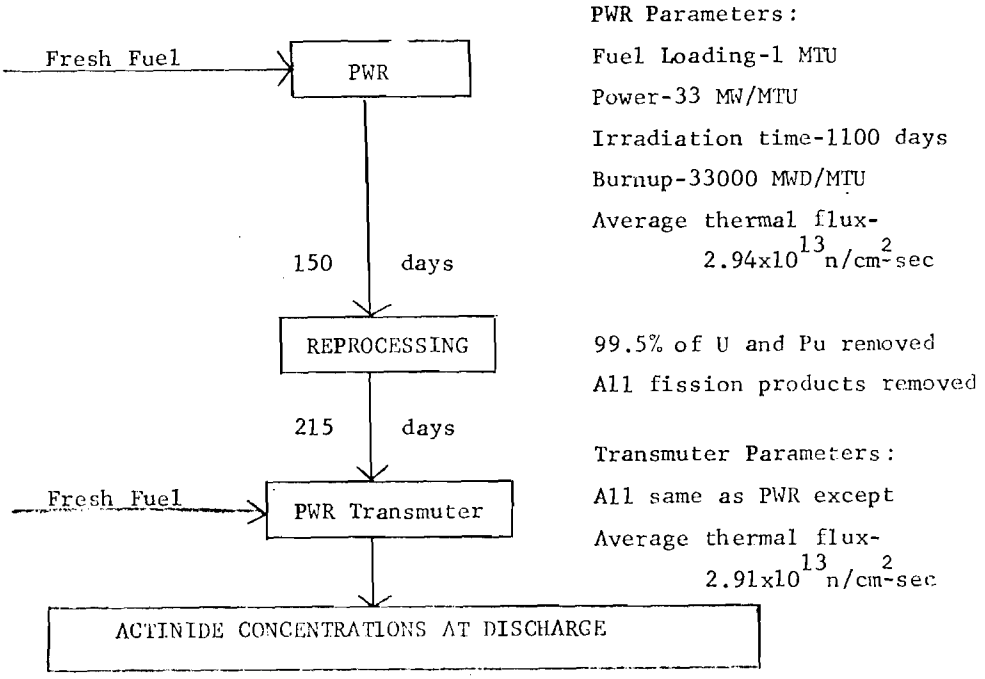

Figure III-1

Sensitivity Analysis Run Scheme With Reactor Parameters

The input parameters for the PWR and the PWR transmuter calculations were the same except that the transmuter had the actinides from the PWR in its core at beginning-of-life. The fresh fuel for each reactor consisted of 3.30% U-235, 96.67% U-238, and 0.027% U-234 for a total of one metric ton of uranium fuel.

Each reactor was run for 1100 days at 33 MW/MTU for a total burnup of 33,000 MWD/MTU. At 150 days after discharge from the PWR, ORIGEN calculated the removal of 100% of the fission products and 99.5% of the uranium and plutonium from the spent fuel. The actinide concentrations at 215 days after reprocessing (365 days after discharge from the PWR) were then calculated and input to the transmuter calculations. The actinide concentrations at discharge from the transmuter were calculated and recorded. These results formed the base case.

Subsequent ORIGEN calculations were duplicates of the base case except that the input cross sections for fission or capture for one isotope were changed to the upper limit values specified by BNL-325. It is important to note that all other parameters were held constant. Table III-5 is a list of the sensitivity runs performed.

2. Discussion of Sensitivity Analysis Results

The basis of comparison between cases was chosen to be the actinide concentrations of several important isotopes at discharge from the transmuter. Since three americium and three curium isotopes were studied by Boccola et al[10] in a somewhat similar study, these were focused upon. Neptunium-237 was also chosen because it is the actinide (excepting uranium and plutonium isotopes) which has the highest concentration at discharge and over a long decay period (10^7 years).

TABLE III-5

List of ORIGEN Sensitivity Runs

Run	Isotope	Reaction
1	BASE CASE	All average cross sections
2	Np-237	CAPTURE
3	Pu-241	"
4	Pu-242	"
5	Am-241	"
6	Am-242m	"
7	Am-243	"
8	Cm-242	"
9	Cm-243	"
10	Cm-244	"
11	Np-237	FISSION
12	Am-241	"
13	Am-242m	"
14	Am-243	"
15	Cm-242	"
16	Cm-243	"
17	Cm-244	"

TABLE III-6

ACTINIDE CONCENTRATIONS VS. SENSITIVITY ANALYSIS RUNS
AT DISCHARGE AFTER REMOVAL OF 99.5% of U and Pu
TRANSMUTATION

UNITS ARE GRAM-ATOMS PER MTU IN FRESH FUEL

Isotope / Base	NP 237	Am 241	AM242A	AM 243	CM 242	CM 243	CM 244	TOTAL(*)
BASE	4.53E+00	2.68E-01	1.18E-02	3.45E-01	2.85E-02	1.46E-03	3.14E-01	2.62E+01
1237(C)	4.41E+00	2.69E-01	1.18E-02	3.45E-01	2.85E-02	1.46E-03	3.14E-01	2.61E+01
1241(C)	4.53E+00	2.67E-01	1.17E-02	3.53E-01	2.84E-02	1.46E-03	3.17E-01	2.62E+01
1242(C)	4.53+00	2.67E-02	1.17E-02	3.53E-01	2.84E-02	1.46E-03	3.17E-01	2.62E+01
1241(C)	4.53E+00	2.62E-01	1.19E-02	3.45E-01	2.88E 02	1.48E-03	3.14E-01	2.62E+01
1242M(C)	4.53E+00	2.68E-01	1.18E-02	3.46E-01	2.84E-02	1.46E-03	3.14E-01	2.62E+01
1243(C)	4.53E+00	2.68E-01	1.18E-02	3.39E-01	2.85E-02	1.46E-03	3.18E-01	2.62E+01
1242(C)	4.53E+0	2.68E-01	1.18E-02	3.45E-01	2.82E-02	1.82E-03	3.15E-01	2.62E+01
1243(C)	4.53E+00	2.68E-01	1.18E-02	3.45E-01	2.85E-02	1.33E-03	3.14E-01	2.62E+01
1244(C)	4.53E+00	2.68E-01	1.18E-02	3.45E-01	2.85E-02	1.46E-03	3.07E-01	2.62E+01
1237(F)	4.53E+00	2.68E-01	1.18E-02	3.45E-01	2.85E-02	1.46E-03	3.14E-01	2.62E+01
1241(F)	4.53E+00	2.68E-01	1.18E-02	3.45E-01	2.84E-02	1.46E-03	3.14E-01	2.62E+01
1242M(F)	4.53E+00	2.68E-01	1.18E-02	3.45E-01	2.84E-02	1.46E-03	3.14E-01	2.62E+01
1243(F)	4.53E+00	2.68E-01	1.18E-02	3.45E-01	2.85E-02	1.46E-03	3.14E-01	2.62E+01
1242(F)	4.53E+00	2.68E-01	1.18E-02	3.45E-01	2.85E-02	1.46E-03	3.14E-01	2.62E+01
1243(F)	4.53E+00	2.68E-01	1.18E-02	3.45E-01	2.85E-02	1.36E-03	3.14E-01	2.62E+01
1244(F)	4.53E+00	2.68E-01	1.18E-02	3.45E-01	2.85E-02	1.46E-03	3.14E-01	2.62E+01

(*) TOTAL OF ALL ACTINIDES AND THEIR DAUGHTERS

TABLE III-7

ACTINIDE PRODUCTION SENSITIVITIES
RELATIVE TO CAPTURE CROSS SECTIONS

REFERENCE NUCLIDE	ADJUSTED NUCLIDE	CHANGE IN σ_c	CHANGE IN I_c	RESULTING CHANGE IN CONCENTRATION
Np-237	Np-237	+ 1.85%	+ 7.58%	- 2.65%
Am-241	Pu-241	+ 2.72%	+ 4.94%	- 0.37%
	Am-241	+ 2.40%	+ 9.46%	- 2.24%
Am-242m	Pu-241	+ 2.72%	+ 4.94%	- 0.85%
	Pu-242	+ 2.16%	+ 2.65%	- 0.85%
	Am-241	+ 2.40%	+ 9.46%	+ 0.85%
	Am-242m	+61.43%	+28.57%	0.00%
Am-243	Pu-241	+ 2.72%	+ 4.94%	+ 2.32%
	Pu-242	+ 2.16%	+ 2.65%	+ 2.32%
	Am-241	+ 2.40%	+ 9.46%	0.00%
	Am-242m	+61.43%	+28.57%	+ 0.29%
	Am-243	+ 2.52%	+ 3.85%	- 1.74%
Cm-242	Am-241	+ 2.40%	+ 9.46%	+ 1.05%
	Am-242m	+61.43%	+28.57%	- 0.35%
	Cm-242	+21.21%	+26.67%	- 1.05%
Cm-243	Am-241	+ 2.40%	+ 9.46%	+ 1.37%
	Am-242m	+61.43%	+28.57%	0.00%
	Am-243	+ 2.52%	+ 3.85%	0.00%
	Cm-242	+21.21%	+26.67%	+24.26%
	Cm-243	+44.44%	+20.00%	- 8.90%

ACTINIDE PRODUCTION SENSITIVITIES

RELATIVE TO CAPTURE CROSS SECTIONS (cont.)

REFERENCE NUCLIDE	ADJUSTED NUCLIDE	CHANGE IN σ_c	CHANGE IN I_c	RESULTING CHANGE IN CONCENTRATION
Cm-244	Am-242m	+61.43%	+28.57%	0.00%
	Am-243	+ 2.52%	+ 3.85%	+ 1.27
	Cm-242	+21.21%	+26.67%	+ 0.32%
	Cm-243	+44.44%	+20.00%	0.00%
	Cm-244	+ 7.19%	+ 7.69%	- 2.23%

TABLE III-8

ACTINIDE PRODUCTION SENSITIVITIES

RELATIVE TO FISSION CROSS SECTIONS

REFERENCE NUCLIDE	ADJUSTED NUCLIDE	CHANGE IN σ_f	CHANGE IN I_f	RESULTING CHANGE IN CONCENTRATION
Np-237	Np-237	+15.79%	0.00%	0.00%
Am-241	Am-241	+ 3.17%	+ 9.52%	0.00%
Am-242m	Am-241	+ 3.17%	+ 9.52%	0.00%
	Am-242m	+18.75%	+ 7.01%	0.00%
Am-243	Am-241	+ 3.17%	+ 9.52%	0.00%
	Am-242m	+18.75%	+ 7.01%	0.00%
	Am-243	0.00%	+126.67%	0.00%
Cm-242	Am-241	+ 3.17%	+ 9.52%	- 0.35%
	Am-242m	+18.75%	+ 7.01%	- 0.35%
	Cm-242	+20.00%	0.00%	0.00%
Cm-243	Am-242m	+18.75%	+ 7.01%	0.00%
	Am-243	0.00%	+126.67%	0.00%
	Cm-242	+20.00%	0.00%	0.00%
	Cm-243	+ 8.33%	+ 21.51%	- 6.85%
Cm-244	Am-242m	+18.75%	+ 7.01%	0.00%
	Am-243	0.00%	+126.67%	0.00%
	Cm-242	+20.00%	0.00%	0.00%
	Cm-243	+ 8.33%	+ 21.51%	0.00%
	Cm-244	+ 8.33%	+ 20.00%	0.00%

The discharge concentrations for each of these isotopes in every case studied are listed in Table III-6. Note that the total amount of actinides is the same for all but the case in which the capture cross sections of Np-237 were changed, and this change was only 0.38%. This indicates that the maximum possible error in the total actinide concentrations due to error in the cross sections of one isotope is very small.

The concentrations listed in Table III-6 were used to create Tables III-7 and III-8. These tables list the change in concentration of these isotopes due to changes in their cross sections or their precursors. In each table, the first column is the nuclide whose concentration is studied. The second column is the nuclide whose cross sections were altered. The next two columns show the percent change in the cross sections of the nuclide listed in column two. The final column lists the resulting change in concentration at discharge of the isotope in the first column.

Generally, an increase in either capture or fission cross sections caused a decrease in the concentration of the adjusted nuclide due to increased removal of that nuclide. The exact change in concentration is difficult to estimate directly because the creation rate of the nuclide is as important as the destruction rate. In fact, if the creation rate is much greater than the destruction rate, the effect of the cross section change is very small. This is the case for most actinides in the transmuter.

The factors affecting the creation rate are as follows:

(1) the amount of precursors present,

(2) cross sections of the precursors,

(3) the transmuter flux.

The factors affecting the destruction rate are:

(1) the amount of the reference nuclide present,

(2) cross sections of the reference nuclide present,

(3) the transmuter flux.

The flux is the same in both cases. Therefore, the ratio of the presursor to reference nuclide concentrations and cross sections gives an indication of the possible effect of varying the cross sections of the reference nuclide. For example, the greatest cross section adjustment was performed for capture by Am-242m. Despite a 61.43% and 28.57% capture increase in the thermal and resonance regions respectively, the total amount of Am-242m remained essentially unchanged ($\leq$0.005%). Referring to Table III-6 one sees that the Am-241 to Am-242m concentration ratio is about 20:1. The Am-241 to Am-242 cross section ratio is about 1:2, leaving an apparent production-destruction ratio of 10:1. The decay scheme must also be taken into effect, however. Figure III-2 is a schematic of the U-238 buildup chain. It shows that about 80% of the Am-242m destruction rate is due to fission. This reduces the effect of a change in the capture cross sections for Am-242m to a negligible amount.

At the other extreme, the concentration of Cm-243 was greatly sensitive to changes in the capture cross sections of Cm-242. This occurs because essentially all of the Cm-242 that is destroyed becomes Cm-243 (see Figure III-2).

These two cases are the extremes. All the other results can be explained by similar reasoning. From Tables III-7 and III-8, it is shown that with few exceptions, the actinide isotopic concentrations are changed by a small amount ($\leq$2.5%) and that the total actinide amount is never significantly altered by an error in the cross sections of one isotope.

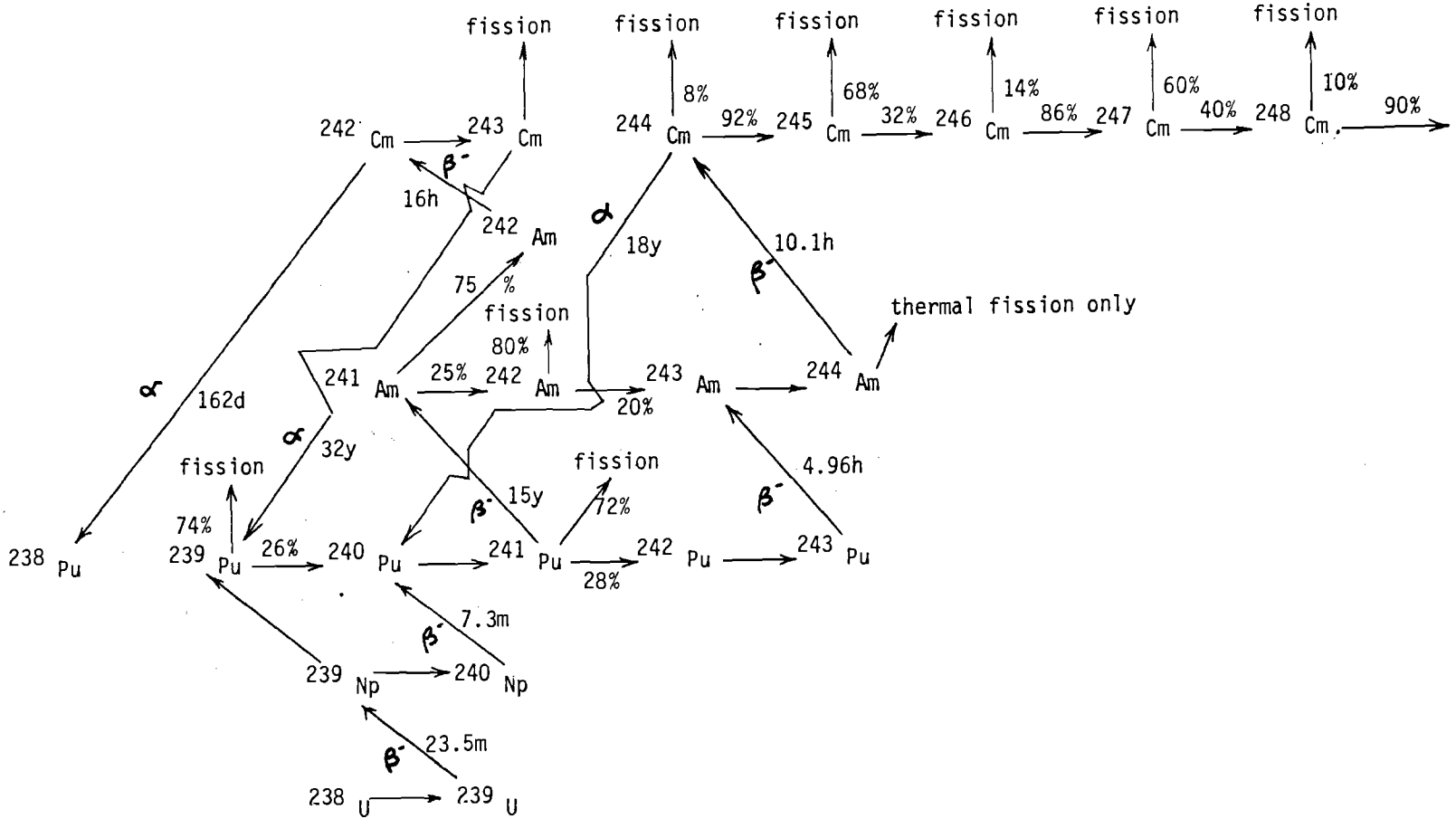

Fig. III-2 ^{238} Buildup Chain

TABLE III-9

ACTINIDE PRODUCTION SENSITIVITIES RELATIVE TO NUCLEAR DATA

Nuclide (Q)	Precursors and nucl. itself (i)	Nuclear datum (q_i)		
		$\sigma_{th}(n,\gamma)$	R.I. (n,γ)	$\lambda(\beta-)$
Am-241	Pu-240	14.35	40.67	
	Pu-241	-0.98	-0.64	96.65
	Am-241	-6.84	-8.24	
Am-242-m	Am-241	37.42	45.08	
	Am-242-m	-10.88	-	
Am-243	Pu-241	39.12	47.08	0.38
	Pu-242	2.36	84.75	
	Pu-243			0.11
	Am-241	0.37	0.44	
	Am-242-m	0.59	-	
	Am-243	-1.00	-7.47	
Cm-242	Am-241	29.31	83.03	
	Am-242			0.55
	Cm-242	-0.17	-	-36.66 (a
Cm-243	Am-242			18.51
	Cm-242	99.86	-	
	Cm-243	-1.12	-1.46	-0.50 (a
Cm-244	Pu-243			0.18
	Am-242-m	0.37	-	
	Am-242			-0.15
	Am-243	10.21	75.63	
	Cm-244	-0.01	-	

Comparison of Sensitivity Analysis Results to Those of Bocola[10]

Bocola, et al[10], performed a sensitivity analysis similar to that previously discussed. In this analysis, the sensitivity of the nuclide concentrations were determined relative to the thermal capture cross sections, capture resonance integrals and decay constants. The Bocola results are reproduced exactly from that paper and listed in Table III-9. Before making this comparison, the following basic differences between this analysis and the Georgia Tech analysis should be pointed out:

1. The Bocola analysis is applicable to a single cycle of LWR fuel whereas the Georgia Tech analysis was done for recycled actinides in a LWR transmutation reactor.
2. The Bocola analysis was done by a perturbation method, in which the cross section of the reference nuclide was perturbed 20%. The Georgia Tech analysis was accomplished by substituting the maximum possible value of the cross section in place of the original cross section. The maximum value was determined by BNL-325[4]. The method used in the Georgia Tech analysis is an exact method, whereas perturbation theory is an approximation that is only applicable for small perturbations. The use of realistic values for the change in cross sections lends more credibility to the Georgia Tech analysis.
3. The Bocola analysis did not include the sensitivities relative to fission cross sections. Therefore, the results may only be compared with respect to capture sensitivities.

4. Since the original concentrations of nuclides and cross section changes are so different for the two studies, the only useful comparison that can be made is whether each cross section change caused a positive or negative change in the nuclide concentration.

Comparing the format of Tables III-7 and III-9, the headings of Table III-9 could be listed from left to right as:

1. Reference Nuclide
2. Adjusted Nuclide
3. Sensitivity of reference nuclide concentration with respect to σ_γ, I_γ, and λ.

The sensitivities listed were obtained from the following formula:

$$S = \frac{\delta Q/Q}{\delta q/q} \tag{3.1}$$

where S = sensitivity

$\delta Q/Q$ = percent change in concentration

$\delta q/q$ = 20.

Comparing the tables it is seen that the signs of each sensitivity match the change in concentration calculation in the Georgia Tech analysis. In some cases, there was no change in the concentration of the reference nuclide in the Georgia Tech analysis, but this is due to the different conditions under which the analysis was run.

References for Chapter III

1. Bell, M. J., "ORIGEN--The ORNL Isotope Generation and Depletion Code," Oak Ridge National Laboratory, Oak Ridge, Tennessee, (May, 1973).

2. Benjamin, R. W., Vandervelde, U. D., Garrell, F. C., McBrosson, F. J., "A Consistent Set of Transpulutonium Multigroup Cross Sections," (1975).

3. Benjamin, R. W., "Status of Measured Neutron Cross Sections of Transactinium Isotopes for Thermal Reactors," Savannah River Laboratory, Aiken, South Carolina, (November 1975).

4. Mughabaghab, S. F., Garber, D. I., "Neutron Cross Sections, Third Edition, Volume One," Brookhaven National Laboratory, Upton, N. Y., (June, 1973).

5. Wright, R. Q., et al, "100G:100 Group Neutron Cross Section Data Based on ENDF/B," Radiation Shielding Information Center, Oak Ridge, Tennessee, (1972).

6. Wright, R. Q., Greene, N. M., Lucius, J. L., Craven, C. W., Jr., "SUPERTOG: A Program to Generate Fine Group Constants and P_n Scattering Matrices from ENDF/B," Oak Ridge National Laboratory, Oak Ridge, Tennessee, (1972).

7. Wright, R. Q., "User's Manual for DLC-2 Data Retrieval Program," informal notes, (July, 1972).

8. Engle, W. W., Jr., "A User's Manual for ANISN," Oak Ridge Gaseous Diffusion Plant, Oak Ridge, Tennessee, (March, 1967).

9. Garber, D. J. and Kinsey, R. R., "Neutron Cross Sections," Third Edition, Volume 2, Curves, Brookhaven National Laboratory, Upton, N. Y., (to be released in 1976).

10. Bocola, W., et al, "Considerations on Nuclear Transmutation for the Elimination of Actinides," C.M.E.N.-C.S.N. Casaccia, Rome, Italy, (1975).

IV. CALCULATIONS OF THE ACTINIDE BURNUP POTENTIAL IN THE GCATR

Before performing detailed calculations, it seemed desirable to explore the potential attractiveness of the GCATR concept making some simplifying approximations and assumptions.

Accordingly, calculations were made using the ORIGEN[1] code for the actinide mass balance in the GCATR. For these calculations, the following assumptions were made:

1. The GCATR services 10 LWR's. The actinide wastes from the LWR's are processed in a reprocessing facility, in which 99.9% of the uranium and plutonium and 100% of the fission products are removed. The reprocessed actinides are then placed in the GCATR core.
2. Reprocessing occurs 160 days after discharge from either the GCATR or LWR's.
3. The GCATR operates on a two-year cycle. Its own wastes are recycled through the reprocessing facility and back into the GCATR.
4. The GCATR uses 100% enriched U-233 fuel in the form of UF_6 gas.
5. The flux in the GCATR core is 1.36×10^{16} neutron per cm^2 per sec. The flux in the actinides in the GCATR is 7.78×10^{15} neutrons per cm^2 per second.

The mass of actinides in the GCATR is shown in Table IV-1 for the entire 40 year life of the reactor. The core region and actinide regions are kept separate, representing the separation of the GCATR core and actinides blanket. The "out" columns list the remaining balance after end of cycle. The difference in these figures is the mass of the fission products produced during the cycle. The "after reprocessing" columns

TABLE IV-1

GCATR ACTINIDE FLOW SCHEME

NOTE: (1) Units are metric tons of actinides (including U and Pu).

(2) In reprocessing, 99.9% of U and Pu are removed.

	CORE			ACTINIDES		
CYCLE	IN	OUT	AFTER REPROCESSING	IN	OUT	AFTER REPROCESSING
1	2.312	0.278	1.096×10^{-3}	1.293	1.108	0.382
2	2.312	0.278	1.096×10^{-3}	1.293	1.108	0.382
3	2.312	0.278	1.096×10^{-3}	1.576	1.404	0.603
4	2.312	0.278	1.096×10^{-3}	1.676	1.404	0.603
5	2.312	0.278	1.096×10^{-3}	1.898	1.574	0.732
6	2.312	0.278	1.096×10^{-3}	1.898	1.574	0.732
7	2.312	0.278	1.096×10^{-3}	2.026	1.672	0.086
8	2.312	0.278	1.096×10^{-3}	2.026	1.672	0.086
9	2.312	0.278	1.096×10^{-3}	2.099	1.729	0.849
10	2.312	0.278	1.096×10^{-3}	2.099	1.729	0.849
11	2.312	0.278	1.096×10^{-3}	2.142	1.762	0.874
12	2.312	0.278	1.096×10^{-3}	2.142	1.762	0.874
13	2.312	0.278	1.096×10^{-3}	2.167	1.781	0.889
14	2.312	0.278	1.096×10^{-3}	2.167	1.781	0.889
15	2.312	0.278	1.096×10^{-3}	2.182	1.793	0.898
16	2.312	0.278	1.096×10^{-3}	2.182	1.793	0.898
17	2.312	0.278	1.096×10^{-3}	2.191	1.800	0.903
18	2.312	0.278	1.096×10^{-3}	2.191	1.800	0.903
19	2.312	0.278	1.096×10^{-3}	2.196	1.804	0.906
20	2.312	0.278	1.096×10^{-3}	2.196	1.804	0.906

show the mass of actinides from that cycle that remain after 99.9% of the uranium and plutonium have been removed.

The results in Table IV-1 were determined by running the ORIGEN code, which calculates the buildup and depletion of each isotope given initial concentrations and reactor conditions. Equilibrium is not yet reached after 40 years with the proposed recycle scheme, due to the two year GCATR cycle. The equilibrium amount of actinides in the GCATR is 2.203 MTA at beginning of life and 1.809 MTA at end of cycle. This results in 0.910 MTA after reprocessing

Table IV-2 is a comparison of the reduction of actinide inventory by three proposed schemes. The first is the Claiborne scheme in which the wastes from one LWR are recycled back into the LWR itself. The second is the Beaman[2] scheme which uses an LMFBR to service three LWR's. The third is the Georgia Tech Gas Core GCATR to service ten LWR's. The corresponding actinide inventories in the GCATR scheme are higher because the system is much larger. The GCATR, however, burns far more actinides than the LMFBR and LWR systems. The important parameter for comparison is the hazard reduction factor, in which the GCATR is superior. This factor is the ratio of the amount produced to the amount remaining. It is the inverse of the percentage of remaining actinides for which the GCATR leaves 16.98%, the LMFBR leaves 19.05%, and the LWR leaves 24.33%.

The comparison, although based upon some simplified approximations, shows that the GCATR is attractive in comparison with the LMFBR and LWR. The GCATR services 10 LWR's for a total of 520,000 MWe years as compared to a total of 3LWR's and 192,000 MWe years for the LMFBR. The hazard

TABLE IV 2. COMPARISON OF ACTINIDE REDUCTION BY LMFBR, GCATR, AND LWR TRANSMUTATION OVER 40 YEAR LIFE. THE ACTINIDE AMOUNTS DO NOT INCLUDE U AND Pu.

	LWR (CLAIBORNE)[3]	LMFBR (BEAMAN)[2]	GCATR (GA. TECH)
System	1 LWR	1 LMFBR and 3 LWR's	1 GCATR and 10 LWR's
Power Production	40,000 MWe Years	192,000 MWe Years	~520,000 MWe Years
Actinide Production	559 KgA	3620 KgA	12,352 KgA
Amount Remaining At End-of-Life		113 (Newly Produced)	618 (Newly Produced)
	102 (In LWR - Near Equilibrium)	351 (Equilibrium in LMFBR)	877 (In GCATR - Near Equilibrium)
	34 (In Reprocessing)	226 (Inreprocessing)	618 (In Reprocessing)
	136 KgA Total	690 KgA Total	2113 KgA Total
Amount Burned Up	423 KgA	2930 KgA	10,239 KgA
Reduction Factor	4.11	5.25	5.85

reduction factor of the GCATR System is 5.85, as compared to values of 5.25 and 4.11 for the LMFBR and LWR, respectively. The GCATR system burns up 10.239 metric tons of actinids in 40 years as compared to 2.930 and 0.423 for the LMFBR and GCTAR, respectively. These comparisons are graphically illustrated in Figures IV-1 through IV-3.

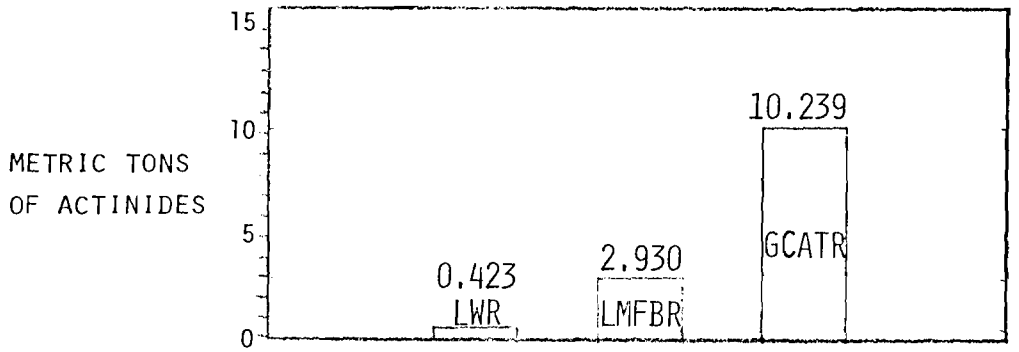

FIGURE IV-1. METRIC TONS OF ACTINIDES BURNED UP IN 40 YEARS BY LWR, LMFBR AND GA. TECH GCATR.

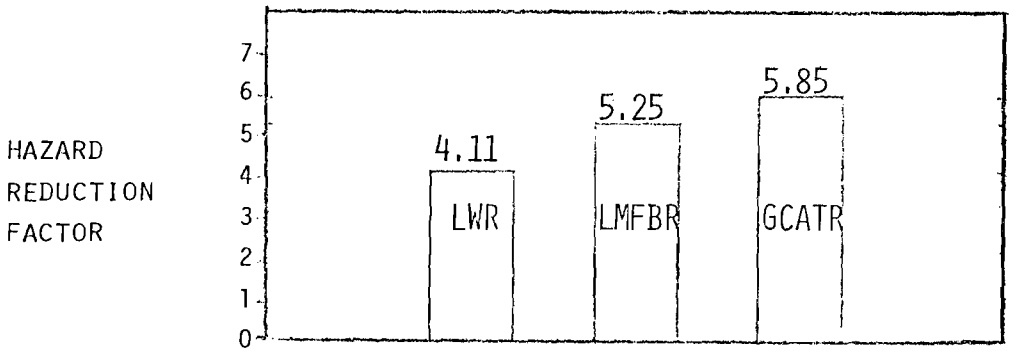

FIGURE IV-2. HAZARD REDUCTION FACTORS OF LWR, LMFBR AND GA. TECH GCATR OVER 40 YEAR LIFE.

(Hazard Reduction Factor = Actinides Produced ÷ Actinides Remaining at End of 40 Year Life)

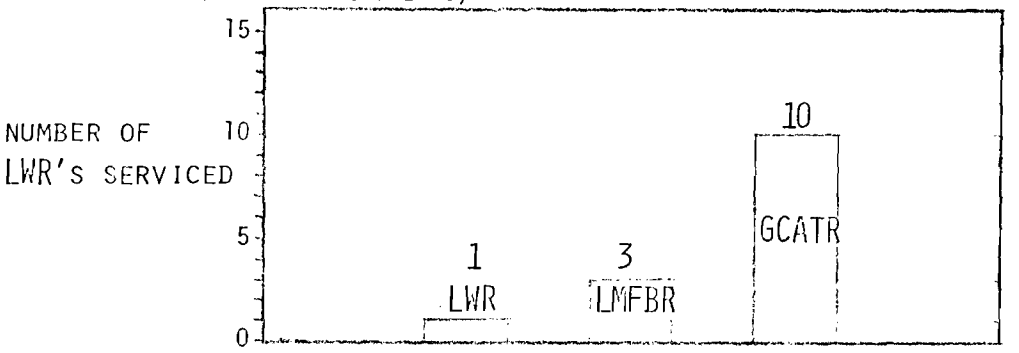

FIGURE IV-3. NUMBER OF LWR'S SERVICED BY LWR, LMFBR AND GA. TECH GCATR SYSTEMS.

References for Chapter IV

1. Bell, M. J., "ORIGEN — The ORNL Isotope Generation and Depletion Code," ORNL-4628, May, 1973.

2. Beaman, S. L., and Aitken, E. A., "Feasibility Studies of Actinide Recycle in LMFBR's as a Waste Management Alternative."

3. Clairborne, H. D., "Neutron Induced Transmutation of High-Level Radioactive Waste," ORNL-TM-3964, December, 1972.

V HEAT TRANSFER ANALYSIS OF ACTINIDE FUEL RODS

The transuranium actinides (neptunium, plutonium, americium, curium, etc.) will not exist in a gaseous state at reasonable temperatures; consequently, it will be necessary to introduce these elements into the GCATR in a solid form. It is thought that the most reasonable approach for placing actinides in an actinide transmutation reactor is in the form of rods encapsulated with a metal cladding. The actinide fuel rods would be in the form of oxides and would be similar to the fuel rods used in present nuclear power plants. These rods would have to be cooled by a suitable coolant and would have the same design constraints that exist for fuel elements used in power reactors. A discussion of the design constraints follows:

1. Thermal outputs of the actinide fuel rods are limited because excessive temperatures may cause undesirable phase changes, fuel melting, or too high a level of stored energy in the fuel from a safety viewpoint.
2. Thermal outputs of the actinide fuel rods may be limited because of excessive temperatures in the cladding. Maximum cladding temperatures will be limited by loss of cladding creep.
3. Thermal outputs of the actinide fuel rods may be limited because the heat flux at the cladding-coolant interface may exceed the departure from nucleate boiling (DNB) heat flux.

There is a scarcity of thermal-physical property data on the oxides of transplutonium actinides. There is no data on the behavior of mixtures. It appears that the densities of all actinide oxides are about the same, being of the order of 11 grams/cc.[1] In addition, the known melting

points of actinide oxides are high, being of the order of 2400°C or higher. Consequently, since little is known about the transplutonium actinide oxides and a sizable fraction of the actinide fuel rods will be uranium oxide, it is assumed that the melting point and thermal conductivity of actinide oxide mixture is the same as UO_2.

For any type of fuel rod, the maximum fuel temperature is proportional to the maximum linear heat rate (watts/cm) of that fuel rod. For conditions in pressurized water reactors, the linear heat rate to cause centerline melting of UO_2 fuel pellets is of the order of 720 watts/cm. Consequently, the early design of pressurized water reactors limited maximum linear heat rates to about 590 watts/cm. More recently maximum linear heat rates have been reduced to about 500 watts/cm because higher linear heat rates allowed too high a level of stored energy in the fuel from the standpoint of the consequences of a loss of coolant accident.

With actinide fuel rods the maximum allowable linear heat rate is established at 590 watts/cm. This is a level which was considered the maximum for water-cooled nuclear power plants prior to 1973 and should not be considered conservative. The melting point for the mixture of actinide oxides may be below 2400°C and, consequently, a lower linear heat rate may be required to prevent centerline melting.

Actinide fuel pellets will be clad with a 300 series stainless steel. The design criteria for the Clinch River Breeder Reactor Core is that maximum stainless steel cladding midwall temperatures not exceed 662°C[2]. Therefore, this criteria will be applied to the cladding for the actinide fuel rods.

Departure from nucleate boiling (DNB) is a possibility whenever a liquid is used as a reactor coolant. For sodium as a coolant, the maximum cladding temperature constraint will preclude the possibility of coolant

boiling during normal reactor operation. Consequently, DNB will not be considered for use of sodium as a coolant. For high pressure water as a coolant, the maximum cladding temperature constraint is at temperatures far in excess of those necessary to produce DNB. Therefore, with a water coolant there will be a constraint on heat flux given by the DNB heat flux. In order to allow a margin of safety in the operation of nuclear reactors, the predicted DNB heat flux divided by the operating heat flux (called the DNB ratio) is not allowed to fall below some prescribed value such as 1.3. For the analysis of water-cooled actinide fuel rods the predicted DNB heat flux will be calculated with the Westinghouse (W-3) correlation which is an accepted standard in the nuclear power industry [3]. The DNB ratio will not be allowed to fall below 1.3.

Table V-1 summarizes the thermal design constraints imposed upon the actinide fuel rods.

TABLE V-1

SUMMARY OF THERMAL CONSTRAINTS ON ACTINIDE FUEL RODS

Linear Heat Rate:	590 watts/cm
Maximum Cladding Temperature:	662°C
Maximum Heat Flux: (applied to water coolant)	Westinghouse (W-3) DNB Heat Flux Divided by 1.3

As previously mentioned the actinide fuel rods need to be cooled by a suitable coolant which can withstand a reactor environment. The coolants selected for consideration are those currently in use in nuclear power plants— pressurized water, helium, and sodium. The specified coolant channel velocities, pressures, and inlet and outlet temperatures for these

coolants, which are somewhat typical of operating power reactors, are given in Table V-2.

TABLE V-2

COOLANT CONDITIONS FOR ACTINIDE FUEL RODS

Coolant	Inlet Velocity	Pressure	Inlet Temperature	Outlet Temperature
Water	8.2 m/sec	156 Bar	294°C	327°C
Helium	82 m/sec	100 Bar	370°C	537°C
Sodium	9.8 m/sec	100 Bar	370°C	537°C

A high burnup rate in the actinide fuel rods is desirable so as to shorten the time required for transforming the actinide by the fission process. The ultimate burnup rate will be limited by the heat transfer limitations discussed at the start of this chapter.

The volumetric heat generation rate in actinide fuel rods, which is proportional to the burnup rate, is given by

$$q''' = \sum_{i=1}^{n} K_i N_i \int_0^{\infty} \phi(E)\, \sigma_{f_i}(E)dE + E_c \qquad (5.1)$$

where

q''' = volumetric heat generation rate, Mev/cm^3-sec

K_i = short range energy released from fission of i th fuel material, Mev/fission

N_i = atom density of i th fuel material, atoms/cm^3

$\phi(E)$ = neutron flux per unit energy, n/cm^2-sec-Mev

$\sigma_{f_i}(E)$ = energy dependent fission cross section of i th fuel material, cm^2

E_c = gamma volumetric heat generation rate, Mev/cm^3-sec

The value of K_i is not known for all the transplutonium actinides, but it should probably be close to that of uranium or plutonium. In addition, the spatial distribution of E_c should be similar to that of the neutron flux and this term can then be incorporated into K_i. For uranium the total recoverable energy release per fission is of the order of 200 Mev/fission. Consequently, by fission cross sections and the total neutron flux, Eq. 5.1 can be simplified to

$$q''' = 200\,\Phi \sum_{i=1}^{n} N_i\,\bar{\sigma}_{f_i}, \quad \text{Mev/cm}^3\text{-sec} \tag{5.2}$$

where $\bar{\sigma}_{f_i}$ is the spectrum-averaged fission cross section of the i th fuel material. From the limitations on q''', the maximum neutron flux permissible in actinide fuel rods can be determined from Eq. 5.2.

For actinide fuel rods of radius r_o cm. encapsulated in stainless steel tubes with a thickness and radial gap between fuel and cladding of ΔC cm., the linear heat rate is given by

$$q' = \pi\, r_o^2\, q''' \tag{5.3}$$

where

q' = linear heat rate, watts/cm

q''' = volumetric heat generation rate, watts/cm^3

The heat flux at the cladding outer surface is given by

$$q''_w = \frac{r_o^2\, q'''}{2(r_o + \Delta C)} \tag{5.4}$$

where q''_w is the heat flux in watts/cm^2.

Inspection of Eq. 5.3 shows that the volumetric heat generation rate is inversely proportional to the the square of the fuel radius. Therefore, for a fixed upper limit for the linear heat rate, the maximum volumetric heat generation rate is found for the smallest possible fuel radius, r_o. From a design point of view there will be a minimum fuel radius for which it is practical to fabricate fuel rods. This minimum radius is assumed to be 0.127 cm.

By examining Eq. 5.4 it is seen that the volumetric heat generation rate is approximately inversely proportional to the fuel radius. Therefore, the maximum volumetric heat generation rate for a fixed heat flux is found for the smallest fuel radius. The minimum fuel radius is determined from a practical fabrication point of view and will be set at 0.127 cm.

From the arguments in the preceding paragraphs it is apparent that the maximum volumetric heat generation rate is achieved with the minimum fuel radius of 0.127 cm. Whether the limiting thermal constraint is due to a maximum linear heat rate (q'), heat flux (q''_w), or cladding temperature will require further analysis of the three reactor coolants and their associated flow conditions. The fuel pellets are assumed to be 0.254 cm. in diameter clad with a 300 series stainless steel of 0.033 cm. thickness with a diametral clearance between the fuel and cladding of 0.015 cm. This results in a fuel rod outside diameter of 0.335 cm. The volumetric heat generation rate in the fuel rods is assumed to have a cosine distribution along the rod axis and the rods are assumed to have an active length of 180 cm.

The thermal design constraints are listed in Table V-1. In order to determine the maximum cladding temperature it is necessary to calculate the heat-transfer coefficients for the various coolants. For a water coolant, the maximum cladding temperature will not be a constraint because the coolant would have gone through a departure from nucleate boiling (DNB) at cladding temperatures far below the 662°C limit. Therefore, it is necessary to calculate heat-transfer coefficients for sodium and helium.

For sodium the heat-transfer coefficient is given by[4]

$$h = \frac{k}{D_e}\left[6.66 + 3.126(P/D) + 1.184(P/D)^2 + 0.0155\left(\frac{\rho v D_e C_p}{k}\bar{\psi}\right)^{0.86}\right] \quad (5.5)$$

where

h = heat-transfer coefficient

k = sodium thermal conductivity

D_e = flow channel equivalent diameter

D = fuel rod diameter

P = rod pitch, spacing between fuel rod centers

ρ = sodium density

v = sodium velocity

C = sodium heat capacity

$\bar{\psi}$ = average ratio of eddy diffusivities

The average ratio of eddy diffusivities is calculated by

$$\bar{\psi} = 1 - \frac{1.82}{N_{Pr}\left(\epsilon_M/\nu\right)_{Max}^{1.4}} \tag{5.6}$$

where

N_{Pr} = sodium Prandtl number

$(\epsilon_M/\nu)_{Max}$ = maximum eddy diffusivity for momentum transfer given graphically in Ref. 4.

The heat-transfer coefficient for helium can be calculated with the Dittus-Boelter equation[5]

$$h = \frac{k}{D_e}\left[0.023\left(\frac{\rho v D_e}{\mu}\right)^{0.8}\left(\frac{C_p \mu}{k}\right)^{0.4}\right] \tag{5.7}$$

where μ is the helium viscosity.

The departure from nucleate boiling heat flux is calculated with an empirical correlation developed by Tong[3]

$$\frac{q''_{DNB,\,EU}}{10^6} = \left\{(2.022 - 0.0004302p) + (0.1722 - 0.0000984p) \times \exp[(18.77 - 0.004129p)\chi]\right\} \times \left[(0.1484 - 1.596\chi + 0.1729\chi|\chi|)G/10^6 + 1.037\right] \times \left[1.157 - 0.869\chi\right] \times \left[0.2664 + 0.8357\exp(-3.151De)\right] \times \left[0.8258 + 0.000794\,(h_{sat} - h_{in})\right], \tag{5.8}$$

where

$q''_{DNB,\,EU}$ = equivalent uniform channel DNB heat flux, Btu/hr-ft^2

p = pressure, psia

χ = quality

G = mass velocity, lb_m/ft^2-hr

h = enthalpy, Btu/lb$_m$

D_e = channel equivalent diameter, in.

For non-uniform axial heat flux distributions Eq. 5.8 is modified by employing a correction factor F such that

$$q''_{DNB,N} = q''_{DNB,EU}/F \tag{5.9}$$

where $q''_{DNB,N}$ = DNB heat flux for the non-uniformly heated channel

$q''_{DNB,EU}$ = equivalent uniform DNB flux from Eq. 5.8

and

$$F = \frac{C \int_o^{\ell_{DNB}} q''(z) \exp[-C(\ell_{DNB,N} - z]dz}{q''_{local}\,[1 - \exp(-C\ell_{DNB,EU})]} \tag{5.10}$$

where

$$C = 0.44 \frac{(1 - \chi_{DNB})^{7.9}}{(G/10^6)^{1.72}} \text{ in.}^{-1}$$

ℓ_{DNB} = axial location at which DNB occurs, in.

The fuel rod thermal-hydraulic analysis will have a variety of uncertainties due to manufacturing tolerances, physical property variations, maldistribution of flow, uncertainty in the correlations, and uncertainty in the fuel heating distribution. The effects of these uncertainties on the thermal-hydraulic performance of fuel rods is accounted for by applying hot channel/hot spot factors to computations based upon nominal conditions in the fuel assembly. Because of the similarity of the actinide fuel rods and

flow conditions to liquid metal-cooled fast breeder reactors, the hot channel/hot spot factors used in the analysis are the same as those used in the analysis of the Clinch River Breeder Reactor Plant[2]. Table V-3 gives values selected.

TABLE V-3

ACTINIDE FUEL ROD HOT CHANNEL/HOT SPOT FACTORS

Axial Nuclear*	Coolant	Film	Heat Flux
(F_Z^N)	$F_{\Delta h}$	$F_{\Delta t}$	F_q
1.57	1.232	1.168	1.081

The solution for the fuel rod geometry and volumetric heat generation rates requires simultaneous application of the thermal constraints listed in Table V-1. For sodium as a coolant the limiting constraint is a maximum linear heat rate of 590 watts/cm to prevent fuel melting. The limiting thermal constraint with helium is on the heat flux to prevent the cladding temperature from exceeding 662°C. With water, the limiting thermal constraint is departure from nucleate boiling.

Table V-4 lists the results of the heat transfer calculations for the three coolants.

---

*This is from the assumed cosine distribution for the axial dependence of the neutron flux.

TABLE V-4

RESULTS OF THERMAL ANALYSES OF ACTINIDE FUEL RODS FOR VARIOUS COOLANTS

	Rod Diameter (cm)	P/D	q' (Max) (watts/cm)	q''_w (Avg) (watts/cm^2)	q''_w (Max) (watts/cm^2)	q''' (Avg) (watts/cm^3)	q''' (Max) (watts/cm^3)
Sodium	0.335	2.21	590	330	560	6,835	11,600
Helium	0.335	2.05	152	85	145	1,780	3,000
Water	0.335	2.00	415	232	394	4,800	8,150

P/D = fuel element pitch-to-diameter ratio; q' (Max) = maximum linear heat rate; q''_w (Avg) = average wall heat flux; q''_w (Max) = maximum wall heat flux; q''' (Avg) = average volumetric heat generation rate; q''' (Max) = maximum volumetric heat generation rate.

One result of great importance is the average volumetric heat generation rate in the fuel rod which is proportional to the maximum average fuel rod burnup rate. Fuel burnup is usually expressed in terms of megawatt-days per tonne of fuel (MWD/t). Maximum burnups proposed in advanced power reactors

such as the Clinch River Breeder Reactor Plant is 150,000 MWD/t[2]. For the average volumetric heat generation rates shown on Table V-4, the time required to achieve these burnups is 202 days with the sodium coolant, 775 days with the helium coolant, and 288 days with the water coolant. The Clinch River Breeder Reactor will require 1100 days to achieve 150,000 MWD/t burnup, so the burnup rate in the actinide fuel rods could be five times as fast as the conventional fuel in an LMFBR.

By taking the maximum volumetric heat generation rates in Table V-4 and applying this data to Eq. 5.2 it is possible to determine the maximum allowable neutron flux in the actinide fuel rods. For spent LWR fuels with a burnup of 33,000 MWD/t in which all fission products and 99.9 percent of the uranium and plutonium have been removed, the maximum neutron fluxes for a fast reactor spectrum are shown in Table V-5 for sodium and helium coolants.

TABLE V-5

MAXIMUM NEUTRON FLUXES IN ACTINIDE FUEL RODS

Coolant	Neutron Flux, n/cm^2-sec
Sodium	4×10^{16}
Helium	10^{16}

The maximum neutron flux in actinide fuel rods with a sodium coolant is about 10 times the maximum neutron flux in LMFBR's. Therefore, it is desirable to be able to construct reactors which are capable of generating

neutron fluxes at this high level. Gas core reactors may be able to generate this high a neutron flux because of their smaller fuel loadings.

References for Chapter V

1. Kirk and Othmer, Encyclopedia of Chemical Technology, Vol. 1, 2nd ed., John Wiley & Sons (1963).

2. Cavelli, M. D., and R. A., Markley, "Preliminary Thermal Hydraulic Design and Predicted Performance of the Clinch Breeder Reactor Core," 75-HT-71, presented at AIChE-ASME Heat Transfer Conference, San Francisco (August 11-13, 1975).

3. Tong, L. S., "Prediction of Departure From Nucleate Boiling for an Axially Non-Uniform Heat Flux Distribution," J. Nuclear Energy, 6, 21 (1967).

4. Dwyer, O. E., and R. N. Lyon, "Liquid Metal Heat Transfer," Proc. 3rd U. N. Intern. Conf. Peaceful Uses of Atomic Energy Geneva, 8, pp 182-189 (1965).

5. Dittus, F. W., and L. M. K., Boelter, University California Pub. Eng., 2, 443 (1930).

VI. REACTOR DESIGN

Any actinide transmutation reactor must satisfy the following general criteria:[1]

a) The transmutation process must not use more energy than was originally produced in the formation of the actinides.

b) The transmutation process must not create more actinides in its operation than it burns.

c) The transmutation process must be rapid enough to burn actinides at a significant rate compared to their creation in the nuclear industry.

Any gas core transmuter developed by this project must satisfy, in addition, the following criteria:

a) UF_6 will be used as the reactor fuel.

b) The reactor must generate a very high neutron flux in order to obtain a significant actinide fission rate.

c) The reactor must produce the neutron spectrum which provides the largest possible net destruction of actinides.

It is necessary to design the gas core actinide transmuter in conjunction with computer design codes. These codes make it possible to optimize the actinide burnup with the constraints of several economic, thermodynamic, and neutronic limitations. The code ORIGEN[2] may be used to determine the actinide burnup with time and the hazard reduction achieved by a specific type of reactor. However, ORIGEN requires as input the neutron flux and spectrum in the actinide region of the reactor to do these calculations.

There are several design codes available which may be used to provide this information. To date this project has worked with MCC (Multigroup Constant Code), THERMOS, ANISN, and MACH-1. For the initial scoping calculations it was found that MACH-1[3] was by far the most useful. While the other codes provided higher accuracy, MACH-1 provided sufficient accuracy for the initial design decisions and was much easier to employ. Because MACH-1 was only a 26-group diffusion code its computer storage requirements were much smaller than with the transport codes.

MACH-1 was utilized for performing neutronic calculations for the following reactor types: spherial core-sodium cooled, cylindrical core-sodium cooled, and cylindrical core-helium cooled. Results of these calculations are presented in Table VI-1. These results were obtained by using MACH-1 to perform core region dimension searches to find the critical core radius ($k = 1$) while holding the thickness of the other regions in the reactor constant. The critical core radii for the three reactor types considered were found to be 68.7 cm., 57.6 cm., and 98.9 cm. respectively. The U-233 critical masses corresponding to these critical radii were found to be 636 kg., 892 kg., and 3600 kg., respectively.

An Actinide Transmuter Reactor can be visualized as a six-region reactor. These regions were of the same general type for each of the three reactors considered. Region 1 was the core region (UF_6), region 2 was the core liner region (Hastelloy-N), region 3 was the actinide region, region 4 was a reflector and coolant region, region 5 was a graphite region, and region 6 was an iron reflector region. Compositions of each region for each reactor type are given in Table VI-2.

The core region contained the UF_6 gaseous fuel. U^{233} was employed to minimize actinide formation in the operation of the reactor itself. Previous work[4] has shown that 540°C. and 100 bar are suitable conditions for such a reactor from thermodynamic and pressure considerations, so these conditions were assumed for the UF_6 gas. This corresponded to a density of 0.69 gm/cm^3 and a uranium aton density of 1.21×10^{21} atoms/cm^3.

Because no actinide compound is gaseous at reasonable temperatures, the actinides in region were assumed to be in the form of oxide rods with properties similar to UO_2 fuel rods. Since a high neutron flux was required to cause a significant fissioning of the actinides, heat generation was a serious concern. Therefore, this region also included a coolant (sodium or helium).

Region 3 initially contains an actinide load of 630 kg. This corresponds to approximately the waste from ten pressurized water reactors per year. It is assumed in the overall reactor design that this amount of actinide material will be loaded each year into the GCATR. As more and more actinides are loaded, the graphite in region 5 will be removed to accommodate the increased actinide load. The actinides will gradually replace the graphite in the reactor.

A major advantage of the Gas Core Transmuter was demonstrated in these calculations, since fluxes several orders of magnitude above those in conventional reactors were achieved. If the flux is to be high and still have a limited power output the critical mass should be as small as possible. However, if the maximum amount of actinides are to be exposed to a high flux, the core should be large. This dictates as low a fuel density as possible. Hence, a Gas Core Reactor is much more suited to this problem

than is a solid fueled reactor. In addition, the Gas Core Reactor has a fast spectrum which contributes significantly toward increased actinide burnup.

TABLE VI-1

MACH-1 Reactor Parameters

REACTOR TYPE	ACTINIDE LOAD (kg)	AVG. FLUX IN ACTINIDES (n/cm^2-sec)	AVG. FLUX IN CORE ($n_1 cm^2$-sec)	ACTINIDES FISSIONED/YR (kg)	CRITICAL CORE RADIUS (cm)	CRITICAL MASS (kg)
Spherical Core-Sodium Cooled (3800 MW_{th})	630	1.8×10^{16}	2.7×10^{16}	136	68.7	636
Cylindrical Core-Sodium Cooled (3800 MW_{th})	630	1.6×10^{16}	1.9×10^{16}	76	57.6	892
Cylindrical Core-Helium Cooled (2120 MW_{th})	630	8.1×10^{14}	3.2×10^{15}	9	98.9	3600

TABLE VI-2

SODIUM COOLED SPHERICAL REACTOR

REGION I - OUTER RADIUS = 68.7 cm.

U^{233} - 1.21×10^{-3} atoms/barn-cm. F^{19} - 7.26×10^{-3}

REGION II - OUTER RADIUS = 71.2 cm.

Cr^{52} - 7.19×10^{-3} Fe^{56} - 4.78×10^{-3} Ni^{59} - 6.887×10^{-2}

Mo^{96} - 6.68×10^{-3} C^{12} - 3.6×10^{-4}

REGION III - OUTER RADIUS = 81.8 cm.

O^{16} - 4.505×10^{-3} Am^{243} - 0.854×10^{-4} Am^{241} 0.725×10^{-4}

Cu^{244} - 2.995×10^{-5} Np^{237} - 0.910×10^{-3} U^{234} - 1.58×10^{-6}

U^{235} - 1.89×10^{-6} U^{238} - 1.135×10^{-3} Pu^{239} - 0.63×10^{-5}

Pu^{240} - 2.7×10^{-6} Pu^{241} - 1.36×10^{-6} Pu^{242} - 4.51×10^{-7}

Na^{23} - 1.72×10^{-2} Fe^{56} - 4.72×10^{-3} Cr^{52} - 1.35×10^{-3}

Ni^{59} - 0.66×10^{-3}

REGION IV - OUTER RADIUS = 91.8 cm.

Na^{23} - 2.205×10^{-2}

REGION V - OUTER RADIUS = 1.06.8 cm.

C^{12} - 9.03×10^{-2}

REGION VI - OUTER RADIUS = 206.8 cm.

Fe^{56} - 8.49×10^{-2}

TABLE VI-2 (cont'd)

SODIUM COOLED CYLINDRICAL REACTOR

REGION I - OUTER RADIUS = 57.6 cm.

U^{233} - 1.21×10^{-3} F^{19} - 7.26×10^{-3}

REGION II - OUTER RADIUS = 58.87 cm.

Cr^{52} - 7.19×10^{-3} Fe^{56} - 4.78×10^{-3} Ni^{59} - 6.887×10^{-2}

Mo^{96} - 6.68×10^{-3} C^{12} - 3.6×10^{-4}

REGION III - OUTER RADIUS = 65.54 cm.

O^{16} - 7.625×10^{-3} Am^{241} - 1.227×10^{-4} Am^{243} - 1.446×10^{-4}

Cu^{244} - 5.08×10^{-5} Np^{237} - 1.54×10^{-3} U^{234} - 2.675×10^{-6}

U^{235} - 1.6×10^{-5} U^{238} - 1.922×10^{-3} Pu^{239} - 1.067×10^{-5}

Pu^{240} - 4.572×10^{-6} Pu^{241} - 2.032×10^{-6} Pu^{242} - 7.64×10^{-7}

Na^{23} - 1.53×10^{-2} Fe^{56} - 5.909×10^{-3} Cr^{52} - 1.689×10^{-3}

Ni^{59} - 8.26×10^{-4}

REGION IV - OUTER RADIUS = 66.54 cm.

Na^{23} - 2.205×10^{-2}

REGION V - OUTER RADIUS = 81.54 cm.

C^{12} - 9.03×10^{-2}

REGION VI - OUTER RADIUS = 181.54 cm.

Fe^{56} - 6.79×10^{-2} Na^{23} - 4.41×10^{-3}

TABLE VI-2 (cont'd)

HELIUM COOLED CYLINDRICAL REACTOR

REGION I - OUTER RADIUS = 98.9 cm.

U^{233} - 1.21×10^{-3} F^{19} - 7.26×10^{-3}

REGION II - OUTER RADIUS = 101.44 cm.

Cr^{52} - 7.19×10^{-3} Fe^{56} - 4.78×10^{-3} Ni^{59} - 6.887×10^{-2}

Mo^{96} - 6.68×10^{-3} C^{12} - 3.6×10^{-4}

REGION III - OUTER RADIUS = 106.34 cm.

O^{16} - 5.852×10^{-3} Am^{241} - 0.942×10^{-4} Am^{243} - 1.11×10^{-4}

Cu^{244} - 3.9×10^{-5} Np^{237} - 1.182×10^{-3} U^{234} - 2.053×10^{-6}

U^{235} - 1.228×10^{-5} U^{238} - 1.475×10^{-3} Pu^{239} - 0.8185×10^{-5}

Pu^{240} - 3.509×10^{-6} Pu^{241} - 1.767×10^{-6} Pu^{242} - 5.86×10^{-7}

He^{4} - 1.817×10^{-5} Fe^{56} - 4.535×10^{-3} Cr^{52} - 1.296×10^{-3}

Ni^{59} - 0.634×10^{-3}

REGION IV - OUTER RADIUS = 107.34 cm.

He^{4} - 2.35×10^{-5}

REGION V - OUTER RADIUS = 122.34 cm.

C^{12} - 9.03×10^{-2}

REGION VI - OUTER RADIUS = 222.34 cm.

Fe^{59} - 6.79×10^{-2} He^{4} - 4.7×10^{-6}

References for Chapter VI

1. Bloemke, J. O., "Technical Alternatives Document," Oak Ridge National Laboratory, Oak Ridge, Tennessee (1976).

2. Bell, M. J., ORIGEN--The ORNL Isotope Generation and Depletion Code, Oak Ridge National Laboratory, Oak Ridge, Tennessee (1973).

3. Menely, D. A., et al, "MACH-1, A One-Dimensional Diffusion Theory Package," ANL-7223 (1966).

4. Clement, J. D., and Rust, J. H., "Analysis of UF_6 Breeder Reactor Power Plants," Final Report, NASA, NSG-1168, Georgia Institute of Technology (1976).

VII. OVERALL SYSTEM DESIGN

The GCATR will be designed to transmute by fission the transuranium actinides from ten light water reactors (LWR's). Figure VII-1 illustrates the fuel cycle for the GCATR. As discussed in Chapter IV., the actinide burnup capability of the GCATR is far in excess of that capable by either LWR's or LMFBR's.

Figure VII-2 and VII-3 illustrate elevation and plan views of a typical GCATR. UF_6 at 100 bar pressure enters the reactor at 482°C and is heated by fissioning to 593°C. The core is a right cylinder with approximate dimensions of a two-meter height and a one-meter diameter. A Hastelloy-N or Monel 404 liner of 1.27 cm thickness will be used to isolate the UF_6 from the rest of the reactor.

Actinide fuel rods, discussed in Chapter V., will be arranged in fuel assemblies for placement along the length of the core outside the liner. These fuel assemblies will require a coolant which can be sodium, helium, or high pressure water. Figure VII-2 indicates sodium is the coolant.

The actinide fuel rod coolant will be at a pressure comparable to that of UF_6 so as to reduce the required thickness of the core liner wall. The reactor will need to be enclosed by a thick-walled pressure vessel which could be made of carbon steel with a stainless steel liner.

Because of its high burnup requirements, the GCATR will generate a considerable amount of thermal power which must be converted into electricity in order to economically justify the concept. Figure VII-4 illustrates the power plant schematic diagram.

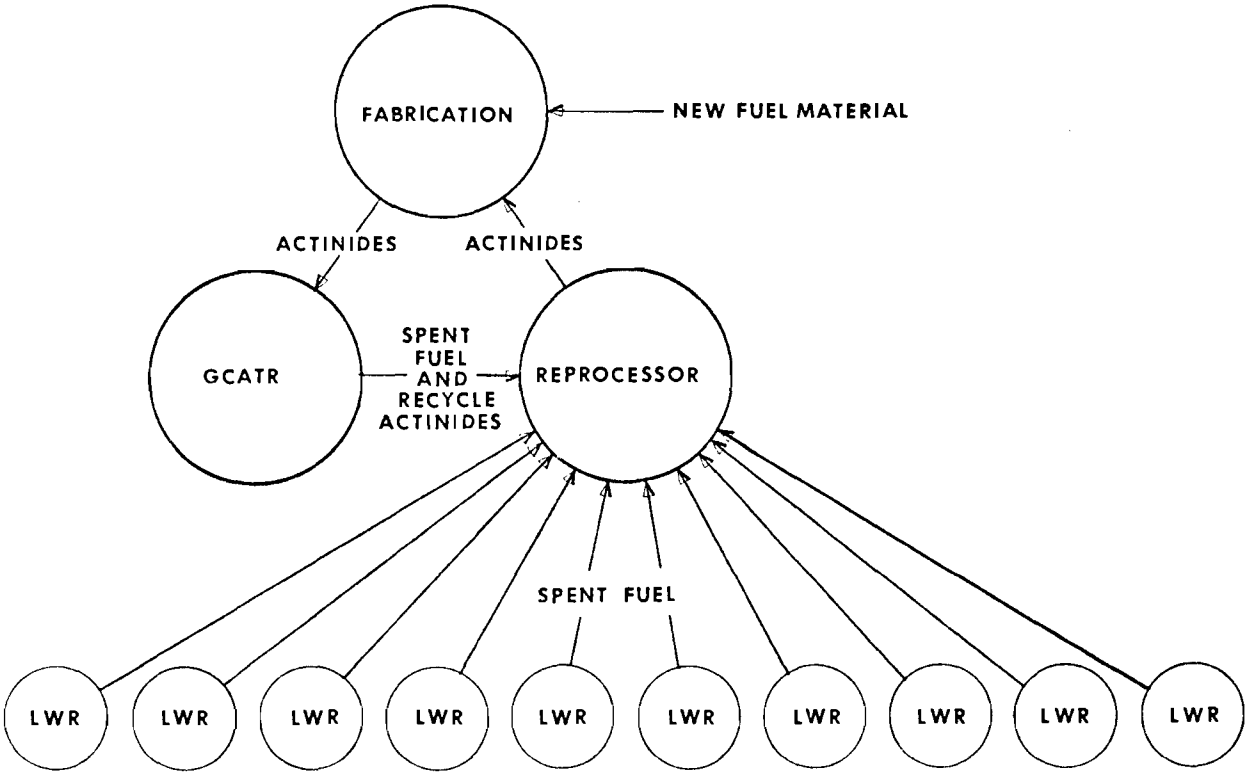

Fig. VII-1 Proposed Fuel Cycle for Gas Core Actinide Transmutation Reactor

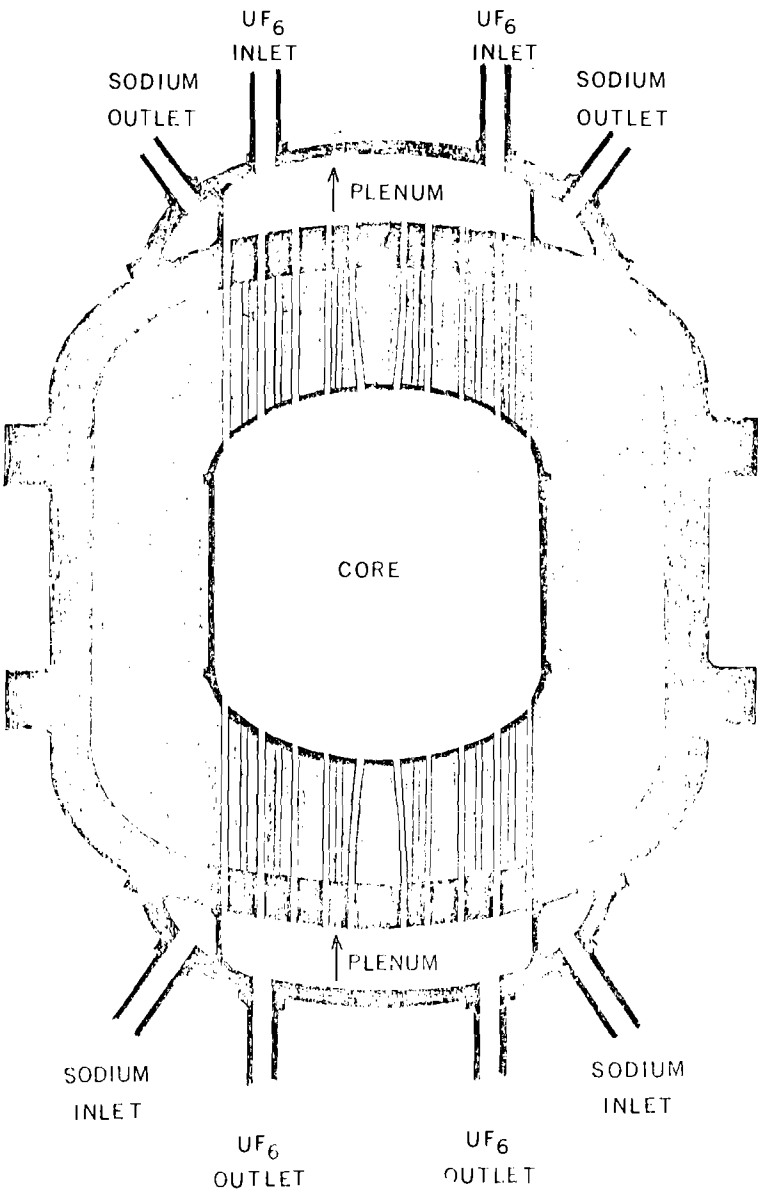

Fig. VII-2 Elevation View of Gas Core Actinide Transmutation Reactor

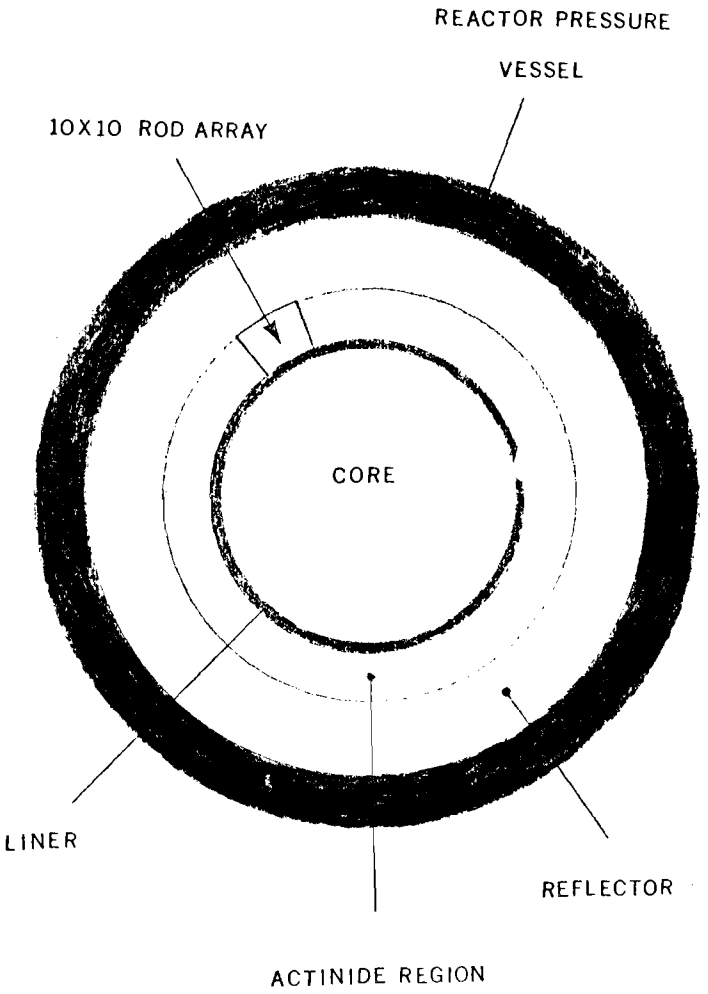

Fig. VII-3 Plan View of Gas Core Actinide Transmutation Reactor

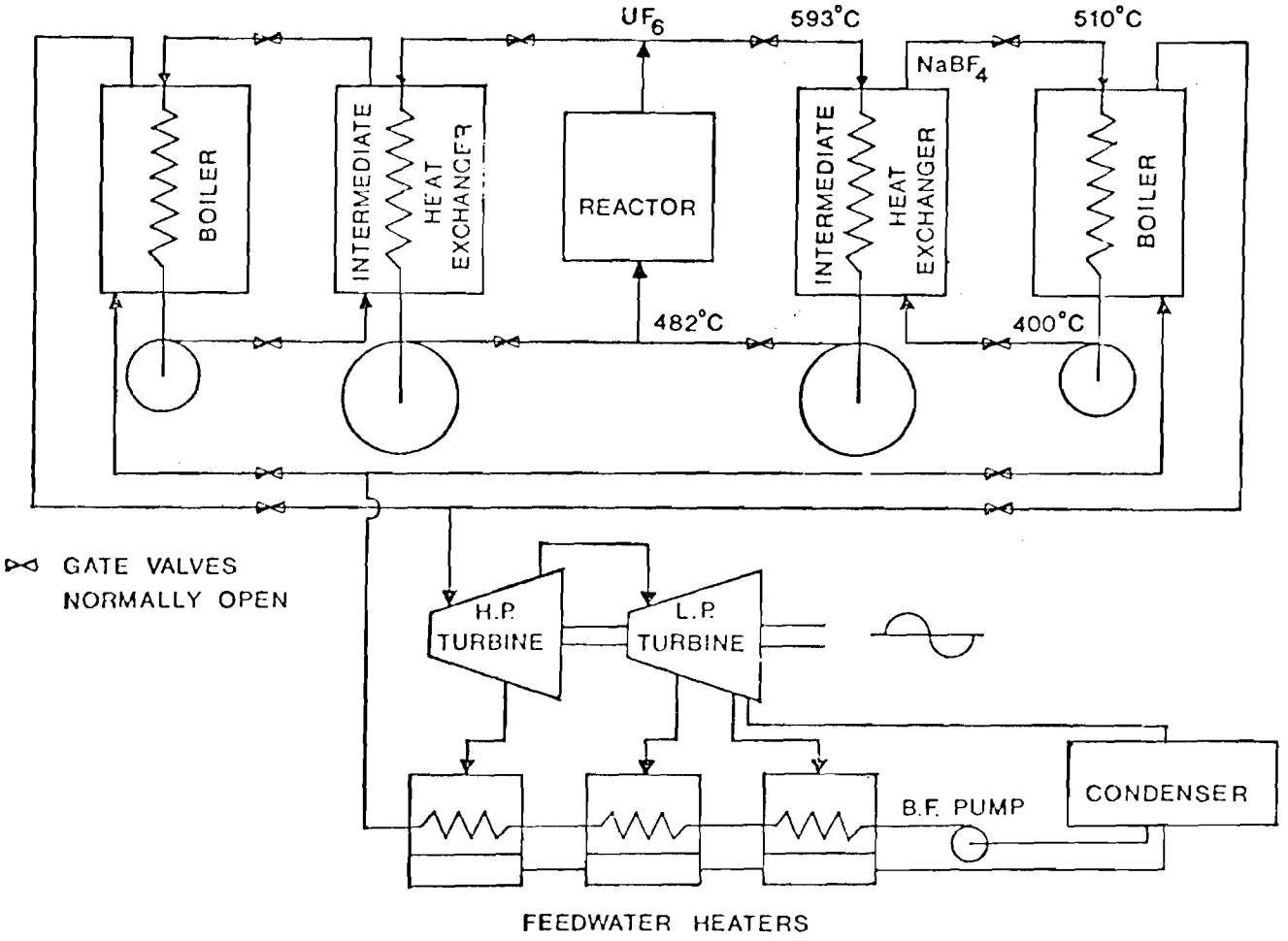

Fig. VII-4 Gas Core Actinide Transmutation Reactor Plant Schematic

Because it was considered undesirable for UF_6 to have the possibility of interacting with water due to failure of a boiler tube, the UF_6 exchanges heat with a molten salt ($NaBF_4$) in an intermediate heat exchanger. $NaBF_4$ was developed as an intermediate coolant for the molten salt breeder reactor and would be inert with UF_6. Another desirable feature of $NaBF_4$ is that the boron present in the salt would eliminate criticality problems with UF_6 in the heat exchanger.

Not shown on Figure VII-4 are flow paths for the coolant used to cool the actinide fuel rods. This coolant, which will be either sodium, helium, or water, will remove a considerable amount of reactor heat. Preliminary calculations with the MACH-I diffusion code indicates that the power generated in the actinide fuel rods ranges from 20-36 percent of the plant output.

Multiple intermediate heat exchangers are employed on the plant so as to keep these heat exchangers compact and also improve upon the reliability and safety by redundancy of equipment. The heat load of these heat exchangers will be of the order of 500 Mw so the plant shown in Figure VII-4 corresponds to 1000 Mw thermal power plant. Plants with higher power generation will have more intermediate heat exchangers.

The $NaBF_4$ enters the intermediate heat exchanger at 400°C and exits at 510°C. It then enters a boiler where it exchanges heat to produce superheated steam at 100 bar pressure and 480°C. The steam is expanded through high and low pressure turbines to a pressure of 0.07 bar. The efficiency of the high pressure turbine is assumed to be 85 percent and that of the low pressure turbine 80 percent. Steam is extracted at optimal temperatures from three locations in the turbines for use in feedwater heaters. The overall efficiency of the plant is 36 percent.

VIII. UF_6 FUEL REPROCESSING

Since the GCATR requires high fluxes and long term burn-up, the gaseous fuel must be reprocessed continuously, i.e. fission products removed. In the literature UF_6 reprocessing is not found as a unique independent process, but as a part of a complex fuel recycling process using uranium oxides or molten salts as reactor fuels. UF_6 reprocessing schemes thus differ from each other, depending on the type of fuel and chemical process used before it is converted to UF_6.

Several nuclear fuel reprocessing schemes have been investigated for this project. The Aquafluor process,[1] cold trap method,[2] and reductive solvent extraction method,[3,4] are some of those worth mentioning here.

The Aquafluor process[1] is designed to reprocess UO_2 fuels utilizing aqueous and fluoride-volatility techniques. The process employs a single-cycle solvent extraction step to separate uranium, plutonium, and neptunium from the bulk of the fission products. The actinides are stripped from the solvent, and plutonium and neptunium are recovered by anion exchange techniques. The uranium effluent stream from the ion-exchange unit is prepared for uranium recovery by concentration of the solution in a reboiler and calcination of the concentrated uranyl nitrate hexahydrate (UNH) solution to UO_3. The UO_3 product from the calciner is mixed with aluminum oxide and then converted into UF_6 by reaction with fluorine.

The off-gas stream from the fluorinator contains, in addition to UF_6 and fluorine, volatile fluorides of fission-product elements such as niobium, ruthenium, technetium, and small quantities of volatile NpF_6 and

PuF_6. Partial decontamination from these elements is effected when the off-gas stream is passed through a bed of NaF pellets maintained at 400°C. Under these conditions some of the volatile impurities are absorbed on NaF, whereas UF_6 is essentially unabsorbed.

The gas stream from the solvent bed is cooled in a finned-tube heat exchanger and then filtered by a system of sintered metal filters to remove particulate material. Uranium hexafluoride is collected in a series of manifolded cold traps. The traps, which are individually heated, are operated in a cyclic manner: On-line operation at low pressure, during which UF_6 is desublimed from the gas stream, and off-line operation at high pressure, during which the solid UF_6 is melted and drained to a product cylinder.

Final decontamination of the UF_6 is effected by vaporizing the liquid UF_6 from the product cylinder through a 10 inch diameter MgF_2 sorption bed followed by a single-stage distillations step.

The cold trapping scheme is presently being used by Allied General Nuclear Services (AGNS).[5] Cold trapping normally operates at 56.4°C and atmospheric pressure. The typical cold trap shell is made from a pipe. The cylindrical geometry is easy to fabricate, insulate, and maintain criticality safe. Refrigerant tubes and resistance heaters (for removing product) are brazed onto the outside of the pipe. They are finned internally to increase the cooling area and decrease the diffusion path length.

A typical cold trap used in the fluoride volatility process at the Oak Ridge National Laboratory is shown in Fig. VIII-1.[6,7] The trap is made from an 8 2/3 ft. long deoxidized copper pipe. The gas inlet and outlet connections were 2 inch copper pipes; a 3/4 inch nozzle was provided for draining liquid uranium hexafluoride from the trap. The inside of the trap

was finned with 1/8 inch copper sheets assembled into square flow sections. Nickel wire-mesh filter cartridges are packed in the last two inches to collect the UF_6 dust. A Freon-11 coolant circulates through four 1 inch extra heavy copper pipes brazed the full length of the shell.

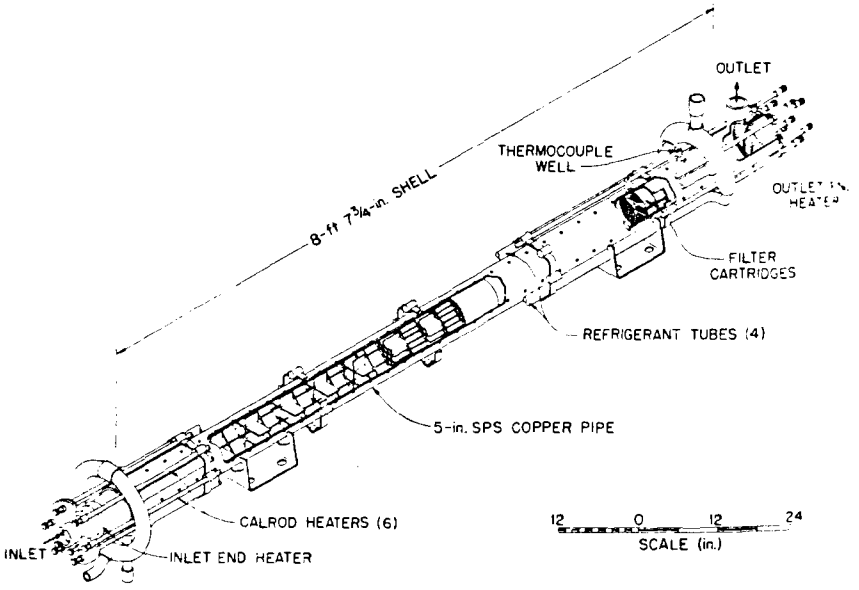

Fig. VIII-1 UF_6 Cold Trap[5]

The reductive solvent extraction method is used in the MSBR as a fuel reprocessing scheme.[3,4] The method is based on selective chemical reduction of various fluoride compounds into liquid bismuth solutions at 600°C utilizing multistage counter-current extraction. The method is based on the fact that a metal fluoride does not dissolve in a bismuth solution. However, when one reduces a metal fluoride into a metallic state, the metal can be dissolved into a bismuth solution. Since each metallic fluoride has a different reductive potential to lithium (where lithium is a reductant) when a solution containing mixtures of fluorides (fluorides of fuel and,

fission products) is counter-currently mixed with a bismuth-lithium solution, the amount of reduction differs from each other, and thus the solubility of each fluoride in the bismuth solution.

In the MSBR all the fission products are first fluorinated to form fluorides. Uranium hexafluoride is then converted into UF_4. After the partial removal of noble metal fission products, the molten salt containing UF_4 and fission product fluorides enters the solvent extraction stage (with bismuth-lithium solution) to separate protactinium from uranium, thorium, and rare earths. In later stages rare earths are separated from thorium by a similar reductive extraction.

The possibility of using the solvent extraction scheme for GCATR fuel reprocessing has been found to be inappropriate for the GCATR fuel system. For a reductive solvent extraction method to be applied successfully, the fluoride fuel and fission-product stream entering the extraction stage should be in liquid form. UF_6 is a gas in the temperature range of the extraction state ($600^{\circ}C$). UF_4 is a solid below $1036^{\circ}C$.[8] Many fluoride fission products are also solids at this temperature ($600^{\circ}C$). Thus, it is impossible to apply the solvent extraction scheme to the GCATR fuel reprocessing at the normal operating temperature range of the extraction stage. In addition, if one increases the temperature of the extraction stage far above the normal operating temperature, many chemical properties, such as fluoride solubility to bismuth solution and reductive potential by lithium, are likely to change in such a way that one can hardly predict any meaningful result.

The cold trap method seems to be feasible for the recovery of UF_6 in the GCATR fuel reprocessing. The amount of UF_6 cold trapped is limited by

the trap physical size and criticality conditions. To handle an appropriate amount of GCATR fuel reprocessing, multi-unit cold traps may be necessary.

Cold trapping is a well known scheme for the recovery of nuclear fuels in many different reprocessing processes. In most of the processes, many of the fission products and other compounds are eliminated in reprocessing earlier stages through chemical treatment. Thus when it reaches the stage of a cold trap the feed contains limited amounts of fission products and volatile elements. In most cases, passing gaseous UF_6 through a bed of absorber (NaF or MgF_2) eliminates the impurities.

The situation is slightly different for GCATR fuels. The gaseous UF_6 stream leaving the reactor contains fission products and fission product fluorides. Suppose one feeds this stream directly to the cold trap, many fission products and fission product fluorides are cold trapped with the UF_6. This will not only increase the number of cold traps, but also requires additional complex UF_6 recovery stages to separate UF_6 from the rest of the old trapped fluorides.

To get around these problems, one may consider removing most of the fission products from the reactor exit fuel stream before it is fed to the cold traps. This can be accomplished by fluorinating first the fuel stream to convert all the fission products into a fluoride form. The fluorides are cooled down to $200^{\circ}C$ to remove non-volatile fluorides as solid or liquid slurries. The extracted gas stream containing UF_6 and other volatile elements is fed into the cold trap for the recovery of UF_6. Solid UF_6 may then be melted and vaporized before it is sent to an impurity removal system. The impurity removal systems are usually a bed of NaF and MgF_2. The use of solid sorbents that selectively collect fluoride impurities from a

UF_6 gas stream while allowing the UF_6 to pass unaffected through the system was investigated at the Oak Ridge gas diffusion plant.[9] Both solvents (NaF and MgF_2) were satisfactory in reducing NbF_5 concentration in UF_6 gas streams from 460 ppm to less than 1 ppm. MgF_2 is a satisfactory sorbent for removing TiF_2 at 120°C from UF_6, if the TiF_4 concentration is less than 10 ppm.[10] Sodium fluoride at 344°C appears to be a good sorbent for RuF_5. MgF_2 is also a satisfactory solvent to remove SbF_5 (at 120°C) and NpF_6 from the UF_6 gas stream.

Proposed UF_6 Reprocessing System

A Schematic diagram for the proposed UF_6 reprocessing system is shown in Fig. VIII-2. The proposed system is basically the combination of a cold trap process and a fluoride volatility process. Partial removal of fission products from the reactor outlet stream has been devised so that the feed stream to the trap contains fewer fission products than the original reactor outlet stream.

A portion of the GCATR exit fuel stream is fluorinated by inserting F_2 into the fluorinator. For the purpose of analysis it is assumed that all the fission products are in fluoride form through this stage. However, it is important to realize that the assumptions are not correct. Even though fluorine is quite reactive with most materials, the reaction in many instances takes certain times. Some of the fission products are also coated with impurities so that physical contact with fluorine is not allowed for a certain period. Thus in practical situations it is not possible for certain fission products to form fluoride. In fact, experience with the MSRE has shown that the noble metal fission products (e.g. Mo, Ru, Tc, Rh, Nb, and Pd) are not present in the molten salt as fluorides.[3,10]

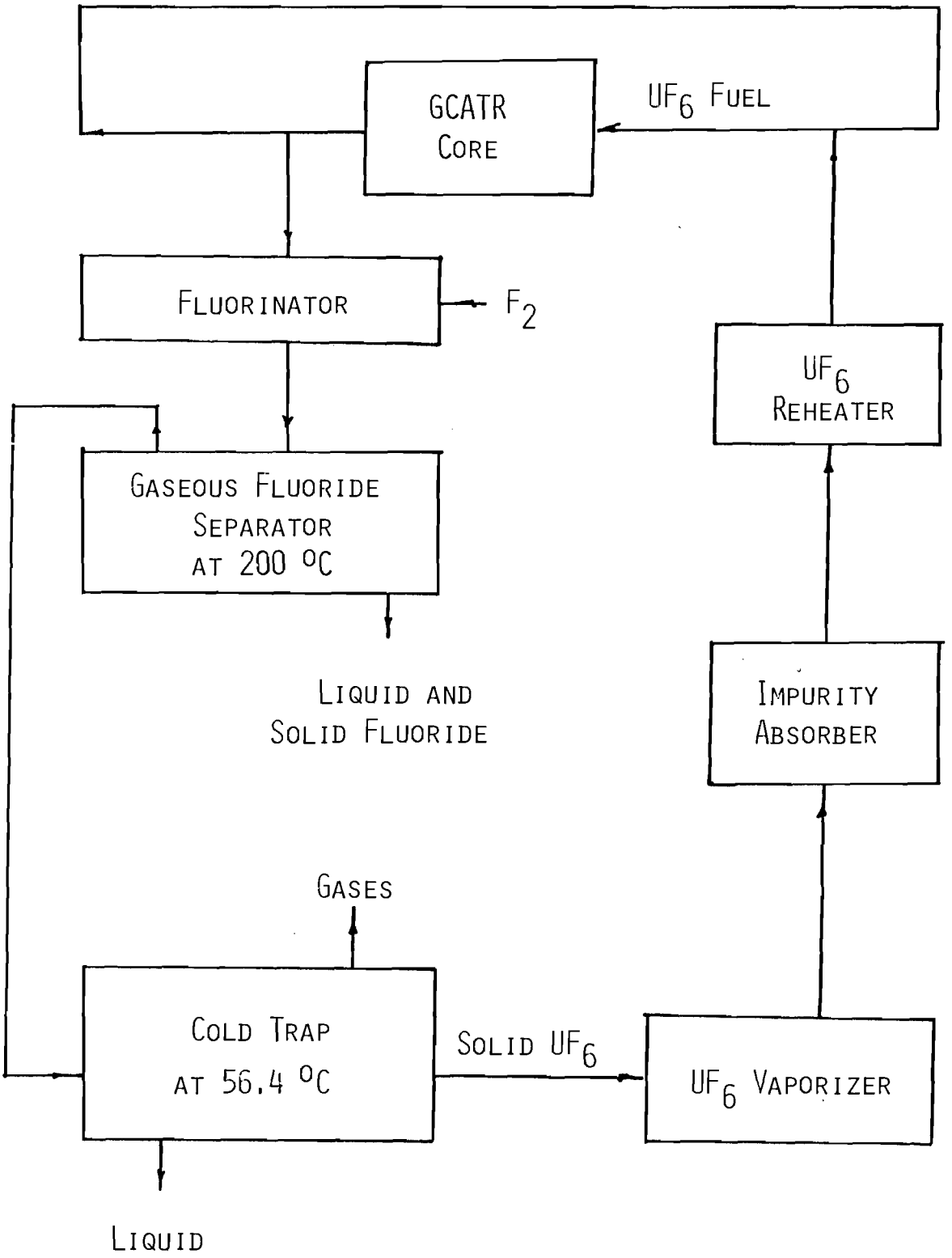

Fig. VIII-2 UF_6 Fuel Reprocessing

After fluorination the fuel and fission-product fluorides are cooled down to 200°C. In this stage, many fluorides listed in Table VIII-1 are solidified or exist as liquid slurries. The exit gas stream from this stage (which contains UF_6, gaseous fission products, and volatile fluorides) is fed into a cold trap. The cold trap operates around 56.4°C. Through this trap UF_6 is recovered (as solid) from liquid wastes (Table VIII-2) and volatile gases (Table VIII-3).

The solid UF_6 is melted and vaporized, and fed into an impurity removal system. The impurity removal system can be a bed of NaF or MgF_2 pellets or a distillation column which selectively absorbs volatile impurities from the UF_6 stream. The purified UF_6 is reheated to an appropriate temperature and sent to the GCATR.

Physical properties of certain fluorides which are not easily available have been estimated (M.P. and B.P. enclosed in parentheses in Table VIII-1 through Table VIII-3 were estimated from ANL-5750).[11] Therefore, the volatility analysis is not really accurate, even though the basic principle is sound.

Fission products, such as Mo, Ru, Tc, Rh, Nb, and Pd, may not form fluorides, but exist as solid particles or plate out inside the reactor.[12] Further study is necessary to make sure that these elements do not create serious complications.

TABLE VIII-1

REMOVABLE SOLID OR LIQUID FLOURIDES AT 200°C

	M.P. (°C)	B.P. (°C)
PdF_2	(952)	(1727)
RhF_2	(937)	(1727)
GeF_2	(877)	(1552)
RbF	775	1410
CsF	682	1251
AgF	435	1147
LaF_3	1527	2327
CeF_3	1460	2300
SrF_2	1450	2489
NdF_3	1410	2300
PmF_3	1400	2300
GdF_3	1400	2300
EuF_3	1390	2280
YF_3	1387	2027
PrF_3	1370	2327
EuF_2	1380	2400
SmF_3	1306	2323
BaF_2	1280	2137
RhF_3	1187	1427
TbF_3	1172	2280
CdF_2	1100	1758
RuF_3	1027	1402
ZrF_4		(903)
RuF_4	(552)	(777)
RhF_4	(507)	(752)
MoF_4	(557)	(613)
SbF_4	(292)	(319)
TeF_4	130	375
RuF_5	101	250
MoF_5	(77)	(227)

TABLE VIII-2

Removable Liquid Flourides at 56.4°C

	M.P.°C	B.P.°C
SbF_5	7	149.5
BrF_3	8.8	135
SeF_4	-13.8	106
IF_5	9.6	98
AsF_3	-8.5	63

TABLE VIII-3

REMOVABLE GASES AT 56.4°C

	M.P. °C	B.P. °C
Kr	-156.6	-152.3
Xe	-111.9	-107.1
AsF_5	-80	-53
SeF_6	-39	-34.5
GeF_4	-37	
BrF	-33	-20
IF_7	4.5	
MoF_6	17.5	35
TeF_6	-36	36
BrF_5	-61.3	40.5

References for Chapter VIII

1. Borghusen, J. J., "Volatility Processes," Reactor and Fuel Processing Technology, 2, No. 1, 54-57 (Winter 1967-1968).

2. Long, Justin. T., "Engineering for Nuclear Fuel Reprocessing," Gordon and Breach Science Publishers, New York (1967).

3. Whatley, M. E., McNeese, L. E., Carter, W. L., Ferris, L. M., and E. L. Nicholson, "Engineering Development of the MSBR Fuel Recycle," Nuclear Applications and Technology, 8, 170-178 (February 1970).

4. McNeese, L. W., "MSR Program Semiannual Progress Report, February 28, 1969," USAEC Report ORNL-4396 Oak Ridge National Laboratory, 273 (1969).

5. Schneider, A., Georgia Institute of Technology, Personal Consultation (May 1976).

6. Milford, R. P., "Engineering Design of the Oak Ridge Fluoride Volatility Pilot Plant," Ind. Eng. Chem., 50, 187-191 (1959).

7. Bresee, J. C., and P. R. Larson, "Continuous Cold Trap for Fluoride Volatility Processing of Uranium," Ind. Eng. Chem., 49, 1349-1354 (1957).

8. Kirk, R. E., and D. E. Othmer, "Encyclopedia of Chemical Technology," 14, 447 (1955).

9. Stephenson, M. J., Merriman, J. R., and H. L. Kaufman, "Removal of Impurities from Uranium Hexafluoride by Selective Sorption Techniques," USAEC Report K-1713 (July 1967).

10. Grimes, W. R., "Molten Salt Reactor Chemistry," Nuclear. App. Tech., 8, 137 (1970).

11. Glamer, Alvin, "The Thermochemical Properties of the Oxides, Fluorides and Chlorides to 2500°K," ANL-5750 (1965).

12. Weast, R. C., "Hand Book of Chemistry and Physics, 57th Edition," B-1 (1976-1977).

IX. ACTINIDE PARTITIONING AND REPROCESSING

Because of the hazardous radionuclides present in high-level wastes from present day reactors, schemes are needed which provide waste management programs of one million years or longer.

One alternative to this would be to remove the long-lived actinides which require long term surveillance. If this could be achieved, the remaining fission products and wastes would require a waste management program on the order of 1000 years. The actinides would then be transmuted in a fission or other type reactor to reduce the long half-lives to short ones, and thus reduce the radioactive hazard. The main problem to be overcome is separation of actinides from the rest of the waste products.

With the assumption that this separation can be done, an investigation was made to determine the necessary separation factors. The study indicated that separations beyond certain limits may not yield enough to substantiate such separation factors. The separations of 99.99% for plutonium, 99.9% for uranium, americium and curium, and 99% for neptunium will reduce the hazard potential to about five percent of that for natural uranium.[1] After 99.9% removal of iodine, it will then be the long-lived remaining fission products which control the waste hazard. Higher removal factors for the actinides do not appear to be warranted unless long-lived fission products are also removed, especially Tc-99.

As means of recovering actinides from the spent waste, several schemes are available. Several schemes can be ruled out mainly due to expense and complexity. For example, centrifuge is too "dirty" because of associated alpha emitters from the actinides.[2] This would require tight contamination

control, and hence much shielding. Other processes require a gaseous form, but there are no gaseous forms of americium or curium.

Present feasibility studies indicate that separations based on solvent extraction, ion exchange, and scavenging precipitation have greatest possibilities. Solvent extraction by itself has not been shown to achieve desired results; however, multi-step solvent extraction processes have a greater probability of success.[3] If particular waste stream recycles are solved, processes based on cation exchange may be a viable method for partitioning the actinides. Another method with potential in waste partitioning may be precipitation.

Figure IX-1 illustrates the reprocessing scheme for fission products and actinides generated from Light Water Reactors. Spent fuel from LWRs containing fission products and actinides listed in Appendix C-1 is sent to storage for about 150 days. The wastes from storage, which is listed in Appendix C-2, is then sent to a reprocessing plant. This plant discharges Kr-85 and tritium to the air. Ninety nine percent of the uranium is removed from the waste and sent for enrichment and 98 percent of the plutonium is separated for further fuel fabrication.

The rest of the high-level waste goes to a high-level liquid waste storage for about 215 days. These high-level wastes are listed in Appendix C-3. After further storage these wastes (listed in Appendix -4) go to a fission product/actinide fractionation plant which is the primary subject of this chapter.

Fractionation Schemes

Studies to date indicate that the best methods for removing actinides

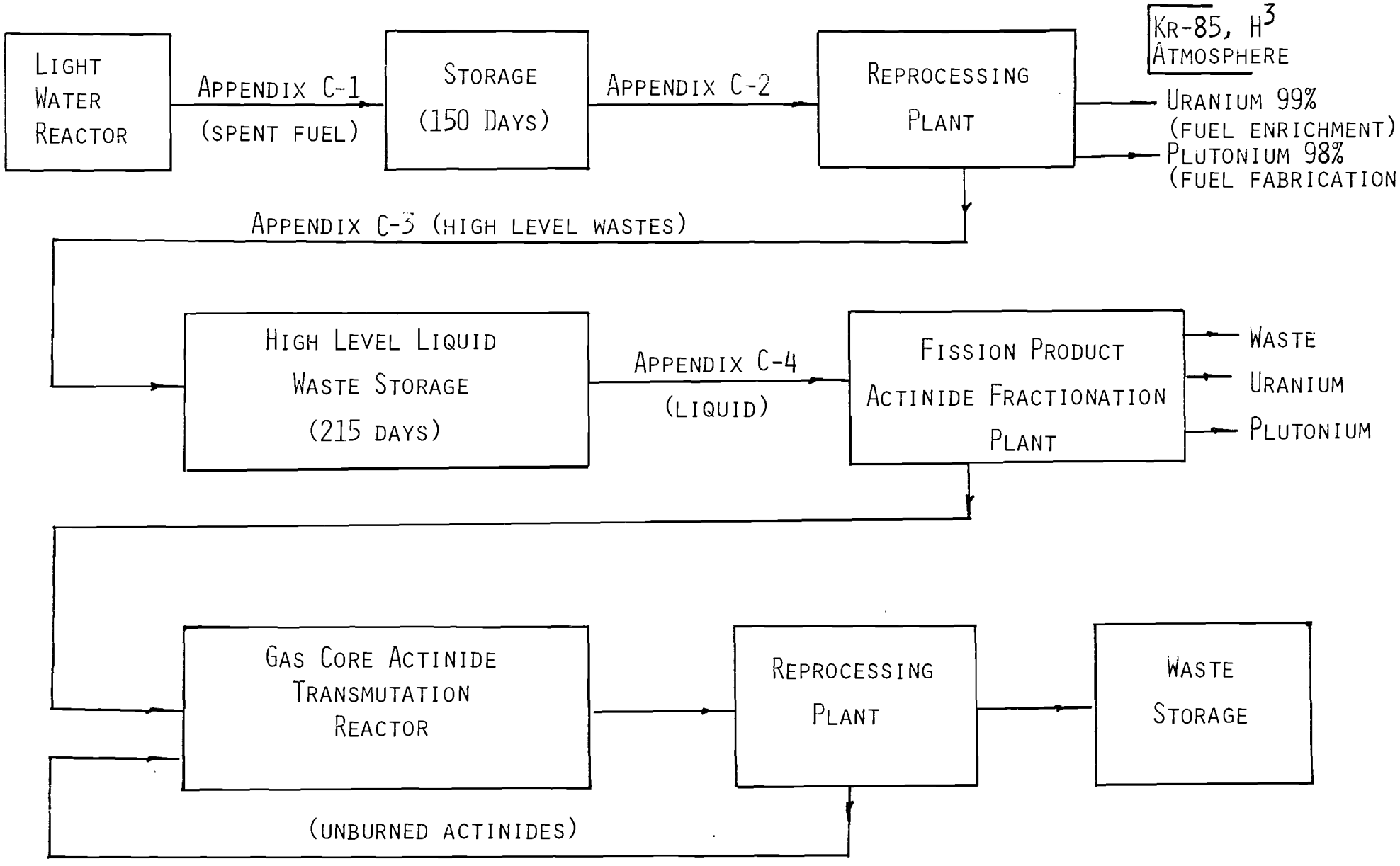

Fig. IX-1 Reprocessing Scheme

from wastes will be obtained by improving present state-of-the-art methods.[4] One of the present schemes is shown in the Fig. IX-2. In this scheme, neptunium, uranium, and plutonium, are recovered in the primary PUREX plant. Various exhaustive extractions or further PUREX processes are used to accomplish complete removal of the neptunium, plutonium, and uranium. Through the PUREX plant process, a recovery rate of 95-99% for neptunium and improvements in uranium and plutonium recover to 99.5% or better are expected.[5]

The interim waste storage is for the purpose of reducing the radiation hazard from the remaining high level wastes during subsequent processing. The radiation hazard will be high unless the fission product yttrium and rare earths, which are associated with americium and curium, are allowed to decay to less hazardous levels.[5] By considering the most important decay times, storage times of ten years would significantly reduce the hazards. Current NRC regulations require that wastes be solidified within five years. However, because of difficulties in working with a solid waste, it will be assumed that the americium and curium are removed from the liquid wastes after a five year period.

One disadvantage of interim waste storage is that the amount of plutonium in the waste grows by curium decay. Therefore, plutonium removal from the stored waste is necessary after several years of interim storage. The process showing most potential for recovering the plutonium is an all ion-exchange process.[6]

After removal of plutonium, the americium and curium are isolated from the rest of the waste. The problems associated with americium and curium removal are centered around finding a suitable chemical separation process

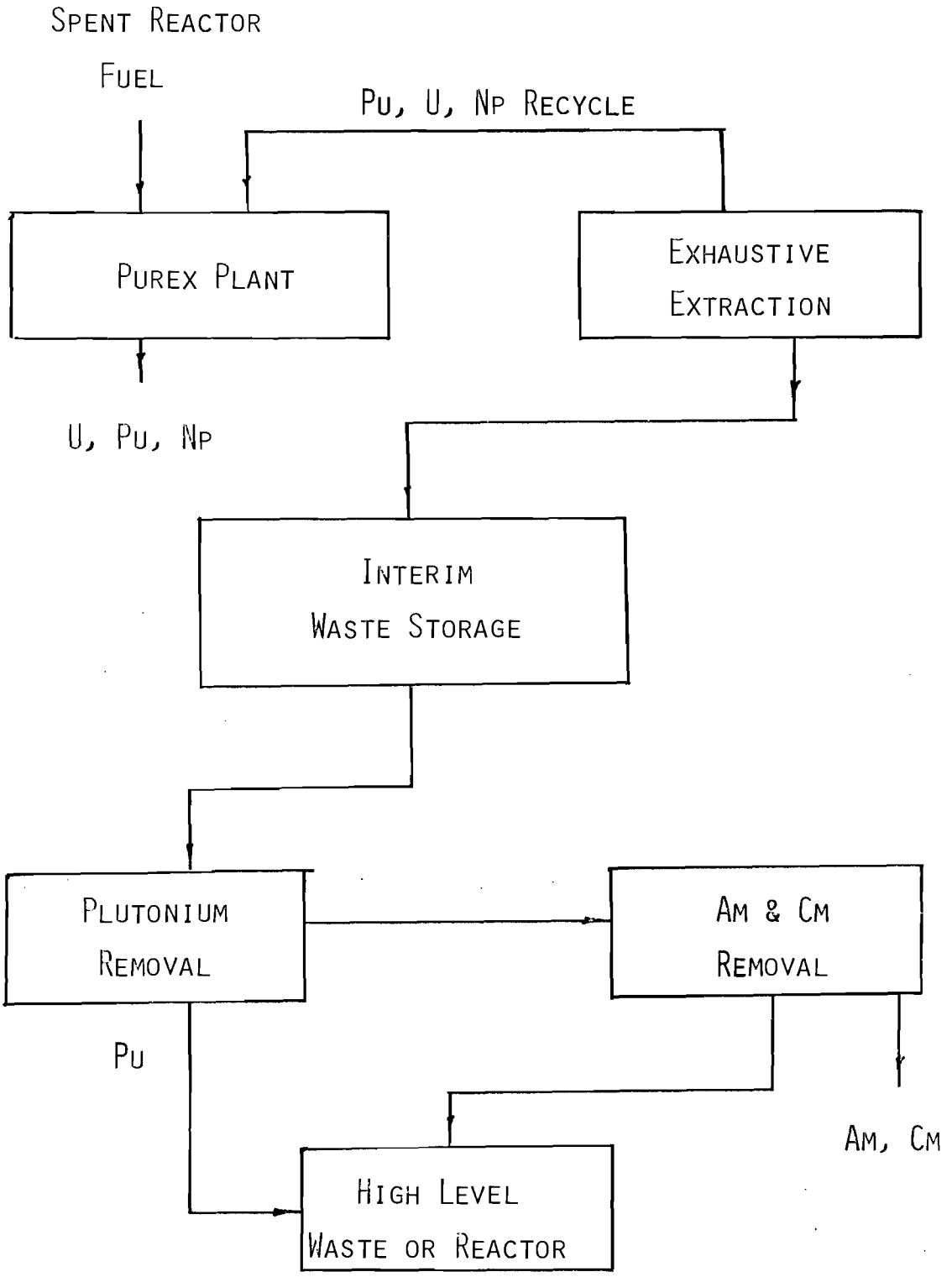

Fig. IX-2 Present Processing Sequence for the Removal of Actinides

for commercial high level wastes. Recovery of americium and currium has been done at Oak Ridge National Laboratory and Savannah River Laboratory on a multigram basis using a Tramex process.[5] This process has problems with corrosive solutions that require processing equipment constructed of special and expensive materials. Because of these reasons, the process is not recommended. However, there is some possibility that the Tramex processing equipment can be constructed so as to allow safe working of both corrosive solutions in the process and toxic radionuclides at little additional cost.

Other processes that have been developed and claim to give high americium and curium separation are Cation Exchange Chromatography (CEC) and Trivalent Actinide-Lanthanide Separation by Phosphorous Reagent Extraction from Aqueous Complexes (TALSPEAK).[5] Cation Exchange Chromatography was developed at the Savannah River Laboratory and successfully used to separate about twenty-five percent of the necessary amounts of americium, curium, and rare earths in one metric ton of Light Water Reactor fuel.[5] A. schematic flowsheet of CEC is shown in Fig. IX-3. The TALSPEAK process, shown in Fig. IX-4, has been developed only to the point of tracer-level laboratory studies at Karlsruhe for americium and curium removal.[5]

As means of separating Am and Cm from other wastes, the Tramex, CEC, and TALSPEAK processes require considerable developmental work and data gathering to determine their applicability to the commercial (high volume) extraction of actinides from high-level wastes.

Proposed Schemes

Present proposals for actinide partitioning are based on a sequence of

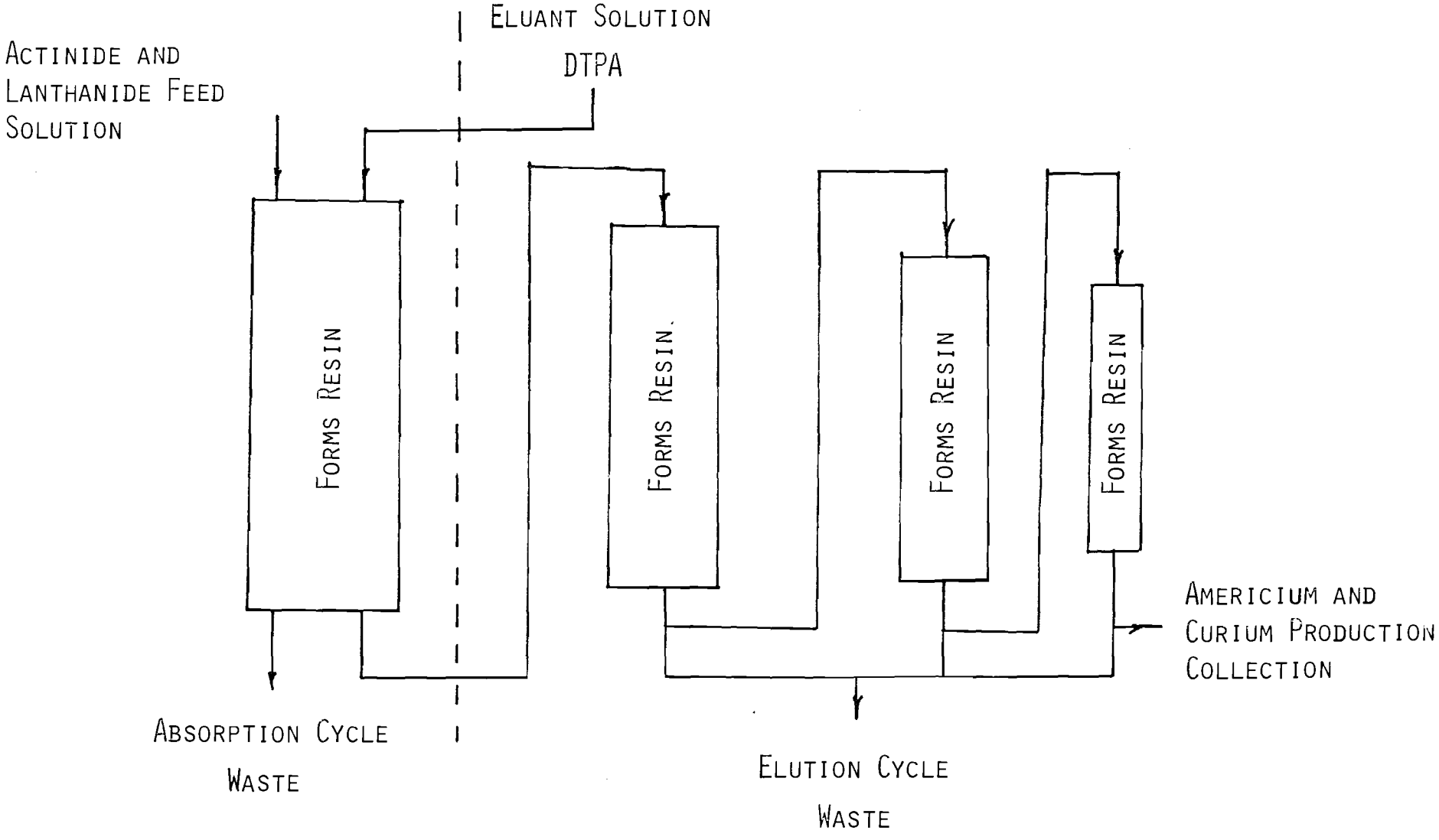

Fig. IX-3 Schematic Flowsheet of Cation Exchange Chromatographic Process for Recovery of Americium and Curium[5]

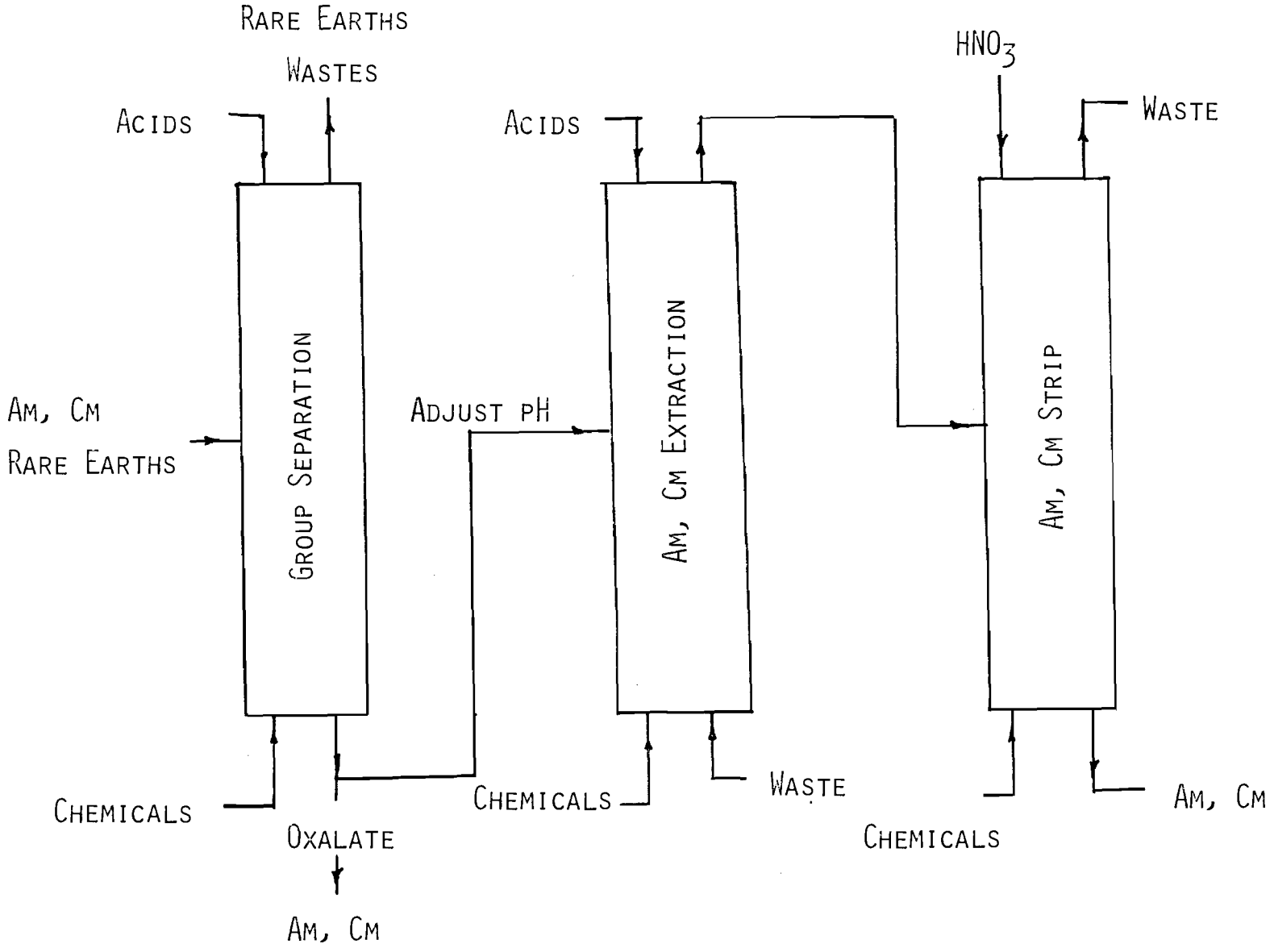

Fig. IX-4 Conceptual Flow Sheet for Recovery of Americium and Curium by a TALSPEAK

separation processes using solvent extraction, ion exchange, and precipitation. These techniques have not yet been developed.[4] A multistep solvent extraction process combined with other processes, such as cation exchange, may work well in the removal of uranium, neptunium, and plutonium, as well as separations of americium and curium from other wastes.

Tributylphosphate (TBP) may be used as the solvent in the solvent extraction method.[4,7] As demonstrated in the PUREX process, TBP achieved highly efficient recovery of uranium, plutonium, and neptunium.[1]

As a means of separating americium and curium from the rest of fission products and wastes, two steps of cation exchange is quite promising. The potential here appears to be 99.9 percent or better.[4] In the first step the lanthanides and actinides are absorbed on a cation exchange resin column and eluted with nitric acid. In the following step the lanthanides and actinides are separated by cation exchange chromatography. Problems to be solved with this process are in converting the spent ion exchange resin to acceptable levels for waste generated in the chromatographic separation.

Precipitation methods combined with ion exchange and/or solvent extraction may be another possible method for partitioning actinides. Even though solid waste handling is unavoidable, ways are now under study for obtaining crude concentrations of plutonium, americium, curium, and fission products. These actinides would then be separated from the lanthanides in further ion exchange or solvent extraction steps. Oak Ridge National Laboratory is studying the use of oxalate[10,6] precipitation together with ion exchange to isolate the lanthanides and actinides.[4,9] A removal factor of 0.95 is achieved by precipitation while the remaining is removed in the cation exchange column.[5] Tracer-level studies indicate removal

of 0.999 for americium and curium.[5] Almost complete removal has been demonstrated for americium and curium by use of multiple oxalate precipitation stages.[4] Further work in this area is still needed to determine the effect of the handling problems.

Technical feasibility, resultant benefits, and costs of partitioning actinides from high-level wastes are yet to be established. It must be decided if the net benefits will justify the use of partitioning. It must also be kept in mind that the separation schemes do not solve the long-term actinide problem. In order to justify this, the actinides must somehow be transmuted to shorter-lived radionuclides or disposed of from our environment. These and many more problems still need research and investigation before a feasible actinide-separation-transmutation process can be substantiated.

From research done to date, it is concluded that much research and development is still needed in the area of actinide partitioning. Work being performed at the Oak Ridge National Laboratory may show encouraging results by the end of 1978. Present state-of-the-art methods will not yield the results needed to establish a practical, economically feasible operating partitioning plant. It is believed that research in the area of combined methods of solvent extraction and ion exchange will yield the necessary separations factors.

References for Chapter IX

1. Claiborne, H. C., "Effect of Actinide Removal on the Long Term Hazard of High-Level Waste," ORNL-TM 4724 (January 1975).

2. Schneider, A., Georgia Institute of Technology, Personal Consultation (April 1976).

3. Bocola, W., Frittelli, L., Gera, F., Grossi, G., Moccia, A., and L. Tondinelli, "Considerations on Nuclear Transmutation for the Elimination of Actinides," IAEA-SM-207/86.

4. Blomeke, J. O., "Technical Alternatives Documents," ORNL, Prepublication Paper (1976).

5. Bond, W. D., and R. E. Leuze, "Feasibility Studies of the Partition of Commercial High-Level Wastes Generated in Spent Nuclear Fuel Processing: Annual Progress Report for FY-1974," ORNL-5012 (January 1975).

6. Bond, W. D., Claiborne, H. C., and R. E. Leuze, "Methods for Removal of Actinides from High-Level Wastes," Nuclear Technology, 24, 367 (1974).

7. LaRiviere, J. R., et al, "The Hanford Isotopes Production Plant Engineering Study," HW-77770, Hanford Atomic Products Operation (July 1963).

8. Rupp, A. F., "A Radioisotope-Oriented View of Nuclear Waste Management," ORNL-4776 (May 1972).

9. Ferguson, D. W., et al., "Chemical Technology Division Annual Progress Report for Period Ending March 31, 1975," ORNL-5050, 6-11, 30-31, (October 1975).

X. FUTURE WORK

TASK 1. GCATR Design Studies

This task is a major thrust of the proposed research program. Four subtasks are considered:

A) Design Studies of Fuel and Actinide Separation and Reprocessing System;

B) Optimization and Design Criteria Studies;

C) Design Studies of the Reactor Subsystem;

C) System Integration.

A) Design Studies of Fuel and Actinide Separation and Reprocessing System.

The spent fuels discharges from a LWR consists of (i) structural materials, (ii) unfissioned uranium, (iii) converted Pu, (iv) "other" actinides, and (v) fission products. The ratio of these components by weight is as follows:

structural	uranium	plutonium	fission products	"other" actinides
256	1023	9	36	1

The other actinides is the smallest component. Thus, a high extraction efficiency of actinides from the other materials is crucial to the feasibility of transmutation schemes. Currently, a research program is underway at the Oak Ridge National Laboratory to improve the extraction efficiency of the "other" actinides. Liaison with ORNL will be established to obtain information on the state-of-the-art of actinide separation. A preliminary design of UF_6 and actinide reprocessing systems will be prepared and system performance analyzed.

B) Optimization and Design Criteria Studies.

In particular, what is the time required for equilibrium to be reached in the GCATR recycling scheme and what is the equilibrium actinide inventory in the core.

C) Design Studies of the Reactor Subsystems.

A multidisciplinary approach will be carried out involving:

(1) Materials

(2) Nuclear Analysis

(3) Thermodynamics and Heat Transfer

(4) Mechanical Design.

In a previous work,[3] one- and two-dimensional survey calculations were carried out for a UF_6-fueled core surrounded by a molten salt blanket and a preliminary mechanical design developed. This work will be extended to include the insertion of fission products and actinides in various locations in the reactor. The effect of other reactor component changes such as using different reflector materials (carbon, beryllium, deuterium oxide) will also be evaluated. The best available cross section data will be used in the computations. A preliminary reactor design will be developed taking into account thermal and mechanical design considerations.

D) System Integration.

This subtask involves putting all the subcomponents together in a workable system taking into account criticality, shielding, and economic consideration.

TASK 2. Comparison of Actinide Production From Th^{232}-U^{233} Fuel Cycle and the U^{238}-Pu^{239} Cycle.

The flow sheet of a standard transmutation scheme is shown in Fig. X-1 The following schemes will be considered:

(1) Scheme A

- assumes 100% extraction of structural materials and fission products from spent LWR fuels and spent GCATR actinide fuels
- assumes 99.9% extraction of U and Pu from spent LWR fuels and spent GCATR actinides.

The results will be compared to those of Claiborne[1] who used a LWR, instead of a GCATR, to transmute the actinides produced by itself.

(2) Scheme B

- assumes 100% extraction of structural materials and fission products from spent LWR fuels and spent GCATR actinide fuels.
- assumes 100% extraction of U and Pu from spent LWR fuels.

The results obtained will be compared to those of Beaman, et al[2] who recycled the actinides through a LMFBR.

(3) Scheme C

- assumes 100% extraction of structural materials and fission products from spent LWR fuels and spent GCATR actinide fuels
- assumes 100% extraction of Pu from spent GCATR actinides.

The following questions will be considered:

(1) What is the hazard associated with the U and Pu storage for these schemes.

(2) What is the hazard associated with the wastes sent to waste storage.

(3) What is the hazard associated with the fuel reprocessing and fabrication.

(4) What is the hazard associated with the operation of the GCATR.

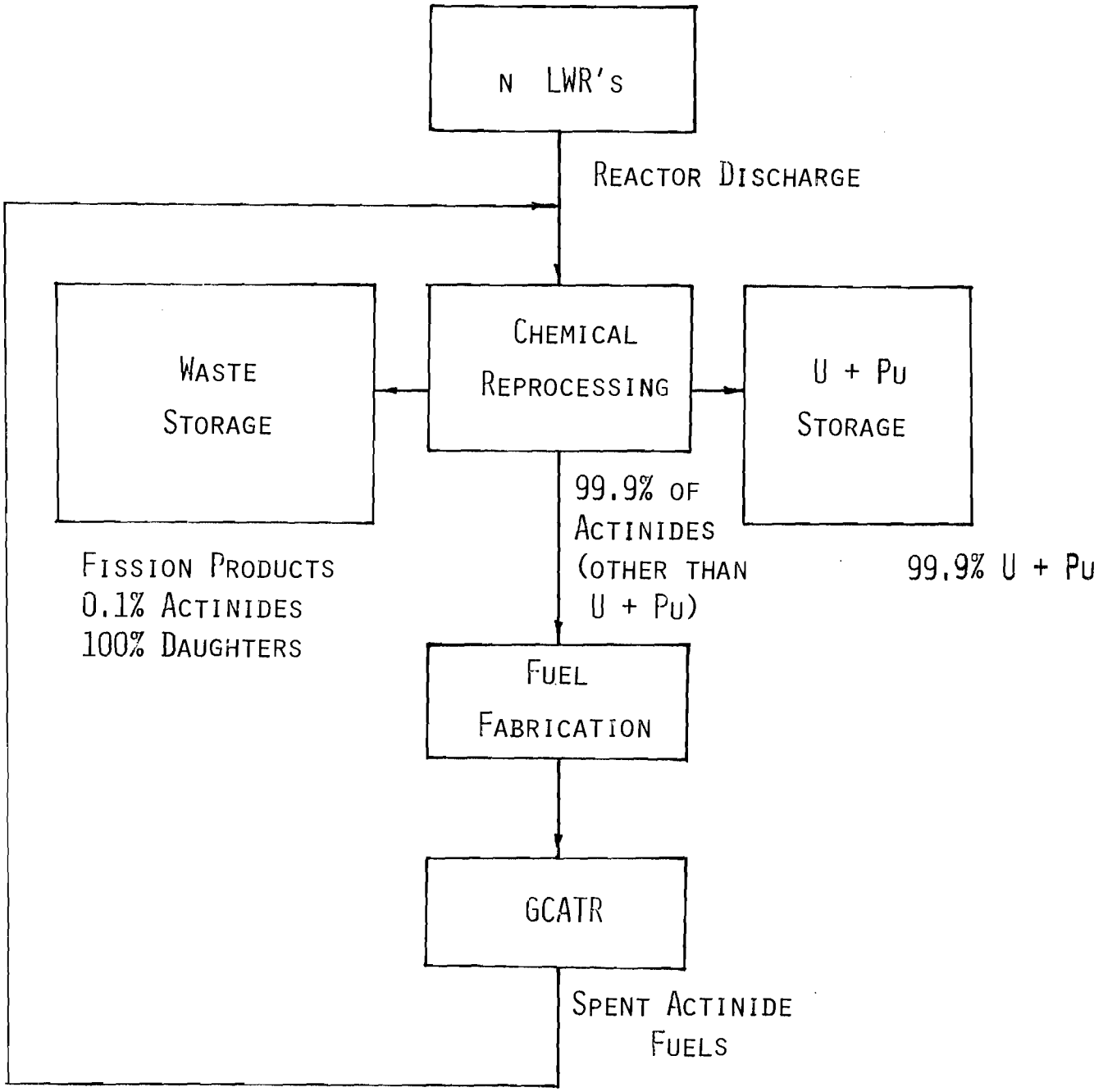

Fig. X-1 Flowsheet for Actinide Recycling

The actinides produced from the Th^{232} cycle consist mostly of Th, Pa, U, Np, and the actinides produced from the U^{238} cycle consist mostly of U, Np, Pu, and Am. The short term and long term hazards associated with the two cycles will be compared.

TASK 3. Gas Core and Gas Core Breeder Studies

In this task work previously carried out at the Georgia Institute of Technology (4-6) will be continued and extended. Specifically, the design of a 1000 MW(e) gas core breeder reactor system will be developed.

For lunar applications it may be more economical to breed using thorium on the moon as a fertile material rather than transport thorium or U^{238} from the earth. However, for low power application (~10MW(e)) transporting the fuels would be more economical than building a heavy and complex reprocessing plant in space.

To prevent the diversion of fissile materials from a nuclear reactor, gas core breeder reactors can be designed with a breeding ratio equal to unity. For such a system, the inventory of fissile material in the core is kept constant, and any diversion will cause the system to go subcritical. In solid fuel reactors, an excess amount of fissile material must be loaded at the beginning of life to accomodate fuel burnup and the production of fission products poisons during operation. Since for fluid fuel reactors fission product reprocessing is done continually, the composition of the core is the same at the beginning of life as at the end of life. This inherent simplicity of fluid fuel reactors allows protection against the diversion of fissile materials from the reactor core.

At the present, chemical reprocessing of Pu^{239} is under controversy. Some people have suggested abandoning spent LWR fuels as waste, i.e., the

throwaway fuel cycle. Others have suggested putting spent LWR fuels in a Heavy Water Reactor to extract more energy from the spent fuels before abandonment. By putting spent LWR fuels in the reflector region of gas core reactors, the high neutron fluxes will allow even higher burnups in spent LWR of HWR fuels. This will enable obtaining the maximum energy from a LWR fuel element.

References for Chapter X

1. Claiborne, H. C., "Neutron Induced Transmutation of High-Level Radioactive Waste," ORNL-TM-3964, (December 1972).

2. Beaman, S. L., and E. A. Aitken, "Feasibility Studies of Actinide Recycle in LMFBRs as a Waste Management Alternative."

3. Clement, J. D., and J. H. Rust, "Analysis of UF_6 Breeder Reactor Power Plants," Final Report, NASA Grant NSG-1168, Georgia Institute of Technology (1976).

4. Clement, J. D., Rust, J. H., and J. R. Williams, "Analysis of UF_6 Breeder Reactor Power Plants," Semi-annual Report, NASA Grant NSG-1168 (October, 1975).

5. Williams, J. R., Clement, J. D., and J. H. Rust, "The UF_6 Breeder: A Solution to the Problems of Nuclear Power," presented at the Inter-Society Energy Conversion Conference (August 11-15, 1975)..

6. Rust, J. H., Clement, J. D., and F. Hohl, "UF_6 Breeder Reactor Power Plants for Electric Power Generation," Proc. Third Symposium on Uranium Plasmas, Princeton University (June 10-12, 1976).

APPENDIX A

GEORGIA INSTITUTE OF TECHNOLOGY RESEARCH ON THE GAS CORE ACTINIDE TRANSMUTATION REACTOR (GCATR)

J. D. Clement, J. H. Rust, and A. Schneider
Georgia Institute of Technology
Atlanta, Georgia 30332

and

F. Hohl
National Aeronautics and Space Administration
Langley, Virginia 23665

Paper presented at the Third Symposium on Uranium Plasmas, Princeton University Conference, Princeton, New Jersey, June 10-12, 1976.

GEORGIA INSTITUTE OF TECHNOLOGY RESEARCH ON THE GAS CORE ACTINIDE TRANSMUTATION REACTOR (GCATR)*

J. D. Clement, J. H. Rust, and A. Schneider
Georgia Institute of Technology
Atlanta, Georgia 30332

and

F. Hohl
National Aeronautics and Space Administration
Langley, Virginia 23665

Abstract

The Gas Core Actinide Transmutation Reactor (GCATR) offers several advantages including (1) the gaseous state of the fuel may reduce problems of processing and recycling fuel and wastes, (2) high neutron fluxes are achievable, (3) the possibility of using a molten salt in the blanket may also simplify the reprocessing problem and permit breeding, (4) the spectrum can be varied from fast to thermal by increasing the moderation in the blanket so that the trade-off of critical mass versus actinide and fission product burnup can be studied for optimization, and (5) the U^{233}-Th cycle, which can be used, appears superior to the U^{235}-Pu cycle in regard to actinide burnup.

The program at Georgia Tech is a study of the feasibility, design, and optimization of the GCATR. The program is designed to take advantage of initial results and to continue work carried out by Georgia Tech on the Gas Core Breeder Reactor under NASA Grant-1168. In addition, the program will complement NASA's program of developing UF_6-fueled cavity reactors for power, nuclear pumped lasers, and other advanced technology applications.

The program comprises:

(1) General Studies -- Parametric survey calculations will be performed to examine the effect of reactor spectrum and flux level on the actinide transmutation for GCATR conditions. The sensitivity of the results to neutron cross sections will be assessed. Specifically, the parametric calculations of the actinide transmutation will include the mass, isotope composition, fission and capture rates, reactivity effects, and neutron activity of the recycled actinides.

(2) GCATR Design Studies -- This task is a major thrust of the proposed research program. Several subtasks are considered: optimization criteria studies of the blanket and fuel reprocessing, the actinide insertion and recirculation system, and the system integration.

The total cost of the GCATR in a nuclear waste management system will be evaluated and compared to the cost of alternate strategies presently being considered.

This paper presents a brief review of the background of the GCATR and ongoing research which has just been initiated at the Georgia Institute of Technology.

*Research sponsored by N.A.S.A.

I. Introduction

The high level radioactive wastes generated in the operation of nuclear power plants contain both fission products and actinide elements produced by the non-fission capture of fissile and fertile isotopes. The fission products, atoms of medium atomic weight formed by the fission of uranium or plutonium, consist mainly of short term (30 years or less half-life) isotopes, including Sr^{90} and Cs^{137}. Tc^{99} and I^{129} are long-lived fission products. The actinide components of radioactive wastes, including isotopes of Np, Am, Cm, and Pu and others are all very toxic and most have extremely long half-lives. The amount of long-lived radioactive material expected to be produced is substantial. Smith[1] has estimated that in 1977, 150 kg of Am^{243}, 150 kg of Am^{241}, and 15 kg of Cm^{244} will be produced. The actinides cause waste management difficulties at two stages in the fuel cycle. Some are carried over with the fission products during fuel reprocessing, but also some dilute plutonium wastes will appear from fuel manufacturing plants. Thus at the entrance to the waste facility are found a mixture of transuranic actinides combined with shorter-lived and temporarily more hazardous fission products.

The safe disposition of the radioactive wastes is one of the most pressing problems of the nuclear industry. Any viable plan must meet the three requirements of

(1) technical soundness
(2) reasonable economics
(3) public acceptance.

II. Background

The strategies which have been suggested for high-level nuclear waste management encompass

(1) terrestrial disposal (geologic, seabed, ice sheet)
(2) extraterrestrial disposal, and
(3) nuclear transmutation,

or some combination of these methods, such as terrestrial burial of the short-lived fission products and extraterrestrial disposal or nuclear induced transmutation of the long-lived actinides. Papers discussing all of these methods were presented at the Waste Management Symposium in December 1974.[2] The technical soundness of terrestrial disposal is a controversial topic, and also public acceptance is questionable. Extraterrestrial disposal is costly. Hence, there is increasing interest in

nuclear transmutation as a potential solution to the nuclear waste disposal problem. Figure 1 summarizes the nuclear waste management schemes which are under consideration.

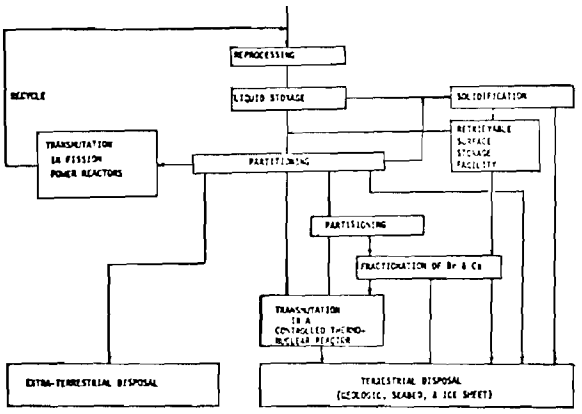

Fig. 1 Schematic representation of schemes for nuclear waste management

The first published suggestion for the use of neutron-induced transmutation of fission products was made in 1964 by Steinberg et al.,[3] who concerned themselves only with the transmutation of Kr^{85}, Sr^{90}, and Cs^{137}. Their calculations assumed that the krypton and cesium fission product wastes had been enriched to 90% in Kr^{85} and Cs^{137}. This was necessary due to the relatively small thermal neutron cross sections of these two nuclides and their small concentration with respect to their stable isotopes found in spent fuel. The Sr^{90} analysis was based on the presence of Sr^{90} and Sr^{89} which has a half-life of 53 days. If the strontium wastes are allowed to decay for one year before being returned to the reactor, then all the Sr^{89} portion will decay to Y^{89} (stable) which can be chemically separated from the Sr^{90}. However, even with these modifications to the waste isotopic composition, Steinberg et al. indicate that a thermal neutron flux of 10^{16} n/cm^2-sec is required before the halving time of Sr^{90} can be reduced from the normal half-life of 28.1 years to 1 year. A flux of 10^{17} n/cm^2-sec was indicated to be necessary before the halving time could be reduced from the natural half-life of 33 years to 1 year. The halving time describes the "total" time spent in a reactor for the inventory of a particular isotope to be reduced to half its value.

In another work, Steinberg and Gregory[4] considered the possibility of fission product burnup (specifically Cs^{137} and Sr^{90}) in a spallation reactor facility. In this scheme a nuclear power reactor is used to "drive" a high-energy proton accelerator with the resultant (p,xn) spallation reactions of the proton beam with the target producing the extreme fluxes of 10^{17} n/cm^2-sec necessary for fission product burnup. However, in addition to economic disadvantages this concept faces serious mechanical and material design problems.

Claiborne[5,6,7] was the first investigator to report detailed calculations of actinide recycling in light water reactors. Claiborne studied actinide recycling in light water reactors (LWR) operating on 3.3% U^{235}-U^{238} fuel cycle. He concluded that it was not practical to burn the fission products because the neutron fluxes were too low and "developing special burner reactors with required neutron fluxes of 10^{17} n/cm^2-sec or in thermonuclear nuclear reactor blankets is beyond the limits of current technology."[5]

For purposes of comparison, Claiborne[5] expressed radioactive waste hazards in terms of the total water required to dilute a nuclide or mixture of nuclides to its RCG (Radiation Concentration Guide Value, also known as the Maximum Permissible Concentration, MPC). Using this criterion, the waste from a PWR spent-fuel reprocessing plant is dominated by fission products for about the first 400 years. After the first 400 years the actinides and their daughters are the dominant factor. The americium and curium components of the actinide waste are the main hazards for the first 10,000 years, after which the long-lived Np^{237} and its daughters become the controlling factor. These data assume that 99.5% of the U and Pu has been removed from the waste.

Claiborne indicates that, if 99.5% of the U and Pu is extracted, then a significant reduction in the waste hazard can be achieved by also removing 99.5% of the other actinides, mainly americium, curium, and neptunium.

For the purpose of calculations, Claiborne assumes that recycling takes place in a typical PWR fueled with 3.3% enriched U and operated with a burnup of 33,000 MWd/metric tonne of uranium. The burnup was assumed continuous at a specific power of 30 MW/metric tonne over a three year period. The calculations also ignored intermittant operation and control rods and assumed that the neutron flux was uniform throughout a region. The recycled actinides were added uniformly to the 3.3% enriched fuel. The actual calculations were performed by a modified version of the nuclide generation and depletion code ORIGEN.[8] The calculations are based on three energy groups (thermal, 1/E energy distribution in the resonance region, and a fast group) with three principal regions in the reactor. Each region was in the reactor for three years while being cycled from the outside to the center so that the innermost region is removed each year.

The "standard" that was used for comparing the effect of the actinide recycle on the actinide waste hazard was the waste obtained after removing either 99.5% or 99.9% of the U and Pu at 150 days after discharge and sending the remaining quantities to waste along with all the other actinides, and all actinide daughters generated since discharge from the reactor. The results of Claiborne's calculations are presented in the form of a hazard reduction factor which he defines as "the ratio of the water required for dilution of the waste to the RCG for the standard case to that required to dilute the waste after each successive irradiation cycle."

The contributions of the actinides, fission products, and structural materials to the total waste hazard are shown in Table 1. Table 2 shows the effect of recycling the actinides in terms of the hazard reduction factor for two cases of actinide extraction efficiency. Note that the values decrease asymptotically with increasing recycles. This is due to the buildup of actinides in the system until decay and burnup equal production, after about 20 cycles. Figures 2 and 3 compare the effect of recycling in a LWR versus no-recycle for the short and long time hazards.

Table 1 Relative contribution of actinides and their daughters to the hazard measure of the waste and of each actinide and its daughters to actinide waste with 99.5% of U + Pu extracted[5]

Nuclides to Waste	Water required for dilution to the RCG[a] (% of total water required for the mixture) for decay times (yr) of: 10^2	5×10^2	10^4	10^5	10^6
	All Components of Waste:[b]				
Actinides	0.3	94	94	98	99
Fission Products	99+	5	6	2	1
Structural	0.04	1	0.2	0.03	4×10^{-4}
	Actinide Waste:[b]				
Americium	51	56	24	8	8
Curium	41	37	59	9	1
Neptunium	0.2	0.3	12	80	89
0.5% U + 0.5% Pu	8	7.7	5	3	1
Other	5×10^{-3}	1×10^{-3}	5×10^{-2}	6×10^{-3}	nil

[a] Using CFR RCGs and recommended default values for the unlisted nuclides.[8]

[b] Round-off may cause column not to total 100.

Table 2 Effect of recycle of actinides other than U and Pu on the hazard measure of waste from PWR spent fuel processing[5]

Recycle No.	Water required for dilution to RCG[a], ratio of standard to recycle[b] case (hazard reduction factor) for decay times (yr) of: 10^2	10^3	10^4	10^5	10^6
	Actinide Extraction Efficiency, 99.5%:				
0	12	15	18	28	52
1	9.3	12	13	20	46
2	8.2	10	11	18	44
3	7.6	8.4	9.3	17	43
4	7.2	7.4	8.3	17	42
5	6.8	6.6	7.5	17	42
10	5.8	4.7	5.8	17	42
20	5.1	3.8	4.9	17	42
30	5.0	3.6	4.6	17	42
	Actinide Extraction Efficiency, 99.9%:				
0	58	73	89	137	256
1	44	59	64	96	224
2	38	48	52	87	213
3	36	40	44	84	210
4	33	35	39	83	209
5	32	31	36	83	208
10	27	22	27	83	207
20	--	18	22	82	206
30	--	17	21	82	206

Using CFR RCGs and recommended default values for the unlisted nuclides.[8]

Chemical processing assumed at 150 days after reactor discharge; one cycle represents 3 years of reactor operation.

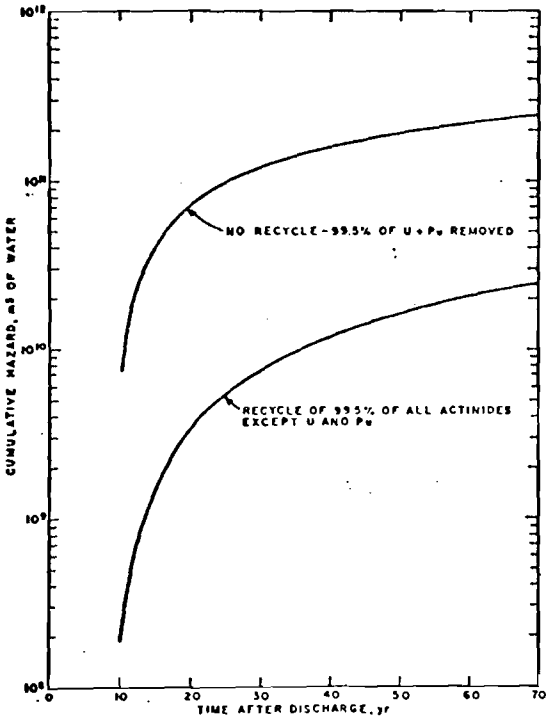

Fig. 2 Short-term cumulative hazard of actinide waste from 60-year operation of a typical PWR[5]

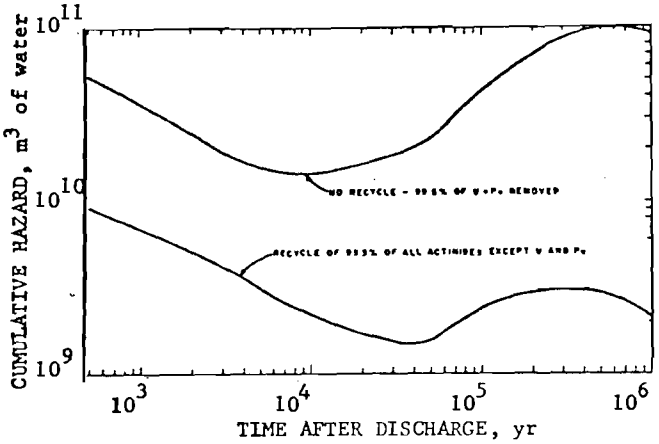

Fig. 3 Long-term cumulative hazard of actinide waste from 60-year operation of a typical PWR[5]

For the PWR examined, the decrease in the average neutron multiplication was only 0.8%. By increasing the fissile enrichment by only 2% (from 3.3 to 3.4% enrichment) the loss in reactivity can be compensated for.

The recycling of reactor actinide waste will increase radiation problems associated with chemical processing and fuel fabrication because of the increased radioactivity of the reactor feed and discharge streams. However, the increased actinide inventory in a reactor will probably have little effect on the potential danger in design basis accidents because the actinides are not volatile and, therefore, will not be significantly dispersed into the environment by any credible reactor accident.

Claiborne also states that the recycle of actinides in LMFBR's should produce even higher hazard reduction factors because of the better fission-to-capture ratio of the actinides in the presence of a fast flux. He also states that the recycling of actinides is well suited for fluid fuel reactors, such as the MSBR, because of the on-stream continuous reprocessing.

A technical group at Battelle Northwest Laboratories[9] extended Claiborne's work to provide a detailed review of the alternative method for long term radioactive waste management. Section 9 of their report was devoted to Transmutation Processing and covered four categories: (1) accelerators, (2) thermonuclear explosives, (3) fission reactors, and (4) fusion reactors. The study identified recycling in thermal power reactors as a promising method and went on to state, "consideration should also be given to evaluating the merit of having special purpose reactors optimized for destroying actinides."[9]

As reported in a review paper by Raman,[10] evaluations made by Raman, Nestor, and Dobbs[11] show that actinide inventories can be reduced further by recycling in a U^{233}-Th^{232} fueled reactor. This is made possible because neutron captures by the fertile Th^{232} produce the fissile U^{233}. Neutron capture by U^{233} results in higher U isotopes until U^{237} is reached. Plutonium and transplutonium isotopes are generated to a far lesser extent in a U^{233}-Th^{232} reactor than in a U^{235}-U^{238} reactor. Raman also stressed the need for more accurate cross section measurements.

The recycling of actinides in fast reactors has also been studied.[12,13,14,15] Greater actinide burnup is achievable in a fast reactor than in a thermal reactor because the fission-to-capture ratio is generally higher as shown in Table 3. In a 1973 review paper in Science, Kubo and Rose[16] suggested that recycling of actinides in an LMFBR has several advantages over recycling in a thermal reactor including the possibility that extreme chemical separations may not be required because fewer actinides are produced in a fast spectrum.

Paternoster, Ohanian, Schneider, Thom, and Schwenk[17,18,19] have studied the use of the gas core reactor for transmutation of fission products and actinide wastes. The fuel was UF_6 enriched to 6% in U^{235}. The four meter diameter core was surrounded by a reflector-moderator of D_2O with a thickness of 0.5 meter. The initial mass was 140 kg of $U^{235}F_6$. Adjustable control rods were located in the outer graphite reflector and the radioactive wastes were loaded in target ports. Figure 4 shows results of calculations, comparing both actinide and fission product waste in current LWR's with the gaseous fuel power reactor. Notice that after 800-1000 days, the actinide wastes in the gaseous core reactor are an order of magnitude less than those in a LWR.

In a study sponsored by NASA, Clement, Rust, and Williams[20,21] analyzed a gas core breeder reactor using a U^{233}-Th^{232} fuel cycle. One- and two-dimensional calculations were carried out for a UF_6 fueled core surrounded by a molten salt blanket. Figure 5 shows a diagram of the reactor. The medium fission energy in the core was found to be 300 keV, and there was some spectrum softening in the blanket.

Table 3 Fission-to-capture ratios of actinides in fast and thermal reactors[10]

Isotope	Half-Life Years	Fast Spectrum	Thermal Spectrum
Np^{237}	2.14×10^{6}	0.213	1.26×10^{-4}
Am^{241}	433	0.115	4.48×10^{-3}
Am^{242m}	152	4.85	1.12
Am^{243}	7370	0.309	4.87×10^{-4}
Cm^{244}	17.9	1.25	0.068

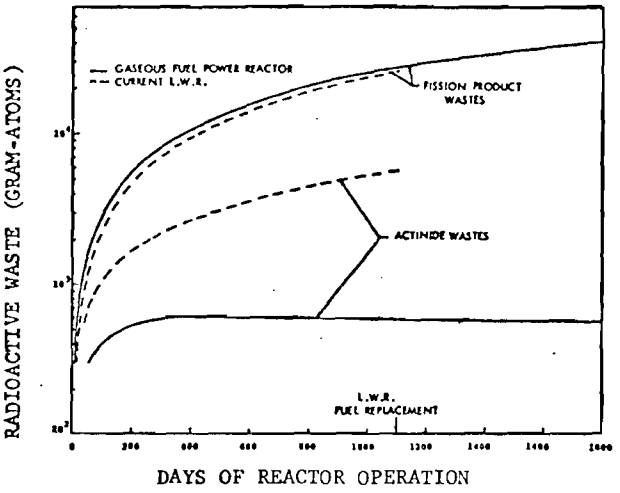

Fig. 4 Radioactive waste production of 3425 MW(t) fission power reactors[19]

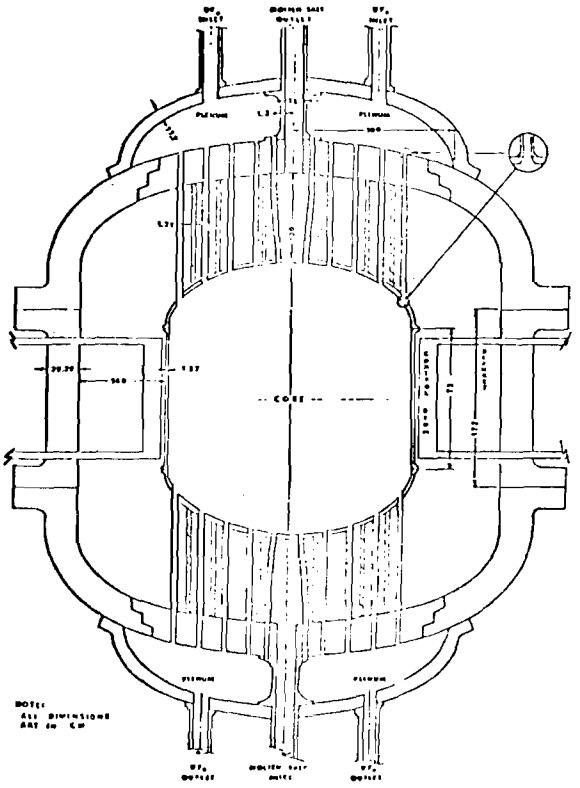

Fig. 5 UF_6 gas-core reactor

Table 4 is a brief summary of some important dates in the history of the GCATR. As previously stated, the burnup of fission products requires thermal neutron fluxes of the order of 10^{17} n/cm^2-sec. In the United States, the two reactors with the highest neutron fluxes are the ORNL High Flux Isotope Reactor (HFIR)[22] and the SRL High Flux Reactor (HFR)[23] which have maximum neutron fluxes of 3×10^{15} and 5×10^{15} n/cm^2-sec, respectively. Both of these reactors employ solid fuels and have essentially reached the upper limit in neutron fluxes because of heat transfer limitations. In addition, when operating at these neutron fluxes the refueling intervals are of the order of two weeks. The gas core reactor does not have the in-core heat transfer limitations posed by solid core reactors employing a coolant and, consequently, higher neutron fluxes should be achievable. In addition, reactor shutdown for refueling is not necessary because new fuel can be continuously added to the UF_6 during reactor operation. Therefore, a gas core reactor may be the only practical reactor for consideration of fission product burnup if such a scheme of waste disposal is considered desirable.

Table 4 Some dates in the history of GCATR

1960-73	- NASA sponsored research on gas-core reactor for rocket propulsion
1964	- Steinberg first suggests neutron-induced transmutation
1972	- Claiborne's studies of actinide recycling in LWR's
1973	- documentation of ORIGEN program
1974	- recycling studies in LWR's, LMFBR's, HTGR's by Croff, Raman, et al.
1974	- suggestion of GCATR by Paternoster, Ohanian, Schneider (University of Florida) and Thom (NASA)
1974-75	- UF_6 breeder reactor study at Georgia Tech sponsored by NASA
1976	- GCATR study at Georgia Tech sponsored by NASA

Table 5 summarizes some of the advantages of the GCATR which appear to make it an attractive candidate for actinide transmutation.

Table 5 Some advantages of the gas-core reactor

(1) The gaseous state of the fuel significantly reduces problems of processing and recycling fuel and wastes.

(2) High neutron fluxes are achievable.

(3) The possibility of using a molten salt in the blanket may also simplify the reprocessing problem and permit breeding.

(4) The spectrum can be varied from fast to thermal by increasing the moderation in the blanket so that the trade-off of critical mass versus actinide and fission product burnup can be studied for optimization.

(5) The U^{233}-Th cycle, which can be used, is superior to the U^{235}-Pu cycle in regard to actinide burnup.

III. GCATR Research Program

The overall objective of the NASA sponsored program is to study the feasibility, design, and optimization of a GCATR. The program involves three interrelated and concurrent tasks, as listed in Table 6.

Table 6 NASA sponsored GCATR research at Georgia Tech

General Studies
Update cross-sections
Sensitivity analysis
Parametric survey
Reactor and System Design
Design criteria
Reactor subsystem
(a) $^{233}UF_6$
(b) plasma core
Fuel and actinide insertion and recycling
Economic Analysis
Comparison of GCATR with other strategies

TASK 1 General Studies

Raman[9] has pointed out the need for more accurate cross section data and the necessity of assessing the sensitivity of the calculational results to the uncertainties in cross sections. This task will include the following subtasks:

A. Literature Survey and Cross Section Tabulation--A literature survey will be carried out and the best available cross sections of the fission products and actinides will be tabulated. Improved values will be used as they become available.

B. Implementation of a Versatile Depletion Program--ORIGEN[8] or a similar computer code will be implemented or developed. A depletion code which solves the equations of radioactive growth and decay and neutron transmutation for large numbers of isotopes is required. ORIGEN has been used previously for LWR's, LMFBR's, MSBR's, and HTGR's, and may also be suitable for the GCATR.

C. Parametric Survey Calculations--Parametric survey calculations will be performed to examine the effort of reactor spectrum, and flux level on the actinide transmutation for GCATR conditions. The sensitivity of the results to neutron cross sections will be assessed. These studies will be related to the nuclear analysis work of TASK 2. Specifically, the parametric calculations of the actinide transmutation will include the mass, isotope composition, fission and capture rates, reactivity effects, and neutron activity of the recycled actinides. Table 7 summarizes the most important parameters to te investigated.

Table 7 Most important parameters to be investigated

(1) The mass and composition of the actinides being recycled
(2) The rate at which the recycled actinides are fissioned and transmuted in the reactor
(3) The effect of the recycled actinides on fission reactor criticality and reactivity
(4) The effect of the recycled actinides on the out-of-reactor nuclear fuel cycle (i.e., fabrication, shipping, reprocessing, actinide inventory, etc.)

TASK 2 GCATR Design Studies

This task is a major thrust of the proposed research program. Four subtasks are considered:

A. Optimization Criteria Studies
B. Design Studies of the Reactor Subsystem
C. Design Studies of the Blanket and Fuel Reprocessing and Actinide Insertion and Recirculation System
D. System Integration

In subtask A, Optimization Criteria Studies, consideration will be given to understanding the trade-offs that are made to achieve a given result. For example, is the GCATR to be used only for actinide burnup? Should we also include breeding (U^{233}-Th) or fission product transmutation? If we reduce the mean neutron energy to achieve faster fission product burnup, how much do we sacrifice in actinide burnup? Should the reactor also be used to produce power? If so, how much power? What are the optimization criteria?

In subtask B, Design Studies of the Reactor Subsystem, a multidisciplinary approach similar to that in Refs. 20, 21 will be carried out involving:

(1) Materials
(2) Nuclear Analysis
(3) Thermodynamics and Heat Transfer
(4) Mechanical Design.

Results of this task will be used iteratively with the parametric study described in TASK 1. In previous work[20,21] one-dimensional and two-dimensional survey calculations were carried out for a UF_6-fueled core surrounded by a molten salt blanket, and a preliminary mechanical design was developed. This work will be extended to include the insertion of fission products and actinides in various locations in the reactor. The effect of other reactor component changes such as using different reflector materials (carbon, beryllium, deuterium oxide) or modifying the molten salt reflector by the addition of moderator will also be evaluated. Best available cross section data from TASK 1 will be utilized. A preliminary reactor design will be developed taking into account thermal and mechanical design considerations.

In subtask C, a preliminary design of the UF_6 and blanket reprocessing system (if molten salt) will be prepared and performance of the systems analyzed. Equilibrium fuel and blanket compositions including fission products and actinides will be computed. These results will provide necessary

information on equilibrium core and blanket compositions for use in the nuclear analyses.

Subtask D, System Integration, involves putting all the sub-components together in a workable system taking account of criticality, shielding, and economic considerations.

TASK 3 Comparison of the GCATR with Other Nuclear Waste Management Strategies

The cost of the GCATR shall be evaluated in terms of mills/kwhre. The cost can be broken down into the components:

(1) solid and liquid storage
(2) shipping
(3) interim retrievable storage separations
(4) separation
(5) disposal or elimination in GCATR

The total cost of the management system will be computed and compared to the cost of alternate strategies presently being considered.

As of June 1976, the research program has been underway for only two months. Table 8 summarizes the status of the program at this time.

Table 8 Summary of Georgia Tech GCATR research program to date

General Studies
1. Actinide cross sections have been updated
2. ORIGEN has been implemented and modified
3. Some sensitivity results and parametric studies have been obtained

Reactor Studies
1. Series of nuclear design codes have been implemented
2. Several configurations of $^{233}UF_6$ reactor are being analyzed

IV. References

1. Smith, J. A., "Proceedings of the Californium-252 Symposium," USAEC Report CONF-681032, p. 179 (1969)

2. "Waste Management Symposium," Nuclear Technology, 24 (December 1974)

3. Steinberg, M., Molzak, G., and Menovita, B., "Neutron Burning of Long-Lived Fission Products for Waste Disposal," BNL-8558, Brookhaven National Laboratory (September 1964)

4. Gregory, M. V. and Steinberg, M., "A Nuclear Transmutation System for Disposal of Long-Lived Fission Product Waste in an Expanding Nuclear Power Economy," BNL-1195 (November 1967)

5. Claiborne, H. C., "Neutron Induced Transmutation of High-Level Radioactive Wastes," ORNL-TM-3964 (December 1972)

6. Claiborne, H. C., "Effect of Actinide Removal on the Long-Term Hazard of High-Level Waste," ORNL Report TM-4724 (1975)

7. Bond, W. D., Claiborne, H. C., and Levze, R. E., "Methods for Removal of Actinides from High Level Wastes," Nuclear Technology, 24, 362-370 (December 1974)

8. Bell, M. J., "ORIGEN--The ORNL Isotope Generation and Depletion Code," ORNL-4628, Oak Ridge National Laboratory (May 1973)

9. Schneider, K. J. and Plat, A. M., "High-Level Radioactive Waste Management Alternatives," BNWL Report 1900 (1974)

10. Raman, S., "Some Activities in the United States Concerning the Physics Aspects of Actinide Waste Recycling," Review Paper from ORNL (1975)

11. Raman, S., Nestor, C. W., Jr., and Dabbs, J. W. T., "The U^{233}-Th^{232} Reactor as a Burner for Actinide Wastes," Proc. of the Conf. on Nuclear Cross Sections and Technology, Washington, D. C. (March 1975)

12. Breen, R., "Elimination of Actinides with LMFBR Recycle," Westinghouse Advanced Reactors Division, private communication reported in Ref. 10

13. Beaman, S. L., "Actinide Recycle Evaluations," General Electric Energy Systems and Technology Division, private communication reported in Ref. 10

14. Croff, A. G., "Parameter Studies Concerning Actinide Transmutation in Power Reactors," Transactions of the American Nuclear Society, 22, 345 (November 1975)

15. Davidson, J. W. and Draper, E. L., Jr., "Costs for Partitioning Strategies in High-Level Waste Management," Transactions of the American Nuclear Society, 22, 348 (November 1975)

16. Kubo, A. S. and Rose, D. J., "On Disposal of Nuclear Waste," Science, 182, No. 4118, 1205-1211 (December 1973)

17. Paternoster, R., Ohanian, M. J., Schneider, R. T. and Thom, K., "Nuclear Waste Disposal Utilizing a Gaseous Core Reactor," Transactions of the American Nuclear Society, 19, 203 (October 1974)

18. Paternoster, R. R., "Nuclear Waste Disposal Utilizing a Gaseous Core Reactor," Master's Thesis, University of Florida (1974)

19. Schwenk, F. C. and Thom, K. T., "Gaseous Fuel Nuclear Reactor Research," Paper presented at the Oklahoma State University Conference on Frontiers of Power Technology (October 1974)

20. Clement, J. D., Rust, J. H., and Williams, J. R., "Analysis of UF_6 Breeder Reactor Power Plants," Semi-annual Report NASA Grant NSG-1168 (October 1975)

21. Rust, J. H. and Clement, J. D., "UF_6 Breeder Reactor Power Plants for Electric Power Generation," Proc. Third Symposium on Uranium Plasmas, Princeton University Conference, June 10-12, 1976

22. Binford, F. T., et al., "The High-Flux Isotope Reactor," ORNL-3572 (Rev. 2) (May 1968)

23. Crandall, J. L., "The Savannah River High Flux Demonstration," USAEC Report DP-999 (1965)

APPENDIX B

UF_6 BREEDER REACTOR POWER PLANTS FOR ELECTRIC POWER GENERATION

J. H. Rust and J. D. Clement
Georgia Institute of Technology
Atlanta, Georgia

and

F. Hohl
National Aeronautics and Space Administration
Langley, Virginia 23665

UF_6 BREEDER REACTOR POWER PLANTS FOR ELECTRIC POWER GENERATION*

J. H. Rust and J. D. Clement
Georgia Institute of Technology
Atlanta, Georgia

F. Hohl
National Aeronautics and Space Administration
Langley, Virginia

Abstract

The concept of a UF_6 fueled gas core breeder reactor (GCBR) is attractive for electric power generation. Studies indicate that UF_6 fueled reactors can be quite versatile with respect to power, pressure, operating temperature, and modes of power extraction. Possible cycles include Brayton cycles, Rankine cycles, MHD generators, and thermionic diodes. Another potential application of the gas core reactor is its use for nuclear waste disposal by nuclear transmutation.

The reactor concept analyzed is a $^{233}UF_6$ core surrounded by a molten salt (Li^7F, BeF_2, ThF_6) blanket. Nuclear survey calculations were carried out for both spherical and cylindrical geometries. A maximum breeding ratio of 1.22 was found. Further neutronic calculations were made to assess the effect on critical mass, breeding ratio, and spectrum of substituting a moderator, Be or C, for part of the molten salt in the blanket.

Thermodynamic cycle calculations were performed for a variety of Rankine cycles. Optimization of a Rankine cycle for a gas core breeder reactor employing an intermediate heat exchanger gave a maximum efficiency of 37%.

A conceptual design is presented along with a system layout for a 1000 MW stationary power plant. The advantages of the GCBR are as follows: (1) high efficiency, (2) simplified on-line reprocessing, (3) inherent safety considerations, (4) high breeding ratio, (5) possibility of burning all or most of the long-lived nuclear waste actinides, and (6) possibility of extrapolating the technology to higher temperatures and MHD direct conversion.

I. Introduction

For about more than a decade, NASA has supported research on gas core reactors which consisted of cavity reactor criticality tests, fluid mechanics tests, investigations of uranium optical emissions spectra, radiant heat transfer, power plant studies, and related theoretical investigations.[1,2,3] These studies have shown that UF_6 fueled reactors can be quite versatile with respect to power, pressure, operating temperature, modes of power extraction, and the possibility of transmuting actinide waste products. Possible power conversion systems include Brayton cycles, Rankine cycles, MHD generators, and thermionic diodes. Additional research has shown the possibility of pumping lasers by fission fragment interactions with a laser gas mixture which leads to the possibility of power extraction in the form of coherent light.[4]

Gas core reactors have many advantages when compared to conventional solid fuel reactors in current use. Table 1 lists several advantages of gas core reactors.

Table 1 Advantages of gas core reactors

I.	Small Fuel Loadings
II.	Simplified On-Line Fuel Reprocessing
III.	Greater Safety due to Small Inventory of Fission Products
IV.	Require Less Structural Material
V.	Higher Breeding Ratios and Shorter Doubling Times
VI.	Potential for Higher Neutron Fluxes Which Makes Actinide Transmutation Practical
VII.	Operates at Higher Temperature with Increased Power Plant Efficiencies
VIII.	Possibility of Extrapolating Technology to Higher Temperatures and Use MHP Direct Conversion

One of the major advantages of UF_6 reactors for power generation is the simplified fuel reprocessing scheme which the gaseous fuel makes possible as shown in Fig. 1.

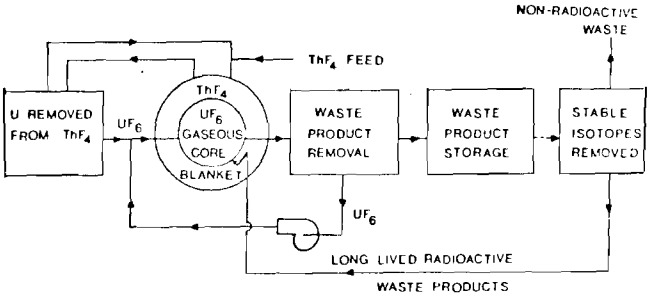

Fig. 1 Simplified diagram of UF_6 breeder reactor fuel cycle.

Part of the UF_6 can be extracted from the core continuously and sent to a fuel reprocessing facility for removal of waste products. The waste product removal can be accomplished by fractional distillation or cold trapping. After an appropriate waiting period, the waste products can be reprocessed for recovering long-lived fission products and actinides for return back to the reactor for transmutation to

*This research was supported by NASA Grants NSG-7068 and NSG-1168.

short-lived isotopes or fissioning of the actinides.

An additional advantage of gas core reactors is that they do not require the core structural materials that are necessary for solid fuel reactors. This lack of materials which undergo parasitic neutron capture enables higher breeding ratios for gas core reactors in comparison to conventional reactors. This paper reports a design study performed at Georgia Tech to evaluate the merits of gas core reactors for use as breeder reactors for electric power generation.

II. Materials

Materials selected for use for the gas core breeder reactor are listed in Table 2.

Table 2 Materials for UF_6 gas core breeder reactor

Core:	UF_6 (U-233)
Blanket:	Molten Salt--LiF-BeF_2-ThF_4 (71.7-16-12.3 mole%)
Structure:	Modified Hastelloy-N
Secondary Coolant:	$NaBF_4$ (92%) NaF (8%)

Uranium hexafluoride was chosen as the fuel because it exists in a gaseous state at low temperatures. U^{233} was selected as the fissionable isotope of the fuel because it enables use of the uranium-thorium fuel cycle which results in the direct production of U^{233} from breeding. An additional advantage is that the U^{233}-Th fuel cycle does not produce as great a buildup of actinides as fuel cycles employing U^{235}-U^{238} or Pu^{239}-U^{238}.

Several concepts were considered for the reactor blanket material. It was throught that a fluid blanket would be desirable so as to capitalize on the continuous reprocessing which is possible with the fluid fuel. The best material for use as the blanket is a molten salt similar to the type employed by the molten salt breeder reactor. This salt has a composition of LiF-BeF_2-ThF_4 which has a melting point of 500°C, has a low vapor pressure at the operating temperature, and is stable in the proposed range of application (540-970°C). In order to reduce parasitic neutron capture in lithium, the lithium is enriched to 99.995% in Li^7.

A modified Hastelloy-N was selected for the core liner, reactor pressure vessel, and primary piping. This material was developed for the molten salt breeder program and is quite compatible with the blanket salt and UF_6 over operating temperatures less than 900°C. Modified Hastelloy-N is very similar in composition and other related physical properties to standard Hastelloy-N; however, the modified version is superior because of its ability to resist helium embrittlement under neutron irradiation.

It was thought that it would be undesirable for UF_6 to interface with water which will be used as the working fluid for the power conversion cycle. Consequently, an intermediate coolant was selected for exchanging heat with the UF_6. This intermediate coolant is a molten salt which is composed of $NaBF_4$ and NaF and is quite compatible with UF_6.

III. Nuclear Analysis

Nuclear calculations were performed using the MACH-I one-dimensional, diffusion code[5] and the THERMOS transport code.[6] MACH-I employs 26 energy groups with the thermal neutron energy being 0.025 eV. Because of the high temperatures of the UF_6 and the blanket, it was thought that more accurate calculations could be performed by using THERMOS to supply thermal neutron cross sections.

The MACH-I code was used to calculate breeding ratios, critical masses, and reactor dimensions for a variety of reactor concepts. The lithium and beryllium contained in the blanket salt will act as a moderator for slowing down fission neutrons from the core. It was thought that additional moderation might be desirable and, consequently, carbon and beryllium were added in varying amounts to the blanket to evaluate the effects upon reactor parameters. Tables 3 and 4 show calculated breeding ratios, critical masses, and reactor dimensions for various percentages of carbon or beryllium in the blanket. As shown, additional moderation does increase breeding ratios and it appears that maximum breeding ratios occur when the blanket volume is about 25% carbon or beryllium. Additional studies showed that blanket thicknesses of 100 cm or greater behaved as though the blanket was of infinite thickness.

It is recognized that gas core reactors will undoubtedly be built in a cylindrical geometry. Since MACH-I is a one-dimensional code it was necessary to perform the survey calculations with a spherical reactor. In order to assess the effects of analyzing two-dimensional reactors with a one-dimensional diffusion code, some of the nuclear calculations were repeated using the EXTERMINATOR[7] diffusion code which is capable of doing calculations in an r-z geometry. The core capacity of the Georgia Tech CYBER-74 computer would not allow performing EXTERMINATOR calculations with more than 4-energy groups. Since the MACH-I calculations were performed with 26-energy groups, it was deemed desirable to collapse the 26-energy groups used in MACH-I down to 4-energy groups and repeat the MACH-I calculations. This enabled comparing the effects of using 4- or 26-energy groups for calculating breeding ratios, reactor dimensions, and critical masses. Table 5 illustrates the results of these calculations and, as seen, there are insignificant differences in using 4- or 26-energy groups with the MACH-I code. Therefore, it may be concluded that computations using 4-energy groups with the EXTERMINATOR code should yield valid results.

Table 5 also shows the results of the 4-energy group EXTERMINATOR calculations for a cylindrical reactor with a core height equal to the core diameter. As seen, the breeding ratio is slightly higher by going from a spherical geometry to a cylindrical geometry. This is to be expected because of the increased neutron leakage from a cylindrical core because of the increased surface-to-volume ratio of a cylinder compared to a sphere.

Table 3 Critical parameters vs volume percent of carbon in blanket (blanket thickness = 114 cm)

Percent of Carbon in Blanket	0	25	50	75	100
Breeding Ratio	1.183	1.196	1.190	1.133	0
Critical Radius (cm)	58.6	60.9	62.6	61.4	39.2
Critical Mass (kg U-233)	379	386	463	436	114

Table 4 Critical parameters vs volume percent of beryllium in blanket (blanket thickness = 114 cm)

Percent of Be in blanket	0	25	50	75	100
Breeding Ratio	1.183	1.223	1.203	1.065	0
Critical Radius (cm)	58.6	61.8	61.1	53.4	29.8
Critical Mass (kg U-233)	379	446	431	287	50

Table 5 Comparison of critical parameters

	Spherical Core (26 group)	Spherical Core (4 group)	Cylindrical Core (4 group)
Breeding Ratio	1.181	1.179	1.219
Critical Radius (cm)	58.6	60.9	54.8
Critical Core Volume	8.4×10^5 cm^3	9.5×10^5 cm^3	1.0×10^6 cm^3
Critical Mass (kg U-233)	379	426	496
Blanket Thickness (cm)	114	114	100

IV. Heat Transfer

Because of high power densities in gas core reactors, it is necessary to analyze the core heat transfer in order to assure that unacceptably high temperatures are not achieved in the UF_6. This requires solving the energy equation for UF_6 flowing through a cylindrical core. Equation 1 gives the energy equation for the UF_6.

$$\rho c_p U_z(r,z) \frac{\partial T}{\partial z} = \frac{1}{r} \frac{\partial}{\partial r}\left(r k_e \frac{\partial T}{\partial r}\right) + q'''(r,z) \quad (1)$$

where

ρ = density
c_p = specific heat at constant pressure
$U_z(r,z)$ = axial velocity
T = temperature
$k_e = k + \rho c_p \epsilon_H$, total conductivity
ϵ_H = eddy diffusivity for heat transfer
q''' = volumetric heat generation rate

Equation 1 is extremely complex because UF_6 physical properties are highly temperature dependent and the volumetric heat generation term is strongly spatially dependent due to the variable UF_6 density in the core and variable neutron flux distributions. Equation 1 was solved for two sets of boundary conditions: (Case 1)--an insulated liner wall in which no heat crosses the wall and (Case 2)--an insulated liner wall until the wall temperature reaches 920°K for the rest of the core length. Equation 1 was solved numerically by using finite difference representations for the partial derivatives and incorporating a MACH-I power distribution computation for the volumetric heat generation term. A marching technique was employed which required iteration at each axial step in order to incorporate the temperature dependence of the UF_6 physical properties. Reference 8 gives a detailed description of the heat transfer modeling and computational techniques.

It was estimated that 9.7% of the reactor power would be deposited in the blanket. Consequently, for a power level of 1000 MWth, 903 MWth would be generated in the reactor core. The UF_6 inlet temperature was specified as 558°K and mass flow rate at 6320 kg per second. The core geometry was a right cylinder with a 100 cm radius and 200 cm length.

Figure 2 illustrates the radial dependence of UF_6 temperatures for various axial positions for the insulated wall boundary condition (Case 1). Temperatures reach a peak at the wall because the volumetric heat generation term is a maximum at the wall and, in particular, the fluid velocity at the wall is zero which means heat is transferred at that location only through conduction. Figure 3 illustrates core liner wall temperatures and UF_6 fuel temperatures at the core axis as a function of core length. As shown by the calculations, after 50 cm down the channel length the liner wall temperatures exceed 920°K, which is considered unacceptably high.

Figure 4 illustrates the radial dependence of UF_6 temperatures for various axial locations for the boundary conditions that liner wall temperatures not exceed 920°K (Case 2). The maximum UF_6 temperature occurs at the core exit and is 1220°K, which is far below temperatures required for substantial UF_6 ionization. Figure 5 illustrates core liner wall temperatures and UF_6 temperatures at the core axis as a function of core length.

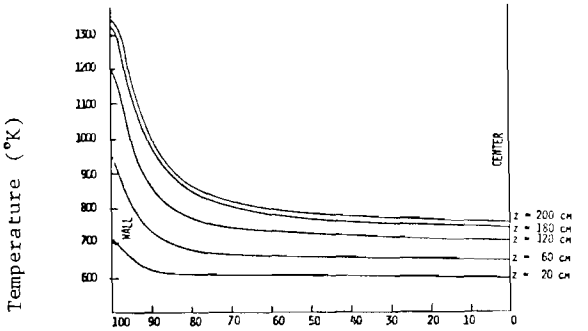

Fig. 2 Temperature vs radial distance (Case 1)

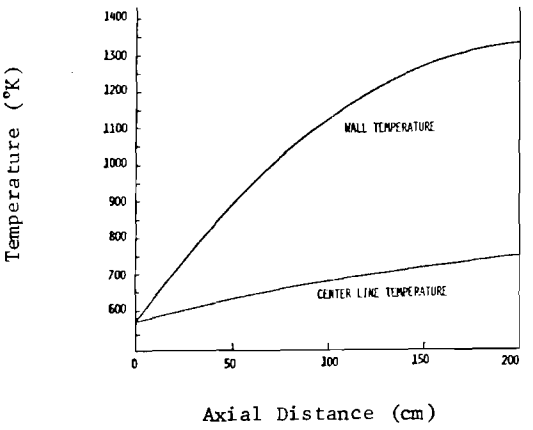

Fig. 3 Wall temperature vs axial distance (Case 1)

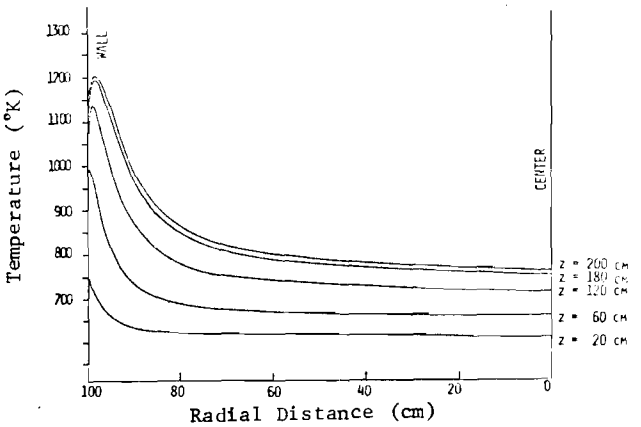

Fig. 4 Temperature vs radial distance (Case 2)

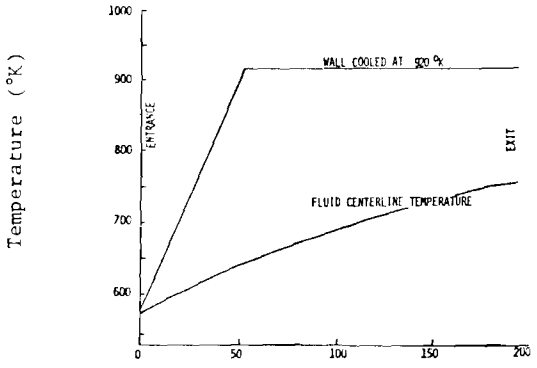

Fig. 5 Wall temperature vs axial distance (Case 2)

The boundary condition that the liner wall temperature not exceed 920°K requires wall cooling after about 40 cm down the core length. Consequently, it is necessary to examine wall heat fluxes in order to determine the extent of the wall cooling. Figure 6 illustrates calculated liner wall heat fluxes as a function of channel length. The maximum heat flux occurs at the channel exit and has a value of 0.205 watt per square centimeter which is a small heat flux for which it will be easy to provide wall cooling.

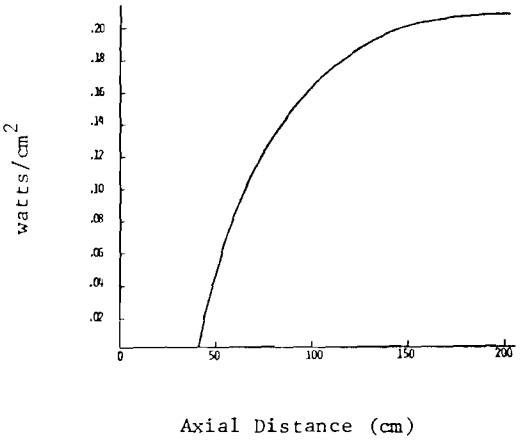

Fig. 6 Wall heat flux vs axial distance (Case 2)

V. System Analysis

It was thought that it would be desirable for the flow through the reactor core to be at a uniform velocity so as to simplify calculations and maximize reactor performance. In order to obtain an approximate uniform velocity distribution in the core it is necessary to employ numerous inlet and outlet nozzles for flow of UF_6 into and out of the core. Figure 7 illustrates the gas core reactor design. The reactor is a right cylinder with ellipsoidal heads and height equal to the diameter. It is easily fabricated and a good geometry to work with from both a practical and a calculational point of view.

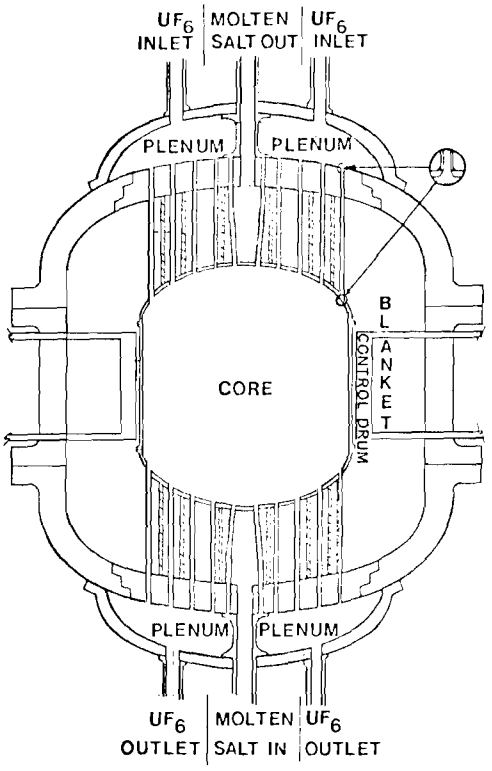

Fig. 7 Reactor configuration

The blanket will be pressurized to the same pressure as the core (on the order of 100 bars). The core liner is designed to withstand a pressure difference of only 15 bars. The outside pressure vessel will need to be capable of containing the 100 bar pressure plus a 20% safety margin, or 120 bar total. These pressures are not extreme and can be easily accommodated. The reactor pressure vessel was designed according to specifications from the ASME Boiler and Pressure Vessel Code; Section III--Rules for Construction of Nuclear Power Plant Components.[9] The core liner was selected at a thickness of 1.3 cm which is adequate for sustaining a 15 bar pressure difference at the reactor operating temperature for a 30-year lifetime. In case of a rapid depressurization of the blanket, the core liner can withstand a pressure difference of approximately 90 bars for a period of 6 minutes.

Many schemes were examined for energy conversion with gas core breeder reactors. The UF_6 can be used as a working fluid for either Brayton or Rankine cycles. However, in order to have reasonable efficiencies, a regenerator is necessary for either cycle. High efficiencies can be achieved using UF_6 in Rankine cycles for the operating temperatures selected for this study. For turbine inlet temperatures of 850°K and pressures of the order of 100 bars, Rankine cycle efficiencies will exceed 41%.

In order to reduce the inventory of UF_6 in the

power plant system, it is desirable to employ another fluid as the working fluid in the energy conversion device. Because of the adverse chemical reaction of UF_6 with water, in the event of a rupture of a boiler tube, it is not advisable for UF_6 to exchange heat directly with water in a boiler. Consequently, a molten salt $NaBF_4$-NaF was selected as an intermediate coolant for transferring heat from UF_6 to water in a boiler. The power plant schematic is shown in Fig. 8. The molten salt has heat transfer characteristics similar to those of water and an additional desirable feature is that it contains boron which is a control material used in conventional reactors and would thus prevent the possibility of criticality inside the intermediate heat exchanger.

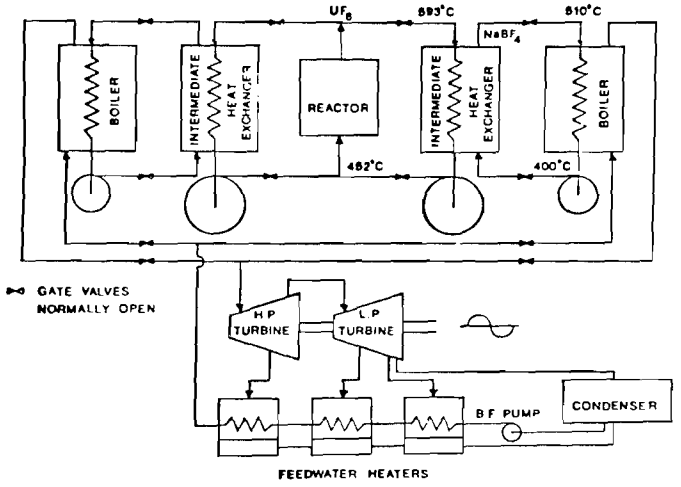

Fig. 8 UF_6 breeder power plant system schematic

The intermediate salt will be used to produce superheated steam at a temperature of 460°C and a pressure of 100 bars. The steam will be passed through high pressure and low pressure turbines for energy extraction. Three feedwater heaters are employed for extracting moisture from the turbines and heating the feedwater before it enters the boiler. By extracting steam at optimum pressures for each feedwater heater stage, the overall cycle efficiency will be 37%.

VI. Conclusions

The design study has shown that it is possible to construct a gas core breeder reactor with a high breeding ratio, of the order of 1.2 or higher, and an overall efficiency of 37%. The plant will not require excessive temperatures or pressures and will use much of the technology already developed for the molten salt breeder reactor program.

References

1. Thom, K., Schneider, R. T., and F. C. Schwenk, "Physics and Potentials of Fissioning Plasmas for Space Power and Propulsion," Paper No. 74-087, International Astronautical Federation 25th Congress, Amsterdam (October, 1974)

2. Williams, J. R., Clement, J. D., and J. H. Rust, "Analysis of UF_6 Breeder Reactor Power Plants," Progress Report No. 1, NASA Grant NSG-7067, Georgia Institute of Technology, Atlanta, Georgia (November, 1974)

3. Walters, R. A., and J. R. Williams, "High Efficiency Laser, MHD and Turbine Power Extraction from a Gas Core Nuclear Reactor," Proc. Southeastern IEEE Conf., Orlando, Florida (April, 1974)

4. Schneider, R. T., "Direct Conversion of Nuclear Energy into Laser Light," The 1976 IEEE International Conference on Plasma Science, Austin, Texas (May 24-26, 1976)

5. Meneley, D. A., et al., "MACH-I, A One-Dimensional Diffusion Theory Package," ANL-7223 (1966)

6. Toppel, B. J., and I. Baksys, "The Argonne-Revised THERMOS Code," ANL-7023 (1965)

7. Fowler, T. B., Tobias, M. L., and D. R. Nondy, "EXTERMINATOR-2; A Fortran IV Code for Solving Multigroup Neutron Diffusion Equations in Two Dimensions," ORNL-4078 (April, 1967)

8. Clement, J. D., and J. H. Rust, "Analysis of UF_6 Breeder Reactor Power Plants," Final Report, NASA Grant NSG-1168, Georgia Institute of Technology, Atlanta, Georgia (February, 1976)

9. "ASME Boiler and Pressure Vessel Code, Section III--Rules for Construction of Nuclear Power Plant Components," American Society of Mechanical Engineers, New York (July, 1971)

APPENDIX C

FISSION PRODUCT AND ACTINIDE CONCENTRATIONS AT VARIOUS STAGES IN WASTE REPROCESSING FOR LWR FUELS

APPENDIX C-1

FISSION PRODUCT AND ACTINIDE CONCENTRATIONS LEAVING A LWR

PWR FUEL CYCLE - DECAY TIMES OF FUEL DURING COOLING PERIOD
POWER= 30.00MW, BURNUP= 33000.MWD, FLUX= 2.92E+13N/CM**2-SEC
NUCLIDE INGESTION HAZARD, M**3 OF WATER AT RCG
BASIS = PER METRIC TONNE OF U LOADED IN REAC

Actinides

	DISCHARGE
PB212	7.50E+01
BI212	3.75E+00
RA223	1.27E+00
RA224	7.50E+02
TH228	6.13E+02
TH230	8.88E+00
TH231	5.96E+03
TH234	1.57E+04
PA231	2.71E+01
PA233	3.24E+03
PA234M	1.60E+01
PA234	6.52E+01
U232	2.00E+02
U233	1.52E+00
U234	2.55E+04
U235	5.70E+02
U236	9.61E+03
U237	8.55E+09
U238	7.85E+03
NP237	1.11E+05
NP239	1.85E+11
PU236	1.17E+04
PU238	5.45E+08
PU239	6.30E+07
PU240	9.55E+07
PU241	5.25E+08
PU242	2.76E+05
AM241	2.15E+07
AM242M	2.29E+06
AM242	6.34E+08
AM243	4.54E+06
CM242	1.67E+09
CM243	7.42E+05
CM244	3.49E+08
CM245	8.54E+04
CM246	1.71E+04
CM248	1.98E+00
BK249	8.96E+00
CF250	3.79E+00
CF252	2.92E+00
SUBTOT	1.98E+11
TOTALS	2.16E+11

Fission Products

	DISCHARGE
H 3	2.36E+05
KR 85	1.13E+04
RB 86	2.47E+07
SR 89	2.39E+11
SR 90	2.59E+11
Y 90	4.03E+09
Y 91	3.13E+10
ZR 93	2.36E+03
NB 93M	3.61E+02
ZR 95	2.29E+10
NB 95M	2.80E+04
NB 95	1.38E+10
MO 99	3.81E+10
TC 99	7.14E+04
RU103	1.52E+10
RH103M	1.22E+08
RU106	5.45E+10
RH106	7.40E+05
PD107	1.10E+02
AG110M	1.23E+08
AG110	1.59E+05
AG111	9.90E+08
CD113M	1.05E+01
IN114M	7.75E+04
CD115M	1.84E+07
SN119M	1.64E+01
SN123	8.88E+03
SB124	2.03E+07
SN125	6.76E+08
SB125	8.70E+07
TE125M	3.11E+07
TE127M	3.07E+08
TE127	3.60E+08
TE129M	2.86E+09
TE129	4.21E+08
I129	6.18E+05
I131	2.87E+12
XE131M	8.39E+03
TE132	5.92E+10
I132	1.53E+11
XE133	1.61E+06
CS134	2.74E+10
CS135	2.86E+03
CS136	1.01E+09
CS137	5.39E+09
BA137M	1.01E+05
BA140	7.27E+10
LA140	7.50E+10
CE141	1.54E+10
PR143	2.41E+10
CE144	1.11E+11
PR144	1.12E+06
ND147	9.81E+09
PM147	5.12E+08
PM148M	3.89E+04
PM148	1.99E+05
SM151	3.12E+06
EU152	1.57E+05
GD153	1.78E+05
EU154	3.49E+08
EU155	3.74E+07
EU156	2.26E+05
TB160	3.21E+07
SUBTOT	4.11E+12
TOTALS	6.40E+12

APPENDIX C-2

FISSION PRODUCT AND ACTINIDE CONCENTRATIONS AFTER 150 DAYS STORAGE

PWR FUEL CYCLE - DECAY TIMES OF FUEL DURING COOLING PERIOD
POWER= 30.00MW, BURNUP= 33000.MWD, FLUX= 2.92E+13N/CM**2-SEC
NUCLIDE INGESTION HAZARD, M**3 OF WATER AT RCG
BASIS = PER METRIC TONNE OF U LOADED IN REAC

Actinides

	150. D
PB212	1.10E+02
BI212	5.49E+00
RA223	1.70E+00
RA224	1.10E+03
TH228	3.18E+02
TH230	1.02E+01
TH231	8.55E+01
TH234	1.57E+04
PA231	2.74E+01
PA233	3.40E+03
PA234M	1.57E+01
PA234	3.14E+00
U232	2.46E+02
U233	1.54E+00
U234	2.52E+04
U235	5.70E+02
U236	9.61E+03
U237	2.65E+04
U238	7.85E+03
NP237	1.13E+05
NP239	1.92E+05
PU236	1.06E+04
PU238	5.64E+08
PU239	6.46E+07
PU240	9.55E+07
PU241	5.15E+08
PU242	2.76E+05
AM241	3.85E+07
AM242M	2.29E+06
AM242	9.15E+04
AM243	4.54E+06
CM242	8.88E+08
CM243	7.36E+05
CM244	6.44E+08
CM245	8.54E+04
CM246	1.71E+04
CM248	1.98E+00
BK249	6.54E+00
CF250	3.09E+00
CF252	2.26E+00
SUBTOT	2.52E+09
TOTALS	2.52E+09

Fission Products

	150. D
H 3	2.31E+05
KR 85	1.10E+04
RB 86	9.49E+04
SR 89	3.24E+10
SR 90	2.56E+11
Y 90	3.84E+09
Y 91	5.37E+09
ZR 93	2.36E+03
NB 93M	4.52E+02
ZR 95	4.62E+09
NB 95M	3.88E+03
NB 95	5.20E+09
MO 99	2.55E-06
TC 99	7.17E+04
RU103	1.10E+09
RH103M	8.83E+06
RU106	4.10E+10
RH106	4.10E+05
PD107	1.10E+02
AG110M	3.14E+07
AG110	3.17E+02
AG111	9.47E+02
CD113M	1.03E+01
IN114M	3.69E+03
CD115M	1.64E+06
SN119M	1.28E+01
SN123	3.86E+03
SB124	3.59E+06
SN125	1.66E+04
SB125	7.95E+07
TE125M	3.23E+07
TE127M	1.23E+08
TE127	3.04E+07
TE129M	1.65E+08
TE129	3.17E+06
I129	5.23E+05
I131	7.28E+06
XE131M	3.19E+00
TE132	7.37E-04
I132	1.95E-03
XE133	3.35E-03
CS134	2.38E+10
CS135	2.36E+03
CS136	3.41E+05
CS137	5.04E+09
BA137M	9.99E+04
BA140	2.16E+07
LA140	2.48E+07
CE141	6.47E+08
PR143	1.36E+07
CE144	7.71E+10
PR144	7.71E+05
ND147	8.39E+05
PM147	4.30E+08
PM148M	3.27E+07
PM148	3.03E+02
SM151	3.12E+06
EU152	1.53E+05
GD153	1.16E+05
EU154	3.43E+08
EU155	2.20E+07
EU156	2.21E+02
TB160	7.38E+06
SUBTOT	4.58E+11
TOTALS	4.58E+11

APPENDIX C-3

FISSION PRODUCT AND ACTINIDE CONCENTRATIONS EXITING FROM THE REPROCESSING PLANT

PWR FUEL CYCLE DECAY TIMES OF FUEL AFTER 1ST PROCESSING
POWER= 30.00MW, BURNUP= 33000.MWD, FLUX= 2.92E+13N/CM**-SEC
NUCLIDE INGESTION HAZARD, M**3 OF WATER AT RCG
BASIS = PER METRIC TONNE OF U LOADED IN REAC

Actinides

	DISCHARGE
PB212	1.10E+02
BI212	5.49E+00
RA223	1.70E+00
RA224	1.10E+03
TH228	3.18E+02
TH230	1.02E+01
TH234	1.57E+04
PA231	2.74E+01
PA233	3.40E+03
U232	2.46E+00
U234	2.52E+02
U235	5.70E+00
U236	9.61E+01
U237	2.65E+02
U238	7.85E+01
NP237	1.13E+05
NP239	1.82E+05
PU236	2.12E+02
PU238	1.13E+07
PU239	1.29E+06
PU240	1.91E+06
PU241	1.03E+07
PU242	5.52E+03
AM241	3.85E+07
AM242M	2.29E+06
AM242	9.15E+04
AM243	4.54E+06
CM242	8.88E+08
CM243	7.36E+05
CM244	3.44E+08
CM245	8.54E+04
CM246	1.71E+04
CM248	1.98E+00
BK249	6.44E+00
CF249	8.96E-01
CF250	3.69E+00
CF252	2.26E+00
SUBTOT	1.30E+09
TOTALS	1.30E+09

Fission Products

	DISCHARGE
H 3	2.31E+05
KR 85	1.10E+04
RB 86	9.49E+04
SR 89	3.24E+10
SR 90	2.56E+11
Y 90	3.84E+09
Y 91	5.37E+09
ZR 93	2.36E+03
NB 93M	4.52E+02
ZR 95	4.62E+09
NB 95M	5.88E+03
NB 95	5.20E+09
TC 99	7.17E+04
RU103	1.19E+09
RH103M	8.83E+06
RU106	4.10E+10
RH106	4.10E+05
PD107	1.10E+02
AG110M	8.14E+07
AG110	8.17E+02
CD113M	1.13E+01
IN114M	9.59E+03
CD115M	1.64E+06
SN119M	1.08E+01
SN123	3.38E+03
SB124	3.59E+06
SB125	7.95E+07
TE125M	3.20E+07
TE127M	1.23E+08
TE127	3.04E+07
TE129M	1.35E+08
TE129	2.17E+06
I129	8.23E+05
I131	7.28E+06
CS134	2.38E+10
CS135	2.85E+03
CS136	3.41E+05
CS137	5.34E+09
BA137M	9.99E+04
BA140	2.16E+07
LA140	2.48E+07
CE141	6.27E+08
PR143	1.36E+07
CE144	7.71E+10
PR144	7.71E+05
ND147	8.39E+05
PM147	4.90E+08
PM148M	3.27E+03
PM148	2.83E+02
SM151	3.12E+06
EU152	1.53E+05
GD153	1.16E+05
EU154	3.43E+08
EU155	3.20E+07
TB160	7.53E+06
SUBTOT	4.58E+11
TOTALS	4.58E+11

APPENDIX C-4

FISSION PRODUCT AND ACTINIDE CONCENTRATIONS AFTER 215 DAYS
STORAGE IN HIGH LEVEL LIQUID WASTE STORAGE FACILITY

PWR FUEL CYCLE DECAY TIMES OF FUEL AFTER 1ST PROCESSING
POWER= 30.00MW, BURNUP= 33000.MWD, FLUX= 2.92E+13N/CM**2-SEC
NUCLIDE INGESTION HAZARD, M**3 OF WATER AT RCG
BASIS = PER METRIC TONNE OF U LOADED IN REAC

Actinides

	CHARGE	215. D
PB212	0.	9.11E+01
BI212	0.	4.55E+00
RA223	0.	2.33E+00
RA224	0.	9.11E+02
TH228	0.	2.59E+02
TH230	0.	1.02E+01
TH234	0.	1.89E+02
PA231	0.	2.74E+01
PA233	0.	3.40E+03
U232	0.	3.56E+00
U234	5.45E+04	2.56E+02
U235	2.36E+03	5.70E+00
U236	0.	9.61E+01
U237	0.	4.81E+02
U238	8.05E+03	7.85E+01
NP237	0.	1.13E+05
NP239	0.	1.82E+05
PU236	0.	1.84E+02
PU238	0.	2.19E+07
PU239	0.	1.29E+06
PU240	0.	1.94E+06
PU241	0.	1.00E+07
PU242	0.	5.52E+03
AM241	0.	3.90E+07
AM242M	0.	2.28E+06
AM242	0.	9.12E+04
AM243	0.	4.54E+06
CM242	0.	3.56E+08
CM243	0.	7.26E+05
CM244	0.	3.36E+08
CM245	0.	8.54E+04
CM246	0.	1.71E+04
CM248	0.	1.98E+00
BK249	0.	4.61E+00
CF249	0.	1.49E+00
CF250	0.	3.58E+00
CF252	0.	1.94E+00
SUBTOT	6.50E+04	7.74E+08
TOTALS	6.50E+04	7.74E+08

Fission Products

	215. D
H 3	2.23E+05
KR 85	1.06E+04
RB 86	3.28E+01
SR 89	1.84E+09
SR 90	2.52E+11
Y 90	3.79E+09
Y 91	4.26E+08
ZR 93	2.36E+03
NB 93M	5.78E+02
ZR 95	4.67E+08
NB 95M	5.94E+02
NB 95	5.96E+08
TC 99	7.17E+04
RU103	2.56E+07
RH103M	2.05E+05
RU106	2.73E+10
RH106	2.73E+05
PD107	1.10E+02
AG110M	4.51E+07
AG110	1.76E+02
CD113M	9.99E+00
IN114M	4.92E+02
CD115M	5.11E+04
SN119M	5.96E+00
SN123	1.17E+03
SB124	2.99E+05
SB125	6.83E+07
TE125M	2.83E+07
TE127M	3.13E+07
TE127	7.74E+06
TE129M	1.69E+06
TE129	2.71E+04
I129	6.24E+05
I131	6.64E-02
CS134	1.95E+10
CS135	2.86E+03
CS136	3.58E+00
CS137	5.27E+09
BA137M	9.85E+04
BA140	1.89E+02
LA140	2.18E+02
CE141	6.31E+06
PR143	2.56E+02
CE144	4.56E+10
PR144	4.56E+05
ND147	1.24E+00
PM147	4.19E+08
PM148M	9.46E+01
PM148	7.55E+00
SM151	3.11E+06
EU152	1.48E+05
GD153	6.25E+04
EU154	3.35E+08
EU155	2.55E+07
TB160	9.80E+05
SUBTOT	3.58E+11
TOTALS	3.58E+11

ANNUAL REPORT

NASA GRANT NSG-1288

GAS CORE REACTORS FOR ACTINIDE TRANSMUTATION AND BREEDER APPLICATIONS

J. D. Clement and J. H. Rust

NASA Program Manager, F. Hohl

Prepared for the

National Aeronautics and Space Administration

by the

School of Nuclear Engineering
Georgia Institute of Technology
Atlanta, Georgia 30332

April 1, 1978

ANNUAL REPORT

NASA GRANT NSG-1288

GAS CORE REACTORS FOR ACTINIDE TRANSMUTATION AND BREEDER APPLICATIONS

J. D. Clement and J. H. Rust

NASA Program Manager, F. Hohl

Prepared for the

National Aeronautics and Space Administration

by the

School of Nuclear Engineering
Georgia Institute of Technology
Atlanta, Georgia 30332

April 1, 1978

ACKNOWLEDGMENTS

This work was supported by NASA Grant NSG-1288, Supplement No. 1. The authors wish to express their appreciation to the program manager, Dr. Frank Hohl, for helpful suggestions during the performance of the research.

The following graduate students, supported by the grant, made significant contributions to the research project: Stanley Chow and Pak Tai Wan.

In addition, the NASA research program was also used as a design project for the Nuclear Engineering design course in the academic curriculum. The following graduate students taking the course were of great assistance in the research work: Constantine Bratianu, Stanley Chow, Trent Primm, and Scott Revolinski.

TABLE OF CONTENTS

LIST OF FIGURES

LIST OF FIGURES (Continued)

LIST OF TABLES

LIST OF TABLES

Abstract

The work summarized in this report, which was carried out as a part of a NASA sponsored fissioning plasma research program, consisted of design power plant studies for four types of reactor systems: uranium plasma core breeder, uranium plasma core actinide transmuter, UF_6 breeder and UF_6 actinide transmuter.

The plasma core systems can be coupled to MHD generators to obtain high efficiency electrical power generation. A power plant employing a ternary cycle of MHD generator, gas turbine, and steam cycle may have efficiencies of 60 to 70 percent for reactor exit temperatures of $3000^{o}K$ to $4000^{o}K$, respectively. The material problems are severe so that this system will require long research and development times and can, therefore, be regarded as an advanced system.

On the other hand, the UF_6 reactor would require only a modest extension of present day technology for its development. A 1074 MWt UF_6 breeder reactor was designed with a breeding ratio of 1.002 to guard against diversion of fuel. Using molten salt technology and a superheated steam cycle, an efficiency of 39.2% was obtained for the plant and the U^{233} inventory in the core and heat exchangers was limited to 105 kg.

It was found that the UF_6 reactor can produce high fluxes (10^{14} n/cm^2-sec) necessary for efficient burnup of actinides. However, the buildup of fissile isotopes posed severe heat transfer problems. Therefore, the flux in the actinide region must be decreased with time. Consequently, only beginning-of-life conditions were considered for the power plant design. A 577 MWt UF_6 actinide transmutation reactor power plant was

designed to operate with 39.3% efficiency and 102 kg of U^{233} in the core and heat exchangers for beginning-of-life conditions. Additional work is needed to solve the heat transfer problems.

1. INTRODUCTION

The need to produce more electricity within certain social, economic, and political constraints has forced the United States to reevaluate many of its energy policies. In particular, the nuclear industry is beset by problems of dwindling uranium resources, waste management, and nuclear proliferation among others. The political and social pressures have been great enough to delay commercialization of the liquid metal fast breeder reactor for an indefinite period and has prompted a growing effort to look at alternative systems.

One such alternative is the gas core reactor which has been supported by the National Aeronautics and Space Administration for almost twenty years. The original goal in research and development of the gas core reactor was to produce a space propulsion reactor that would be capable of fast, manned expeditions to neighboring planets.[1]

Although budgetary and policy factors terminated the development of nuclear powered propulsion engines, NASA has continued to sponsor fissioning plasma research consisting of cavity reactor criticality tests, fluid mechanics tests, investigation of uranium optical emission spectra, radiant heat transfer studies, and related theoretical work.[2,3] Research has shown that UF_6 fueled reactor can be quite versatile with respect to power, pressure, operating temperature, and modes of power extraction.[4] Possible power conversion systems include Brayton cycles, Rankine cycles, MHD generators, and thermionic diodes. Power extraction may also be possible in the form of coherent light from interactions of fission fragments with a laser gas mixture.

NASA is also conducting a series of UF_6 non-flowing and flowing critical experiments at the Los Alamos Scientific Laboratory.[5] If preceding steps are successful, a reactor experiment may be performed in the early 1980's at the Nuclear Rocket Development Station for a uranium plasma at 6000°K and producing 5 MW of thermal power.

In addition, the International Security Affairs Office of the U.S. Energy Research and Development Administration (now the Department of Energy) has sponsored research on non-proliferating gas core reactor power plants.[6-9] Initial studies show that fuel inventories may be a factor of 10 less than those in current U.S. power reactors.

A study[10] was also conducted by the University of Florida on heterogeneous gas core reactors (HGCR) for power generation. An approximately 50-50 mixture of UF_6 and He was used as the gaseous fuel. Designs for a 3000 MWt light-water moderated, and a 1000 MWt heavy-water moderated HGCRs were presented.

The Georgia Institute of Technology has been engaged in various gas core reactor power plant concepts under NASA sponsorship. One such concept utilized a uranium plasma, breeder reactor employing a MHD generator for the topping cycle.[11,12] Power plant efficiencies of 70 percent are attainable with this high temperature reactor.

More recent work done at Georgia Tech involves the application of UF_6 reactors for breeding and actinide transmutation purposes.[13,14] Several advantages of these systems were identified.

An advantage of UF_6 reactor systems is the continuous on-line reprocessing of fluid fuels. By bleeding off a small percentage of the UF_6 from the primary loop, fission product and actinide buildup can be continuously removed by reprocessing. This results in a better fuel economy for the reactor.

The UF_6 reactor is inherently safe because the conventional loss-of-coolant accident cannot occur, the core contains a minimum amount of radioactive fission products, and the temperature coefficient of reactivity is negative which prevents accidental power excursions.

Reference 13 indicates that UF_6 breeder reactors may have breeding ratios of 1.25 - 1.26 for core diameters varying from 1 to 5 m and that fuel doubling times may be as small as a few years. Reference 14 shows that the gas core actinide transmutation reactor may be capable of burning up 10.3 metric tons of actinides in 40 years as compared to 2.93 and 0.423 for the liquid metal fast breeder reactor and the light water reactor, respectively.

One significant advantage of the gas core reactors over conventional reactors is that it has a smaller critical mass. This is important since reducing system uranium inventory may reduce the risk of fuel diversion. However, this will place an added design constraint. For example, a breeder reactor may be designed with a breeding ratio just sufficient to fuel itself. The rationale behind this design is that any diversion of fuel would cause the reactor to shut down. The resulting loss of the use of a power reactor may be a deterrent to fuel diversion.

This report reexamines both plasma core and UF_6 breeder and actinide transmutation reactors in the light of reducing fuel inventories. However, full optimizations of these systems were beyond the scope of this study.

Chapter 2 summarizes the results for high temperature uranium plasma breeder and actinide transmutation power plants employing MHD topping cycles. A detailed study was made in Ref. 15. Chapter 3 analyzes the UF_6 breeder power plants while Chapter 4 analyzes UF_6 actinide transmutation power plants. Finally, conclusions and recommendations are presented in Chapter 5.

References for Chapter 1

1. Ragsdale, R. G., "To Mars in 30 Days by Gas Core Nuclear Rocket," Astronautics and Aeronautics, 10, No.1 (1971).

2. Thom, K., Schneider, R. T., and Schwenk, F.C., "Physics and Potentials of Fissioning Plasmas for Space Power and Propulsion," International Astronautical Federation 25th Congress, Paper No. 74087, Amsterdam (October 1974).

3. Schwenk, F. C. and Thom, K. T., "Gaseous Fuel Nuclear Reactor Research," paper presented at the Oklahoma State University Conference on Frontiers of Power Technology (October 1974).

4. Rodgers, R. J., Latham, T. S., and Krascella, N. L., "Investigation of Applications for High-Power, Self-Critical Fissioning Uranium Plasma Reactors," NASA CR-145048 (September 1976).

5. Rodgers, R. J., Latham, T. S., and Krascella, N.L., "Analyses of Low-Power and Plasma Core Cavity Reactor Experiments," United Aircraft Research Laboratories Report R75-911908-1 (May 1975).

6. Lowry, L. L., "Gas Core Reactor Power Plants Designed for Low Proliferation Potentials," LA-6900-MS (September 1977).

7. Soran, P. D. and Hansen, G. E., "Neutronics of a Mixed-Flow Gas-Core Reactor," LA-7036-MS (November 1977).

8. Lowry, L. L., Helmick, H. H., and Kendall, J. S., "The Nonproliferation Features of the Gas Core Reactor," Transactions of the American Nuclear Society, 27, 933 (November 27-December 2, 1977).

9. Mc Laughlin, T. P., Soran, P. D., and Hansen, G.E., "Gas Core Reactors: Neutronics, SNM Proliferation, and Resource Utilization," Transactions of the American Nuclear Society, 27, 934-35 (November 27-December 2, 1977).

10. Han, K. I., Dugan, E. T., and Diaz, N. J., "Heterogeneous Gas Core Reactor Power Plants," Transactions of the American Nuclear Society, 27, 722-724 (November 27-December 2, 1977).

11. Williams, J. R. and Clement, J.D., "Exploratory Study of Several Advanced Nuclear-MHD Power Plant Systems," Final Status Report, NASA Grant NGR-11-002-145, Georgia Institute of Technology, Atlanta, Georgia (March 1973).

12. Williams, J. R. and Clement, J.D., "Satellite Nuclear Power Station - An Engineering Analysis," NASA Grant NGR-11-002-145, Georgia Institute of Technology, Atlanta, Georgia (March 1973).

13. Clement, J. D. and Rust, J. H., "Analysis of UF_6 Breeder Reactor Power Plants," Final Report, NASA Grant NSG-1168, Georgia Institute of Technology, Atlanta, Georgia (February 1976).

14. Clement, J. D. and Rust, J. H.,"Analysis of the Gas Core Actinide Transmutation Reactor (GCATR)," Annual Report, NASA Grant NSG-1288, Georgia Institute of Technology, Atlanta, Georgia (February 1977).

15. Clement, J. D. and Rust, J.H., "Analysis of the Gas Core Actinide Transmutation Reactor (GCATR)," Semi-Annual Report, NASA Grant NSG-1288, Supplement No.1, Georgia Institute of Technology, Atlanta, Georgia (September 1977).

2. HIGH TEMPERATURE URANIUM PLASMA POWER PLANTS

The work summarized in this chapter, which is described in detail in Ref. 1, consists of design power plant studies for applications of the plasma core reactor as a breeder and as an actinide transmuter. In addition to these applications, the system produced electrical power with a high efficiency.

A reactor subsystem was designed for each of the two applications. Tables 2.1 and 2.2 summarize the reactor design parameters for the breeder and the actinide transmuter, respectively.

For the breeder reactor, neutronics calculations were carried out for a U-233 plasma core with a molten salt breeding blanket. The primary objectives of the overall nuclear design were to design a reactor with a low critical mass (less than a few hundred kilograms U-233) and also a breeding ratio of 1.01. The later objective was a safety precaution to guard against diversion of fissionable material during blanket reprocessing. Since only enough U-233 would be bred in the blanket to replenish the amount depleted in the core, any diversion of U-233 during reprocessing would result in an insufficient amount of fissionable material to replenish the core and the reactor would shut down. Both of the above objectives were met in the final design. It is also possible to design for much higher breeding ratios in the range 1.1-1.2.

The Plasma Core Actinide Transmutation reactor was designed to transmute the nuclear waste from conventional LWR's. Each LWR is loaded with

Table 2.1 Plasma Core Breeder Reactor Reference Design

Dimensions of Reactor Regions	
U^{233} Plasma	- 165 cm O.D.
Helium	- 285 cm O.D.
BeO Moderator	- 325 cm O.D.
Molten Salt*	- 355 cm O.D.
BeO Reflector	- 375 cm O.D.
Fe Pressure Shell	- 415 cm O.D.
Critical Mass	- 26.3 kg
Breeding Ratio	- 1.0099
Power	- 2000 MWt
Average Thermal Flux in Plasma	- 3.42×10^{15} n/cm^2-sec
Reactor Pressure	- 200 atm
Average Temperatures	
U^{233} Plasma	- 25,000°K
Helium	- 3,000°K
Molten Salt	- 1,015°K
Molten Salt Mass Flow Rate	- 542 kg/sec

*Molten Salt Composition - 71.7% LiF (99.995% Li^7), 16% BeF_2, 12.3% ThF_4

Table 2.2 Plasma Core Actinide Transmutation Reactor Reference Design

Dimensions of Reactor Regions

U^{233} Plasma	-	200 cm thickness
He	-	120 cm thickness
Be Moderator	-	17 cm thickness
*Act. Oxide + Zr + He	-	0.85 cm thickness
Be Reflector	-	80-90 cm thickness

Critical Mass	-	380 kg
Mass of Actinides	-	1.27 metric tonne
Power	-	2000 MWt
Average Thermal Flux in Plasma	-	2.06×10^{14} n/cm^2-sec
Average Thermal Flux in Actinides	-	1.23×10^{14} n/cm^2-sec
Reactor Pressure	-	200 atm.

Temperatures

U^{233} Plasma	-	25000°K
He	-	3000°K
Be Moderator	-	1000°K
Act. Oxide + Zr + He	-	800°K
Be Reflector	-	400-600°K

*Actinide Composition: 74% Np^{237}; 7% Am^{241}; 14% Am^{24}; 4% Cm^{244}.

88 metric tonnes of uranium (3.3% U^{235}) and operated until a burnup of 33,000 MWD/MTU is reached. The fuel is discharged from the reactor and cooled for 160 days. Next, the spent fuel is reprocessed during which 100% of Np, Am, Cm, and higher actinides are separated from the other components. The concentrations of these actinides are calculated by ORIGEN[2] and tabulated. These actinides are then manufactured as oxides into zirconium clad fuel rods and charged as fuel assemblies in the reflector region of the plasma core actinide transmutation reactor. Results of actinide burnup calculations for an equilibrium plasma core transmuter servicing 27 PWR's show that after 12 cycles the actinide inventory has stabilized to about 2.6 times its initial loading. There are two mechanisms for the removal of actinides:

(1) They are fissioned directly in the plasma core actinide transmuter

(2) They are removed as U or Pu.

The U and Pu can be used in other reactors. In the equilibrium cycle, about 7% of the actinides are directly fissioned away, while about 31% is removed by reprocessing.

Fluid mechanics, heat transfer, and mechanical design considerations for both reactors are also described in Ref. 1.

Since it is desirable to have the Plasma Core Breeder Reactor (PCBR) be a self-contained unit, generating its own new fuel, an on-line reprocessing system for the molten salt blanket is a necessity. Reference 1 describes protactinium removal and salt purification processes, calculations of expected flow rates, and equilibrium concentrations of various isotopes present in the system.

In order to achieve maximum effectiveness from the high temperature coolants from either of the two plasma core reactors, it was decided that a ternary power cycle would produce the highest efficiency power plant. The ternary cycle consists of a combination of MHD, gas turbine, and Rankine cycle energy conversion units. Two concepts were investigated — a system with a high temperature regenerator in the helium loop, shown in Fig. 2.1, and a system without a regenerator, shown in Fig. 2.2.

The achieved objectives of the study were as follows:

(1) Model the nuclear MHD power plant cycle.

(2) Analyze the power output from the three energy conversion units and evaluate plant overall efficiency.

(3) Make a parametric study of the effect of changing operating variables on plant overall performance.

All studies used values for input data according to current commercial technology (i.e. efficiencies for steam cycle components, gas turbine, and compressors) or with current use in MHD research.

The modeling of the MHD cycle consisted of defining a pseudo-Brayton cycle and treating the expansion within the MHD generator in a similar manner as in a gas turbine. In order to analyze the two systems it was necessary to write two computer codes:

(1) NMHD-1 — code to analyze the nuclear MHD power plant without regeneration in the helium loop

(2) NMHD-2 — code to analyze the nuclear MHD power plant with regeneration in the helium loop.

Table 2.3 lists input parameters for each system.

A study was made of the effect on overall efficiency of varying the reactor coolant outlet temperature from $3000^{o}K$ to $4000^{o}K$ for the two

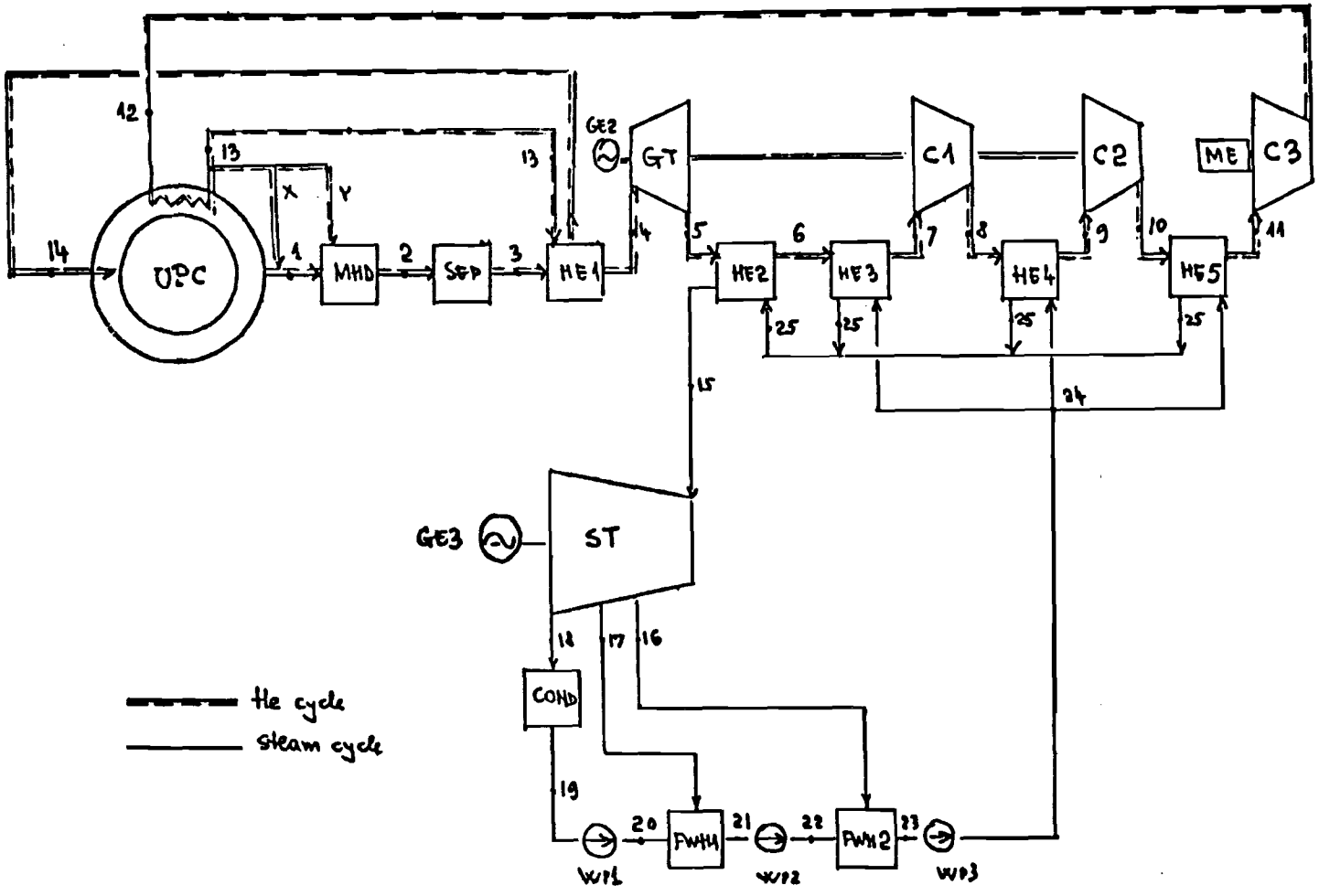

UPC - Uranium Plasma Core; MHD - MHD Generator; SEP - Diffuser and Separator; HE1 - Regenerative Heat Exchanger; HE2,3,4 and 5 - Heat Exchangers; GE - Electric Generator; GT - Gas Turbine; C - Compressor; ME - Electric Motor; ST - Steam Turbine; COND - Condenser; WP - Water Pump; FWH - Feed Water Heater.

Fig. 2.1 Nuclear MHD Power Plant With Regeneration

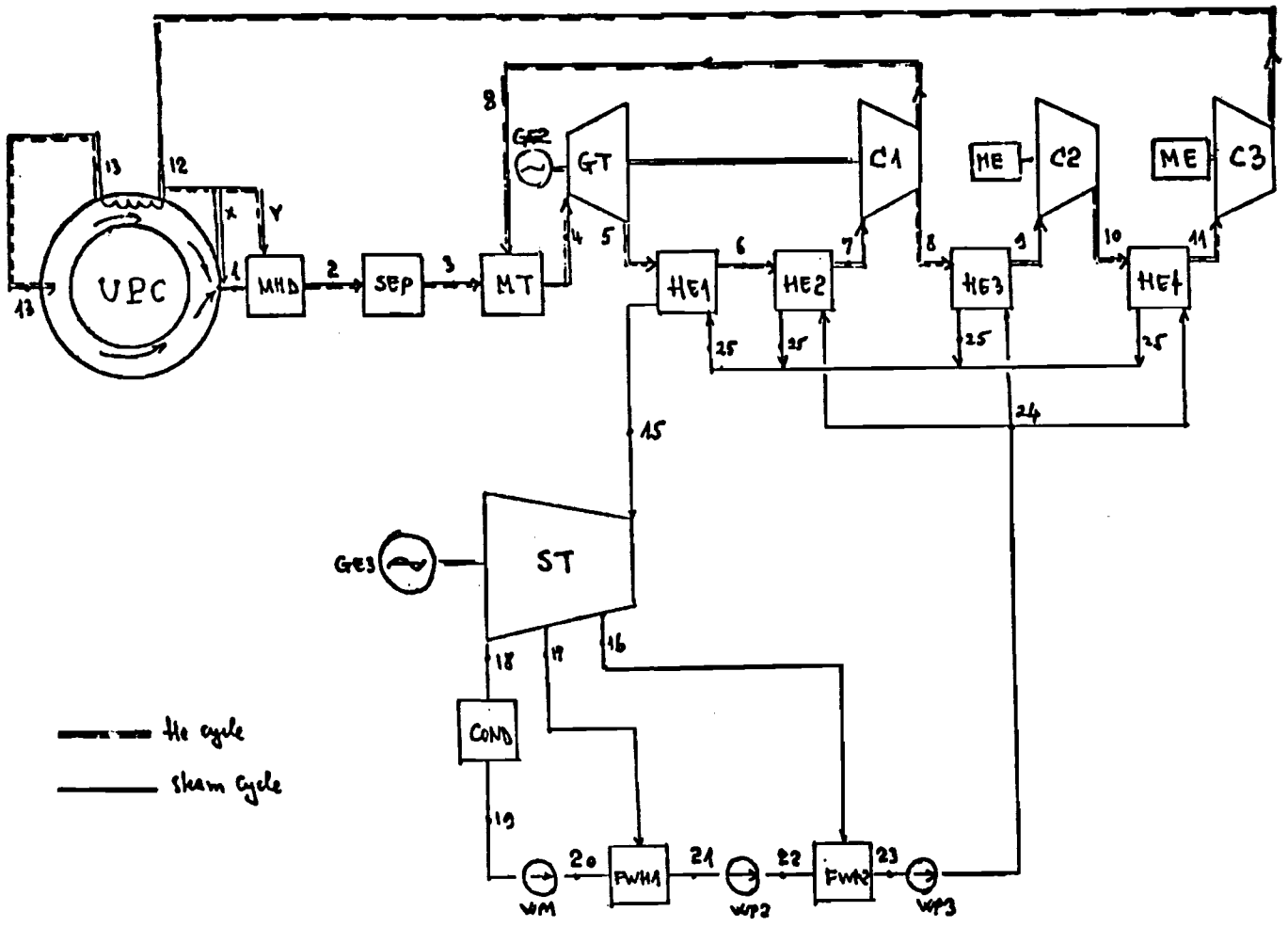

UPC - Uranium Plasma Core; MHD - MHD generator; SEP - Diffuser and Separator; MT - Mixing Tank; GE - Electric Generator; GT - Gas Turbine; C - Compressor; HE - Heat Exchanger; ME - Electric Motor; ST - Steam Turbine; COND - Condenser; WP - Water Pumps; FWH - Feed Water Heater.

Fig. 2.2 Nuclear MHD Power Plant Without Regeneration

Table 2.3 Input Data for NMHD-1 and NMHD-2

Index	NMHD-1		NMHD-2	
1	Boiler Temperature ----	1000°F	Boiler Temperature ----	1000.°F
2	Boiler Pressure -------	1600 psia	Boiler Pressure -------	1600 psia
3	Condenser Pressure ----	1.0 psia	Condenser Pressure ----	1.0 psia
4	Steam Turbine Efficiency	81%	Steam Turbine Efficiency	81%
5	Pump Efficiency -------	80%	Number of Feed Heaters	0,1 or 2
6	Number of Feed Heaters	0,1 or 2	Reactor Temp Difference	200°K
7	Compressor Efficiency -	85%	Compressor Efficiency -	85%
8	MHD Inlet Temp --------	3000°K	MHD Inlet Temp --------	3000°K
9	MHD Inlet Press -------	200 bar	MHD Inlet Press -------	200 bar
10	MHD Pressure Ratio ----	5.0	MHD Pressure Ratio ----	3.0
11	Gas Turbine Pressure Ratio	2.0	Gas Turbine Press. ratio	3.0
12	Feed Heater 1 Pressure	12. psia	Feed Heater 1 press. --	12. psia
13	Feed Heater 2 Pressure -	4. psia	Feed Heater 2 press. --	4.0 psia
14	Bottom Temp Difference -	150°K	Bottom Temp Diff. ----	150°K
15	MHD Inlet Mach No. ----	0.5	MHD Inlet Mach No. ----	0.5
16	Sep Outlet Mach No. ----	0.1	Sep Outlet Mach No. ---	0.1
17	Gas Turbine Inlet Temp -	1500°K	Gas Turbine Inlet Temp	1500°K
18	MHD Efficiency ---------	49%	MHD Efficiency --------	49%
19	Gas Turbine Efficiency -	85%	Gas Turbine Efficiency	85%
20	Number of Compress Stages	3.0	Number of Compress Stages	3.0

systems. Tables 2.4 and 2.5 list typical results, showing an overall plant efficiency as high as 70%.

For Nuclear MHD Power Plant with regeneration (Fig. 2.1), the major contribution of the electric power is produced in the top of the power cycle by the MHD subsystem (33.97% - 45.49% from 100% heat produced by the reactor). The power production has been shifted toward the top of the ternary cycle with a large increase in overall efficiency. This system produces overall efficiencies that are 60 - 80% higher than actual power plants in use and 25 - 45% higher than expected coal-fired MHD power plants.

For Nuclear MHD Power Plants without regeneration (Fig. 2.2), the major contribution of electric power is due to the steam turbine subsystem (36.03% - 36.36% from 100% heat produced by the reactor). Due to a significant fraction of the electric power being produced by the steam cycle at lower efficiencies (40%), it is desirable to shift the power production toward the top of the cycle to improve the overall efficiency. This can be achieved by reducing the mass flow rate of helium within the inner loop and increasing the pressure ratio of the MHD generator. This system produced overall efficiencies that are 40 - 50% higher than actual power plants in use, and 10 - 15% higher than expected coal-fired MHD power plants. Due to the relatively low temperatures within the helium loop, this type of power plant could be considered as a first step in a national program of implementation of MHD power plants with a nuclear source.

Table 2.4 Plant Overall Efficiencies with High Temperature Regenerator

MHD Inlet Temperature	3000°K		3250°K		3500°K		3750°K		4000°K	
Q_R	4973.45	100.0%	5138.94	100.00%	5299.94	100.00%	5458.27	100.0%	5693.55	100.0%
W_{MHD}	1689.52	33.97%	1914.65	37.26%	2139.78	40.37%	2139.78	43.44%	2590.04	45.49%
W_{GT}	319.12	6.42%	319.12	6.21%	319.12	6.02%	319.12	5.85%	319.12	5.60%
W_{ST}	1112.20	22.36%	1112.20	21.64%	1112.20	20.99%	1112.20	20.38%	1112.20	19.53%
η_{PLANT}	62.75%		65.11%		67.38%		69.56%		70.62%	

Q_R = REACTOR HEAT RATE

W_{MHD} = MHD NET ELECTRIC POWER: $W_{MHD} = W_{MHD\ OUTPUT} - W_{COMPRESSOR}$

W_{GT} = GAS TURBINE ELECTRIC POWER: $W_{GT} = W_{GT\ OUTPUT} - 2 \times W_{COMPRESSOR}$

W_{ST} = STEAM TURBINE ELECTRIC POWER: $W_{ST} = W_{ST\ OUTPUT} - W_{PUMP}$

$$\eta_{PLANT} = \left(\frac{W_{MHD}}{Q_R} + \frac{W_{GT}}{Q_R} + \frac{W_{ST}}{Q_R}\right) \times 100 = \left(\frac{W_{MHD}}{Q_R}\,100\right) + \left(\frac{W_{GT}}{Q_R}\,100\right) + \left(\frac{W_{ST}}{Q_R}\,100\right) \quad [\%]$$

Table 2.5 Plant Overall Efficiencies without High Temperature Regenerator

MHD Inlet Temperature	3000°K		3250°K		3500°K		3750°K		4000°K	
Gas Flow Rate Through the GT.	2.33 kg/sec		2.60 kg/sec		2.88 kg/sec		3.15 kg/sec		3.42 kg/sec	
Q_R	12265.71	100.0%	13563.96	100.0%	14862.21	100.0%	16160.46	100.0%	17458.71	100.0%
W_{MHD}	1777.71	14.49%	2077.87	15.32%	2378.55	16.0%	2679.22	16.58%	2929.90	17.07%
W_{GT}	456.46	3.72%	510.00	3.76%	563.54	3.79%	617.68	3.82%	670.62	3.84%
W_{ST}	4419.73	36.03%	4901.75	36.14%	5383.76	36.22%	5865.78	36.30%	6347.80	36.36%
η_{PLANT}	54.24%		55.22%		56.01%		56.70%		57.27%	

Q_R = REACTOR HEAT RATE

W_{MHD} = MHD NET ELECTRIC POWER : $W_{MHD} = W_{MHD\ OUTPUT} - 2W_{COMPRESSOR}$

W_{GT} = GAS TURBINE ELECTRIC POWER : $W_{GT} = W_{GT\ OUTPUT} - W_{COMPRESSOR}$

W_{ST} = STEAM TURBINE ELECTRIC POWER: $W_{ST} = W_{ST\ OUTPUT} - W_{PUMP}$

$$\eta_{PLANT} = \left(\frac{W_{MHD}}{Q_R} + \frac{W_{GT}}{Q_R} + \frac{W_{ST}}{Q_R}\right) \times 100 = \left(\frac{W_{MHD}}{Q_R}\,100\right) + \left(\frac{W_{GT}}{Q_R}\,100\right) + \left(\frac{W_{ST}}{Q_R}\,100\right) \quad [\%]$$

References for Chapter 2

1. Clement, J. D. and Rust, J. H., "Analysis of the Gas Core Actinide Transmutation Reactor," Semi-Annual Report, NASA Grant NSG-1288, Georgia Institute of Technology (September 1977).

2. Bell, M. J., "ORIGEN-The ORNL Isotope Generation and Depletion Code," ORNL-4628 (May 1973).

3. UF_6 BREEDER REACTOR POWER PLANT

A. Neutronics

Neutronics calculations were carried out for a uranium hexafluoride breeder reactor (UF_6BR). The primary objectives of the overall nuclear design were to design a reactor with a low critical mass (less than a few hundred kilograms U-233) and a breeding ratio of 1.0. The latter objective was a precaution to guard against diversion of fissionable material at any stage in the fuel cycle. Since only enough U-233 would be bred in the blanket to replenish the amount depleted in the core, any diversion of U-233 from the fuel cycle would result in an insufficient amount of fissionable material to replenish the core and the reactor would shut down. Both of the objectives were met in the final design.

The MACH-I Code[1] was used as the primary computational tool in the nuclear analysis. MACH-I is a one-dimensional, diffusion theory code. The 26-group ABBN cross section set of Bondarenko, et al[2] was used.

A cylindrical geometry was chosen which is shown in Fig. 3.1. The core consists of a $He - UF_6$ mixture flowing through a beryllium matrix. Addition of helium improves the heat transfer characteristics of the $He - UF_6$ mixture and is important in maintaining a small inventory of U-233 in the heat exchanger(s). The beryllium matrix provides the moderation needed by the neutrons. The partial pressures of He and UF_6 are 99 atm. and 0.69 atm., respectively. The core diameter is 200 cm and its height is 600 cm. Surrounding the core radially is a 60 cm thick breeding blanket. The breeding salt composition is 71.7 mole % LiF,

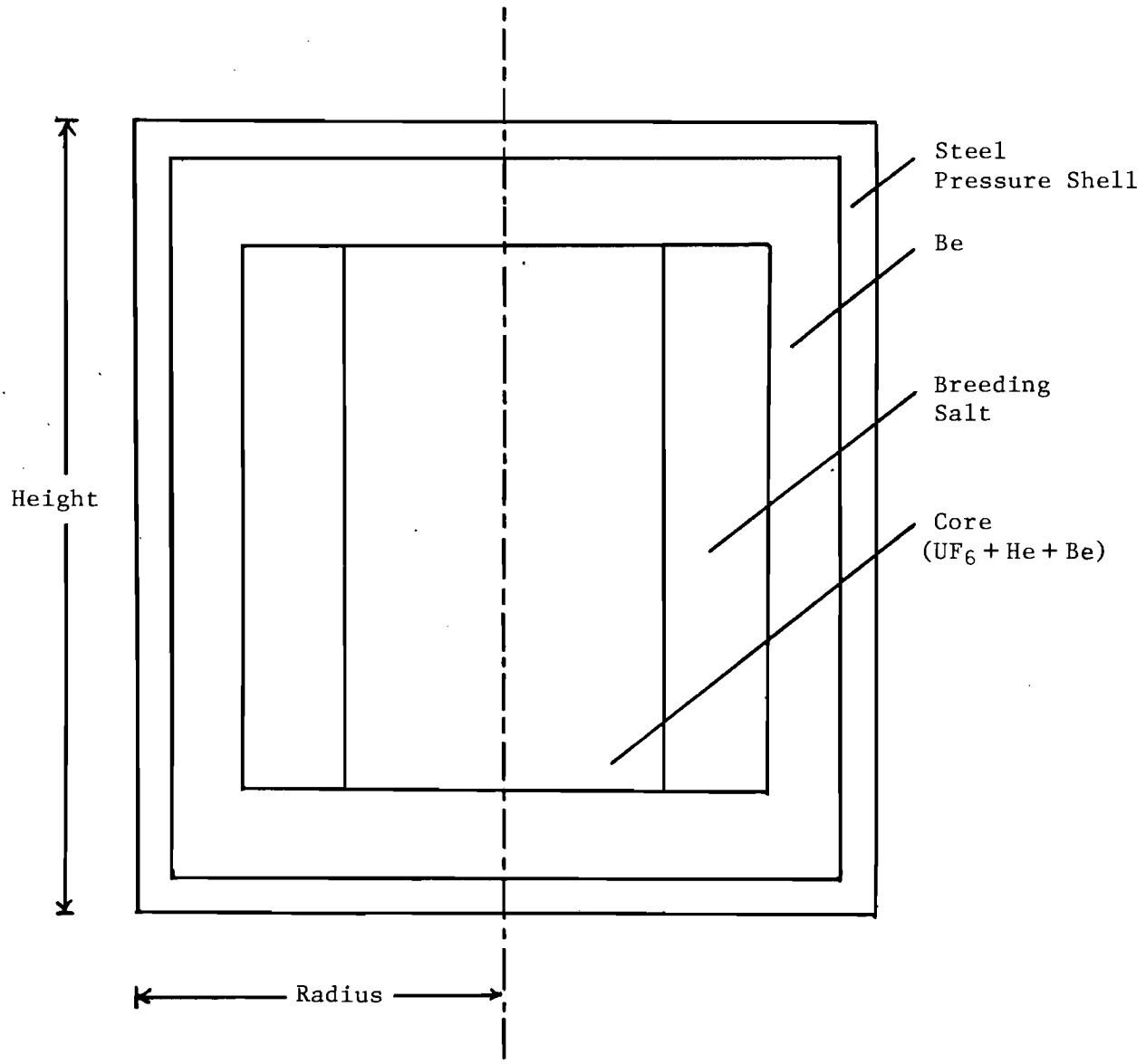

Fig. 3.1 Reactor Configuration of UF_6BR

16 mole % BeF_2, and 12.3 mole % ThF_4. The Li is enriched to essentially 100% Li^7. This composition is based on work done on the molten salt breeder reactor (MSBR) by the Oak Ridge National Laboratory.[3] Beryllium was used as a reflector both axially (20 cm) and radially (50 cm). The entire reactor is encased in a 20 cm thick stainless steel pressure shell.

Since the ABBN cross section set does not have cross sections for helium and fluorine, these were generated from cross section data from BNL-325.[4,5] The group-averaged cross sections were calculated as follows:

$$\langle \sigma_x \rangle_i = \frac{\int_{E_i} \sigma_x(E)\, \phi(E)\, dE}{\int_{E_i} \phi(E)\, dE} \tag{3.1}$$

where $\phi(E) = 0.77E^{\frac{1}{2}}\, e^{-0.776E}$ $\qquad 2.5 \text{ MeV} \leq E \leq 10 \text{ MeV}$

$= \frac{1}{E}$ $\qquad E \leq 2.5 \text{ MeV}$

The elastic and inelastic downscattering cross sections were calculated by:

$$\langle \sigma \rangle_{i \to j} = \frac{\int_{E_i} \int_{E_j} \sigma(E)\, \phi(E)\, P(E \to E')\, dE'\, dE}{\int_{E_i} \phi(E)\, dE} \tag{3.2}$$

for elastic scattering, $P(E \to E') = \frac{1}{(1-\alpha)E}$ $\qquad \alpha E < E' < E$

$= 0$ $\qquad$ otherwise $\qquad$ (3.3)

where $\alpha = \left(\frac{A-1}{A+1}\right)^2$

for inelastic scattering, $P(E \rightarrow E') = \frac{E'}{T^2} e^{-E'/T}$ (3.4)

with $T = 3.2\sqrt{\frac{E}{A}}$

A = Atomic no. of nuclide

The transport cross section was calculated by

$$\langle \sigma_{tr} \rangle = \langle \sigma_e \rangle (1 - \bar{\mu}_e) + \langle \sigma_{in} \rangle + \langle \sigma_c \rangle + \langle \sigma_f \rangle \quad (3.5)$$

where $\langle \sigma_{tr} \rangle$ = group averaged transport cross section

$\langle \sigma_e \rangle$ = group averaged elastic scattering cross section

$\bar{\mu}_e$ = average cosine of scattering angle

$= \frac{2}{3A}$

$\langle \sigma_{in} \rangle$ = group averaged inelastic scattering cross section

$\langle \sigma_c \rangle$ = group averaged capture cross section

$\langle \sigma_f \rangle$ = group averaged fission cross section

For helium, there are no resonances and all cross sections are smooth functions of energy. Fluorine-19 has a few elastic scattering resonances. It was estimated that for the fluorine in UF_6 and the breeding blanket, the effect of these resonances is small compared to the moderation in the beryllium and lithium. Hence, these resonances were neglected.

In the core and the breeding blanket, self shielding factors were used to take care of dilution effects. For the uranium in the core infinite dilution factors were used because of the low density of the UF_6

gas. For the thorium-232 in the blanket, a self shielding cross section of 61 barns was determined, and appropriate self shielding factors were accounted for.

Since the ABBN cross section set does not treat thermal cross sections accurately, the effective neutron temperature model was used. The thermal flux was assumed to be Maxwellian, $\phi(E) \alpha E\, e^{-E/kT_n}$, where T_n = effective neutron temperature. Following the treatment of Wescott[6] the average thermal cross section is given by

$$\langle \sigma_x \rangle_{th} = \sigma_x(E_o) \frac{\sqrt{\pi}}{2} \sqrt{\frac{T_o}{T}}\, g_x(T) \qquad (3.6)$$

where (E_o, T_o) is, by convention, (0.025 eV, 293.16 °K) and $g_x(T)$ is the non $\frac{1}{v}$ factor for reaction x.

A neutron temperature of 783°K was assumed for the calculations. For this neutron temperature, groups 25 and 26 were combined as the thermal group.

For the cylindrical geometry chosen, a complete calculation would require a two-dimensional calculation. Since MACH-I is a one-dimensional code, the infinite slab and infinite cylinder geometries were used to model the axial and radial neutronics of the reactor. The two geometries were coupled together by group dependent bucklings in the axial and radial directions. Iteration between the axial and radial calculations were carried out until a consistent set of axial and radial bucklings was obtained.

To insure adequate leakage of neutrons to the breeding blanket, a height to diameter ratio of $\frac{600}{200} = 3.0$ was chosen. This was essential to the breeding of the reactor.

In all the MACH-1 calculations, a search was made for the Be concentration in the core. The critical mass of the core could be reduced substantially by increasing the Be to U^{233} ratio, i.e. by making the neutron spectrum more and more thermal. However, for breeding of thorium-232, which has numerous resonances in the epithermal range, too thermal a neutron spectrum would be detrimental. The concentration of Be in the core chosen was a compromise between the requirements of criticality and breeding.

When thorium-232 absorbs a neutron, thorium-233 is formed, and a 7.5 MeV gamma is emitted. Thorium-233 undergoes β^- decay to Pa^{233} emitting a β^- particle of 1.23 MeV. Pa^{233} undergoes further β^- decay to form U^{233} emitting a β^- particle of 0.25 MeV. The reaction is given by:

$$Th^{233}(n,\gamma)\, Th^{233} \xrightarrow[22\ \text{min.}]{\beta^-} Pa^{233} \xrightarrow[27.4\ \text{days}]{\beta^-} U^{233}$$

For a breeding ratio of 1.0, this added up to 8.98 MeV per fission in core. Furthermore, from a MACH-1 calculation, it was found that 0.08%. of the total fissions occurs in the blanket, i.e., 0.157 MeV is available per fission. Assuming a recoverable energy of 196 MeV per fission, the percent of heat generated in the blanket is about 5%.

Characteristics of the reference UF_6BR design are discussed in Section D.

B. Heat Transfer and Thermal Hydraulics

It is necessary to size the heat exchangers in order to determine the total U^{233} inventory in the system. The primary heat exchanger analysis is the same for both the actinide transmutation reactor and the breeder reactor.

The heat exchangers used in this study are simple tube-in-shell counterflow heat exchangers. In the primary heat exchanger (Fig. 3.2) the UF_6-helium mixture passes through a number of modified Hastelloy-N tubes where heat is transferred to a flowing salt mixture composed of 92% $NaBF_4$ and 8% NaF (mole percent). This salt mixture was chosen to eliminate the possibility of criticality occurring in the primary heat exchangers and for its chemical inertness to UF_6. Modified Hastelloy-N was used for the tubing because of its corrosion resistance in a fluoride environment. Properties of UF_6, helium, $NaBF_4$-NaF salt, and modified Hastelloy-N are given in Appendix A.

The primary loop shown in Fig. 3.3 consists of the reactor core, primary heat exchanger, and compressor. The objectives of the analysis was to determine the heat exchanger size so as to determine the amount of fissile uranium in the heat exchanger and to determine the compressor power.

The analysis proceeds as follows. Given the core power, Q_{core}, and the inlet and exit temperatures of the core, T_3 and T_1, respectively, the flow rate in the loop is determined from

$$\dot{m} = \frac{Q_{core}}{C_p(T_1 - T_3)} \tag{3.7}$$

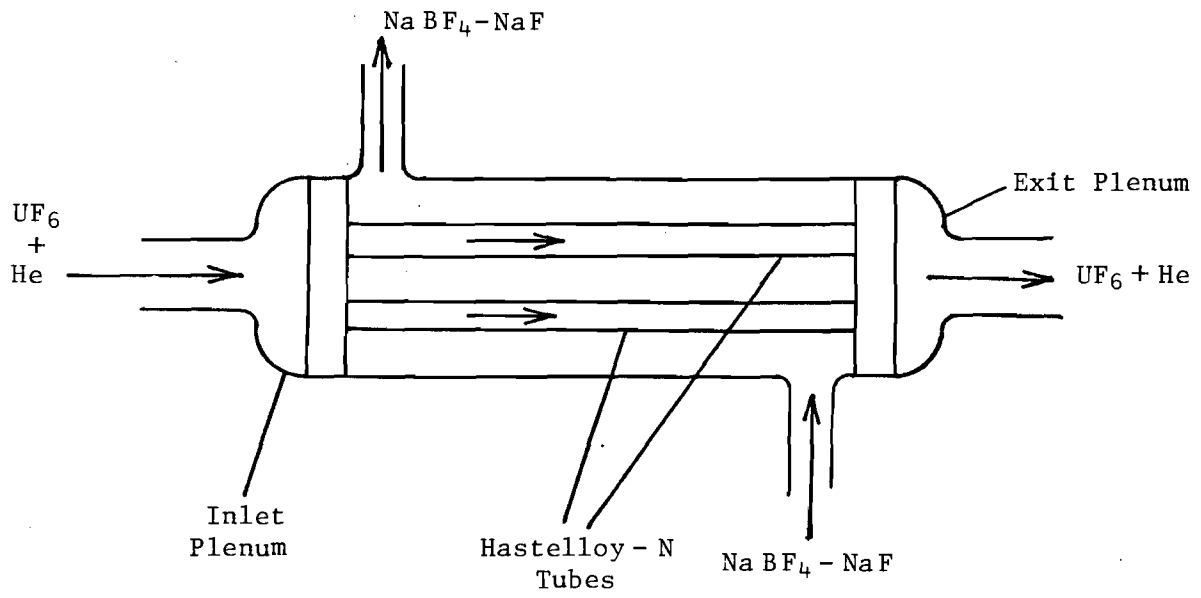

Fig. 3.2 Primary Heat Exchanger

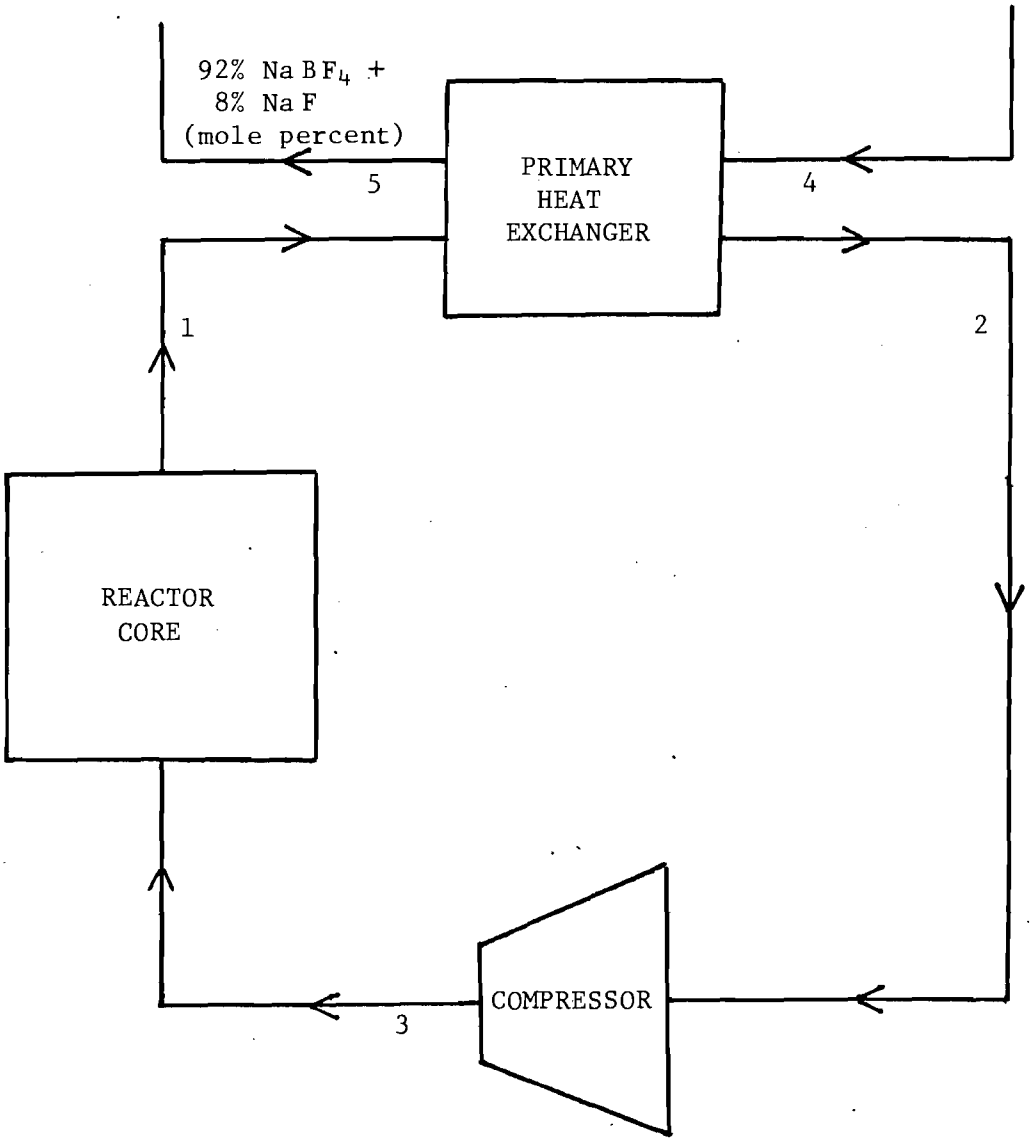

Fig. 3.3 Primary Flow Loop

where C_p is the specific heat of the helium-UF_6 gas mixture.

If the primary heat exchanger exit temperature, T_2, is given, then the power transferred from the UF_6-helium loop to the Na B F_4-Na F salt loop is given by

$$Q_{PHX} = \dot{m}\, C_p (T_1 - T_2) \tag{3.8}$$

The size of the heat exchanger can now be estimated. The equivalent diameter is determined by assuming the tubes are arranged in a triangular lattice structure (Fig. 3.4) and is given by

$$d_{eq} = \frac{4\, A_f}{P_w} = \frac{2\sqrt{3}\, c^2 - \pi d_o^{\,2}}{\pi\, d_o} \tag{3.9}$$

where A_f is the channel flow area, P_w is the wetted perimeter, c is the pitch, and d_o is the tube outside diameter. The channel flow area is

$$A_f = \frac{\sqrt{3}}{4}\, c^2 - \frac{\pi\, d_o^{\,2}}{8} \tag{3.10}$$

The Reynolds and Prandtl numbers for the UF_6-helium mixture in the heat exchanger tubes are

$$Re = \frac{\rho\, u\, d_i}{\mu} \tag{3.11}$$

$$Pr = \frac{C_p\, \mu}{K} \tag{3.12}$$

where ρ, μ, and K are the density, viscosity, and thermal conductivity of the mixture. The average velocity in the tube, u, and tube inside diameter, d_i, must be specified. Similarly, the Reynolds and Prandtl

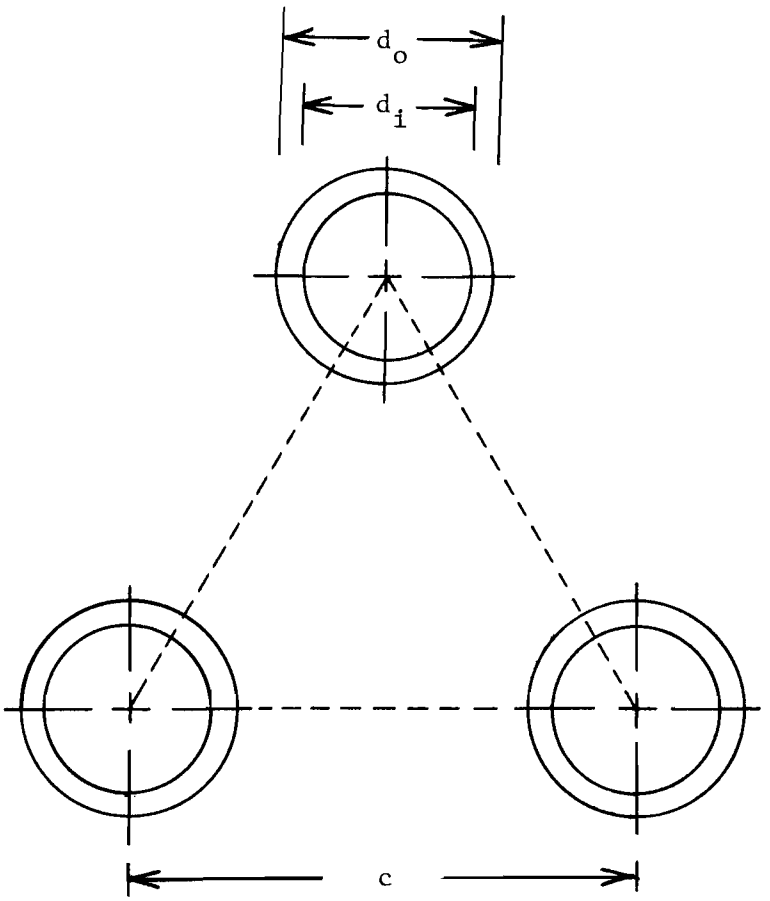

Fig. 3.4 Heat Exchanger Tube
Triangular Lattice Arrangement

numbers for the $NaF - NaBF_4$ salt are

$$Re' = \frac{\rho' u' d_{eq}}{\mu'} \tag{3.13}$$

$$Pr' = \frac{C_p' \mu'}{K'} \tag{3.14}$$

where primes are used to distinguish the salt from the gas mixture.

The convective heat transfer coefficients for the mixture and salt are estimated from the Dittus-Boelter equation[7]

$$h_i = 0.023 \frac{K}{d_i} (Pr)^{0.4} (Re)^{0.8} \tag{3.15}$$

$$h_o = 0.023 \frac{K'}{d_{eq}} (Pr')^{0.4} (Re')^{0.8} \tag{3.16}$$

The overall heat transfer coefficient for flows on each side of a tube is given by[8]

$$U = \frac{1}{\frac{1}{h_o} + \frac{d_o}{2 K_T} \ln \frac{d_o}{d_i} + \frac{d_o}{h_i d_i}} \tag{3.17}$$

where K_T is the thermal conductivity of the tube material.

The total cross sectional area of tubing required is

$$A_t = \frac{\dot{m}}{\rho u} \tag{3.18}$$

or, the number of tubes required is

$$n_t = \frac{4A_t}{\pi d_i^2} \tag{3.19}$$

It is then possible to compute the heat exchanger exit temperature on the salt side from

$$T_5 = T_4 + \frac{Q_{PHX}}{c_p' \rho' u' A_f n_t} \tag{3.20}$$

The log mean temperature difference for counterflow is given by[8]

$$\Delta T_m = \frac{(T_1 - T_5) - (T_2 - T_4)}{\ln \frac{T_1 - T_5}{T_2 - T_4}} \tag{3.21}$$

from which the heat transfer surface area is determined from

$$S = \frac{Q_{PHX}}{U \Delta T_m} \tag{3.22}$$

and the length of the tubes is then

$$L_t = \frac{S}{n_t \pi d_o} \tag{3.23}$$

The volume of helium-UF_6 mixture in the tubes is

$$V_t = n_t \frac{\pi d_i^2}{4} L_t \tag{3.24}$$

Additional UF_6 and helium reside in the inlet and exit plenums of the heat exchanger. The additional volume is calculated from

$$V_p = n_t L_p \frac{\pi d_i^2}{4 \sigma} \tag{3.25}$$

where L_p is the additional length of the heat exchanger due to the plenums and was taken to be 0.3048 m (1 ft.). Each tube flow area opens up to two corresponding triangular areas so that

$$\sigma = \frac{\pi d_i^2}{2\sqrt{3}\, c^2} \tag{3.26}$$

Therefore, the mass of UF_6 and helium in the heat exchanger is

$$m = \rho(V_t + V_p) \tag{3.27}$$

of which $\frac{233}{347} \frac{\rho^{UF_6}}{\rho}$ is the mass of U^{233}. The salt volume in the heat exchanger is

$$V' = n_t A_f L_t \tag{3.28}$$

and the salt mass is

$$m' = \rho' V' \tag{3.29}$$

The pressure drop has two components. The first is the pressure drop due to the change in flow areas between the plenums and tubes. This drop is given by[9]

$$\Delta P_p = \frac{\rho u^2}{2} (K_c + K_e) \tag{3.30}$$

where K_c and K_e are contraction and expansion coefficients which are functions of σ and the Reynold's number. Reference 9 gives values for K_c and K_e.

The second component is the friction loss in the tubing for the friction factor, f_w. For implementation in a computer code, the Colebrook equation is used[9]:

$$\frac{1}{f_w^{1/2}} = -2 \text{Log}_{10}\left[\frac{\epsilon/d_i}{3.70} + \frac{2.51}{\text{Re } f_w^{1/2}}\right] \tag{3.31}$$

where ϵ is a roughness parameter and is 1.524×10^{-6}m (5×10^{-6} ft.) for drawn tubing. f_w is solved iteratively and is used to compute the tube pressure drop

$$\Delta P_t = f_w \frac{\rho u^2}{2} \frac{L}{d_i} \tag{3.32}$$

The compressor power for circulating the UF_6-helium mixture is

$$Q_{comp} = \frac{\dot{m} C_p T_2}{\eta_c} \left[\left(\frac{P_3}{P_2}\right)^{\frac{\gamma - 1}{\gamma}} - 1\right] \tag{3.33}$$

where η_c is the compressor efficiency and γ is the mixture specific heat ratio.

Each heat exchanger and superheater were modeled in the same manner. However, pumps are used in the remaining loops. The pump power is calculated from

$$Q_{pump} = \frac{\dot{m} \Delta P}{\eta_p \rho} \tag{3.34}$$

where ΔP is the pressure drop across the pump, and η_p is the pump efficiency.

The boiler is treated differently because water changes into steam over the length of the boiler tubes. Therefore, the boiler is split into two regions for the purposes of analysis. The first region is the subcooled liquid region where the Dittus-Boelter equation is used to calculate the convective heat-transfer coefficient. The second region consists of saturated liquid changing to saturated steam. In this region, the Dittus-Boelter equation cannot be used so a heat-transfer coefficient of $5.68 \times 10^4 \ \frac{W}{m^2 K} \left(10^4 \ \frac{Btu}{ft^2 hr F}\right)$ was assumed.

C. Thermodynamic Cycle Analysis

Using the analysis from the previous section, a computer code was written to analyze the breeder power plant cycle. A separate code supplied by Professor R. W. Carlson of the Georgia Institute of Technology was used to obtain the efficiency of the steam cycle.

Several constraints are imposed on temperatures and velocities in the system by the following considerations:

(1) Uranium inventory in the primary heat exchanger cannot be excessive,

(2) Compressor and pump powers must be kept low for good power plant efficiencies,

(3) The breeding salt must be kept above 772°K and the coolant salt must be kept above 658°K to avoid solidification.

Figure 3.5 shows the power plant schematic. The steam cycle consists of high pressure and low pressure turbines, a condenser operating at 1 psia, five feedwater heaters operating at 7, 41, 141, 371, and 820 psia, a boiler operating at 1600 psia and a superheater in which steam is heated to 670°K.

The work used in circulating the various fluids (excluding water) through the heat exchangers is 13.1 MW which is multiplied by 1.5 to account for pressure losses in the piping. An overall plant efficiency of 39.3% is obtained for a steam cycle efficiency of 40.4%.

D. Summary

The design parameters for the breeder reactor are summarized in Table 3.1 while the power plant parameters are summarized in Table 3.2 Temperatures and velocities in the loop are shown in Fig. 3.5.

The critical parameters of interest are the power plant efficiency, reactor thermal power, and the U^{233} inventory. They are 39.3%, 1074 MWt, and 104.8 kg, respectively. In computing the uranium inventory, the uranium in the piping and reprocessing system was not included.

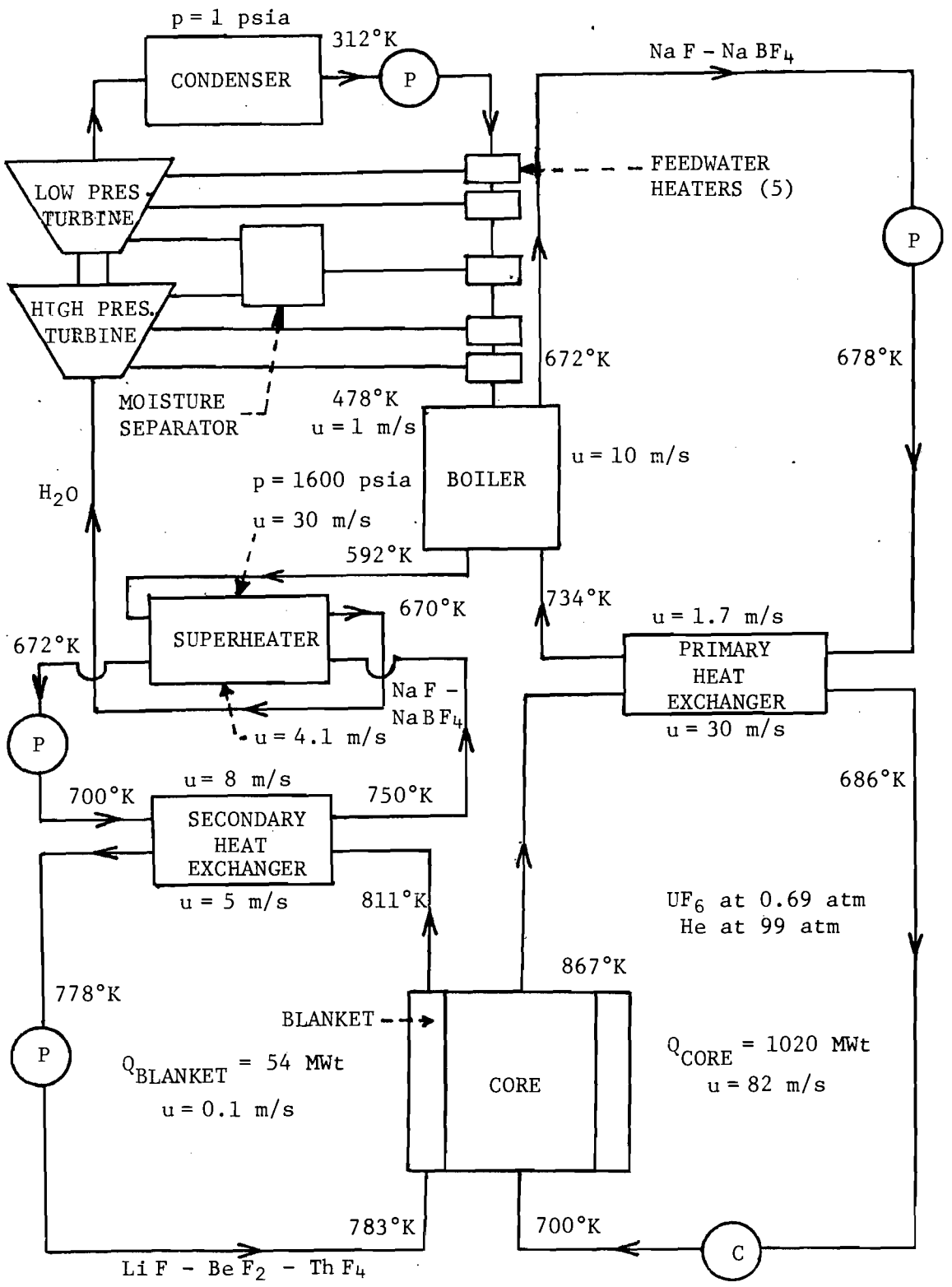

Fig. 3.5 UF_6 Breeder Reactor Power Plant Schematic

Table 3.1. UF_6BR Reactor Design Data Summary

Core Composition

$U^{233}F_6$ partial pressure	=	0.69 atm.
He partial pressure	=	99 atm.
Volume percent of UF_6 + He	=	70%
Volume percent of Be	=	30%

Dimensions

Geometry	=	Cylindrical
Core Diameter	=	2.0 m
Core Height	=	6.0 m
Thickness of Breeding Blanket	=	0.6 m
Thickness of Axial Be Reflector	=	0.5 m
Thickness of Radial Be Reflector	=	0.2 m
Thickness of Steel Pressure Shell	=	0.2 m
Reactor Diameter	=	4.0 m
Reactor Height	=	7.4 m
Core Volume	=	18.85 m^3

Neutronics

Breeding Ratio	=	1.0022
Be to U^{233} Atom Density Ratio	=	8111
Average Core Thermal Flux	=	1.34×10^{15} n/cm^2-sec
Average Core Fission Density	=	1.68×10^{18} fissions/m^3 - sec
Average Core Power Density	=	5.4×10^7 W/m^3
Peak to Average Ratio of Radial Fission Densities	=	1.78
Peak to Average Ratio of Axial Fission Densities	=	1.24
Percent Fission in Blanket	=	0.08%
Average Thermal Flux in Blanket	=	5.3×10^{13} n/cm^2-sec

Table 3.1. UF_6BR Reactor Design Data Summary
(continued)

Masses

U^{233} Mass in Core = 32.8 kg

UF_6 Mass in Core = 48.8 kg

Be Mass in Core = 10,300 kg

Th^{232} Mass in Blanket = 44,465 kg

Reactor Heat Transfer and Thermal Hydraulics

Total Reactor Power = 1074 MWt

Core Power = 1020 MWt

Blanket Power = 54 MWt

Core Region:

Inlet Temperature = 700°K

Exit Temperature = 867°K

Average UF_6 + He Velocity = 82 m/sec

Mass Flow Rate of UF_6 + He = $1.8 \times 10^3 \frac{kg}{sec}$

Blanket Region:

Inlet Temperature = 783°K

Exit Temperature = 811°K

Average Salt Velocity = 8.5×10^{-2} m/sec

Mass Flow Rate of Salt = $1.42 \times 10^3 \frac{kg}{sec}$

Table 3.2. UF_6BR Power Plant Design Data Summary

Number of Loops = 2

Power Plant Efficiency = 39.3%

Uranium Mass:

Core = 32.8 kg

Primary Heat Exchangers = 72.0 kg

Total = 104.8 kg (Excluding U^{233} in piping and reprocessing system)

Electric Power Output = 426 MWe

UF_6 - He Loop Parameters:

Primary Heat Exchanger:

Number of Tubes = 63595

Inner Tube Diameter = 7.745×10^{-3} m

Outer Tube Diameter = 9.525×10^{-3} m

Pitch to Diameter Ratio = 1.3

Length of Tubes = 3.81 m

Mass Flow Rate = 1.8×10^{3} kg/sec

Compressor Power = 8.6 MW

Na F - $Na BF_4$ Primary Loop Parameters

Boiler:

Number of Tubes = 3585

Inner Tube Diameter = 1.4148×10^{-2} m

Outer Tube Diameter = 1.5875×10^{-2} m

Pitch to Diameter Ratio = 1.6

Length of Tubes = 7.95 m

Mass Flow Rate = 1.30×10^{4} kg/sec

Pump Power = 3.7 MW

Table 3.2. UF_6BR Power Plant Design Data Summary (continued)

Li F - Be F_2 - Th F_4 Loop Parameters

Secondary Heat Exchanger:

Number of Tubes	=	886
Inner Tube Diameter	=	7.745×10^{-3} m
Outer Tube Diameter	=	9.525×10^{-3} m
Pitch to Diameter Ratio	=	1.3
Length of Tubes	=	4.09 m

Mass Flow Rate = $1.42 \times 10^3 \frac{kg}{sec}$

Pump Power = 0.37 MW

NaF - Na BF_4 Secondary Loop Parameters

Superheater:

Number of Tubes	=	628
Inner Tube Diameter	=	1.4148×10^{-2} m
Outer Tube Diameter	=	1.5875×10^{-2} m
Pitch to Diameter Ratio	=	1.3
Length of Tubes	=	11.6 m

Mass Flow Rate = 844.5 kg/sec

Pump Power = 0.46 MW

Steam Cycle Parameters

Condenser Pressure = 1 psia

Boiler Pressure = 1600 psia

Feedwater Heater Pressures:

No. 1	=	7 psia
No. 2	=	41 psia
No. 3	=	141 psia
No. 4	=	371 psia
No. 5	=	820 psia

Maximum Steam Temperature = 670°K

Steam Cycle Efficiency = 40.4%

References for Chapter 3

1. Meneley, D. A., et al., "Mach-1, A One-Dimensional Diffusion Theory Package," ANL-7223 (1966).

2. Bondarenko, I. I., Ed., Group Constants for Nuclear Reactor Calculations. Consultants Bureau, New York (1964).

3. Grimes, W. R., "Molten Salt Reactor Chemistry," Vol. 8, Nuclear Applications and Technology 8 (February 1970).

4. Garber, D. I., and Kinsey, R. R., "Neutron Cross Sections," 3rd Edition, Vol. II, BNL-325 (January 1976).

5. Hughes, D. J., and Schwartz, R. B., "Neutron Cross Sections," 2nd Edition, BNL-325 (July 1958).

6. Westcott, C. H., "Effective Cross Section Values for Well-Moderated Thermal Reactor Spectra," 3rd Edition, AECL-1101 (November 1960).

7. El-Wakil, M. M., Nuclear Heat Transport, International Textbook Company (1971).

8. Steam/Its Generation and Use, Babcock and Wilcox Company (1975).

9. Rust, J. H., "Nuclear Power Plant Engineering," Unpublished Notes, Georgia Institute of Technology.

4. UF_6 ACTINIDE TRANSMUTATION REACTOR POWER PLANT

One consequence of the large scale use of fission reactors for production of energy is the accumulation of radioactive wastes. The spent fuel discharged from a LWR consists of structural materials, unfissioned uranium, converted plutonium, other actinides, and fission products. The ratio of these components by weight is as follows:

structural	:	uranium	:	plutonium	:	fission products	:	other actinides
= 256	:	1023	:	9	:	36	:	1

Although the other actinides are the smallest component, they are very important because of their long half lives. After 10^3 years most of the other materials will have decayed to stable isotopes; these actinides will still be radioactive and may present significant health hazards in the future.

Steinberg,[1,2] proposed use of neutron induced transmutation for the disposal of long-lived fission wastes. Under such a scheme, these fission wastes are separated from gross wastes during fuel reprocessing, and converted into forms suitable for insertion into a neutron field, e.g., a fission reactor. In this neutron environment, these nuclides will be converted, or fissioned into short-lived isotopes. The resulting wastes will then be stored for a short period until a harmless activity level is reached. This method allows the possibility of reducing long-lived fission waste inventory at a faster rate than natural decay, and hence of reducing the long-term risk of exposure to radioactivity.

The first step in the actinide transmutation scheme is the chemical extraction of actinides from the bulk wastes. The Oak Ridge National Laboratory is currently performing a fairly extensive study in this area.[3]

Since no chemical extraction process is 100% efficient, there will always be a small quantity of actinides left unextracted in the bulk wastes. What, then, should the extraction efficiency be so that the risk associated with the unextracted actinides be considered acceptable? Radioactive material has been present in the earth's crust and surface at all times in the form of uranium and thorium minerals and ores. Claiborne[4] compared the long-term hazard of actinides for different extraction efficiencies with the calculated hazard of pitchblende (~ 70% U), the most radioactive mineral, and with the calculated hazard of high grade uranium ore (~ 0.2% U). He showed that it is possible to reduce the hazard (after 1000 years) associated with high-level wastes to values comparable to those from high grade uranium ore provided that 99.99% of Pu, 99.9% of U, Am, Cm, and ^{129}I and 95% of the Np are recovered from LWR fuels.

After the actinides are extracted from the bulk wastes, they are placed into a reactor for irradiation.

Claiborne[5] performed detailed calculations on actinide transmutation in LWR's. Assuming separation efficiencies of 99.5% and 99.9% for U, Pu, and the other actinides, the actinides (no U and Pu) are recycled back into a PWR for many cycles. A thermal flux of 3×10^{13} n/cm^2-sec was used. With this strategy the actinides are removed by two paths. One, they are converted to plutonium and uranium, and are then extracted during chemical reprocessing. Most of the plutonium extracted is Pu^{238}, formed by the reaction Np^{237} (n,γ) $Np^{238} \xrightarrow{\beta-} Pu^{238}$. A small quantity of Pu^{239} is also formed. This mix of Pu^{238} - Pu^{239} can be used as reactor fuel just like Th^{232} - U^{233}. The other path is for the actinides to be fissioned directly inside the PWR. The total

actinide inventory approaches an equilibrium value that is several times that produced in the first cycle (1.6 times for Np, 1.2 times for Am, 9.0 times for Cm). Np reaches equilibrium after ~ 4 to 5 recycles, Am after ~ 2 to 3 recycles, and Cm after 50 to 60 recycles. Claiborne also concluded that the introduction of actinide wastes perturbs the reactor very slightly. Similar results have been obtained at Battelle Northwest Laboratories.[6]

Beaman et al.[7] performed actinide transmutations calculations for an LMFBR. His scheme consisted of an LMFBR recycling the actinide wastes produced by itself and 3 BWR's. The actinides are removed in 2 ways: (1) by conversion to Pu, and (2) by fission. Equilibrium concentrations of recycled actinides in a LMFBR are qualitatively similar to the LWR case. In Np^{237} equilibrium is reached after about 14 recycles; for Cm about 30 recycles. An equilibrium concentration of the actinide mixture is achieved after approximately 26 recycles. The equilibrium inventory is 3.1 times the quantity charged in the first cycle. Introduction of the actinide wastes into an LMFBR have a very slight effect on other reactor characteristics. Similar studies were done by Oliva, et al.[8]

These schemes for recycling actinide wastes in LWRs and LMFBRs are not satisfactory in two respects. First, since only a small number of reactors are serviced by a LWR or a LMFBR, many transmuters (LWRs and/or LMFBRs) will be required. Second, even then it will require very long irradiation times (> 20 recycles) to reach equilibrium. This gives rise to the idea of designing of a special burner reactor capable of servicing a large number of LWRs and operating at high fluxes to shorten the irradiation time.

One candidate for this special burner reactor is the gas core reactor. Because of the low fissile fuel inventory a high flux can be maintained. Continuous reprocessing of the fuel means better fuel economy and the possibility of continuous irradiation.

Clement and Rust[9] performed actinide burnup calculations in a plasma core actinide transmutation reactor. The calculations assumed 100% extraction efficiency for U, Pu and other actinides and the reactor was designed to dispose of actinide wastes from 27 LWRs. Due to constraints imposed by the high temperature uranium plasma, the neutron flux in the actinide region was only 7×10^{12} n/cm^2-sec. Approximate equilibrium actinide inventory is reached after 13 recycles, and the equilibrium actinide inventory is about 2.6 times the initial actinide loading.

This study continues the previous investigation; however, a uranium hexafluoride fueled reactor was investigated for its potential as a gas core actinide transmuter (UF_6ATR).

A. Neutronics

A flow chart of the computation strategy is shown in Fig. 4.1. The ABBN[10] cross section set is used for imput into the MACH-I[11] code. Cross sections for Np^{237}, Am^{241}, Am^{243}, Cm^{244} are generated from ENDF/III by the code MC^2.[12] Cross sections for the He and fluorine are generated from the cross section data from BNL-325.[13,14] The detailed formalism is described in Chapter 3. The depletion and decay of the actinide isotopes are calculated by the code ORIGEN.[15]

The cylindrical reactor configuration is shown in Fig. 4.2. Since MACH-I is a one-dimensional code, the infinite slab and cylinder geometries were used to model the axial and radial neutronics of the reactor. The two calculations were coupled together by group dependent bucklings in

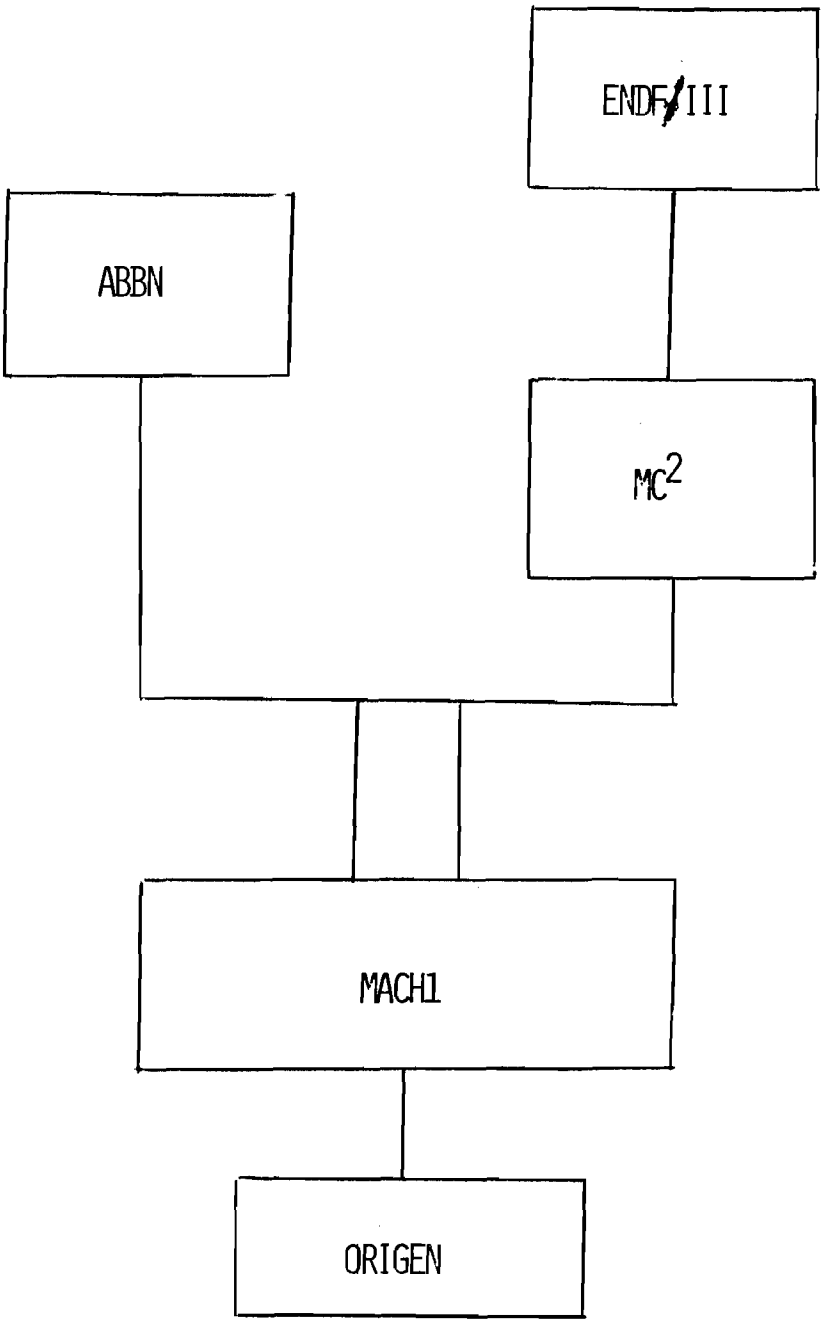

Fig. 4.1 Flowsheet of Nuclear Analysis Computation

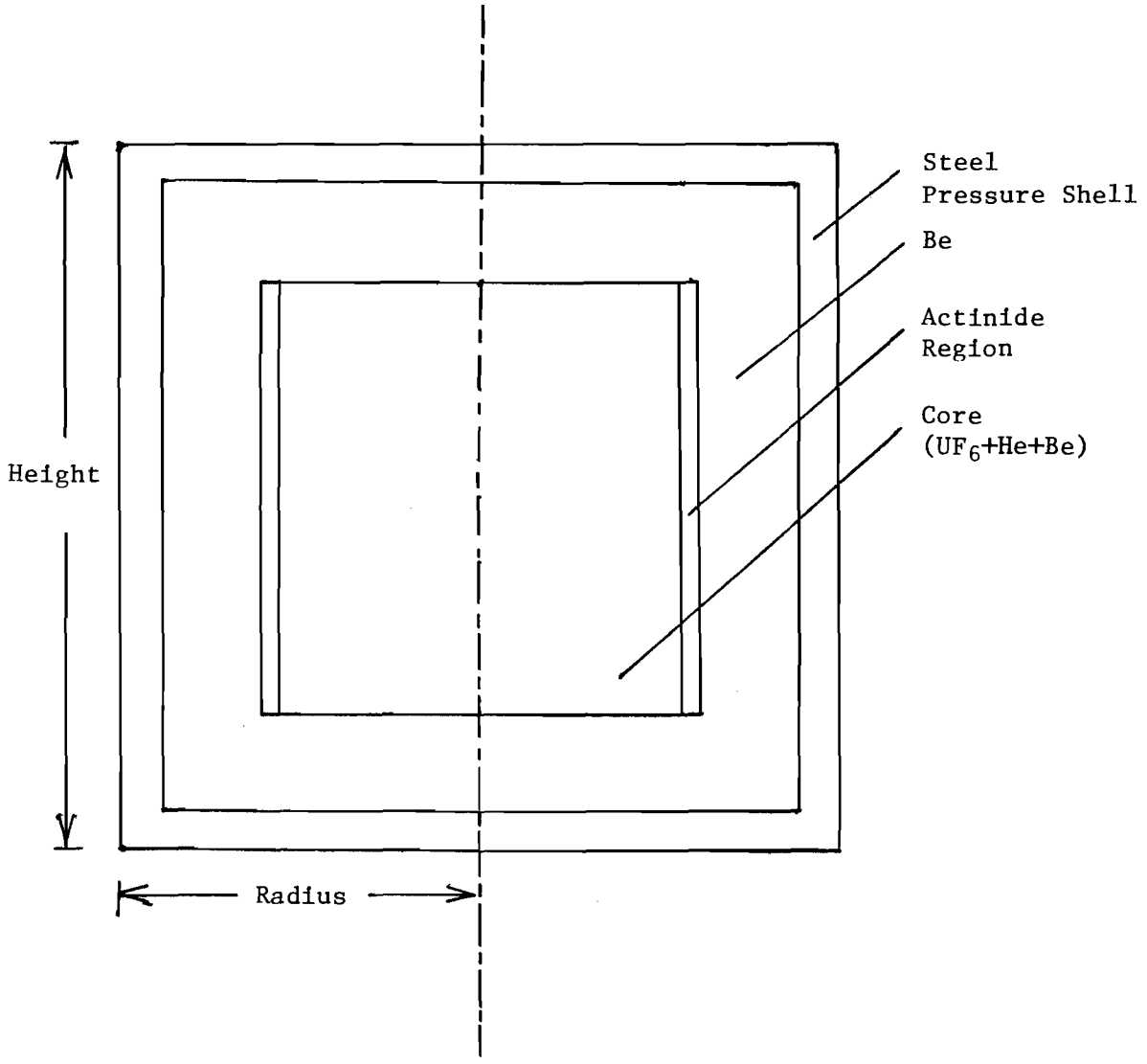

Fig. 4.2 Reactor Configuration of UF_6ATR

the axial and radial directions. Several iterations were required before a consistent set of axial and radial bucklings was obtained.

The core consists of a He-UF_6 mixture flowing through a beryllium matrix. Addition of helium greatly improves the heat transfer characteristics of the gas, since UF_6 is a very poor heat transfer agent. The neutron spectrum is thermalized by a beryllium matrix in the core. Surrounding the core is an actinide blanket region consisting of He cooled, zirconium clad actinide fuel rods. The actinides are assumed to be present as oxides. Only the principal actinides, Np^{237}, Am^{241}, Am^{243}, and Cm^{244} are included. The actinide blanket is surrounded by a beryllium reflector and a steel pressure shell. Characteristics of the reactor are summarized in Section 4D.

B. Heat Transfer and Thermal Hydraulics

The analysis for the heat exchangers is the same as that described in Section 3.B. The heat transfer for the actinide transmuter reactor is unique in that the core power decreases from 504 MWt at beginning of life to 180 MWt at the end of life of the first core. This is due to buildup of fissile plutonium in the actinide blanket. Therefore, the flux in the actinide region and the core has to be decreased to maintain the same volumetric heat generation rate in the actinide rods. The consequence is that a time dependent study is needed. However, in this study, heat transfer calculations were only made for beginning-of-life conditions.

C. Thermodynamic Cycle Analysis

Figure 4.3 shows the schematic for the actinide power plant at beginning-of-life conditions. The overall plant efficiency is 39.2%.

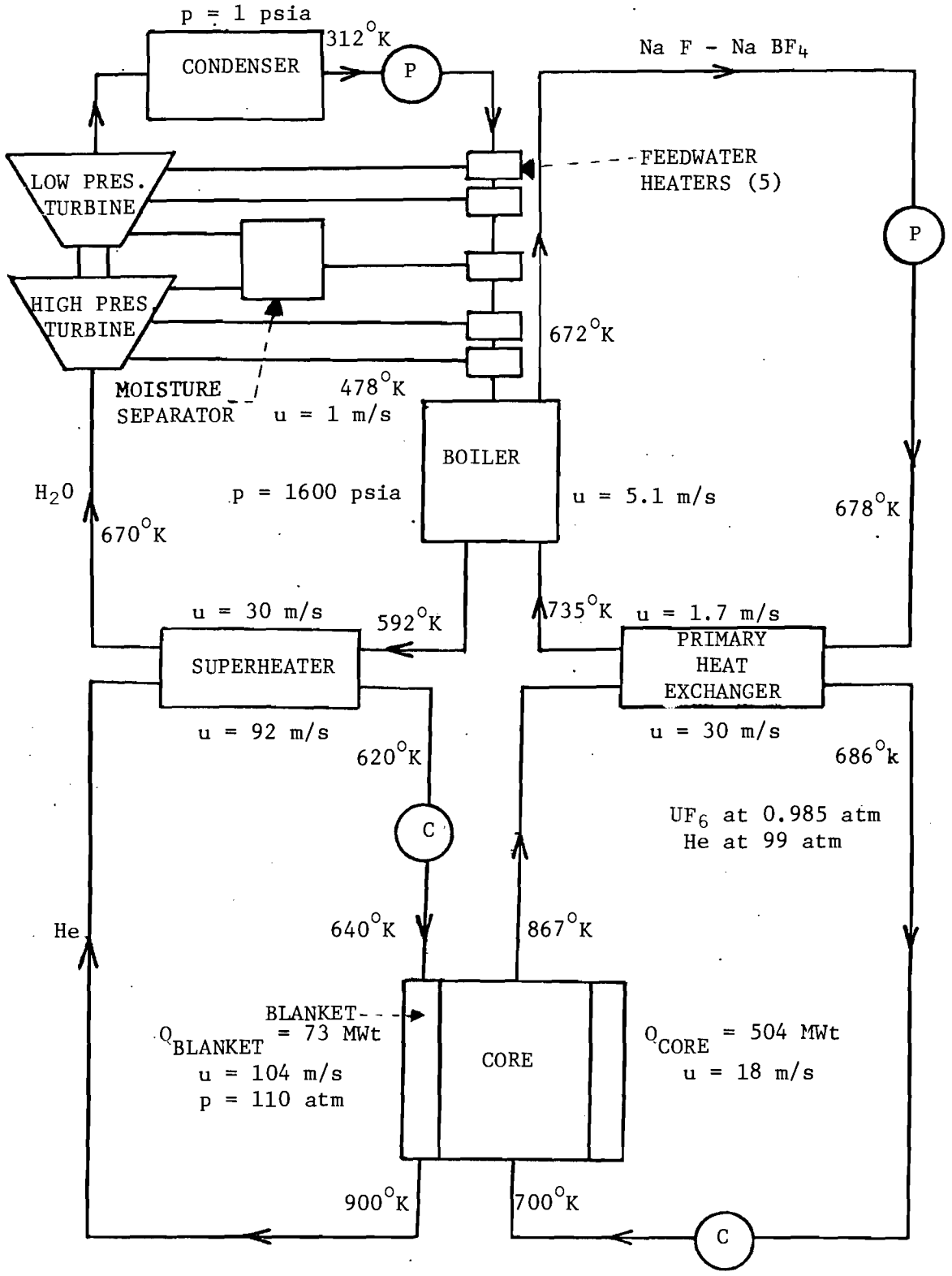

Fig. 4.3 UF_6 Actinide Transmutation Reactor Power Plant
(Beginning-of-Life Conditions)

D. Summary

Characteristics of the beginning-of-life UF_6ATR are shown in Table 4.1 By virtue of the low density of the U^{233} fuel, an average flux of 4×10^{14} n/cm^2 sec can be reached in the core, and an average flux of 1.3×10^{14} n/cm^2 sec can be reached in the actinide region. This high actinide region flux will bring about a very rapid transmutation of the actinides. However, as the quantity Pu^{239} and other fissile isotopes increases, the flux in the actinide region must be lowered to stay within the safety limits of the actinide rods. Thus the flux in the actinide region must be gradually lowered, as the inventory of fissile isotopes gradually builds up so as to maintain an acceptable volumetric heat generation rate (q''') in the actinide region.

The transmutation strategy used for the present study is shown in Fig. 4.4. Each LWR is loaded with 88 metric tonnes of uranium (3.3% U^{235}) and operated at a constant and average specific power of 30 MW/MTU. At the end of 1100 days, a burnup of 33,000 MWD/MTU is reached. The fuel is discharged from the reactor and cooled for 160 days. Next, the spent fuel is reprocessed during which 100% of Np, Am, Am, and higher actinides are separated from the bulk wastes. The concentrations of these actinides are calculated by ORIGEN. These actinides are then manufactured into fuel rods and charged into the UF_6ATR. These actinides are irradiated for 1100 days in the UF_6ATR until an average burnup of 100,000 MWD/MTA is attained. The actinide rods are discharged from the UF_6ATR and undergo reprocessing during which fission products and converted U and Pu are extracted. These actinides are mixed with a batch of freshly produced actinides from the LWRs and manufactured into oxide rods and charged back into the UF_6ATR. In the present calculation the UF_6ATR services 14 PWRs,

Table 4.1 UF_6ATR Reactor Design Data Summary
(Beginning-of-Life)

Core Composition

U^{233} F_6 partial pressure	=	0.985 atm.
He partial pressure	=	99 atm.
Volume percent of UF_6 + He	=	83.3%
Volume percent of Be	=	16.7%

Actinide Composition

Actinide Dioxide	=	28 volume %
Zirconium Clad	=	7 volume %
Helium Coolant	=	65 volume %
Actinides		
Np^{237}	=	74 atomic %
Am^{241}	=	7 atomic %
Am^{243}	=	14 atomic %
Cm^{244}	=	5 atomic %

Dimensions

Geometry = Cylindrical

Core Diameter = 2.74 m

Core Height = 3.0 m

Thickness of Actinide Blanket = 1.32×10^{-2} m

Thickness of Axial Be Reflector = 0.5 m

Thickness of Radial Be Reflector = 0,43 m

Thickness of Pressure Shell = 0.2 m

Reactor Diameter = 4.0 m

Reactor Height = 4.4. m

Core Volume = 17.7 m^3

Volume of Actinide Region = 0.343 m^3

Fuel Pins in Actinide Region

Fuel Pin Radius	=	2.175×10^{-3} m
Gap Thickness	=	1.5×10^{-4} m
Clad Thickness	=	3.5×10^{-4} m
Wire Wrap Diameter	=	1.42×10^{-3} m

Table 4.1 UF_6ATR Reactor Design Data Summary
(continued)

Neutronics

Type of Reactor = Thermal

Be to U^{233} Atom Density Ratio = 2660

Average Core Thermal Flux = 4.07×10^{14} n/cm^2-sec

Average Core Fission Density = 8.90×10^{17} fissions/m^3 sec

Peak to Average Ratio of Radial Fission Densities = 1.82

Peak to Average Ratio of Axial Fission Densities = 1.42

Percent Fissions in Actinide Blanket = 12.6%

Average Thermal Flux in Actinide Region = 1.26×10^{14} n/cm^2-sec

Masses

U^{233} Mass in Core = 52.5 kg

UF_6 Mass in Core = 78.2 kg

Actinide Mass = 800 kg (~ output from 14 LWRs)

Reactor Heat Transfer and Thermal Hydraulics

Total Reactor Power = 577 MWt

Core Power = 504 MWt

Actinide Region Power = 73 MWt

Core Region

- Inlet Temperature = 700^{o}K
- Exit Temperature = 867^{o}K
- Average UF_6 + He Velocity = 18 m/sec
- Mass Flow Rate = 1008 kg/sec
- Average Core Power Density = 28.5 MW/m^3

Actinide Region

- He Coolant Pressure = 110 atm.
- Inlet Temperature = 640^{o}K
- Exit Temperature = 900^{o}K
- Average He Velocity = 104 m/sec
- Mass Flow Rate = 54 kg/sec
- Average Power Density of Region = 210 MW/m^3

Table 4.1 UF_6ATR Reactor Design Data Summary
(continued)

Average q''' of Actinide Rod	=	760 MW/m^3
Average q''_w of Actinide Rod	=	0.83 MW/m^2
Average q' of Actinide Rod	=	11.3 kW/m

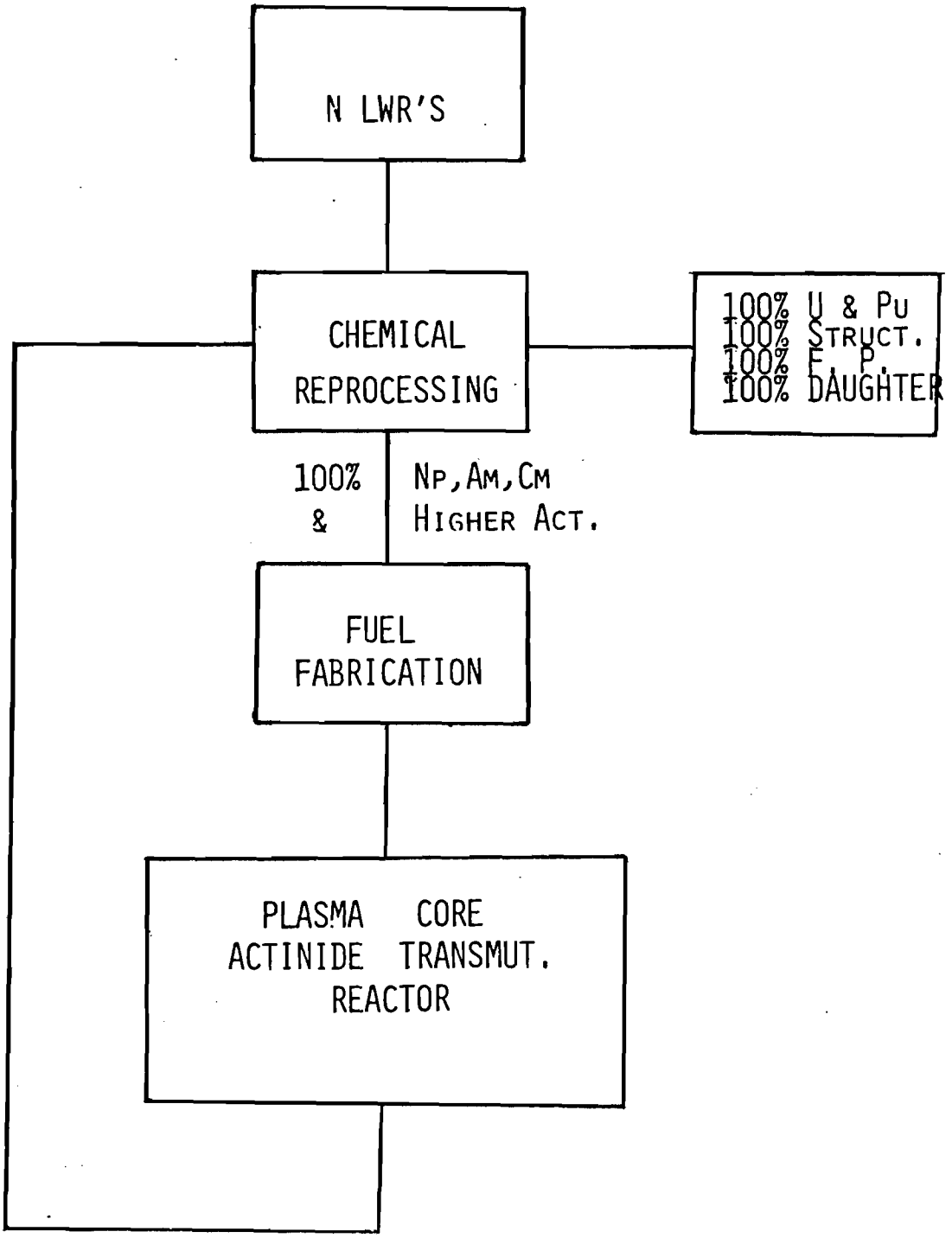

Fig. 4.4 Strategy for Actinide Transmutation

i.e., 800 kg of actinides per cycle. To maintain an acceptable volumetric heat generation rate (q''') in the actinide region, the flux must be varied as a function of time. To approximate this occurrence, a flux of 5.6×10^{13} n/cm^2-sec was used for the first 100 days and a flux of 1.6×10^{13} n/cm^2-sec for the rest of the 1100 day period. Approximate equilibrium is reached after 15 recycles. The equilibrium actinide inventory is about 2.3 times its initial loading. In the equilibrium cycle, about 10.8% of the actinides are fissioned and about 32.1% is removed by reprocessing. These results are shown in Table 4.2.

The UF_6ATR is capable of maintaining a flux of 10^{14} n/cm^2-sec in the actinide region; however, heat transfer limitations in the actinide region force the UF_6ATR to operate at a much lower flux. Assuming that the heat transfer problem in the actinide region can be solved, an ORIGEN calculation was performed for a UF_6ATR with a constant flux of 1.25×10^{14} n/cm^2-sec in the actinide region. The actinides were irradiated for 165 days. The results were compared with those of a typical low flux UF_6ATR case with 1100 days of irradiation in Table 4.3. As shown, the 2 cases are comparable, indicating that with a high flux of 1.25×10^{14} n/cm^2-sec it may be possible to cut the irradiation time by a factor of 6-7.

Table 4.4 summarizes the power plant parameters for beginning-of-life conditions. The power plant operates at 577 MWt with an efficiency of 39.2% and with 102.2 kg of U^{233} in the core and heat exchanger.

Table 4.2 Actinide Burnup in Uranium Hexafluoride Actinide Transmutation Reactor 1100 Days of Irradiation, 365 Days of Cooling, 730 Days of Reprocessing (100% Removal of U and Pu, F. P. and Daughters, and Fuel Fabrication, 14 PWRs Serviced (0.800 Metric Tonne of Actinides Charged per Cycle) THERM = 0.54227, RES = 0.375, FAST = 1.50, Φ(0-100 days) = 1.6×10^{13}.

Batch No.	Cycle No.														
	1	2	3	4	5	6	7	8	9	10	11	12	13	14	15
1	0.800	0.426	0.233	0.128	0.073	0.045	0.030	0.022	0.017	0.015	0.013	0.012	0.011	0.011	0.010
2		0.800	0.426	0.233	0.128	0.073	0.045	0.030	0.022	0.017	0.015	0.013	0.012	0.011	0.011
3			0.800	0.426	0.233	0.128	0.073	0.045	0.030	0.022	0.017	0.015	0.013	0.012	0.011
4				0.800	0.426	0.233	0.128	0.073	0.045	0.030	0.022	0.017	0.015	0.013	0.012
5					0.800	0.426	0.233	0.128	0.073	0.045	0.030	0.022	0.017	0.015	0.013
6						0.800	0.426	0.233	0.128	0.073	0.045	0.030	0.022	0.017	0.015
7							0.800	0.426	0.233	0.128	0.073	0.045	0.030	0.022	0.017
8								0.800	0.426	0.233	0.128	0.073	0.045	0.030	0.022
9									0.800	0.426	0.233	0.128	0.073	0.045	0.030
10										0.800	0.428	0.233	0.128	0.073	0.045
11											0.800	0.426	0.233	0.128	0.073
12												0.800	0.426	0.233	0.128
13													0.800	0.426	0.233
14														0.800	0.426
15															0.800
TOTAL	**0.8**	**1.23**	**1.46**	**1.59**	**1.66**	**1.69**	**1.71**	**1.73**	**1.74**	**1.76**	**1.77**	**1.78**	**1.79**	**1.80**	**1.81**

Table 4.3 Comparison of Low Flux UF_6ATR and High Flux UF_6ATR for the First Cycle.

Avg. flux	$5.60 \times 10^{13} - 1.60 \times 10^{13}$	1.25×10^{14}
Irradiation time	1100 days	165 days
Burnup	59,900 MWD/MTA	47,800 MWD/MTA
% Actinides fissioned	6.0%	5.2%
% Actinides removed by reprocessing	32.3%	27.9%

Table 4.4 UF_6ATR Power Plant Design Data Summary
(Beginning-of-Life)

Number of Loops = 1

Power Plant Efficiency = 39.2%

Uranium Mass:

Core = 52.5 kg

Primary Heat Exchanger = 49.7 kg

Total = 102.2 kg (Excluding U^{233} in piping and reprocessing system)

Electric Power Output = 226 MWe

UF_6 - He Loop Parameters:

Primary Heat Exchanger:

Number of Tubes = 61496

Inner Tube Diameter = 7.74×10^{-3} m

Outer Tube Diameter = 9.525×10^{-3} m

Pitch to Diameter Ratio = 1.3

Length of Tubes = 3.81 m

Mass Flow Rate = 1015 kg/sec

Compressor Power = 4.73 MW

NaF - $NaBF_4$ Loop Parameters:

Boiler:

Number of Tubes = 3535

Inner Tube Diameter = 1.4148×10^{-2} m

Outer Tube Diameter = 1.5875×10^{-2} m

Pitch to Diameter Ratio = 1.6

Length of Tubes = 9.19 m

Mass Flow Rate = 6308 kg/sec

Pump Power = 0.66 MW

He Coolant Loop Parameters

Superheater:

Number of Tubes = 994

Inner Tube Diameter = 1.4148×10^{-2} m

Outer Tube Diameter = 1.5875×10^{-2} m

Pitch to Diameter Ratio = 1.3

Length of Tubes = 9.95 m

Mass Flow Rate = 54 kg/sec

Compressor Power = 2.42 MW

Table 4.4 UF_6ATR Power Plant Design Data Summary
(continued)

Steam Cycle Parameters

Condenser Pressure = 1 psia

Boiler Pressure = 1600 psia

Feedwater Heater Pressures:

No. 1 = 7 psia

No. 2 = 41 psia

No. 3 = 141 psia

No. 4 = 371 psia

No. 5 = 820 psia

Maximum Steam Temperature = $670^{\circ}K$

Steam Cycle Efficiency = 40.4%

References for Chapter 4

1. Steinberg, M., Wotzak, G. and Manowitz, B., "Neutron Burning of Long-Lived Fission Products for Waste Disposal," BNL-8558 (September 1964).

2. Gregory, M. V., and Steinberg, M., "A Nuclear Transformation System for Disposal of Long-Lived Fission Product Waste in an Expanding Nuclear Power Economy," BNL-11915 (November 1967).

3. Blomeke, J. O., "A Program to Establish the Technical Feasibility and Incentives for Partitioning," NR-CONF-001, Proceedings of Nuclear Regulatory Commission Workshop (June 1976).

4. Claiborne, H. C., "Effect of Actinide Removal on the Long-Term Hazard of High-Level Waste," ORNL-TM-4724 (January 1975).

5. Claiborne, H. C., "Neutron-Induced Transmutation of High-Level Radioactive Waste," ORNL-TM-3964 (December 1972).

6. Schneider, K. J., and Platt, A. M., "High-Level Radioactive Waste Management Alternative," BNWL-1900, Battelle Pacific Northwest Laboratories (1974).

7. Beaman, S. L., and Aitken, E. A., "Feasibility Studies of Actinide Recycling in LMFBRs as a Waste Management Alternative," General Electric Company.

8. Oliva, G., Palmiotti, G., Salvatores, M., and Tondinelli, L., "Elimination of Transuranium Elements by Burnup in a Power Fast Breeder Reactor," Nuclear Science and Engineering 37 (March 1978).

9. Clement, J. D., and Rust, J. H., "Analysis of the Gas Core Actinide Transmutation Reactor (GCATR)," NASA-GRANT-NSG-1288 (September 1977).

10. Bondarenko, I. I., Ed., Group Constants for Nuclear Reactor Calculations, Consultants Bureau, New York (1964).

11. Meneley, D. A., et al., "MACH-I, A One-Dimensional Diffusion Theory Package," ANL-7223 (1966).

12. Toppel, B. J., Rago, A. L., and O'Shea, D. M., "MC^2 - A Code to Calculate Multigroup Cross Sections," ANL-7318 (1967).

13. Garber, D. I., and Kinsey, R. R., "Neutron Cross Sections," 3rd Edition, Vol. II, BNL-325 (January 1976).

14. Hughes, D. J., and Schwartz, R. B., "Neutron Cross Sections," 2nd Edition, BNL-325 (July 1958).

15. Bell, M. J., "ORIGEN - The ORNL Isotope Generation and Depletion Code," ORNL-4628 (May 1973),

5. CONCLUSIONS AND RECOMMENDATIONS

This report shows that gas core reactors can be very versatile in terms of power, temperature, and application. Four types of systems were studied: plasma core breeder, plasma core actinide transmuter, UF_6 breeder, and UF_6 actinide transmuter.

In addition to breeding and transmuting actinides, the plasma core reactor can serve as a high temperature source for MHD power conversion. For a reactor exit temperature of 4000°K, a power plant employing a ternary cycle consisting of a MHD generator, gas turbine, and steam cycle with a high temperature regenerator may have an efficiency as high as 70%. However, great advances in materials technology are necessary for the development of this system. If the reactor exit temperature is decreased to 3000°K, the power plant efficiency is decreased to 63%, but materials requirements would be considerably lessened. For exit temperatures considerably below 3000°K, advanced solid core reactors such as high temperature gas cooled reactors and liquid metal fast breeder reactors utilizing plasma or liquid metal MHD may become competitive with the gas core reactor - MHD system.

The on-going UF_6 reactor experiments at Los Alamos and the DOE coal-fired MHD program will provide valuable information on the feasibility of a plasma core reactor - MHD system. However, research and development of this system is a long term proposition so that studies are needed now to define the problems and to formulate a modest research program.

On the other hand, the UF_6 reactor would require only a modest extension of present day technology for its development. In particular, the UF_6 breeder reactor is an attractive near term application. The

on-line reprocessing systems for the core and blanket are major features of this system since they improve the fuel economy. Although no calculations were made on the reprocessing systems, they are qualitatively discussed in Appendix B. It is important to note that much of the molten salt technology is available from the molten salt breeder program, helium purification techniques are available from the high temperature gas-cooled reactor program, and UF_6 handling techniques are available from the gaseous diffusion program. It appears that no radically new technology is required for the development of this reactor.

Both this report and that of Ref. 1 show attractive features of the UF_6 breeder reactor. A comparison of the two systems is given in Table 5.1. The Los Alamos core design is unique in that seven cylindrical cells are arranged in a scalloped fashion while the Georgia Tech design uses a beryllium matrix. The former design allows a wider design range based on breeding ratio.

The Los Alamos reactor is designed for 200 MWt while the Georgia Tech reactor is designed for 1074 MWt. These powers are low but acceptable for use in developing countries where the power grid system is not well developed. Higher powers may be obtained by increasing the reactor pressure, but this introduces materials problems.

It is seen that the uranium inventories are small (less than 100 Kg for the Los Alamos system). Only the uranium inventory in the core and heat exchangers were estimated in the Georgia Tech design; but, if the uranium in the piping, circulators, and reprocessing system were added, the inventory would still be small compared to present day reactor power plants.

Table 5.1 Comparison of Los Alamos[1] and Georgia Tech UF_6 Breeder Power Plants

	Los Alamos[1]	Georgia Tech
Core Configuration	Seven Cylindrical Cells Scallop Design	Beryllium Matrix
Reactor Power, MWt	200	1074
UF_6 Partial Pressure, atm.	0.6	0.69
He Partial Pressure, atm.	99	99
Reactor Exit Temperature, °K	1225	867
Type of Cycle	Brayton - Steam	Superheated Steam
Power Plant Efficiency, %	36.6	39.3
U^{233} in Core, kg	45.0	32.8
U^{233} in Heat Exchangers, kg	4.0	72.0
Total U^{233} in Core and Heat Exchangers, kg	49.0	104.8
Total U^{233} in Entire System, kg	91.0	---

The efficiency was slightly higher for the Georgia Tech UF_6 breeder power plant due to the superheated steam cycle which has an efficiency of 40.4% compared to the 34% steam cycle employed in the Los Alamos design.

The main advantage of the Georgia Tech reactor versus the Los Alamos reactor is that the reactor exit temperature is much less for the Georgia Tech reactor. This is important because more UF_6 dissociates at higher temperatures creating fluorine which may cause corrosion problems. Operating at lower temperatures will also alleviate materials problems and increase the lifetime of the power plant. In addition, the Los Alamos design used a Brayton cycle which needs additional development work, whereas the superheated steam cycle is already used in most power plants.

Therefore, UF_6 breeder reactor power plants can be developed using present day or near term technology with power plant efficiencies comparable or slightly greater than present day nuclear power plants and with a lower uranium inventory.

For the purpose of transmutation of actinides, gas core reactors can be designed to act as special burner reactors; servicing large numbers of LWRs and capable of maintaining a high flux. The plasma core actinide transmuter was designed to service 27 LWRs. Due to the many constraints imposed on the high temperature uranium plasma core, a low flux of 7×10^{12} n/cm^2-sec was used for the actinide region. As a result of the low flux, long irradiation times (~ 13 recycles) are required to attain equilibrium. These irradiation times were comparable to those obtained by Claiborne[2] and Beaman.[3] The uranium hexafluoride gas core

reactor can sustain higher fluxes (10^{14} n/cm^2-sec) in the actinide region. However, since the actinide region consisted of conventional solid actinide fuel rods, the buildup of fissile isotopes in this high flux actinide region posed severe heat transfer problems. As a result, the actinide region neutron flux must be decreased with increasing time to maintain a constant volumetric heat generation rate.

The heat transfer problems in the actinide region arise principally from the buildup of fissile plutonium isotopes. If the actinides can be used in a molten salt blanket, the converted plutonium isotopes can be continually removed and the heat transfer problems greatly alleviated.

One consequence of loading a large quantity of actinide nuclides into a transmuter is that the core and the actinide region become closely coupled. Hence, the criticality of the reactor is greatly affected by the composition change in the actinides. A detailed neutronic study of such a reactor will require a detailed set of cross sections for the actinides.

Again, the U^{233} inventory in the core and heat exchanger is seen to be low (102 kg for the case under study). The power plant efficiency at the beginning of life was 39.2%, assuming that the heat transfer problems mentioned previously can be solved in such a way that the model in Section 4.C is feasible.

The UF_6 reactor need not be designed for breeding and actinide transmutation applications. The relaxation of some of the constraints enables the reactor to operate at high powers under different conditions. Examples of UF_6 power reactors is given in Table 5.2 which summarizes work done by the University of Florida.[4] The main criticism of these

Table 5.2 University of Florida's UF_6 Reactor Designs[4]

Characteristics	HGCR1	HGCR2
Total Power	3000 MW(th)	1000 MW(th)
Moderator/coolant Material	H_2O	D_2O
Core Barrel Material	Be or BeO	Be or BeO
Moderator/coolant Channel Tube Material	Nb-alloy	Be or BeO
Reflector Material	H_2O	D_2O
Core Diameter	340 cm	340 cm
Core Height	360 cm	360 cm
Core Volume	32.69 m^3	32.69 m^3
Tube Thickness	0.1 cm	0.5 cm
Core Barrel Thickness	20 cm	20 cm
Reflector Thickness	40 cm	80 cm
Unit Cell Radius	3.2 cm	7.5 cm
Number of Coolant Channels	2800	514
Fuel Volume Fraction in the Core	0.88	0.64
Average UF_6 Pressure	20 atm	20 atm
U_{235} Enrichment (Average)	12 wt%	3 wt%
He Pressure	21 atm	21 atm
Coolant Pressure	1100 psi	1100 psi
Power Density	92 kW/litre	31 kW/litre
Uranium Mass in the Core	1665 kg	1665 kg
U_{235} Mass in the Core	200 kg	50 kg
Average Gas Temperature	~1000 K	~1000 K
Average Coolant Temperature	~540 K	~540 K
Estimated HGCR Overall Efficiency	~40%	~40%

designs is that the UF_6 to He partial pressure ratio is too high so that excessive amounts of uranium will be present in the heat exchangers.

In conclusion, it can be seen that the gas core reactor can operate under a wide range of conditions. No optimization was performed in this study, but it was shown that the UF_6 reactor can be used as a breeder with low uranium inventory and high power plant efficiency. The superior actinide transmutation features of the UF_6 reactor was also demonstrated, but further work is needed to solve the heat transfer problems. Plasma core reactors will require more extensive research, but the high power plant efficiencies that may be obtained when the reactor is coupled to a MHD generator is a strong motivating factor for further investigation of this system.

References for Chapter 5

1. Lowry, L. L., "Gas Core Reactor Power Plants Designed for Low Proliferation Potential," LA-6900-MS (September, 1977).

2. Claiborne, H. C., "Neutron Induced Transmutation of High-Level Radioactive Waste," ORNL-TM-3964 (December, 1972).

3. Beaman, S. L. and Aitken, E. A., "Feasibility Studies of Actinide Recycling in LMFBRs as a Waste Management Alternative," General Electric Company.

4. Han, K. I., Dugan, E. T., and Diaz, N. J., "Heterogeneous Gas Core Reactor Power Plants," Transactions of the American Nuclear Society, 27, 721-724 (November 27 - December 2, 1977).

Appendix A. Material Properties

UF_6 - helium gas mixture properties were calculated in the manner suggested by Ref. 1. The UF_6 thermophysical properties listed in Table A.1 were obtained from Ref. 2 which used data from Ref. 3. Helium properties shown in Table A.2 were obtained from Refs. 4 and 5. The properties of pure UF_6 and helium were used to obtain mixture properties following the procedures given in Ref. 6.

The mixture density is calculated from

$$\rho_{mix} = \rho_{UF_6} + \rho_{He} \tag{A.1}$$

while the specific heat at constant pressure of the mixture is obtained from

$$C_p^{mix} = \frac{C_p^{UF_6} \rho_{UF_6} + C_p^{He} \rho_{He}}{\rho_{mix}} \tag{A.2}$$

The specific heat at constant volume for UF_6 and for helium are

$$C_v^{UF_6} = \frac{C_p^{UF_6}}{\gamma_{UF_6}} \tag{A.3}$$

$$C_v^{He} = \frac{C_p^{He}}{\gamma_{He}} \tag{A.4}$$

which are used to determine the ratio of specific heats for the mixture,

$$\gamma_{mix} = \frac{C_p^{UF_6} \rho_{UF_6} + C_p^{He} \rho_{He}}{C_v^{UF_6} \rho_{UF_6} + C_v^{He} \rho_{He}} \tag{A.5}$$

Table A.1

UF_6 Thermophysical Properties[2]

Density, $\rho = 4.2675 \times 10^{-2} \frac{p}{T}, \frac{kg}{m^3}$
Specific Heat, $C_p = 391.22 + 0.09574\,T - \frac{3.8685 \times 10^6}{T^2}, \frac{J}{kg\ °K}$
Thermal Conductivity, $k = [0.0257\,T - 0.9093] \times 10^{-3}, \frac{W}{m\ °K}$
Viscosity, $\mu = [0.469 + 0.0044\,T] \times 10^{-5}$, pascal - sec
Ratio of Specific Heats, $\gamma = 1.06$

Pressure is in pascals
Temperatures are in degrees Kelvin

Table A.2

Helium Thermophysical Properties[4,5]

Density, $\rho = 4.8146 \times 10^{-4} \frac{p}{T}, \frac{kg}{m^3}$
Specific Heat, $C_p = 5192.6, \frac{J}{kg\ °K}$
Thermal Conductivity, $k = [6457 + 28.285\ T] \times 10^{-5}, \frac{W}{m\ °K}$ $200\ °K \leq T \leq 1000\ °K$
Viscosity, $\mu = 8.358 \times 10^{-6} + 3.659 \times 10^{-8}\ T$, pascals-sec $200\ °K \leq T \leq 1000\ °K$
Ratio of Specific Heat, $\gamma = 1.6667$

Pressure is in pascals
Temperatures are in degrees Kelvin

Given the mixture mass flow rate, $\dot{m}_{mix}$, and the ratio of UF_6 partial pressure to total pressure, r, the mass flow rates of UF_6 and helium are found from

$$\dot{m}_{UF_6} = \frac{\dot{m}_{mix}}{1 + \frac{M_{He}}{M_{UF_6}} \frac{1-r}{r}} \tag{A.6}$$

$$\dot{m}_{He} = \dot{m}_{mix} - \dot{m}_{UF_6} \tag{A.7}$$

where M_{He} and M_{UF_6} are the molecular weights of helium and UF_6, respectively.

The mole flow rates are defined by

$$\dot{x}_{UF_6} = \frac{\dot{m}_{UF_6}}{M_{UF_6}} \tag{A.8}$$

$$\dot{x}_{He} = \frac{\dot{m}_{He}}{M_{He}} \tag{A.9}$$

The mixture viscosity and conductivity are then given by

$$\mu_{mix} = \sum_i \frac{\dot{x}_i \mu_i}{\sum_j \dot{x}_j \Phi_{ij}} \tag{A.10}$$

$$k_{mix} = \sum_i \frac{\dot{x}_i k_i}{\sum_j \dot{x}_j \Phi_{ij}} \tag{A.11}$$

where the summation is taken over the helium and UF_6 species and Φ_{ij} is given by

$$\Phi_{ij} = \frac{1}{\sqrt{8}} \frac{\left[1 + \left(\frac{\mu_i}{\mu_j}\right)^{\frac{1}{2}} \left(\frac{M_j}{M_i}\right)^{\frac{1}{4}}\right]^2}{\left[1 + \left(\frac{M_i}{M_j}\right)\right]^{\frac{1}{2}}} \qquad \text{(A.12)}$$

Values of C_p^{mix}, μ_{mix}, and k_{mix} as functions of helium mole fraction are given in Tables A.3 to A.5 for various temperatures. These properties are also shown graphically in Figs. A.1 to A.3.

The molten salt used in the breeding blanket is composed of LiF (71.7 mole %), BeF_2 (16 mole %), and ThF_4 (12.3%). Its properties listed in Table A.6 were obtained from Ref. 7.

The properties of NaF (8 mole %)-$NaBF_4$ (92 mole %) salt is given in Table A.7 and were obtained from Ref. 8.

Hastelloy-N is a nickel alloy which is compatible with fluorides. Modified Hastelloy-N is very similar in composition and other related physical properties to standard Hastelloy-N, but the addition of 2% titanium increases the ability of Hastelloy-N to resist helium embrittlement due to neutron irradiation. A thorough discussion of this material is given in Ref. 9 as only the physical properties are summarized in Table A.8 which was obtained from Ref. 10.

Further discussion of the corrosion problem is made in Ref. 11. As pointed out in that report, nickel or one of its alloys, is the best candidate for containing UF_6. However, nickel has a high capture cross section which prevents it from being used in large amounts in the reactor core. But it may be possible to use small amounts of nickel in the core by utilizing it as a clad. For example, nickel may be electroplated onto a beryllium substrate. Further work is needed to determine the optimum material and geometry of structural material in the core.

Table A.3. Specific Heats at Constant Pressure for UF_6-Helium Mixtures For Various Mole Fractions of He

$$C_p \left(\frac{J}{kg\ °K}\right)$$

$\frac{x^{He}}{x^{TOT}}$	T = 600°K	T = 700°K	T = 800°K
0	437.92	450.35	461.76
0.1	443.87	456.29	467.68
0.2	451.29	463.69	475.06
0.3	460.80	473.17	484.52
0.4	473.41	485.75	497.07
0.5	490.96	503.25	514.54
0.6	517.04	529.27	540.49
0.7	559.87	571.99	583.10
0.8	643.22	655.12	666.03
0.9	876.20	887.49	897.84
0.91	924.77	935.93	946.16
0.92	983.96	994.97	1005.1
0.93	1057.7	1068.5	1078.4
0.94	1152.1	1162.7	1172.3
0.95	1277.2	1287.5	1296.8
0.96	1451.0	1460.8	1469.8
0.97	1708.8	1717.9	1726.2
0.98	2130.6	2138.7	2146.0
0.99	2946.6	2952.5	2957.8
0.995	3727.4	3731.3	3734.8
0.998	4475.4	4477.3	4479.0
1.0	5192.6	5192.6	5192.6

Table A.4. Viscosities for UF_6-Helium Mixtures at Various Mole Fractions of He

$\frac{x^{He}}{x^{TOT}}$	μ (pascal-sec)		
	T = 600°K	T = 700°K	T = 800°K
0	3.1090×10^{-5}	3.5490×10^{-5}	3.9890×10^{-5}
0.1	3.1444×10^{-5}	3.5889×10^{-5}	4.0335×10^{-5}
0.2	3.1860×10^{-5}	3.6359×10^{-5}	4.0857×10^{-5}
0.3	3.2356×10^{-5}	3.6917×10^{-5}	4.1478×10^{-5}
0.4	3.2955×10^{-5}	3.7590×10^{-5}	4.2224×10^{-5}
0.5	3.3689×10^{-5}	3.8412×10^{-5}	4.3135×10^{-5}
0.6	3.4601×10^{-5}	3.9430×10^{-5}	4.4258×10^{-5}
0.7	3.5735×10^{-5}	4.0687×10^{-5}	4.5636×10^{-5}
0.8	3.7071×10^{-5}	4.2143×10^{-5}	4.7213×10^{-5}
0.9	3.8007×10^{-5}	4.3071×10^{-5}	4.8132×10^{-5}
0.91	3.7971×10^{-5}	4.3008×10^{-5}	4.8043×10^{-5}
0.92	3.7877×10^{-5}	4.2878×10^{-5}	4.7876×10^{-5}
0.93	3.7708×10^{-5}	4.2660×10^{-5}	4.7608×10^{-5}
0.94	3.7439×10^{-5}	4.2325×10^{-5}	4.7207×10^{-5}
0.95	3.7036×10^{-5}	4.1834×10^{-5}	4.6630×10^{-5}
0.96	3.6452×10^{-5}	4.1134×10^{-5}	4.5814×10^{-5}
0.97	3.5619×10^{-5}	4.0147×10^{-5}	4.4673×10^{-5}
0.98	3.4435×10^{-5}	3.8757×10^{-5}	4.3078×10^{-5}
0.99	3.2748×10^{-5}	3.6791×10^{-5}	4.0833×10^{-5}
1.00	3.0312×10^{-5}	3.3971×10^{-5}	3.7630×10^{-5}

Table A.5. Thermal Conductivities For UF_6-Helium Mixtures at Various Mole Fractions of He

$$k \left[\frac{W}{m\ °K}\right]$$

$\frac{x^{He}}{x^{TOT}}$	T = 600°K	T = 700°K	T = 800°K
0	1.4511×10^{-2}	1.7081×10^{-2}	1.9651×10^{-2}
0.1	1.8913×10^{-2}	2.2076×10^{-2}	2.5239×10^{-2}
0.2	2.4178×10^{-2}	2.8049×10^{-2}	3.1918×10^{-2}
0.3	3.0591×10^{-2}	3.5316×10^{-2}	4.0038×10^{-2}
0.4	3.8569×10^{-2}	4.4349×10^{-2}	5.0125×10^{-2}
0.5	4.8765×10^{-2}	5.5880×10^{-2}	6.2989×10^{-2}
0.6	6.2251×10^{-2}	7.1107×10^{-2}	7.9954×10^{-2}
0.7	8.0919×10^{-2}	9.2139×10^{-2}	1.0335×10^{-1}
0.8	1.0843×10^{-1}	1.2304×10^{-1}	1.3763×10^{-1}
0.9	1.5286×10^{-1}	1.7267×10^{-1}	1.9245×10^{-1}
0.91	1.5883×10^{-1}	1.7931×10^{-1}	1.9977×10^{-1}
0.92	1.6518×10^{-1}	1.8637×10^{-1}	2.0753×10^{-1}
0.93	1.7195×10^{-1}	1.9388×10^{-1}	2.1579×10^{-1}
0.94	1.7917×10^{-1}	2.0188×10^{-1}	2.2958×10^{-1}
0.95	1.8688×10^{-1}	2.1042×10^{-1}	2.3394×10^{-1}
0.96	1.9512×10^{-1}	2.1954×10^{-1}	2.4393×10^{-1}
0.97	2.0395×10^{-1}	2.2928×10^{-1}	2.5458×10^{-1}
0.98	2.1340×10^{-1}	2.3968×10^{-1}	2.6594×10^{-1}
0.99	2.2351×10^{-1}	2.5078×10^{-1}	2.7804×10^{-1}
1.00	2.3428×10^{-1}	2.6257×10^{-1}	2.9085×10^{-1}

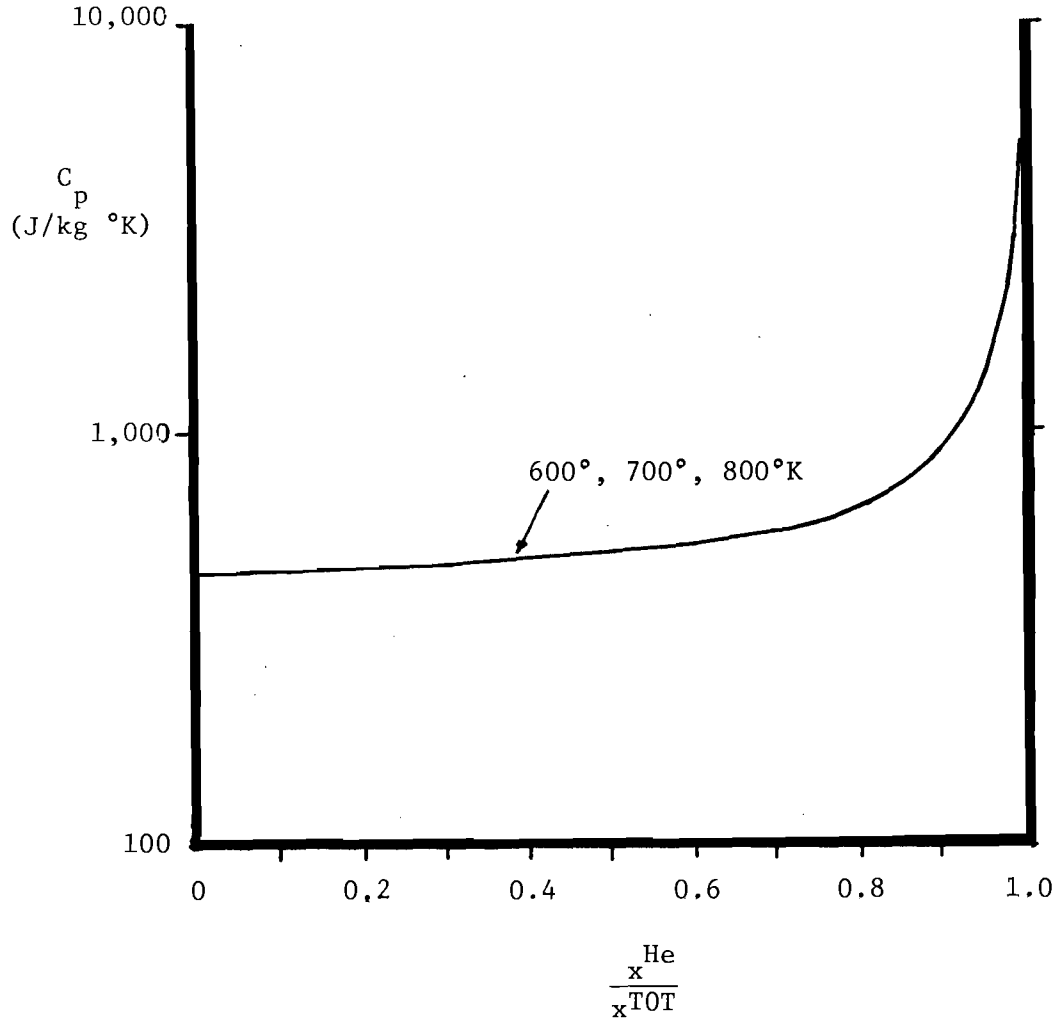

Fig. A.1. Specific Heats at Constant Pressure for UF_6-Helium Mixtures at Various Mole Fractions of He

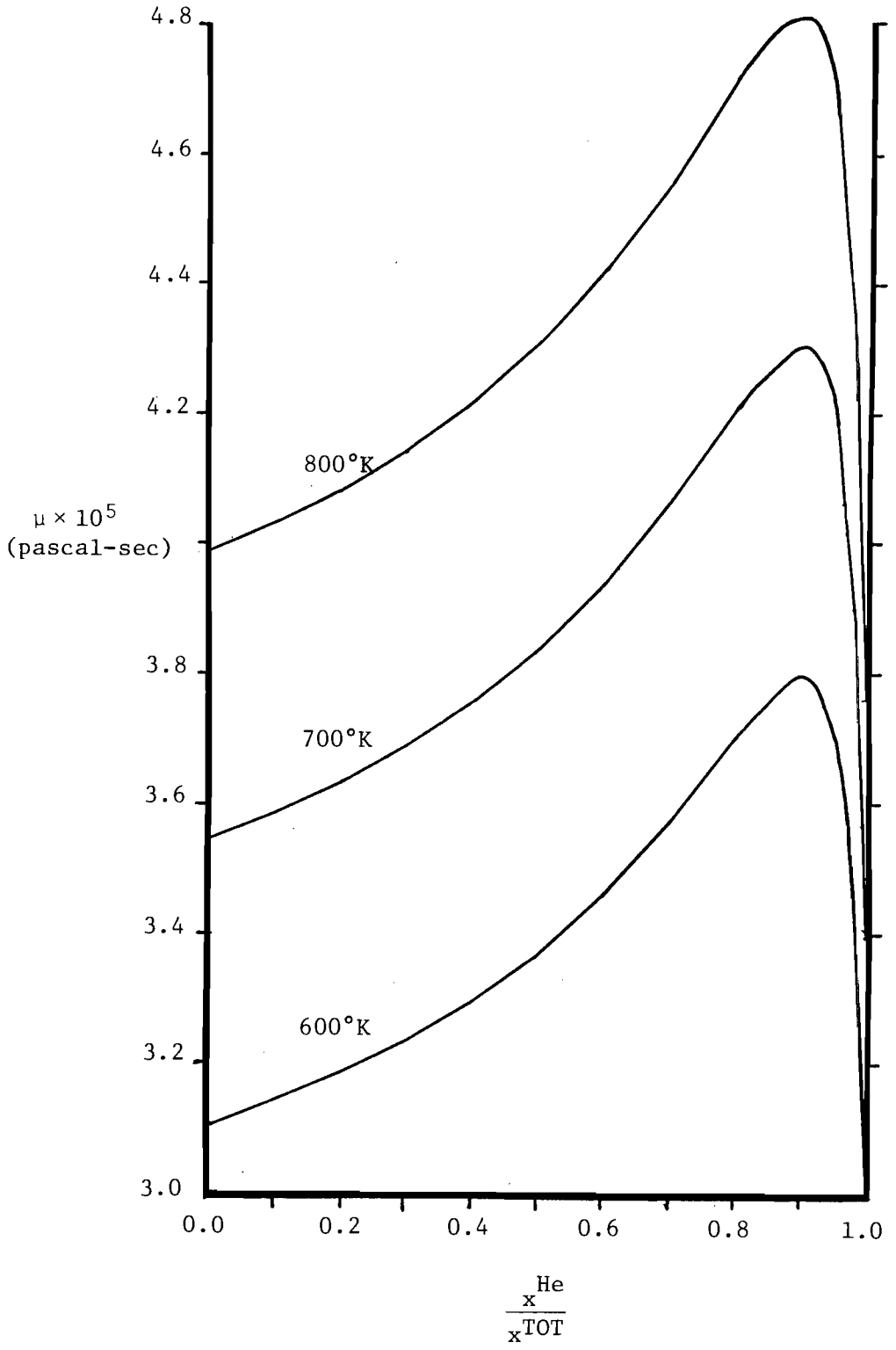

Fig. A.2. Viscoscities of UF_6-Helium Mixtures at Various Mole Fractions of He

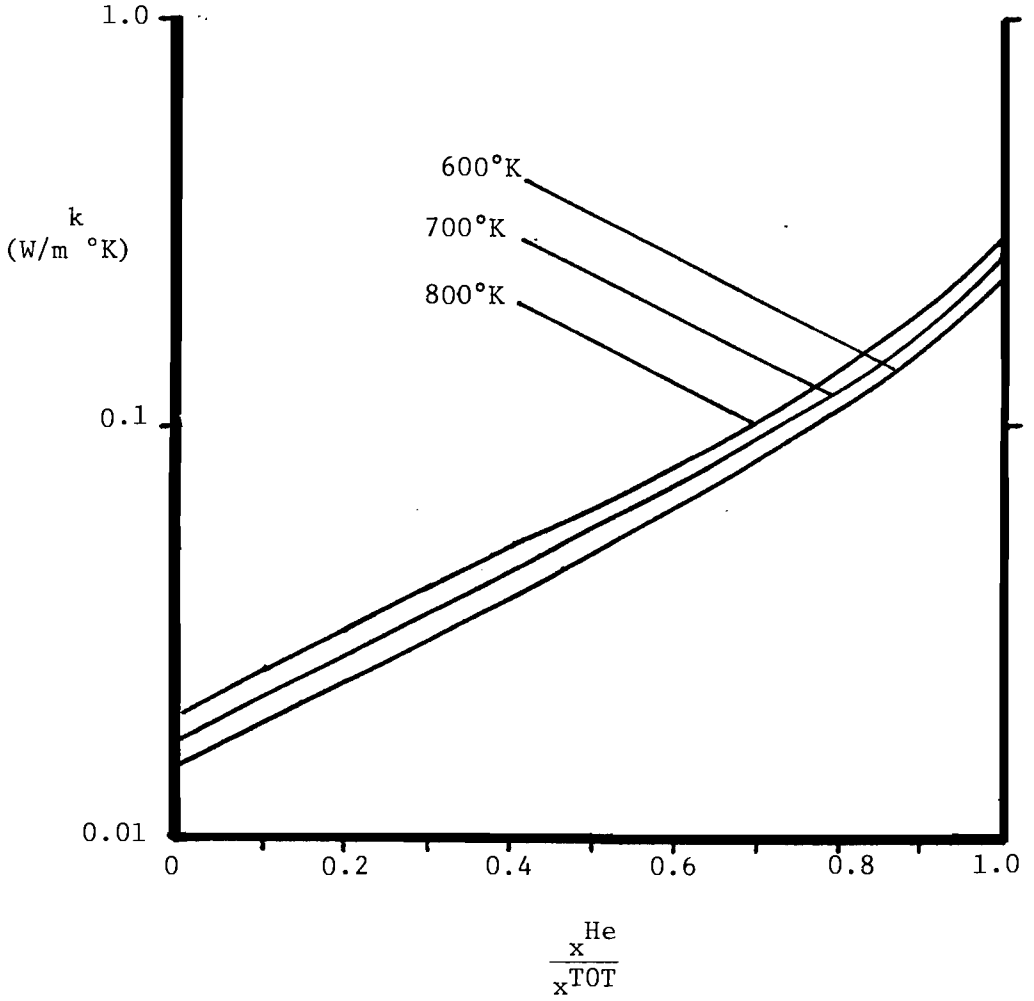

Fig. A.3. Thermal Conductivities for UF_6-Helium Mixtures at Various Mole Fractions of He

Table A.6. Thermophysical Properties of LiF (71.7 mole %), BeF_2 (16 mole %), and ThF_4 (12.3 mole %) Molten Salt (7)

Molecular Weight = 64

Melting Point = 772 °K

Specific Heat at Constant Pressure = 1356.6 $\frac{J}{kg\ °K}$

Density = 3935.4 - 0.6682 T $\frac{kg}{m^3}$, T is in °K

Viscosity = 1.0901×10^{-4} exp (4090/T) pascals-sec , T is in °K

Thermal Conductivity = 1.19 $\frac{W}{m\ °K}$ at 978 °K

1.23 $\frac{W}{m\ °K}$ at 908 °K

1.19 $\frac{W}{m\ °K}$ at 839 °K

Vapor Pressure at 894 °K is less than 13.33 pascals (1 mm Hg)

Table A.7. Thermophysical Properties of NaF (8 mole %), $NaBF_4$ (92 mole %) Salt[8]

Melting Point = 658 °K

Physical Properties at 727 °K

Density = 1938.4 $\frac{kg}{m^3}$

Specific Heat at Constant Pressure = 1507.3 $\frac{J}{kg\ K}$

Viscosity = 0.0025 pascals-sec

Thermal Conductivity = 0.5 $\frac{W}{m\ °K}$

Vapor Pressure at 880 °K* = 2.667×10^3 pascals (200 mm Hg)

*Highest permissible operating temperature.

Table A.8. Properties of Hastelloy N [9]

Yield Strength	3.103×10^8 pascals
Tensile Strength	7.929×10^8 pascals
Elongation	51%
Brinell Hardness	96
Density	8489.3 $\frac{kg}{m^3}$
Specific Gravity	8.79
Melting Point	1672 °K
Specific Heat	418.7 $\frac{J}{kg\ °K}$
Coefficient of Thermal Expansion	3.44 m/m/°K
Thermal Conductivity	10.25 $\frac{W}{m\ °K}$
Electrical Resistivity	1.388×10^{-6} ohm-m
Young's Modulus of Elasticity	2.186×10^{11} pascals

Nominal Composition

Chromium	7%	Molybdenum	16.5%
Iron	8%	Nickel	65.5%
Titanium	3%		

References for Appendix A

1. Private communication with John S. Kendall of the United Technologies Research Center, East Hartford, Connecticut (January 25, 1978).

2. Rodgers, R. J., Latham, T. S., and Krascella, M. L., "Analysis of Low-Power and Plasma Core Cavity Reactor Experiments," United Aircraft Research Laboratories Report, R75-911908-1 (May 1975).

3. Katz, J. J. and Rabinowitch, E., Chemistry of Uranium, USAEC, Technical Information Service, Oak Ridge, Tennessee (1958).

4. Lick, W. J. and Emmons, H. W., Thermodynamic Properties of Helium to 50,000°K, Harvard University Press (1962).

5. Lick, W. J. and Emmons, H. W., Transport Properties of Helium to 50,000°K, Harvard University Press (1965).

6. Holmes, J. T. and Baerns, M. G., "Predicting Physical Properties of Gases and Gas Mixtures," Chemical Engineering (May 24, 1965).

7. Robertson, R. C., "Conceptual Design Study of a Single-Fluid Molten Salt Breeder Reactor," ORNL-4541 (June 1971).

8. Grimes, W. R., "Molten Salt Reactor Chemistry," Nuclear Applications and Technology, 8 (February 1970).

9. Clement, J. D. and Rust, J. H., "Analysis of UF_6 Breeder Reactor Power Plants," Final Report, NASA Grant NSG-1168, Georgia Institute of Technology (February 1976).

10. Properties of Some Metals and Alloys, International Nickel Company, Inc., New York (1968).

11. Wagner, P., "Materials Considerations for UF_6 Gas-Core Reactor. Interim Report for Preliminary Design Study," LA-6776-MS (April 1977).

Appendix B Reprocessing Systems

No quantitative analysis was made of the reprocessing systems for the UF_6 breeder and actinide transmutation reactors. However, since the reprocessing systems are important to the operation of the power plants, a qualitative discussion is included in this study which is based on proposed systems given in Refs. 1-3. Although these studies were preliminary in nature, they did not encounter major obstacles.

There are three major reprocessing systems to be considered. The first is the cleanup of fission products in the UF_6-helium mixture. For the breeder power plant, the bred material must be separated from the breeding salt. Finally, actinides must be separated from other waste products to be used in the actinide transmutation reactor. These systems will be described in the following sections.

B.1 Fission Product Cleanup

Fission products must be removed from the UF_6-helium mixture continuously to avoid buildup of reactor poisons and condensation of volatiles. Fortunately, the technology for UF_6 separation and purification is available from the Molten Salt Breeder Reactor Program at Oak Ridge National Laboratory and helium purification technology is available from the High Temperature Gas Cooled Reactor developed by General Atomics.

It is expected that some UF_6 will dissociate in the core and that the fluorine formed will combine with metallic fission products to form fluorides. According to Ref. 1, the fluorides and gases in Table B.1 will be formed. The fluorides are divided into volatile, mobile, intermediate and refractory fluorides according to their boiling points. The mole

Table B.1

Gaseous and Fluoride Fission Products[1]

Gases	Volatile Fluorides	Mobile Fluorides	Intermediate Fluorides	Refractory Fluorides
Kr	SeF_6 (236°K)*	SbF_5 (423°K)	Cs F (1524°K)	RaF_2 (2410°K)
Xe	MoF_6 (308°K)	NbF_5 (509°K)	Rb F (1663°K)	YF_3 (2500°K)
I	TeF_6 (309°K)	RuF_5 (523°K)		CeF_3 (2573°K)
Br		ZrF_5 (873°K)		NdF_3 (2573°K)
		SuF_4 (978°K)		PrF_4 (2600°K)
				LaF_3 (2600°K)
				SrF_2 (2762°K)

*numbers in parantheses are the boiling points of the various fluorides

fractions of the fission product gases, volatile fluorides, and mobile fluorides are on the order of 10^{-5} less than the mole fraction of helium while the mole fractions of the intermediate and refractory fluorides are 10^{-3} less than the other fluorides.

Due to their low boiling points, the volatile and some of the mobile fluorides will remain in the UF_6-helium circulating gas loop until they are removed for reprocessing. The other fluorides will be deposited in the heat exchangers and piping. The problem is further complicated by radioactive decay of various species, resulting in a change of their chemical nature and the relocation of their deposition sites.

Reference 1 suggests that replaceable getter pads made of nickel wire be placed in the reactor outlet piping to capture the intermediate and refractory fluorides.

Lowry[1] of the Los Alamos Scientific Laboratory proposed the fission product cleanup system shown in Fig. B.1. A small amount of UF_6-helium gas mixture is bled from the circulating loop and is reduced in pressure to 1.5 atmospheres. The mixture then passes into a high temperature bed of Na F pellets at 500°K where most of the volatile fluorides are absorbed and is cooled to 300°K before entering a low temperature bed of Na F pellets. The low temperature bed absorbs the UF_6 and remaining metal fluorides while the helium containing xenon, krypton, bromine, iodine and other gases pass through the filter to the helium purification system.

Two low temperature beds are utilized. When one bed becomes loaded with UF_6, the flow into this bed is valved out and the fresh bed is placed in service. The bed loaded with UF_6 is then heated to 700°K which drives

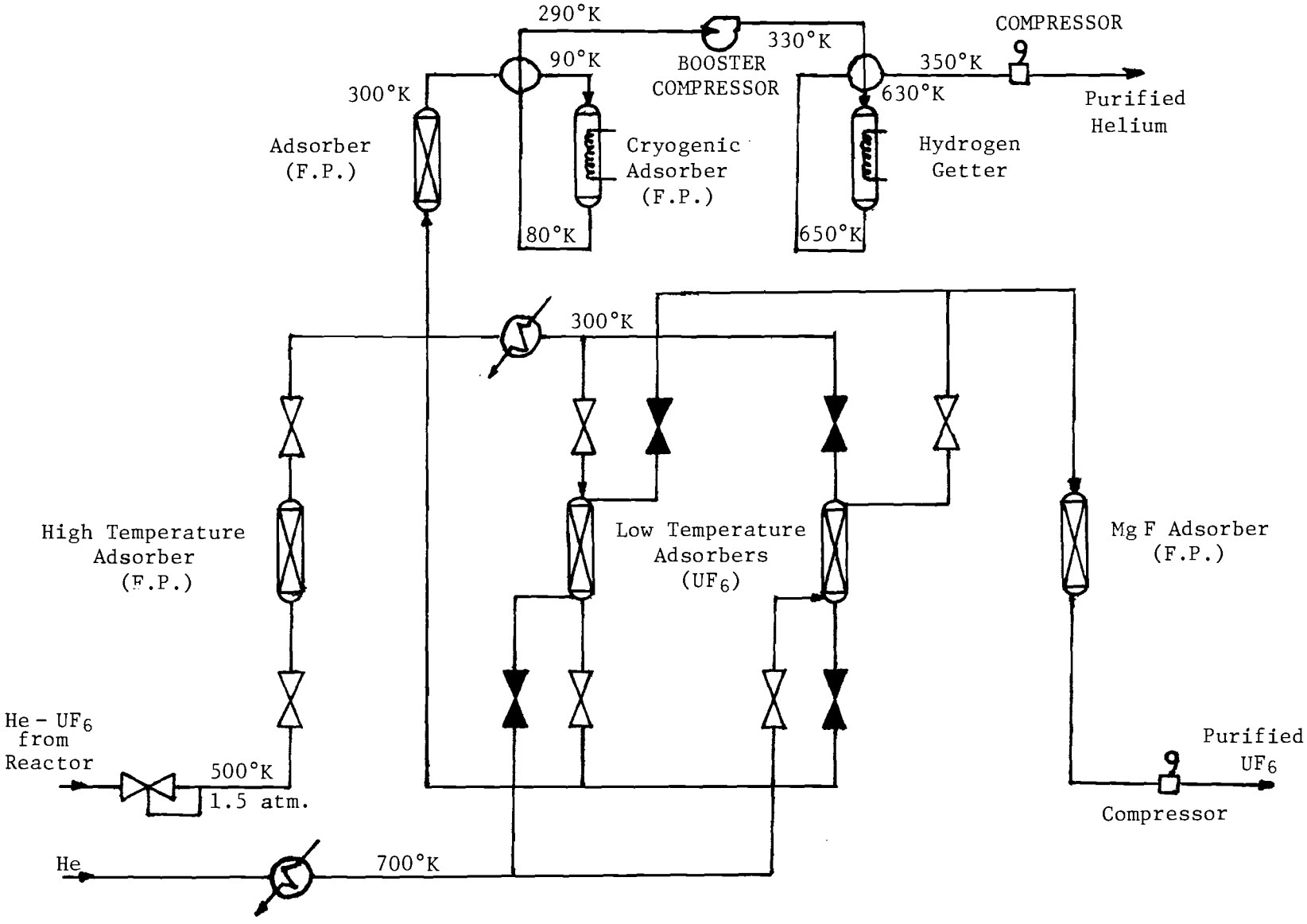

Fig. B.1 Fission Product Removal System[1]

off UF_6 as a gas along with small amounts of TeF_6. A helium purge gas is used to help remove the UF_6. Finally, the UF_6 passes through a bed of MgF_2 to remove the TeF_6 before being filtered, pressurized, and cooled to produce a purified liquid which is recycled to the reactor. The NaF and MgF_2 beds containing fission products are either stored or sent to a waste treatment plant.

Helium at 300°K flows into one of two parallel systems consisting of high and low temperature charcoal absorbers. The high temperature absorber contains activated charcoal impregnated with potassium. The charcoal removes the condensable metallic fission products while the potassium removes iodine by chemisorption.

The helium is then cooled to 90°K in a helium regenerator and passes through the low temperature absorber which removes krypton, xenon, nitrogen, and some hydrogen and tritium. Helium is cooled in the absorber to 80°K by liquid nitrogen. The purified helium then enters the cold side of the regenerator where it is heated to 290°K and is filtered to remove dust before being compressed and sent to the hydrogen removal section.

Helium leaving the compressor enters another regenerator before passing through one of two parallel hydrogen getters consisting of titanium sponges to remove hydrogen and tritium. Helium enters the getters at 630°K and is heated by the electrically heated sponges to 650°K. The helium then reenters the regenerator and is cooled to 350°K, filtered and recompressed.

The uranium inventory in the reprocessing system is not a function of reactor power but of regeneration frequency and volume of the NaF bed.

Distillation[1] is an alternative method for fission product removal especially if a large part of the primary stream must be cleaned up. The bled stream enters a distillation column where most of the fluorides are removed as a concentrate at the bottom of the column. An aqueous wash removes the fluorides from the concentrate and residual UF_6 is returned to the column for further purification. The UF_6 and volatile fluorides are condensed and fed to a second column which produces pure UF_6 at the bottom of the column.

Another method for UF_6 purification is a combination of a cold trap process and fluoride volatility process proposed by Rust and Clement.[2]

Clearly, there are several possible methods for UF_6 purification. The method that will be selected should be based on consideration of economics, minimum uranium inventory, effectiveness in keeping the system as clean as possible, and compatibility with power plant operation.

B.2 Breeding Salt Reprocessing System

The description of the molten salt breeding blanket reprocessing system is summarized from Ref. 3. Additional information was taken from Ref. 1.

Since it is desirable to have the Gas Core Breeder Reactor (GCBR) be a self-contained unit, generating its own new fuel, an on-line reprocessing system for the molten salt blanket is a necessity. This section describes protactinium removal and salt purification processes, and calculational procedures for expected flow rates and equilibrium concentrations of various isotopes present in the system.

The salt used in the blanket is an eutectic mixture composed of LiF, BeF_2, and ThF_4 in the ratios of 72:16:12 mole percent. This particular combination was developed at the Oak Ridge National Laboratory in conjunction with the Molten Salt Breeder Reactor program.

When thorium atoms contained in the salt are irradiated with neutrons, some of the atoms absorb a neutron and transmute to protactinium as shown in Fig. B.2. The protactinium eventually decays to uranium which can then be fed to the core as new fuel. However, as seen in Figure B.2, Pa^{233} has a substantial cross section (22 barns) and since its half life is 27 days, Pa acts as a poison, siphoning off neutrons which could otherwise irradiate Th atoms. In addition, the daughter of Pa^{233} $\left(U^{233}\right)$ would be lost. For these reasons, it is desirable to remove Pa from the molten salt loop and allow it to decay outside the core.

However, since it is impossible to have a zero protactinium concentration in the molten salt blanket, there will be some uranium present in the core. Some of these atoms will fission and, consequently, there will be some uranium fission products in the molten salt loop. Some of these fission products have large cross sections as shown in Table B.2. Note that Xe and other gaseous fission product poisons are not listed because it is assumed that the blanket can be vented and these gaseous products easily removed. As will be shown later, the necessity of keeping the concentration of fission products at a low level determines the amount of time which the salt can stay in the irradiated blanket region.

In order to achieve the above neutronics goals, a fluorination-reductive extraction system was developed at Oak Ridge National Lab. A description of this process is as follows:[5]

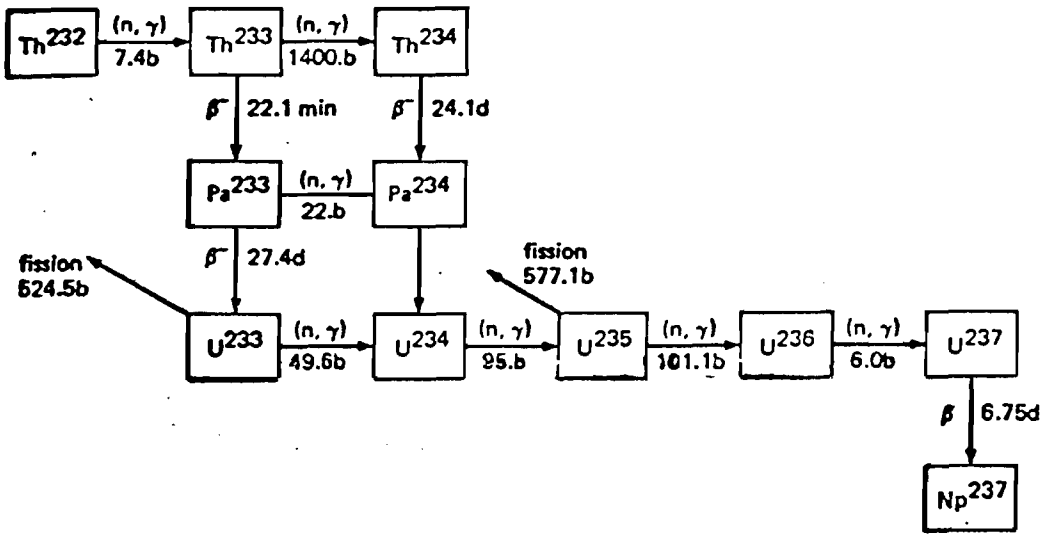

Fig. B.2 The chain of isotopes created by neutron irradiation of Th232.

Table B.2

Rare Earth Fission Product Absorption Cross Section

Nd-143	330 barns
La-139	8.9 barns
Eu-153	320 barns

The fluorination-reductive extraction system for isolating protactinium is shown in its simplest form in Figure B.3. The salt stream from the reactor first passes through a fluorinator, where most of the uranium is removed by fluorination. Approximately 90% of the salt leaving the fluorinator is fed to an extraction column, where it is countercurrently contacted with a bismuth stream containing lithium and thorium. The uranium is preferentially removed from the salt in the lower extractor, and the protactinium is removed by the upper contactor. A tank through which the bismuth flows is provided for retaining most of the protactinium in the system.

The bismuth stream leaving the lower contactor contains some protactinium as well as the uranium that was not removed in the fluorinator and the uranium that was produced by the decay of protactinium. This stream is contacted with a H_2-HF mixture in the presence of approximately 10% of the salt leaving the flourinator in order to transfer the uranium and the protactinium to the salt. The salt stream, containing UF_4 and PaF_4, is then returned to a point upstream of the fluorinator, where most of the uranium is removed. The protactinium passes through the fluorinator and is subsequently extracted into the bismuth. Reductant (Li and Th) is added to the Bi stream leaving the oxidizer, and the resulting stream is returned to the upper contractor. The salt stream leaving the upper contactor is essentially free

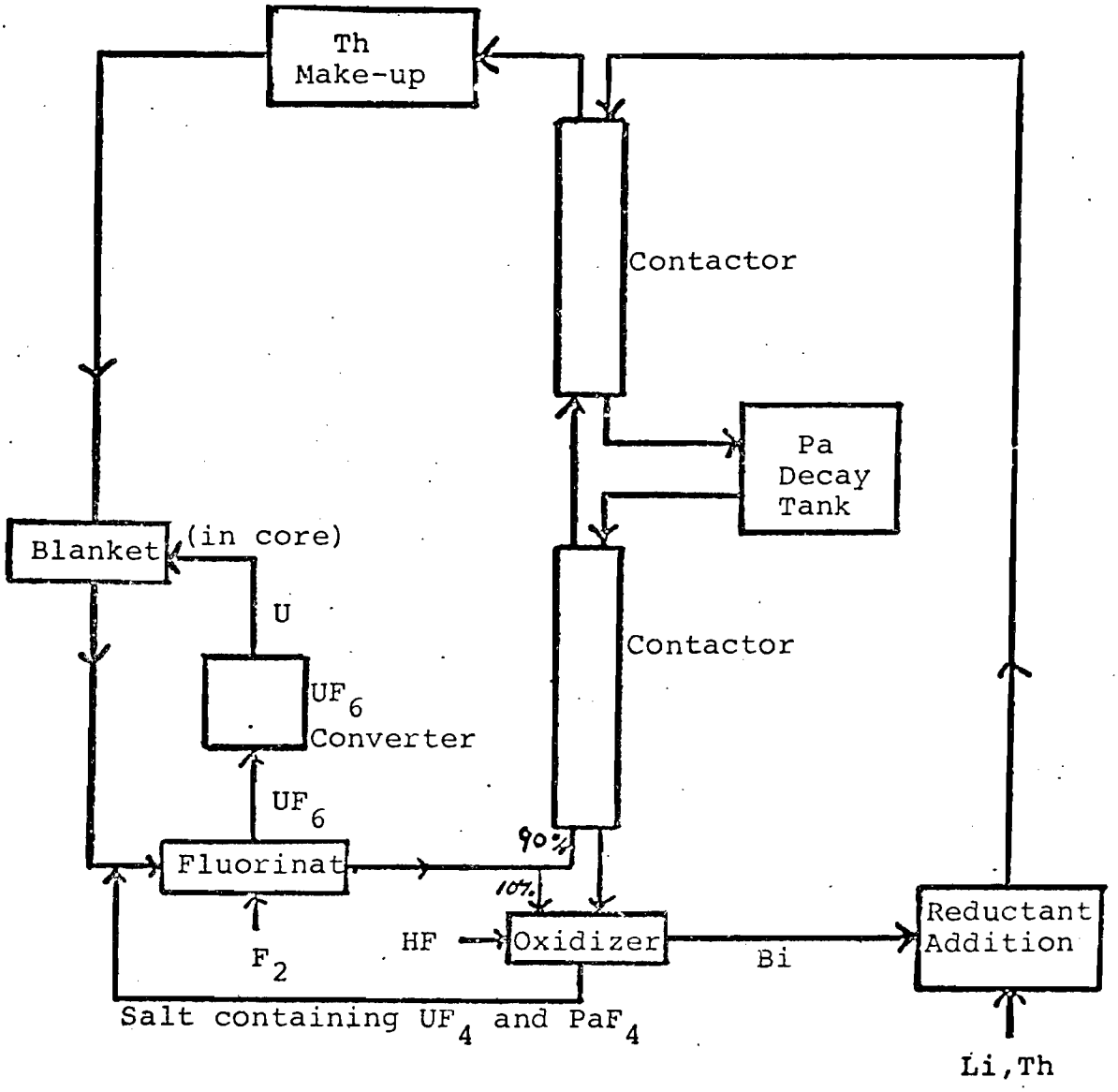

Fig. B.3 UF_6 Breeder Reactor Salt Reprocessing System

of uranium and protactinium and would be processed for removal of any fission product gases and additional thorium added to compensate for that which had been consumed.

Figure B.4 describes the UF_6 to U metal conversion process. Unfortunately this is a batch process instead of a continuous flow system as is present in the remainder of the reprocessing set-up. However, there should be no problem providing temporary storage tanks for UF_6.

The UF_6 initially enters a reaction chamber where it is mixed with hydrogen. A reaction is triggered and UF_4 powder and HF gas is produced. The UF_4 is then loaded into a steel "bomb" which has been coated with fused dolomitic lime--lime is one of the few oxides that does not react with molten uranium. The "bomb" is then heated to 565°C where an exothermic reaction takes place and uranium metal solidifies on the bottom of the "bomb". The MgF_2 is removed and U metal of high purity can then be taken from the bottom of the "bomb" and sent to the plasma core reactor.[7]

Given certain constraints on the reprocessing system it is possible to calculate the flow rates which would exist in both the molten salt and bismuth loops. It is also possible to calculate protactinium concentrations throughout the reprocessing system and therefore determine uranium concentrations throughout the system. The constraints which are placed on the reprocessing system are as follows:

1) The protactinium concentration in the molten salt blanket is allowed to reach 95% of the equilibrium value obtained if the salt remained in the active region of the reactor for an infinite amount of time, provided that the concentration of protactinium does not cause

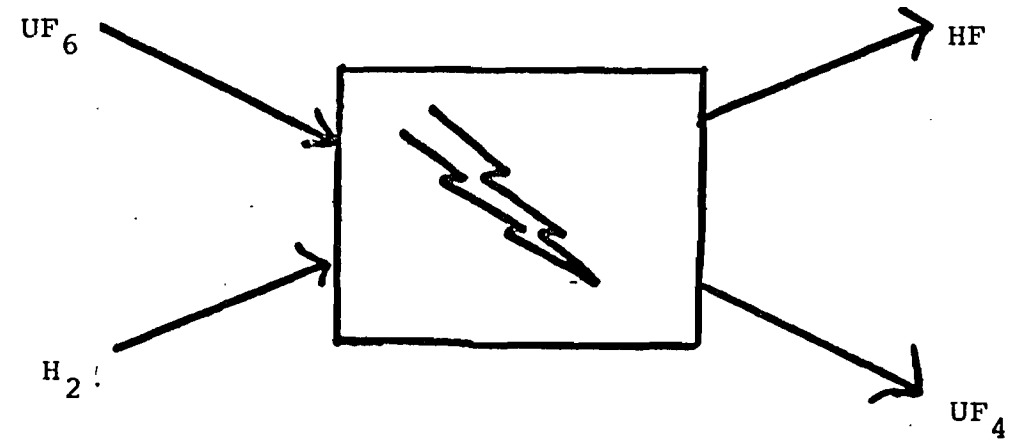

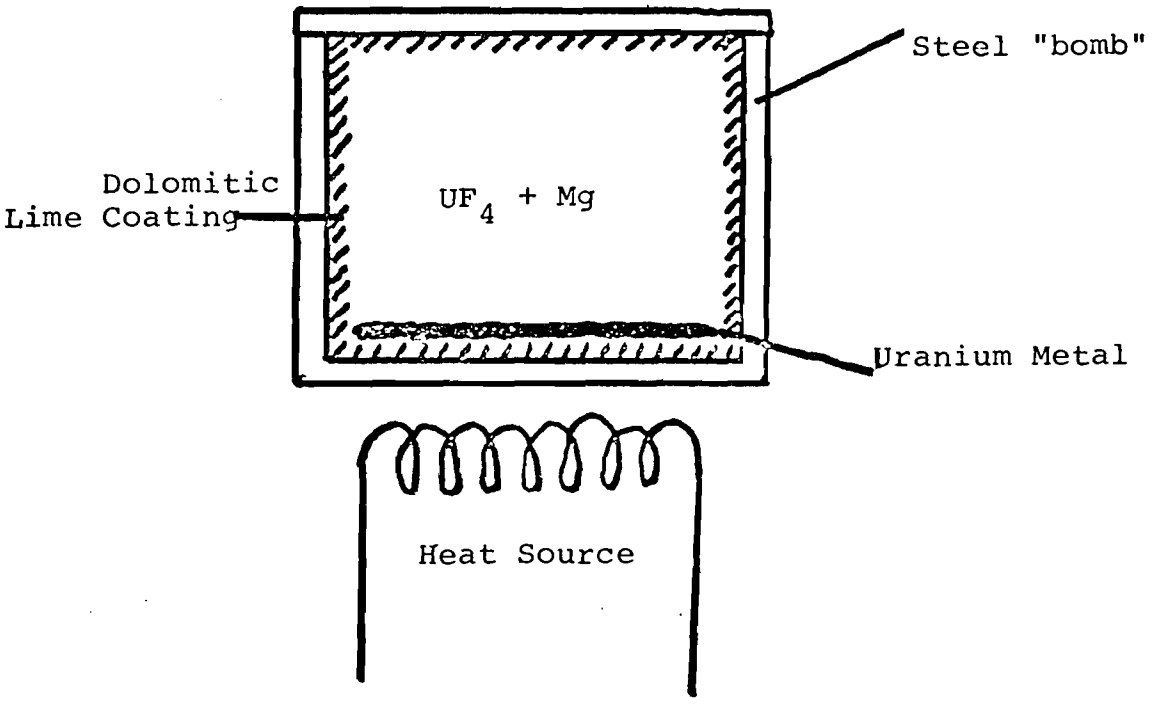

Fig. B.4 UF_6 to U Metal Batch Process

parasitic absorption of neutrons by fission products greater than 1% of the absorptions which are due to thorium captures.

2) The volume of the blanket and the flux in the blanket is determined by breeding ratio constraints as explained elsewhere in this report.

3) The uranium removal efficiency of the fluorinator and oxidizer is 98%.[7]

4) The operating temperature of the system is 640°C (necessary because the salt is a eutectic mixture).[7]

5) The Li concentration in the Bi loop is 1%. The Th concentration in the Bi loop is held at less than 50% of the solubility of Th in Bi.[8]

6) The Pa distribution coefficient for the contactors, defined as (mole fraction of Pa in Bi at equilibrium)/(mole fraction of Pa in salt at equilibrium), can be taken to be 100.[8]

The following physics data is required:

Neutron Flux

Volume of Blanket

Molar Volume of Salt

Molar Volume of Bi

Pa Absorption Cross Section

Th Absorption Cross Section

U Absorption Cross Section

U Fission Cross Section

Pa Decay Constant

Concentration of Th in Salt

To satisfy assumption 1, it is necessary to examine if the Pa concentration in the salt from the output of the blanket will be governed by the rate of fission product captures. To determine the number of fission product captures the Pa and U concentrations are first calculated as follows:

$$\frac{d\ Pa}{dt} + \lambda Pa = \sigma_a^{Th}\ \phi\ Th \tag{B.1}$$

where ϕ is the flux, Th is the thorium concentration, and λ the Pa decay constant.

Solving Eq. B.1 gives

$$Pa = \frac{\sigma_a^{Th}\phi\ Th}{\lambda} - e^{-\lambda t}\left[\frac{\sigma_a^{Th}\phi\ Th}{\lambda} - Pa_o\right] \tag{B.2}$$

The equation for the uranium concentration as a function of time is

$$\frac{dU}{dt} = -\ \phi\ \sigma_a^{u}\ U + \lambda\ Pa \tag{B.3}$$

where U is the U-233 concentration.

Solving this equation we have

$$U = U_o e^{-\sigma_a^{u}\phi t} + \frac{\sigma_a^{Th}\ Th}{\sigma_a^{u}}\left(1 - e^{-\sigma_a^{u}\phi t}\right) - \lambda\left[\frac{\sigma_a^{Th}\phi\ Th}{\lambda} - Pa_o\right]\left[\frac{e^{-\lambda t} - e^{-\sigma_a^{u}\phi t}}{\sigma_a^{u}\phi - \lambda}\right] \tag{B.4}$$

If a material is assumed to spend time T in the blanket, then the number of fissions which occurs during this time is

$$\text{No. of fissions} = \int_o^T \sigma_f{}^u \phi \; U(t)\,dt \tag{B.5}$$

Evaluating this integral we have

$$\text{No. of fissions} = \sigma_f{}^u \phi \left[\frac{\sigma_a{}^{Th}\, Th}{\sigma_a{}^u} \left(T - \frac{e^{-\sigma_a{}^u \phi T} - 1}{\sigma_a{}^u \phi} \right) - \right.$$

$$\left. \frac{\lambda}{(\sigma_a{}^u \phi - \lambda)} \left[\frac{\sigma_a{}^{Th} \phi Th}{\lambda} - P_{ao} \right] \left[\frac{1-e^{-\lambda T}}{\lambda} + \frac{e^{-\sigma_a{}^u \phi T} - 1}{\sigma_a{}^u \phi} \right] \right] \tag{B.6}$$

and the fission product concentration at the end of a cycle of length T is given by

$$[\text{F.P.}] = \left[\int_o^T \sigma\phi \; U(t) \; e^{\sigma_f{}^u \phi t} \, dt \right] e^{-\sigma_f{}^u \phi T} \ll \gamma \; (\text{No. of fissions}) \tag{B.7}$$

where γ is the probability per fission of getting a particular fission product. Since the fluorinater removes 98% of the uranium in the molten salt on each pass through the system, the entering concentration to the blanket region can be taken as effectively zero.

Solving Eq. B.7 for a variety of times T, the results can be given as $\frac{\Sigma_{Eu}}{\Sigma_{Th}}$ where Σ_{Eu} is the absorption cross section of one of the most troublesome rare earth fission products, Eu^{153}. It should be stated that the estimate of the Eu^{153} concentration is high due to the approximation in Eq. B.7. If the concentration is sufficiently small, no fission product removal system is necessary; otherwise, a removal system similar to those discussed in Section B.1 is needed.

To determine the flow rates and concentrations in the system, use must be made of the following mass balance equations.[9] Referring to the hypothetical exchange column shown in Fig. B.5

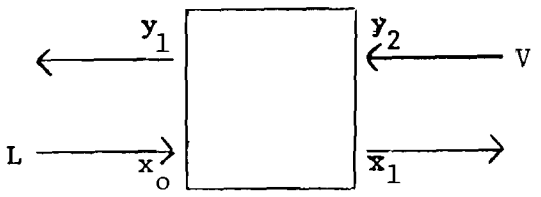

Figure B.5: Exchange Column Flows

then a material balance yields the following equation:

$$Lx_o + Vy_2 = Lx_1 + Vy_1 \tag{B.8}$$

or

$$L\,(x_o - x_1) = V\,(y_1 - y_2) \tag{B.9}$$

where L and V are flow rates in moles/sec and x and y are concentrations of the transferring material expressed in mole fractions. Now at equilibrium

$$y_1 = K \cdot x_1 \tag{B.10}$$

where K is a constant known as the distribution coefficient. Substituting for x_1 in Equation B.9 and solving for y_1 we have

$$y_1 = \frac{y_2 + \frac{L}{V} x_o}{\frac{L}{KV} + 1} \tag{B.11}$$

So if the two inlet concentrations and the flow rates are known, then the outlet concentrations can be calculated.

The value of the flow rates in the Bi and blanket loops must be solved for iteratively. A flow chart of the solution process is shown in Fig. B.6. A value for the Bi flow rate is assumed and for given Pa core concentration, neutron flux, and core volume, the flow rate in the blanket, residence time in the core, and input concentration of Pa to the core can be solved for iteratively.

Reference 8 gives the distribution coefficient of Pa as a function of time of contact and relative volumes of salt and Bi. Picking a specific distribution coefficient determines the time of contact and the relative volume of the two components. A new value for the Bi flow rate can then be calculated by using the value of the blanket flow rate calculated above. The entire iterative procedure is then repeated with the new Bi flow rate.

Once the flow rates have been calculated, the output Pa concentration in the Bi loop from the contactor can then be found from Eq. B.11 and the input concentration from Eq. B.9.

It should be noted at this point that if a contactor is composed of several stages with K being the distribution coefficient in each stage, then the procedure described above can be applied to the whole system with the number of stages, N, given by the expression[9]

$$N = \frac{\log \left[\frac{A-1}{A} \left(\frac{y_{n+1} - Kx_o}{y_1 - Kx_o} \right) + \frac{1}{A} \right]}{\log A} \qquad \text{(B.12)}$$

where A is the absorption factor and is defined by $A = L/(KV)$.

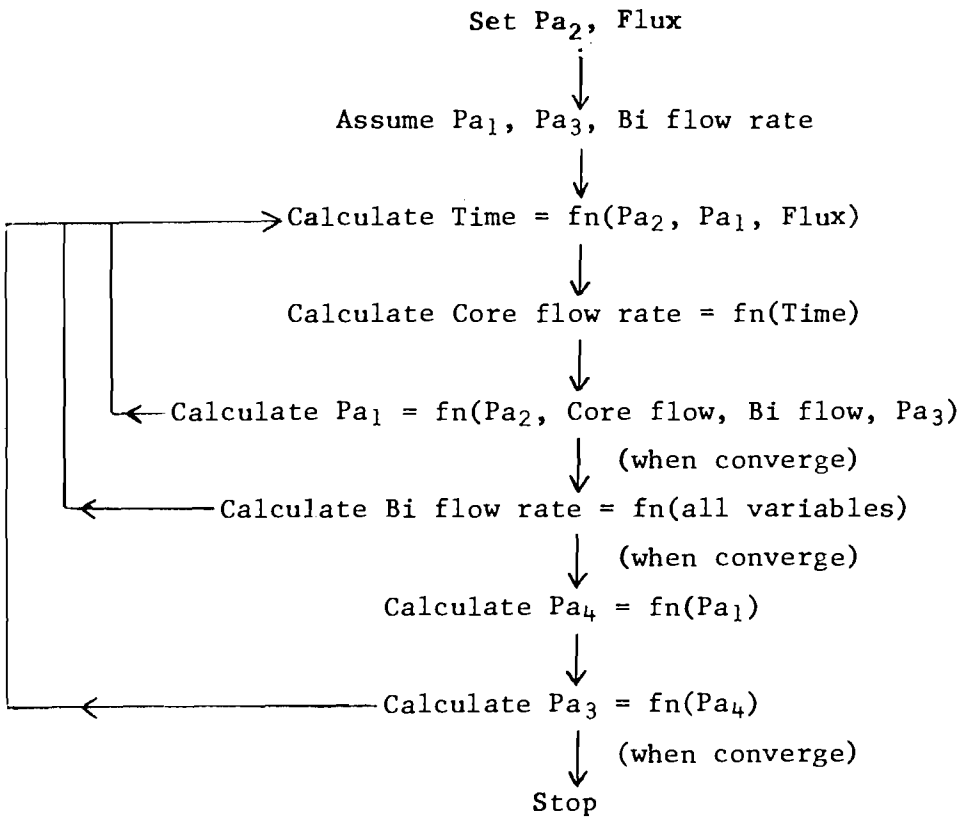

Pa_1 = Core input Pa concentration

Pa_2 = Core output Pa concentration

Pa_3 = Bi loop contactor input Pa concentration

Pa_4 = Bi loop contactor output Pa concentration

Fig. B.6 Flowchart for Calculation of Reprocessing System Flow Rates and Pa Concentration

Calculations performed for the Plasma Core Breeder Reactor salt reprocessing system[3] indicate the proposed system is feasible. The technology is presently available and the chemical processes involved in uranium separation have been proven by experiments in connection with the Molten Salt Breeder program.

Reference 1 points out that extraction of U^{233} from the salt requires a concentration of 100 parts per million or more.[10] At start-up, no U^{233} exists in the blanket so that the reactor must run from an auxiliary bottle until enough has formed. This would add to the uranium inventory.

B.3 Actinide Reprocessing System

Because of the hazardous radionuclides present in high-level wastes from present day reactors, schemes are needed which provide waste management programs of one million years or longer.

One alternative to this would be to remove the long-lived actinides which require long term surveillance. If this could be achieved, the remaining fission products and wastes would require a waste management program on the order of 1000 years. The actinides would then be transmuted in a fission or other type reactor to reduce the long half-lives to short ones, and thus reduce the radioactive hazard. The main problem to be overcome is separation of actinides from the rest of the waste products.

With the assumption that this separation can be done, an investigation was made to determine the necessary separation factors. The study indicated that separations beyond certain limits may not yield enough to substantiate such separation factors. The separations of 99.99% for plutonium, 99.9% for uranium, americium and curium, and 99% for neptunium will reduce the hazard potential to about five percent of that for natural uranium.[11] After 99.9% removal of iodine, it will then be the long-lived remaining fission products which control the waste hazard. Higher removal factors for the actinides do not appear to be warranted unless long-lived fission products are also removed, especially Tc-99.

As means of recovering actinides from the spent waste, several schemes are available. Several schemes can be ruled out mainly due to expense and complexity. For example, a centrifuge is too "dirty" because of associated alpha emitters from the actinides.[12] This would require tight contamination control, and hence much shielding. Other processes require a gaseous form, but there are no gaseous forms of americium or curium.

Present feasibility studies indicate that separations based on solvent extraction, ion exchange, and scavenging precipitation have greatest possibilities. Solvent extraction by itself has not been shown to achieve desired results; however, multi-step solvent extraction processes have a greater probability of success.[13] If particular waste stream recycles are solved, processes based on cation exchange may be a viable method for partitioning the actinides. Another method with potential in waste partitioning may be precipitation.

Figure B.7 illustrates the reprocessing scheme for fission products and actinides generated from Light Water Reactors. Spent fuel from LWRs containing fission products and actinides listed in Table B.3 is sent to storage for about 150 days. The wastes from storage, which is listed in Table B.4, is then sent to a reprocessing plant. This plant discharges Kr-85 and tritium to the air. Ninety nine percent of the uranium is removed from the waste and sent for enrichment and 98 percent of the plutonium is separated for further fuel fabrication.

The rest of the high-level waste goes to a high-level liquid waste storage for about 215 days. These high-level wastes are listed in Table B.5. After further storage these wastes (listed in Table B.6) go to a fission product/actinide fractionation plant.

Fractionation Schemes

Studies to date indicate that the best methods for removing actinides from wastes will be obtained by improving present state-of-the-art methods.[14] One of the present schemes is shown in the Fig. B.8. In this scheme, neptunium, uranium, and plutonium, are recovered in the primary PUREX plant. Various exhaustive extractions or further PUREX processes are used to accomplish complete removal of the neptunium, plutonium, and uranium. Through the PUREX plant process, a recovery rate of 95-99% for neptunium and improvements in uranium and plutonium recovery to 99.5% or better are expected.[15]

The interim waste storage is for the purpose of reducing the radiation hazard from the remaining high level wastes during subsequent processing. The radiation hazard will be high unless the fission product yttrium and rare earths, which are associated with americium and curium, are allowed to

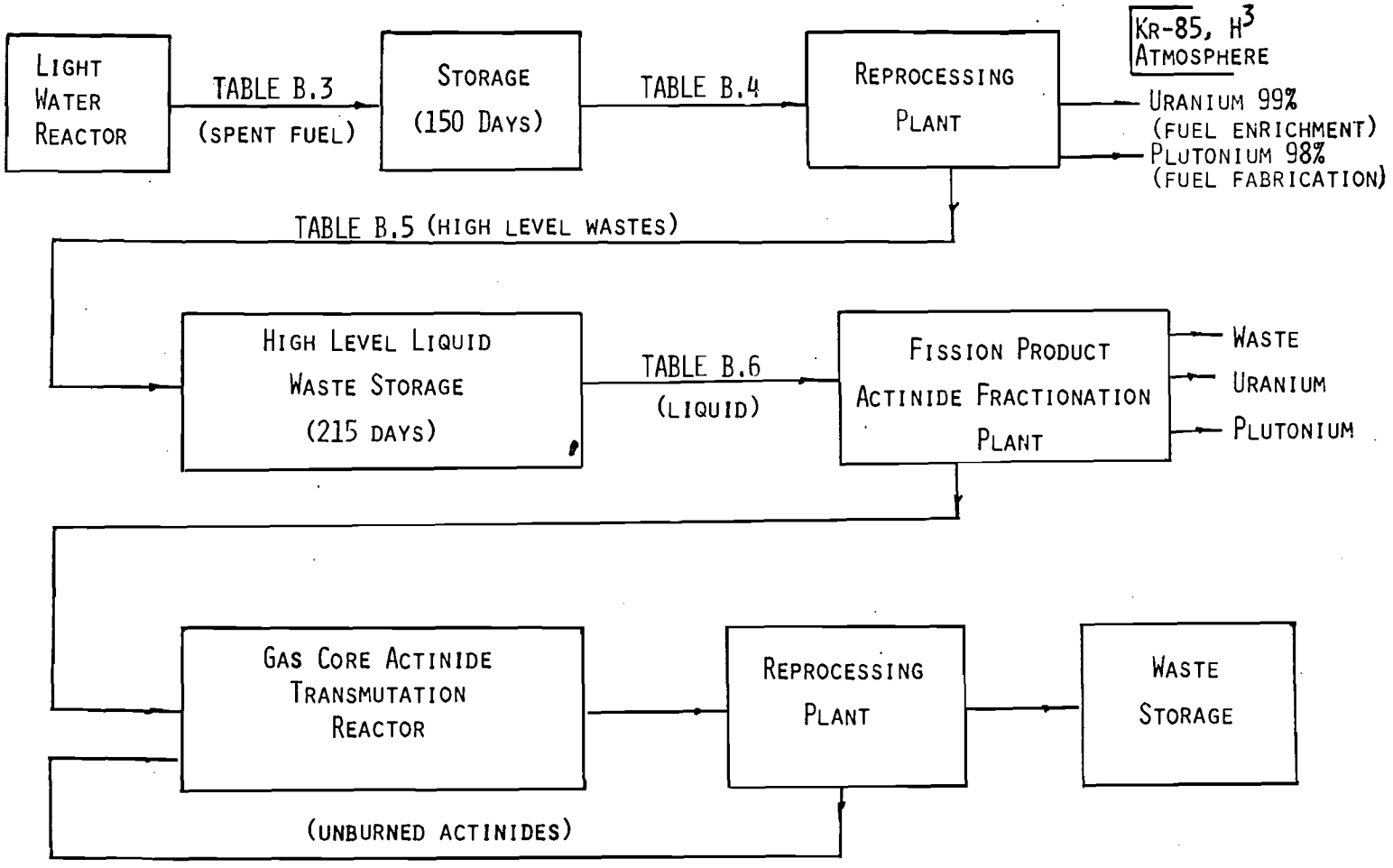

Fig. B.7. Actinide Reprocessing Scheme

Table B.3

FISSION PRODUCT AND ACTINIDE CONCENTRATIONS LEAVING A LWR

PWR FUEL CYCLE - DECAY TIMES OF FUEL DURING COOLING PERIOD
POWER= 30.00MW, BURNUP= 33000.MWD, FLUX= 2.92E+13N/CM**2-SEC
NUCLIDE INGESTION HAZARD, M**3 OF WATER AT RCG
BASIS = PER METRIC TONNE OF U LOADED IN REAC

Actinides

	DISCHARGE
PB212	7.50E+01
BI212	3.75E+00
RA223	1.27E+00
RA224	7.50E+02
TH228	2.13E+02
TH230	8.88E+00
TH231	3.98E+03
TH234	1.57E+04
PA231	2.71E+01
PA233	3.24E+03
PA234M	1.60E+01
PA234	6.52E+01
U232	2.03E+02
U233	1.52E+00
U234	2.50E+04
U235	5.70E+02
U236	9.61E+03
U237	8.55E+09
U238	7.85E+03
NP237	1.11E+05
NP239	1.85E+11
PU236	1.17E+04
PU238	5.45E+08
PU239	6.86E+07
PU240	9.55E+07
PU241	5.25E+08
PU242	2.76E+05
AM241	2.15E+07
AM242M	2.29E+06
AM242	6.34E+08
AM243	4.5+E+06
CM242	1.67E+09
CM243	7.42E+05
CM244	3.49E+08
CM245	8.54E+04
CM246	1.71E+04
CM248	1.98E+00
BK249	8.96E+06
CF250	3.79E+00
CF252	2.52E+00
SUBTOT	1.98E+11
TOTALS	2.16E+11

Fission Products

	DISCHARGE
H 3	2.36E+05
KR 85	1.13E+04
RB 86	2.47E+07
SR 89	2.39E+11
SR 90	2.59E+11
Y 90	4.03E+09
Y 91	3.13E+10
ZR 93	2.36E+03
NB 93M	3.61E+02
ZR 95	2.29E+10
NB 95M	2.80E+04
NB 95	1.38E+10
MO 99	3.81E+10
TC 99	7.14E+04
RU103	1.52E+10
RH103M	1.22E+08
RU106	5.45E+10
RH106	7.40E+05
PD107	1.10E+02
AG110M	1.23E+08
AG110	1.59E+05
AG111	9.90E+08
CD113M	1.05E+01
IN114M	7.75E+04
CD115M	1.84E+07
SN119M	1.64E+01
SN123	8.88E+03
SB124	2.03E+07
SN125	5.76E+08
SB125	8.70E+07
TE125M	3.11E+07
TE127M	3.07E+08
TE127	3.60E+08
TE129M	2.86E+09
TE129	4.21E+08
I129	6.18E+05
I131	2.87E+12
XE131M	6.39E+03
TE132	5.92E+10
I132	1.53E+11
XE133	1.61E+06
CS134	2.74E+10
CS135	2.86E+03
CS136	1.01E+09
CS137	5.39E+09
BA137M	1.01E+05
BA140	7.27E+10
LA140	7.50E+10
CE141	1.54E+10
PR143	2.41E+10
CE144	1.11E+11
PR144	1.12E+06
ND147	9.81E+09
PM147	5.12E+08
PM148M	3.89E+04
PM148	1.99E+05
SM151	3.12E+06
EU152	1.57E+05
GD153	1.78E+05
EU154	3.49E+08
EU155	6.74E+07
EU156	4.26E+05
TB160	3.21E+07
SUBTOT	4.11E+12
TOTALS	6.40E+12

Table B.4

FISSION PRODUCT AND ACTINIDE CONCENTRATIONS AFTER 150 DAYS STORAGE

PWR FUEL CYCLE - DECAY TIMES OF FUEL DURING COOLING PERIOD
POWER= 30.00MW, BURNUP= 33000.MWD, FLUX= 2.92E+13N/CM**2-SEC
NUCLIDE INGESTION HAZARD, M**3 OF WATER AT RCG
BASIS = PER METRIC TONNE OF U LOADED IN REAC

Actinides

	150. D
PB212	1.10E+02
BI212	5.49E+00
RA223	1.70E+00
RA224	1.10E+03
TH228	3.18E+02
TH230	1.02E+01
TH231	8.55E+01
TH234	1.57E+04
PA231	2.74E+01
PA233	3.40E+03
PA234M	1.57E+01
PA234	3.14E+00
U232	2.46E+02
U233	1.54E+00
U234	2.52E+04
U235	5.70E+02
U236	9.61E+03
U237	2.03E+04
U238	7.85E+03
NP237	1.13E+05
NP239	1.92E+05
PU236	1.06E+04
PU238	5.64E+08
PU239	6.46E+07
PU240	9.55E+07
PU241	5.15E+08
PU242	2.76E+05
AM241	3.85E+07
AM242M	2.29E+06
AM242	9.15E+04
AM243	4.34E+06
CM242	8.38E+08
CM243	7.66E+05
CM244	3.44E+08
CM245	8.54E+04
CM246	1.71E+04
CM248	1.98E+00
BK249	6.64E+00
CF250	3.03E+00
CF252	2.26E+00
SUBTOT	2.52E+09
TOTALS	2.52E+09

Fission Products

	150. D
H 3	2.31E+05
KR 85	1.10E+04
RB 86	9.49E+04
SR 89	3.24E+10
SR 90	2.56E+11
Y 90	3.84E+09
Y 91	5.37E+09
ZR 93	2.36E+03
NB 93M	4.52E+02
ZR 95	4.62E+09
NB 95M	5.88E+03
NB 95	5.23E+03
MO 99	2.55E-06
TC 99	7.17E+04
RU103	1.10E+09
RH103M	8.83E+06
RU106	4.10E+10
RH106	4.10E+05
PD107	1.10E+02
AG110M	3.14E+07
AG110	3.17E+02
AG111	9.47E+02
CD113M	1.03E+01
IN114M	9.69E+03
CD115M	1.64E+06
SN119M	1.28E+01
SN123	3.86E+03
SB124	3.99E+06
SN125	1.06E+04
SB125	7.95E+07
TE125M	3.22E+07
TE127M	1.26E+08
TE127	3.04E+07
TE129M	1.35E+08
TE129	3.17E+06
I129	5.23E+05
I131	7.28E+06
XE131M	3.19E+00
TE132	7.57E-04
I132	1.95E-03
XE133	5.35E-03
CS134	2.38E+10
CS135	2.86E+03
CS136	3.41E+05
CS137	5.04E+09
BA137M	9.99E+04
BA140	2.16E+07
LA140	2.48E+07
CE141	6.27E+08
PR143	1.36E+07
CE144	7.71E+10
PR144	7.71E+05
ND147	8.39E+05
PM147	4.90E+08
PM148M	3.27E+03
PM148	2.66E+02
SM151	3.12E+05
EU152	1.53E+05
GD153	1.16E+05
EU154	5.43E+08
EU155	2.20E+07
EU156	2.01E+02
TB160	7.58E+06
SUBTOT	4.58E+11
TOTALS	4.58E+11

Table B.5

FISSION PRODUCT AND ACTINIDE CONCENTRATIONS EXITING FROM THE REPROCESSING PLANT

PWR FUEL CYCLE DECAY TIMES OF FUEL AFTER 1ST PROCESSING
POWER= 30.00MW, BURNUP= 33000.MWD, FLUX= 2.92E+13N/CM**-SEC
NUCLIDE INGESTION HAZARD, M**3 OF WATER AT RCG
BASIS = PER METRIC TONNE OF U LOADED IN REAC

Actinides

	DISCHARGE
PB212	1.16E+02
BI212	5.49E+00
RA223	1.79E+00
RA224	1.10E+02
TH228	3.18E+02
TH230	1.02E+01
TH234	1.57E+04
PA231	2.74E+01
PA233	3.40E+03
U232	2.45E+00
U234	2.52E+02
U235	5.70E+00
U236	9.61E+01
U237	2.65E+02
U238	7.85E+01
NP237	1.13E+05
NP239	1.82E+05
PU236	2.12E+02
PU238	1.13E+07
PU239	1.29E+06
PU240	1.91E+06
PU241	1.03E+07
PU242	5.52E+03
AM241	3.85E+07
AM242M	2.29E+06
AM242	9.15E+04
AM243	4.54E+06
CM242	3.88E+08
CM243	7.36E+05
CM244	3.44E+08
CM245	8.54E+04
CM246	1.71E+04
CM248	1.96E+00
BK249	6.44E+00
CF249	6.96E-01
CF250	3.69E+00
CF252	2.26E+00
SUBTOT	1.30E+09
TOTALS	1.30E+09

Fission Products

	DISCHARGE
H 3	2.31E+05
KR 85	1.10E+04
RB 86	9.49E+04
SR 89	3.24E+10
SR 90	2.56E+11
Y 90	3.84E+09
Y 91	5.37E+09
ZR 93	2.36E+03
NB 93M	4.52E+02
ZR 95	4.02E+09
NB 95M	5.88E+03
NB 95	5.20E+09
TC 99	7.17E+04
RU103	1.10E+09
RH103M	8.82E+06
RU106	4.10E+10
RH106	4.10E+05
PD107	1.10E+02
AG110M	8.14E+07
AG110	3.17E+02
CD113M	1.63E+01
IN114M	9.89E+03
CD115M	1.64+06
SN119M	1.08E+01
SN123	3.30E+05
SB124	3.59E+06
SB125	7.95E+07
TE125M	3.20E+07
TE127M	1.23E+08
TE127	5.04E+07
TE129M	1.35E+08
TE129	2.17E+06
I129	6.23E+05
I131	7.28E+06
CS134	2.58E+10
CS135	2.69E+03
CS136	3.41E+05
CS137	5.34E+09
BA137M	9.39E+04
BA140	2.16E+07
LA140	2.48E+07
CE141	6.27E+08
PR143	1.36E+07
CE144	7.71E+10
PR144	7.71E+05
ND147	8.08E+05
PM147	4.90E+08
PM148M	3.07E+03
PM148	2.63E+02
SM151	3.12E+06
EU152	1.93E+05
GD153	1.16E+05
EU154	3.43E+08
EU155	3.20E+07
TB160	7.53E+06
SUBTOT	4.58E+11
TOTALS	4.58E+11

Table B.6

FISSION PRODUCT AND ACTINIDE CONCENTRATIONS AFTER 215 DAYS
STORAGE IN HIGH LEVEL LIQUID WASTE STORAGE FACILITY

PWR FUEL CYCLE DECAY TIMES OF FUEL AFTER 1ST PROCESSING
POWER= 30.00MW, BURNUP= 33000.MWD, FLUX= 2.92E+13N/CM**2-SEC
NUCLIDE INGESTION HAZARD, M**3 OF WATER AT RCG
BASIS = PER METRIC TONNE OF U LOADED IN REAC

Actinides

	CHARGE	215. D
PB212	0.	9.11E+01
BI212	0.	4.55E+00
RA223	0.	2.33E+00
RA224	0.	9.11E+02
TH228	0.	2.59E+02
TH230	0.	1.02E+01
TH234	0.	1.89E+02
PA231	0.	2.74E+01
PA233	0.	3.40E+03
U232	0.	3.56E+00
U234	5.45E+04	2.56E+02
U235	2.36E+03	5.70E+00
U236	0.	9.61E+01
U237	0.	4.81E+02
U238	8.05E+03	7.85E+01
NP237	0.	1.13E+05
NP239	0.	1.82E+05
PU236	0.	1.84E+02
PU238	0.	2.19E+07
PU239	0.	1.29E+06
PU240	0.	1.94E+06
PU241	0.	1.00E+07
PU242	0.	5.52E+03
AM241	0.	3.90E+07
AM242M	0.	2.28E+06
AM242	0.	9.12E+04
AM243	0.	4.54E+06
CM242	0.	3.56E+08
CM243	0.	7.26E+05
CM244	0.	3.36E+08
CM245	0.	8.54E+04
CM246	0.	1.71E+04
CM248	0.	1.98E+00
BK249	0.	4.01E+00
CF249	0.	1.49E+00
CF250	0.	3.58E+00
CF252	0.	1.94E+00
SUBTOT	6.50E+04	7.74E+08
TOTALS	6.50E+04	7.74E+08

Fission Products

	215. D
H 3	2.23E+05
KR 85	1.06E+04
RB 86	3.28E+01
SR 89	1.84E+09
SR 90	2.52E+11
Y 90	3.79E+09
Y 91	4.26E+08
ZR 93	2.36E+03
NB 93M	5.78E+02
ZR 95	4.67E+08
NB 95M	5.94E+02
NB 95	5.96E+08
TC 99	7.17E+04
RU103	2.56E+07
RH103M	2.05E+05
RU106	2.73E+10
RH106	2.73E+05
PD107	1.10E+02
AG110M	4.51E+07
AG110	1.76E+02
CD113M	9.99E+00
IN114M	4.92E+02
CD115M	5.11E+04
SN119M	5.96E+00
SN123	1.17E+03
SB124	2.99E+05
SB125	6.83E+07
TE125M	2.83E+07
TE127M	3.13E+07
TE127	7.74E+06
TE129M	1.69E+06
TE129	2.71E+04
I129	6.24E+05
I131	6.64E-02
CS134	1.95E+10
CS135	2.66E+03
CS136	3.58E+00
CS137	5.27E+09
BA137M	9.85E+04
BA140	1.89E+02
LA140	2.18E+02
CE141	6.31E+06
PR143	2.56E+02
CE144	4.56E+10
PR144	4.56E+05
ND147	1.24E+00
PM147	4.19E+08
PM148M	9.40E+01
PM148	7.55E+00
SM151	3.11E+06
EU152	1.48E+05
GD153	6.25E+04
EU154	3.35E+08
EU155	2.55E+07
TB160	9.80E+05
SUBTOT	3.58E+11
TOTALS	3.58E+11

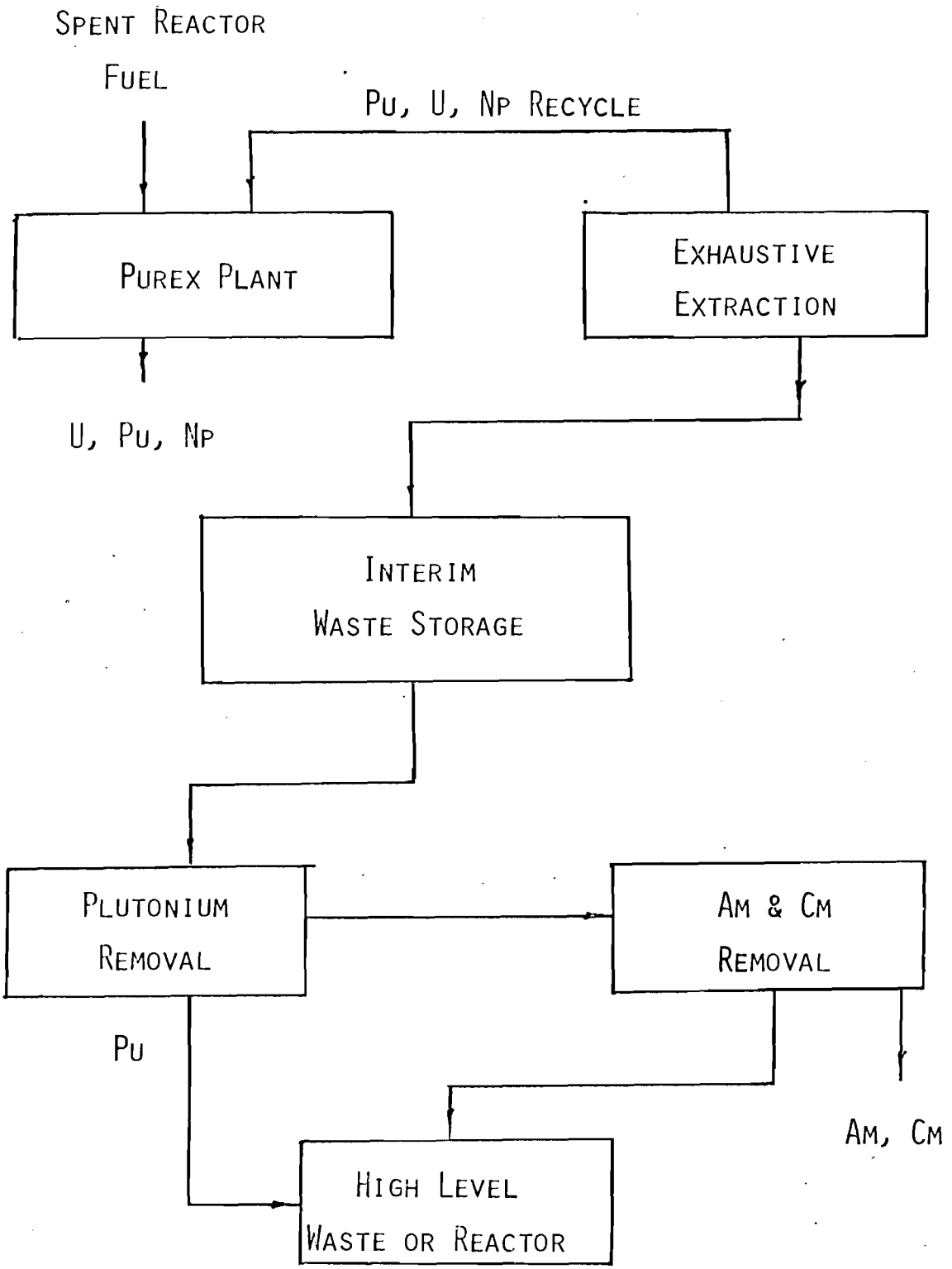

Fig. B.8 Present Processing Sequence for the Removal of Actinides

decay to less hazardous levels.[15] By considering the most important decay times, storage times of ten years would significantly reduce the hazards. Current NRC regulations require that wastes be solidified within five years. However, because of difficulties in working with a solid waste, it will be assumed that the americium and curium are removed from the liquid wastes after a five year period.

One disadvantage of interim waste storage is that the amount of plutonium in the waste grows by curium decay. Therefore, plutonium removal from the stored waste is necessary after several years of interim storage. The process showing most potential for recovering the plutonium is an all ion-exchange process.[16]

After removal of plutonium, the americium and curium are isolated from the rest of the waste. The problems associated with americium and curium removal are centered around finding a suitable chemical separation process for commercial high level wastes. Recovery of americium and curium has been done at the Oak Ridge National Laboratory and Savannah River Laboratory on a multigram basis using a Tramex process.[15] This process has problems with corrosive solutions that require processing equipment constructed of special and expensive materials. Because of these reasons, the process is not recommended. However, there is some possibility that the Tramex processing equipment can be constructed so as to allow safe working of both corrosive solutions in the process and toxic radionuclides at little additional cost.

Other processes that have been developed and claim to give high americium and curium separation are Cation Exchange Chromatography (CEC) and Trivalent Actinide-Lanthanide Separation by Phosphorous Reagent Extraction from Aqueous

Complexes (TALSPEAK).[15] Cation Exchange Chromatography was developed at the Savannah River Laboratory and successfully used to separate about twenty-five percent of the necessary amounts of americium, curium, and rare earths in one metric ton of Light Water Reactor fuel.[15] A schematic flowsheet of CEC is shown in Fig. B.9. The TALSPEAK process, shown in Fig. B.10, has been developed only to the point of tracer-level laboratory studies at Karlsruhe for americium and curium removal.[15]

As means of separating Am and Cm from other wastes, the Tramex, CEC, and TALSPEAK processes require considerable developmental work and data gathering to determine their applicability to the commercial (high volume) extraction of actinides from high-level wastes.

Proposed Schemes

Present proposals for actinide partitioning are based on a sequence of separation processes using solvent extraction, ion exchange, and precipitation. These techniques have not yet been developed.[14] A multistep solvent extraction process combined with other processes, such as cation exchange, may work well in the removal of uranium, neptunium, and plutonium, as well as separations of americium and curium from other wastes.

Tributylphosphate (TBP) may be used as the solvent in the solvent extraction method.[14,17] As demonstrated in the PUREX process, TBP achieved highly efficient recovery of uranium, plutonium, and neptunium.[11]

As a means of separating americium and curium from the rest of fission products and wastes, two steps of cation exchange is quite promising. The potential here appears to be 99.9 percent or better.[14] In the first step the lanthanides and actinides are absorbed on a cation exchange resin

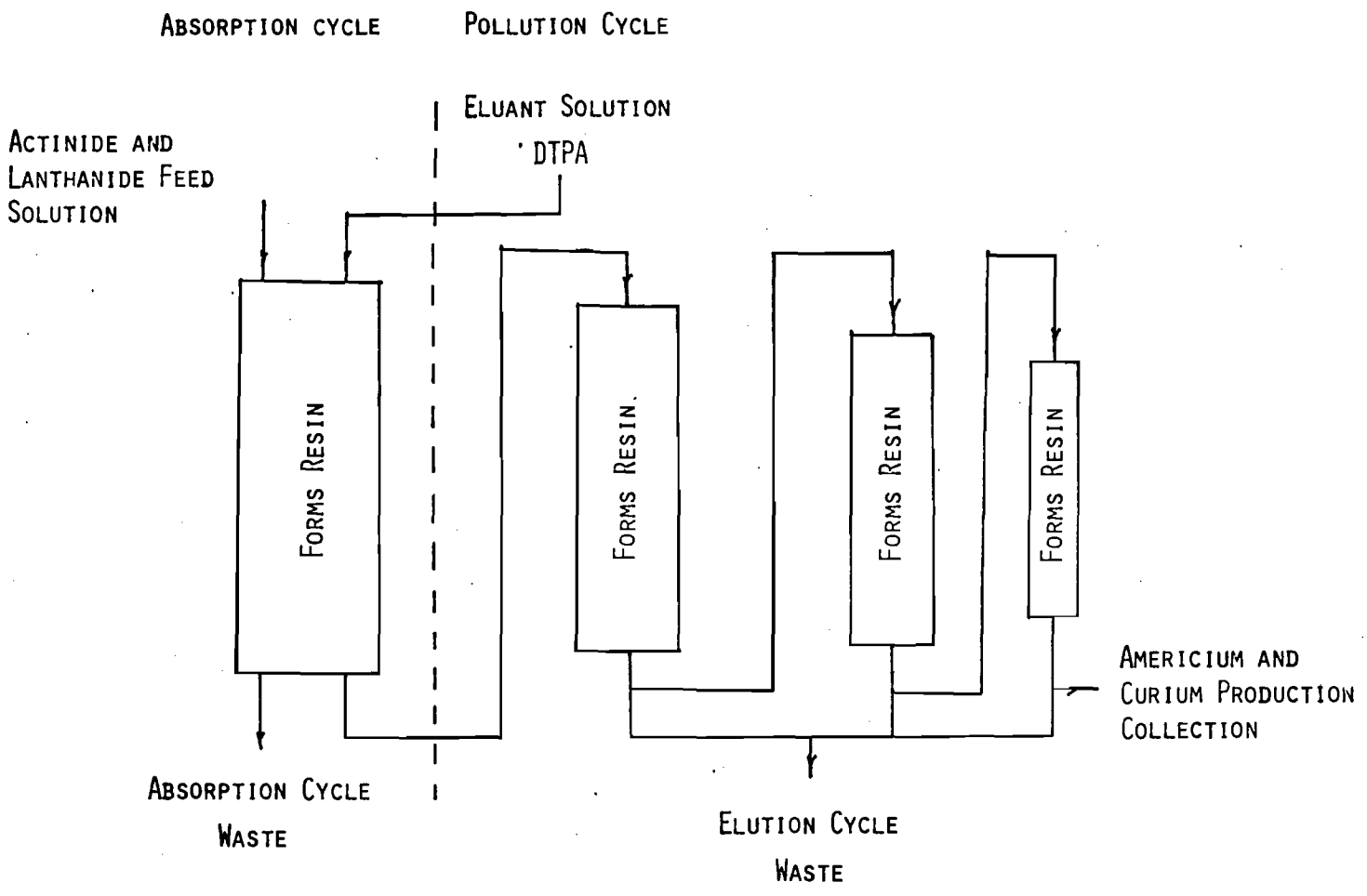

Fig. B.9. Schematic Flowsheet of Cation Exchange Chromatographic Process for Recovery of Americium and Curium[15]

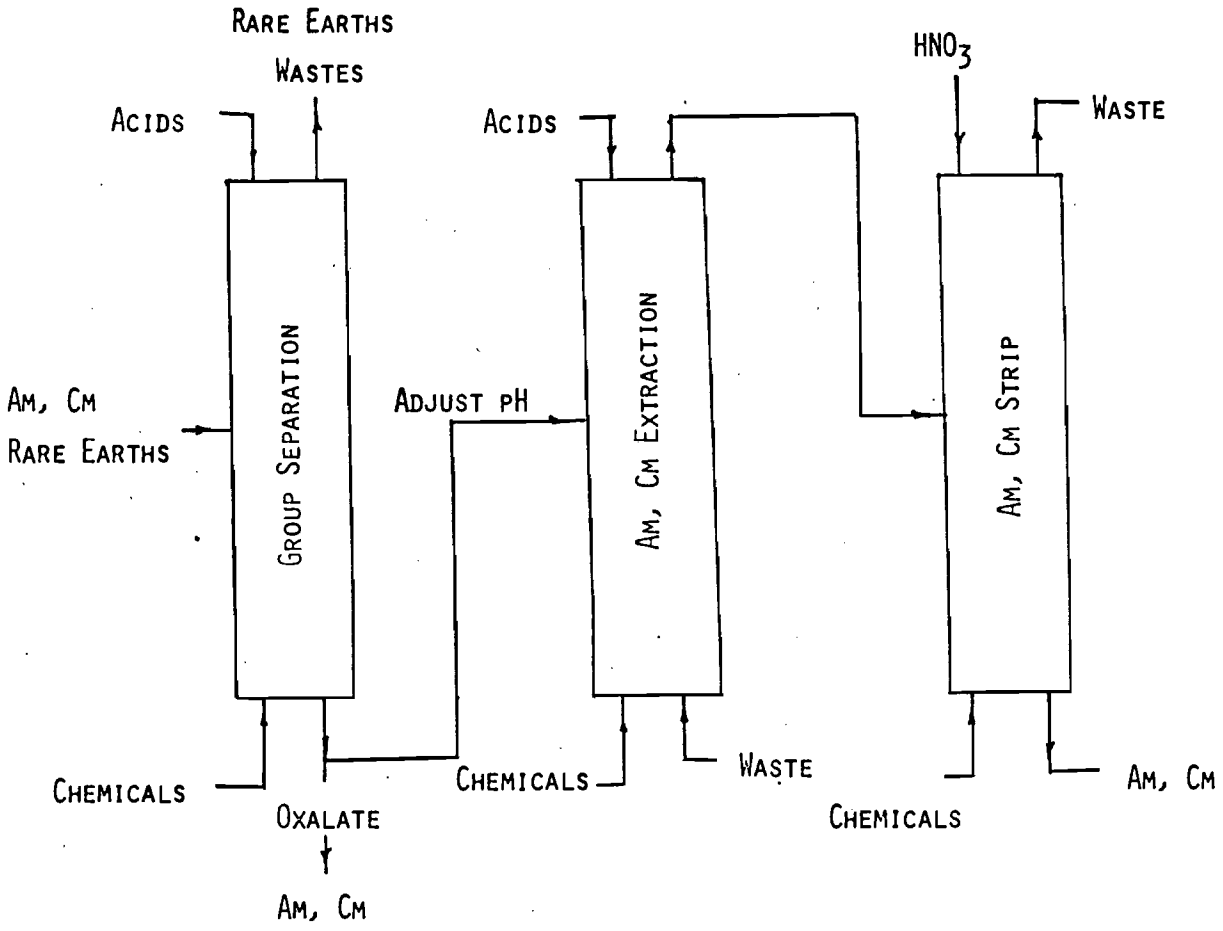

Fig. B.10. Conceptual Flow Sheet for Recovery of Americium and Curium by a TALSPEAK

column and eluted with nitric acid. In the following step the lanthanides and actinides are separated by cation exchange chromatography. Problems to be solved with this process are in converting the spent ion exchange resin to acceptable levels for waste generated in the chromatographic separation.

Precipitation methods combined with ion exchange and/or solvent extraction may be another possible method for partitioning actinides. Even though solid waste handling is unavoidable, ways are now under study for obtaining crude concentrations of plutonium, americium, curium, and fission products. These actinides would then be separated from the lanthanides in further ion exchange or solvent extraction steps. Oak Ridge National Laboratory is studying the use of oxalate[16] precipitation together with ion exchange to isolate the lanthanides and actinides.[14,19] A removal factor of 0.95 is achieved by precipitation while the remaining is removed in the cation exchange column.[15] Tracer-level studies indicate removal of 0.999 for americium and curium.[15] Almost complete removal has been demonstrated for americium and curium by use of multiple oxalate precipitation stages.[14] Further work in this area is still needed to determine the effect of the handling problems.

Technical feasibility, resultant benefits, and costs of partitioning actinides from high-level wastes are yet to be established. It must be decided if the net benefits will justify the use of partitioning. It must also be kept in mind that the separation schemes do not solve the long-term actinide problem. In order to justify this, the actinides must somehow be transmuted to shorter-lived radionuclides or disposed of from our environment. These and many more problems still need research and investigation before a feasible actinide-separation-transmutation process can be substantiated.

From research done to date, it is concluded that much research and development is still needed in the area of actinide partitioning. Work being performed at the Oak Ridge National Laboratory may show encouraging results by the end of 1978. Present state-of-the-art methods will not yield the results needed to establish a practical, economically feasible operating partitioning plant. It is believed that research in the area of combined methods of solvent extraction and ion exchange will yield the necessary separations factors.

References for Appendix B

1. Lowry, L. L., "Gas Core Reactor Power Plants Designed for Low Proliferation Potentials," LA-6900-MS (September 1977).

2. Clement, J. D. and Rust, J. H., "Analysis of the Gas Core Actinide Transmutation Reactor (GCATR)," Annual Report, Georgia Institute of Technology, NASA Grant NSG-1288 (February 1977).

3. Clement, J. D. and Rust, J. H., "Analysis of the Gas Core Actinide Transmutation Reactor (GCATR)," Semi-Annual Report, Georgia Institute of Technology, NASA Grant NSG-1288, Supplement No. 1 (September 1, 1977).

4. Henry, A. F., Nuclear Reactor Analysis, M.I.T. Press, 763 (1975).

5. McNeese, L. E., "Engineering Development Studies for Molten-Salt Breeder Reactor Processing No. 5," ORNL-TM-3140, 15-16 (October 1971).

6. Benedict, M. and Pigford, T. H., Nuclear Chemical Engineering, McGraw-Hill, 156-158 (1957).

7. McNeese, L. E., Op. Cit., 18.

8. "Molten Salt Reactor Program Semiannual Progress Report for Period Ending August 31, 1968," ORNL-4344, 292-298 (1969).

9. Foust, A. S., Principal of Unit Operations, Wiley, 45, 77 (1964).

10. Rosenthal, M. W., Houbenreich, P. N., and Briggs, R. B., "The Development Status of the Molten Salt Breeder Reactors," ORNL-4812 (August 1972).

11. Claiborne, H. C., "Effect of Actinide Removal on the Long Term Hazard of High-Level Waste," ORNL-TM-4724 (January 1975).

12. Schneider, A., Georgia Institute of Technology, Personal consultation (April 1976).

13. Bocola, W., Frittelli, L., Gera, F., Grossi, G., Moccia, A., and Tondinelli, L., "Considerations on Nuclear Transmutation for the Elimination of Actinides," IAEA-SM-207/86.

14. Blomeke, J. O., "Technical Alternatives Documents," ORNL, Prepublication Paper (1976).

15. Bond, W. D., and Leuze, R. E., "Feasibility Studies of the Partition of Commercial High-Level Wastes Generated in Spent Nuclear Fuel Processing: Annual Progress Report for FY-1974," ORNL-5012 (January 1975).

16. Bond, W. D., Claiborne, H. C., and Leuze, R. E., "Methods for Removal of Actinides from High-Level Wastes," Nuclear Technology, 24, 367 (1974).

17. LaRiviere, J. R., et al., "The Hanford Isotopes Production Plant Engineering Study," HW-77770, Hanford Atomic Products Operation (July 1963).

18. Rupp, A. F., "A Radioisotope-Oriented View of Nuclear Waste Management," ORNL-4776 (May 1972).

19. Ferguson, D. W., et al., "Chemical Technology Division Annual Progress Report for Period Ending March 31, 1975," ORNL-5050, 6-11, 30-31 (October 1975).

ANNUAL REPORT

NASA GRANT NSG-1288

GAS CORE REACTORS FOR ACTINIDE TRANSMUTATION

J. D. Clement, J. H. Rust, Pak Tai Wan, S. Chow

NASA Program Manager, F. Hohl

Prepared for the

National Aeronautics and Space Administration

by the

School of Nuclear Engineering
Georgia Institute of Technology
Atlanta, Georgia 30332

April 1, 1979

ANNUAL REPORT

NASA GRANT NSG-1288

GAS CORE REACTORS FOR ACTINIDE TRANSMUTATION

J. D. Clement, J. H. Rust, Pak Tai Wan, S. Chow

NASA Program Manager, F. Hohl

Prepared for the

National Aeronautics and Space Administration

by the

School of Nuclear Engineering
Georgia Institute of Technology
Atlanta, Georgia 30332

April 1, 1979

TABLE OF CONTENTS

LIST OF FIGURES

LIST OF TABLES

SUMMARY

The Georgia Institute of Technology, under the sponsorship of the National Aeronautics and Space Administration, has undertaken a research program on the design and analysis of a uranium hexafluoride gas core actinide transmutation reactor (UFATR). This report summarizes results up to February 28, 1979.

One consequence of nuclear fission reactors is the accumulation of radioactive wastes. The long-term hazard of these wastes is dominated by actinides. Plutonium and uranium can be recycled within the nuclear fuel cycle, but disposal of other actinides is still a problem. If the actinides can be chemically extracted from bulk wastes, then the long-lived nuclides can be transmuted to short-lived fission products in a neutron environment. Past studies on actinide transmutation were reviewed. The UF_6 gas core reactor was selected for this application.

The core is spherical and consists of four regions. Region I is the UF_6-He fuel mixture, region II is a beryllium reflector-moderator, region III is a liquid bismuth-actinide blanket and region IV is a graphite reflector. The gaseous fuel and liquid metal blanket are continuously circulated for heat removal, reprocessing of fission products, and refueling of depleted nuclides. For the present UFATR design, the core provides an abundant supply of thermal neutrons for transmutation use and yet is insensitive to composition changes in the blanket.

To study burnup of actinides in the blanket, a three-group cross section set was generated. The codes MACH I and ORIGEN were used iteratively to study the neutronics and depletion of the actinide blanket. An initial load of 6 metric tonnes of actinides was loaded into the blanket.

This quantity of actinides is produced by 300 LWR-years of operation. At the beginning, the core produces 2000 MWt while the blanket generates only 239 MWt. After four years of irradiation, the actinide mass is reduced to 3.9 metric tonnes. During this time, the blanket is becoming more fissile and its power rapidly approaches 1600 MWt. At the end of four years, continuous refueling of actinides is carried out and the actinide mass is held constant. Equilibrium is essentially achieved at the end of eight years. At equilibrium, the core is producing 1400 MWt and the blanket 1600 MWt. At this power level, the actinide destruction rate is equal to the production rate from 32 LWRs.

Chapter 1

INTRODUCTION

As part of its policy of supporting research and development programs which reside on the frontier of power technology, the National Aeronautics and Space Administration has sponsored work in gaseous-fueled reactors and plasma research. The original goal in research and development of the gas core reactor was to produce a space propulsion reactor capable of fast, manned expeditions to neighboring planets.[1] Although budgetary and policy factors terminated the development of nuclear powered propulsion engines, NASA has continued to sponsor fissioning plasma research consisting of cavity reactor criticality tests, fluid mechanics tests, investigation of uranium optical emission spectra, radiant heat transfer studies, and related theoretical work.[2,3] Research has shown that UF_6 fueled reactors can be quite versatile with respect to power, pressure, operating temperature, and modes of power extraction.[4] Possible power conversion systems include Brayton cycles, Rankine cycles, MHD generators, and thermionic diodes. Power extraction may also be possible in the form of coherent light from interactions of fission fragments with a laser gas mixture.

In addition, the International Security Office of the U. S. Energy Research and Development Administration (now the Department of Energy) has sponsored research on non-proliferating gas core reactor power plants.[5,6] Initial studies show that fuel inventories may be a factor of 10 less than those in current U. S. power reactors.

The Georgia Institute of Technology has been engaged in various gas core reactor power plant concepts under NASA sponsorship. One concept

utilized a uranium plasma, breeder reactor employing a MHD generator for the topping cycle.[7,8] Power plant efficiencies of 70 percent are attainable with this high temperature reactor.

More recent work done at Georgia Tech involves the application of plasma and UF_6 reactors for breeding and actinide transmutation purposes.[9-11]

This report summarizes results for the design and analysis of UF_6 gas core actinide transmutation reactor.

References for Chapter 1

1. Ragsdale, R. G., "To Mars in 30 Days by Gas Core Nuclear Rocket," Astronautics and Aeronautics, 10, No. 1 (1971).

2. Thom, K., Schneider, R. T. and Schwenk, F.C., "Physics and Potentials of Fissioning Plasmas for Space Power and Propulsion," International Astronautical Federation 25th Congress, Paper No. 74087, Amsterdam (October, 1974).

3. Schwenk, F. C. and Thom, K. T., "Gaseous Fuel Nuclear Reactor Research," paper presented at the Oklahoma State University Conference on Frontiers of Power Technology (October, 1974).

4. Rodgers, R. J., Latham, T. S., and Krascella, N. L., "Investigation of Applications for High-Power, Self-Critical Fissioning Uranium Plasma Reactors," NASA CR-14508 (September, 1976).

5. Lowry, L. L., "Gas Core Reactor Power Plants Designed for Low Proliferation Potentials," LA-6900-MS (September, 1977).

6. Soran, P. D. and Hansen, G. E.," Neutronics of a Mixed Flow Gas-Core Reactor," LA-7036-MS (November, 1977).

7. Williams, J. R. and Clement, J. D., "Exploratory Study of Several Advanced Nuclear-MHD Power Plant Systems," Final Status Report, NASA Grant NGR-11-002-145, Georgia Institute of Technology, Atlanta, Georgia (March, 1973).

8. Williams, J. R. and Clement, J. D., "Satellite Nuclear Power Station - an Engineering Analysis," NASA Grant NGR-11-002-145, Georgia Institute of Technology, Atlanta, Georgia (March, 1975).

9. Clement, J. D. and Rust, J. H., "Analysis of UF_6 Breeder Reactor Power Plants," Final Report, NASA Grant NSG-1168, Georgia Institute of Technology, Atlanta, Georgia (February, 1976).

10. Clement, J. D. and Rust, J. H., "Analysis of the Gas Core Actinide Transmutation Reactor (GCATR)," Annual Report, NASA Grant NSG-1288, Georgia Institute of Technology, Atlanta, Georgia (February,1977).

11. Clement, J. D. and Rust, J. H., "Gas Core Reactors for Actinide Transmutation and Breeder Applications," Annual Report, NASA Grant NSG-1288, Supplement No. 1, Georgia Institute of Technology, Atlanta, Georgia (April, 1978).

Chapter 2

THE ACTINIDE TRANSMUTATION PROBLEM

One consequence of large scale use of fission reactors for power production is the accumulation of radioactive wastes. The spent fuel discharged from a LWR consists of structural materials, unfissioned uranium, converted plutonium, fission products and other actinides. These actinides are formed from the neutron capture reaction of fertile and fissile isotopes. Figures 2.1 and 2.2 illustrate the radioactivity and toxicity* of spent LWR-UO_2 fuel, respectively. Up to 300 years the fission product component dominates; but from then onwards, the actinide component is dominant. Most of the actinide toxicity is due to uranium and plutonium. If the plutonium is recycled in LWRs or LMFBRs, it does not have to be considered in the waste managment category. The uranium will most likely be recycled through the enrichment plant. Thus, the other actinides will be the principal contributors to the long term hazards of reactor wastes. The composition and radioactivity of the actinide portion of the high-level waste is shown in Table 2.1.

The ultimate method for the disposal of high-level radioactive wastes in the U. S. is still being evolved. For the short-lived component, it seems that ultimate storage in deep geologic formations of known characteristics (such as salt mines) remains the best method since less than one thousand years is required to reduce the activity to an innocuous level.

---

*The toxicity of a radioactive substance is defined as the quantity of water or air that would be required to dilute the substance to the RCG level — a level considered acceptable for ingestion or inhalation by the general public.

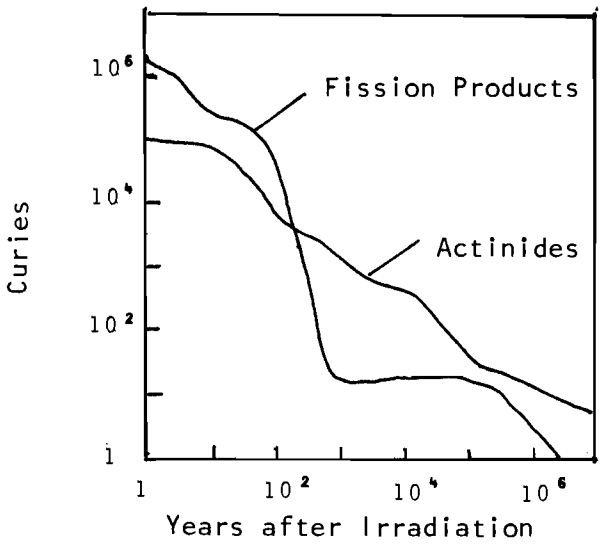

Fig. 2-1. Radioactivity of 1 MT of LWR UO_2 Spent Fuel (1)

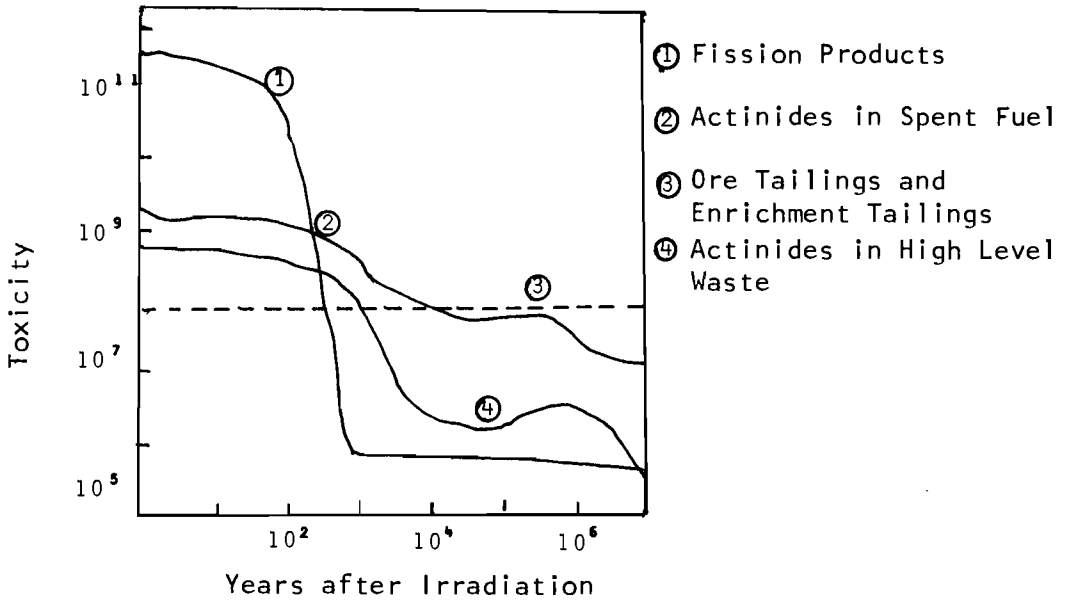

Fig. 2-2. Toxicity of 1 MT of LWR-UO_2 Spent Fuel (1)

TABLE 2.1

LWR Waste Concentrations (Separate @ 10 yr. 99.5% Removal of U and Pu; per MT of Fuel) (1)

Isotope	Grams	Curies	Toxicity, M^3 of Water
^{234}U	1.10	-	- - -
^{235}U	39.5	-	- - -
^{236}U	20.7	-	- - -
^{238}U	4730	-	- - -
^{237}Np	532	-	1.25 + 5
^{239}Np	-	13.6	1.36 + 5
^{234}Pu	0.709	12.0	2.39 + 6
^{239}Pu	23.8	1.46	2.92 + 5
^{240}Pu	10.4	2.30	4.61 + 5
^{241}Pu	3.58	359	1.79 + 6
^{242}Pu	2.07	-	- - -
^{241}Am	456	1560	3.91 + 8
^{242m}Am	1.12	10.9	2.73 + 6
^{242}Am	-	10.9	1.09 + 5
^{243}Am	70.9	13.6	3.41 + 6
^{242}Cm	0.00271	3.31	6.62 + 5
^{243}Cm	0.0720	8.98	4.49 + 5
^{244}Cm	10.7	864	1.23 + 8
^{245}Cm	0.928	-	4.1 + 4
^{246}Cm	0.099	-	- - -
TOTAL	5910	2870	5.27 + 8

Assurance of tectonic stability for thousands of years with a very high degree of confidence is quite possible in some geologic formations. For the treatment of the long-lived component, much uncertainty exists because the effects of geologic, climatic, and other natural phenomena cannot be reliably extrapolated in the time span of thousands to millions of years. This study deals with one alternative, the neutron-induced transmutation of actinide wastes.

Review of Past Transmutation Studies

The objective of actinide transmutation is to convert the waste from an actinide waste composition to a fission product composition. The actinide elements typically have very long half lives and relatively large neutron cross sections for transmutation, especially for the fission process. After being converted to fission products, these wastes would require much shorter storage times to decay to background radiation levels.

A technical hurdle that must be overcome before actinide transmutation can become a reality is the chemical extraction of actinides at high efficiencies from bulk waste. Numerous studies have been performed on the chemical removal of actinides from high-level wastes.[2-5] Studies to date have not been able to determine the feasibility (or infeasibility) of chemical processes for the satisfactory removal of actinides wastes. The Oak Ridge National Laboratory is currently conducting an extensive study in this area.[5]

Many research organizations have performed studies on transmutation using different reactor systems. A chronological list of (1) the principal investigator(s), (2) the investigator's affiliation(s), and (3) a brief description of the transmutation studies conducted is given in Table 2.2.

TABLE 2.2

Summary of Past Actinide Transmutation Studies

Investigator(s) (Organization)	Description	Reference (Date)
M. Steinberg G. Wotzak B. Manowitz (BNL)	Physics and economics of transmuting Kr-85, Sr-90, and Cs-137	6 (1964)
M. Steinberg M. V. Gregory (BNL)	Transmutation of fission product in a spallation reactor	7 (1967)
H. C. Claiborne (ORNL)	Discussion of fission product transmutation; investigation of actinide recycling in a PWR	8 (1972)
W. C. Wolkenhauer (PNL)	Physics of transmuting Sr-90 and Cs-137 in CTR	9 (1972)
W. C. Wolkenhauer B. R. Leonard, Jr. B. E. Gore (PNL)	Evaluation of potential of a CTR for transmuting fission products and actinides	10 (1973)
B. E. Gore B. R. Leonard, Jr. (PNL)	Physics of transmuting massive amounts Cs-137 in a CTR blanket	11 (1974)
K. J. Schneider A. M. Platt (PNL)	Comprehensive overview of waste management alternatives including actinide transmutation	12 (1974)
R. R. Paternoster (U. of Florida)	Calculation of actinide transmutation with a UF_6 Gas Core reactor	13 (1974)
R. J. Breen (WARD)	Actinide transmutation rates in oxide and carbide fueled LMFBR	14 (1975)
S. Raman (ORNL)	Review of actinide transmutation in many devices	15 (1975)
S. Raman C. W. Nestor, Jr. J. W. T. Dabbs (ORNL)	Actinide transmutation in a U^{233}-Th^{232} reactor	16 (1975)
A. G. Croff (ORNL)	Review of actinide transmutation studies	17 (1975)
A. G. Croff (ORNL)	Parametric survey of actinide transmutation	18 (1976)

TABLE 2.2

Summary of Past Actinide Transmutation Studies (cont'd)

S. L. Beaman E. A. Aitken (GE)	Physics of recycling wastes from 3 BWRs and 1 LMFBR in an LMFBR	19 (1976)
J. J. Prabulos (CE)	Calculation of actinide transmutation in a 1500 MWe carbide fueled LMFBR	20 (1976)
W. Bocola L. Frittelli G. Grossi A. Moccia L. Tondinelli (CNEN-CSN, Italy)	Calculation of sensitivities of actinide buildup to cross section changes; comparison of risks from nuclear transmutation and geologic disposal	21 (1976)
T. A. Parish E. L. Draper, Jr. (U. of Texas)	Engineering and physics design of a CTR for long-lived fission product transmutation	22 (1976)
R. H. Clarke G. A. Harte (GEGB,UK)	Actinide production and transmutation in MAGNOX and sodium cooled fast reactors	23 (1976)
R. P. Rose (EPRI)	Engineering and physics design of a tokamak fusion actinide transmuter	24 (1976)
U. P. Jenquin B. R. Leonard, Jr. (PNL)	Physics of transmuting actinides in CRT blankets	25 (1976)
D. H. Berwald (U. of Michigan)	Engineering and physics design of a laser driven fusion actinide transmuter	26 (1977)
T. H. Pigford J. Choi (U. C. Berkeley)	Calculation of approach-to-equilibrium times for PWR and LMFBR as actinide transmuter	27 (1978)
J. D. Clement J. H. Rust (Ga. Tech)	Analysis of gas core actinide transmutation reactor	28 (1977)
G. Oliva G. Palmiotti M. Salvatores L. Tondinelli (Italy)	Comparison of actinide transmutation in LWRs and LMFBRs	29 (1978)
J. D. Clement J. H. Rust (Ga. Tech)	Design of plasma core reactors for actinide transmutation	30 (1978)

The list is restricted mainly to studies with fission and fusion reactor systems. Those interested in other systems, such as accelerator or nuclear explosive transmutation, are referred to Ref. 12, which gives a discussion of these transmutation devices and an extensive list of references.

The effectiveness of an actinide transmutation system depends on numerous factors. The principal ones are (i) neutron flux level, (ii) neutron energy spectrum, and (iii) logistics of the transmutation strategy.

The most important parameter affecting actinide transmuation rates is the neutron flux in the actinide region. All studies strive to maintain as high a flux as possible. Studies using commercial power reactors as transmuters are hampered by fixed flux levels determined by power production considerations. Typical LWR thermal fluxes are on the order of 10^{13} to 10^{14} n/cm^2-sec. Typical LMFBR fast fluxes are on the order of 10^{15} to 10^{16} n/cm^2-sec. For fusion reactors, Rose[24] indicated that a high neutron wall loading (about 10 MW/m^2) is required for effective transmutation rates. However, tokamak fusion reactors probably cannot achieve such high wall loadings due to high plasma beta stability considerations[24] and laser driven fusion reactors will be required.

Complications may also arise due to changing characteristics of the actinide region. As actinides are irradiated, they are fissioned or converted to higher actinides by capture. Hence, the composition of the actinide mix is gradually changing with time. Initially, it consists mostly of Np^{237}, Am^{241}, and Am^{243}. Upon irradiation, some are converted to nuclides with large fission cross sections. This may cause problems because the neutron flux is usually set at the maximum permissible value

consistent with thermal hydraulic constraints. As the actinide mix becomes more fissile, the neutron flux may have to be lowered to maintain a constant volumetric heat generation rate. Upon further irradiation, fission product poisons become dominant and the flux may have to be readjusted.

The energy spectrum of neutrons irradiating the actinides is a significant factor. Many authors[8,15,19] stated that fast reactors are superior to thermal reactors because the fission-to-capture ratio is generally higher for fast reactor neutron spectra. Rose found that thermal spectrum actinide burner concepts have difficulty achieving a high k_{eff} (about 0.85 - 0.95), whereas fast burners can attain such high neutron multiplication. However, on the basis of reaction rates, a study by Oliva, et al.[28] showed that LWRs are better than LMFBRs. This is because the fast neutron fluxes of present day LMFBRs are not large enough to compensate for the drop in neutron cross sections at fast energies so that their product, i.e. the reaction rate, is less than that of the LWR case. One clear advantage that fast reactors have over thermal reactors is that their criticality is less sensitive to the introduction of foreign materials in the core. This means that for the same reactivity penalty, larger quantities of actinides can be inserted in fast reactors and that these actinides can have more fission product impurities. For fusion reactors, the mean energy of neutrons emerging from fusion reactions is very high (14 MeV for the deuterium-tritium reaction). Theoretically, a greater number of neutron reactions, e.g. (n,2n), (n,3n), (n,p) is available as transmutation channels. In practice, the cross sections of these high energy reactions are small and they were found to contribute insignificantly to the overall reaction rates.

In fact, many fusion transmutation studies utilize well-moderated actinide blankets to maximize transmutation rates.

Another major factor affecting the overall effectiveness of actinide transmutation is the logistics of the transmutation strategy. Some studies make the simplifying assumption that actinides are loaded into the transmuter once and for all, and that they are irradiated continuously for long periods of time (typically 30 years) with no reprocessing. Under such a strategy, the actinide inventory in the transmuter will decrease almost exponentially. Some studies utilize the concept of actinide recycling. The irradiated actinides are discharged to reprocessing after one cycle of irradiation. At reprocessing a fresh batch of actinides is added to the unfissioned actinides. Together, they are extracted, made into forms suitable for irradiation and inserted back into the transmuter. After many cycles, an equilibrium is reached. From then onwards, the quantity of actinides removed in one cycle is equal to the quantity of fresh actinides added during reprocessing. For actinide recycling schemes, the actinide extraction efficiency is of vital importance. Since each time the actinides pass through the reprocessing step, a fraction is lost to waste storage together with the fission products. Consequently, these actinides are not transmuted and contribute to the long-term hazard of storage wastes. On the other hand, if all actinides are kept within the transmutation system, they will eventually be beneficially transmuted. A subtle point that affects the overall transmutation rates concerns whether converted uranium and plutonium are removed during reprocessing. During reprocessing, the fission products are removed. In the studies of Claiborne[8] and Beaman,[19] the converted uranium and plutonium are also

removed. The nuclides removed are mostly Pu^{238}, formed from neutron capture of Np^{237} and decay of Am and Cm isotopes. For such a transmutation strategy, there will be two main pathways for removal of actinides. One is via direct fission during irradiation and the other is via reprocessing as converted uranium and plutonium. Claiborne's data showed that in one equilibrium cycle, about 35% of the in-core actinides are removed — 12% is fissioned directly and 23% is removed in reprocessing. The extracted Pu^{238} can be used as a breeding material for Pu^{239}. From the point of view of ultimate waste disposal, the removal of Pu^{238} constitute a postponement since Pu^{238} is a highly hazardous nuclide with toxic decay daughters. A proper disposal strategey must be developed for the extracted Pu^{238}.

Proposed Work

There is a need for the study of fission reactors specifically designed to burn actinides. As actinide transmuters, commercial power reactors have two shortcomings. The flux level is limited by power production considerations and the number of reactors serviced by one power reactor is small. Consequently, many power reactors would have to be used as transmuters. Fusion reactors do produce an abundant supply of high-energy neutrons. However, a considerable amount of basic research and developmental work is required before fusion reactors can be expected to be commercially available. Hence, there is motivation to use near-term technology to design fission reactors, especially engineered for the burnout of actinide elements. The present study is concerned about the design and analysis of a uranium hexafluoride gas core reactor for such as application.

References for Chapter 2

1. Jenquin, U. P. and Leonard, B. R., Jr., "Evaluations of Fusion-Fission (Hybrid) Concepts: Transmutation of High-Level Actinide Waste in Hybrids," Part B, EPRI-ER-469 (1976).

2. Bond, W. D., Claiborne, H. C. and Leuze, R. E., "Methods for Removal of Actinides from High-Level Wastes," Nuclear Technology, 24, 362 (December, 1972).

3. Bond, W. D. and Leuze, R. E., "Feasibility Studies of the Partitioning of Commercial High-Level Wastes Generated in Spent Fuel Reprocessing: Annual Progress Report for FY-1974," ORNL-5012 (January, 1975).

4. Bond, W. D. and Leuze, R. E., "Removal of Actinides from High Level Wastes Generated in the Reprocessing of Commercial Fuels," Transplutonium Elements, 423 (1976).

5. Blomeke, J. O. and Tedder, D. W., "Actinide Partitioning and Transmutation Program Progress Report for October 1, 1976 to March 31, 1977," ORNL-TM-5888 (June, 1977).

6. Steinberg, M., Wotzak, G. and Manowitz, B., "Neutron Burning of Long-Lived Fission Products for Waste Disposal," BNL-8558 (September, 1964).

7. Gregory, M. V. and Steinberg, M., "A Nuclear Transformation System for Disposal of Long-Lived Fission-Product Waste in an Expanding Nuclear Power Economy," BNL-11915 (November, 1967).

8. Claiborne, H. C., "Neutron-Induced Transmutation of High-Level Radioactive Waste," ORNL-TM-3984 (December, 1972).

9. Wolkenhauer, W. C., "The Controlled Thermonuclear Reactor as a Fission Product Burner, " BNWL-SA-4232 (1972).

10. Wolkenhauer, W. C., Gore, B. F. and Leonard, B. R., Jr., "Transmutation of High-Level Radioactive Waste with a Controlled Thermonuclear Reactor," BNWL-1772 (1973).

11. Gore, B. E. and Leonard, B. R., Jr., "Transmutation of Massive Loadings of Cesium-137 in the Blanket of a Controlled Thermonuclear Reactor," Nuclear Science and Engineering, 53, 319-323 (1974).

12. Schneider, K. J. and Platt, A. M., "High-Level Radioactive Waste Management Alternatives," BNWL-1900, Battelle Pacific Northwest Laboratories (May, 1974).

13. Paternoster, R. R., "Radioactive Waste Disposal by Nuclear Transmutation in a UF_6 Gaseous-Core," M.S. Thesis, U. of Florida (1974).

14. Breen, R. J., "Elimination of Actinides with LMFBR Recycle," Trans. Am. Nucl. Soc., 21, 262 (June, 1975).

15. Raman, S., "Some Activities in the United States Concerning the Physics Aspects of Actinide Waste Recycling, "Proc. IAEA Advisory Group Mtg. Transactinium Isotope Nuclear Data, CONF-751104-4 (1975).

16. Croff, A. G., "Actinide Transmutation Studies: A Review," Trans. Am. Nucl. Soc., 23, 545 (June, 1976).

17. Croff, A. G. , "Parametric Studies Concerning Actinide Transmutation in Power Reactors," Trans. Am. Nucl. Soc., 22, 345 (1975).

18. Raman, S., Nestor, C. W., Jr. and Dabbs, J.W.T., "The U^{233}- Th^{232} Reactor as a Burner for Actinide Wastes," CONF-750303-36 (1975).

19. Beaman, S. L. and Aitken, E. A., "Feasibility Studies of Actinide Recycling in LMFBRs as a Waste Management Alternative," CONF-760622-48 (1976).

20. Prabulos, J. J., "Actinide Destruction in a 1500 MWe Carbide Fueled LMFBR," Trans. Am. Nucl. Soc., 23, 548-549 (June, 1976).

21. Bocola, W., Fritelli, L., Gera, F., Grossi G., Moccia, A. and Tondinelli, L., "Considerations on Nuclear Transmutation for Elimination of Actinides," IAEA-SM-207/86 (1976).

22. Parish, T. A. and Draper, E. L, Jr., "Determination of Procedures for Transmutation of Fission Product Wastes by Fusion Neutrons," UTNRL-FU101, U. of Texas (1976).

23. Harte, G. A. and Clarke, R. H., "Investigation into the Use of a Fast Breeder Reactor to Incinerate Actinide Waste from the U.K. Nuclear Power Programme," CEGE-RD/B/N-3903 (1976).

24. Rose, R. P., "Fusion-Driven Actinide Burner Design Study," EPRI-ER-451 (1976).

25. Berwald, D.H., "Preliminary Design and Neutronic Analysis of a Laser Fusion Driven Actinide Waste Burning Hybrid Reactor," Ph.D. Thesis, Dept. of Nuclear Engineering, U. of Michigan (1977).

26. Pigford, T. H. and Choi, J., "Actinide Transmutation in Fission Reactors," Trans. Am. Nucl. Soc., 27, 450-451 (1977).

27. Clement, J. D. and Rust, J. H., "Analysis of the Gas Core Actinide Transmutation Reactor (GCATR)," Georgia Institute of Technology, NASA Grant NSG-1288 (1977).

28. Oliva, G., Palmiotti, G., Salvatores, M. and Tondinelli, L., "Elimination of Transuranium Elements by Burnup in a Power Fast Breeder Reactor," Nuclear Technology, 37 (March, 1978).

29. Clement, J. D. and Rust, J. H., "Gas Core Reactors for Actinide Transmutation and Breeder Applications," Georgia Institute of Technology, NASA Grant NSG-1288 (1978).

Chapter 3

DESIGN OF REFERENCE UF_6 ACTINIDE TRANSMUTER

Validity of MACH-1 Calculation for Gas Core Reactors

The MACH-1 code[1] was chosen to perform neutronic calculations. MACH-1 is a one-dimensional, multi-group, diffusion code. It has one thermal group. At Georgia Tech, it uses a 26-group cross section set derived from the ABBN set.[2]

Due to the low density of fuel in gas core reactors, there is some doubt as to whether a simple code like MACH-1 can describe the neutronics accurately. The calculations of Mills[3,4] were chosen as the standard. Mills used a multigroup S_n theory code. He obtained good agreement between calculation and experimental data for low fuel density reactors. Figure 3.1 shows plots of critical concentration and critical masses of U^{235} gas as a function of D_2O, Be, and C—reflected reactors as a function of core radius. Table 3.1 shows U^{235} critical masses for a spherical reactor with 50 cm of Be reflector as calculated by MACH-1.

TABLE 3.1

U^{235} Critical Masses (kg) for a Spherical Reactor with 50 cm. Be Reflector for Different Core Radii. (Tn = 400°C)

	Radius						
	20 cm.	30 cm.	40 cm.	50 cm.	60 cm.	100 cm	300 cm.
MACH-1 result	4.44	2.10	2.34	2.85	3.49	7.09	46.6

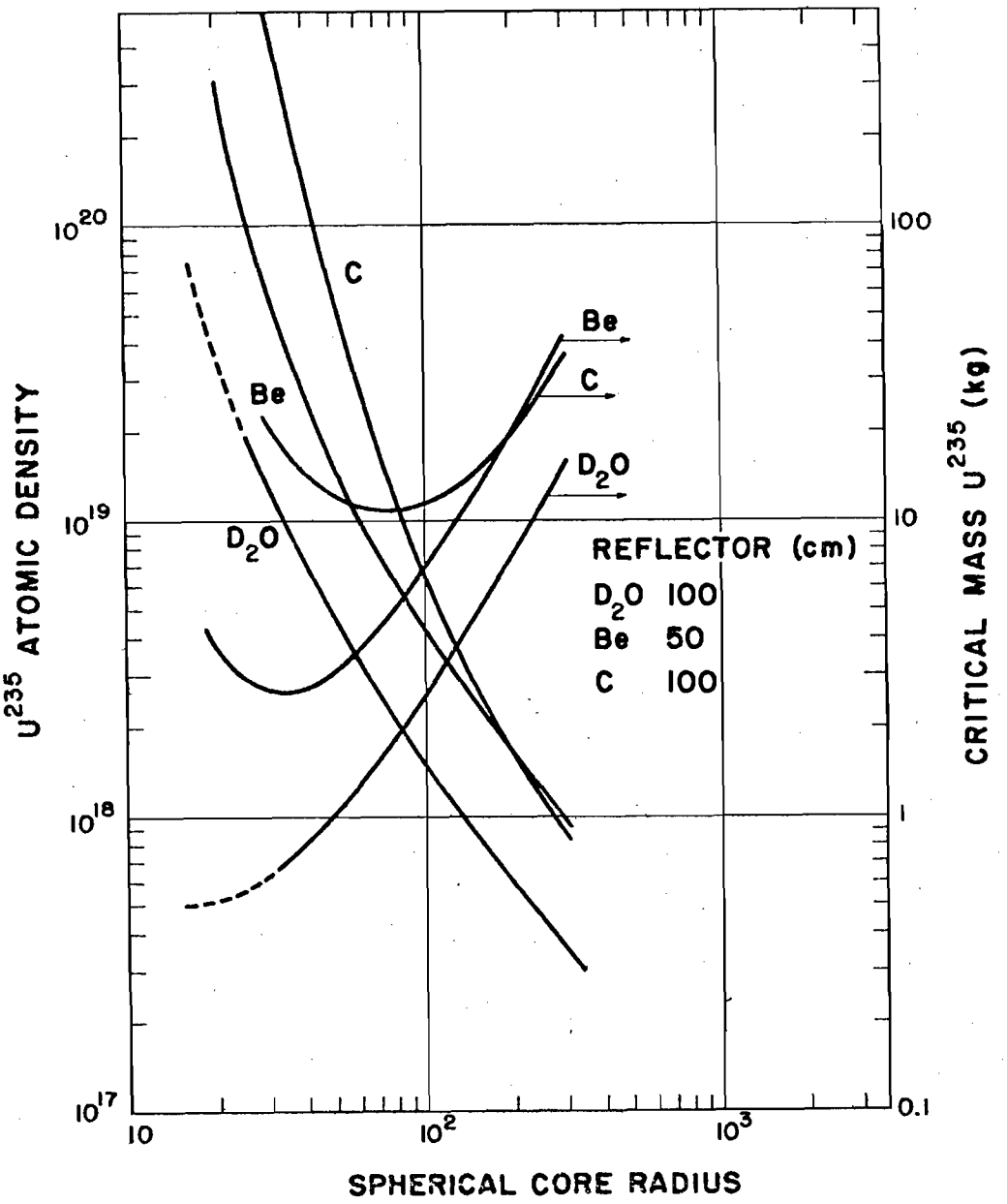

Fig. 3.1. Critical Concentration of U^{235} Gas as a Function of D_2O, Be, and C-reflected Core Radius.

For treatment of the thermal group cross sections in MACH-1, the Wescott[5] formulation is followed. The MACH-1 results well match the shape of Mills curves. By adjusting the effective neutron temperature, good agreement (< 10% discrepancy) is obtained.

Reference Reactor Design

The configuration of the UF_6 transmuter is shown in Fig. 3.2. It consists of four regions. Region I is the gaseous fuel region with a mixture of UF_6 and He as fuel. Region II consists of the beryllium reflector-moderator. Region III consists of the liquid bismuth-actinide blanket. Region IV is the graphite reflector. Table 3.2 is a summary of the operating reactor parameters.

Core Design Considerations

Spherical geometry is chosen for simplicity of design. A fuel mixture of UF_6 and He is used. The uranium is essentially 100% U^{233}. Since UF_6 is a very poor heat transfer agent, helium is added to improve the overall heat transfer characteristics of the mixture. Addition of helium helps to maintain a small inventory of U-233 in the heat exchangers. The fission energy is deposited in the UF_6-He mixture in reactor core. It is pumped out of the core through heat exchangers where the fission energy is transferred. The fuel mixture is passed through reprocessing and refueling systems, where fission product poisons are removed and fresh UF_6 fuel added.

Since the ABBN cross section set does not have cross sections for helium and fluorine, these were generated from cross section data from BNL-325.[6,7] The formalism is described previously.[8] It is estimated that due to the low neutron cross sections and density of helium and fluorine, they do not effect the neutonics calculations significantly.

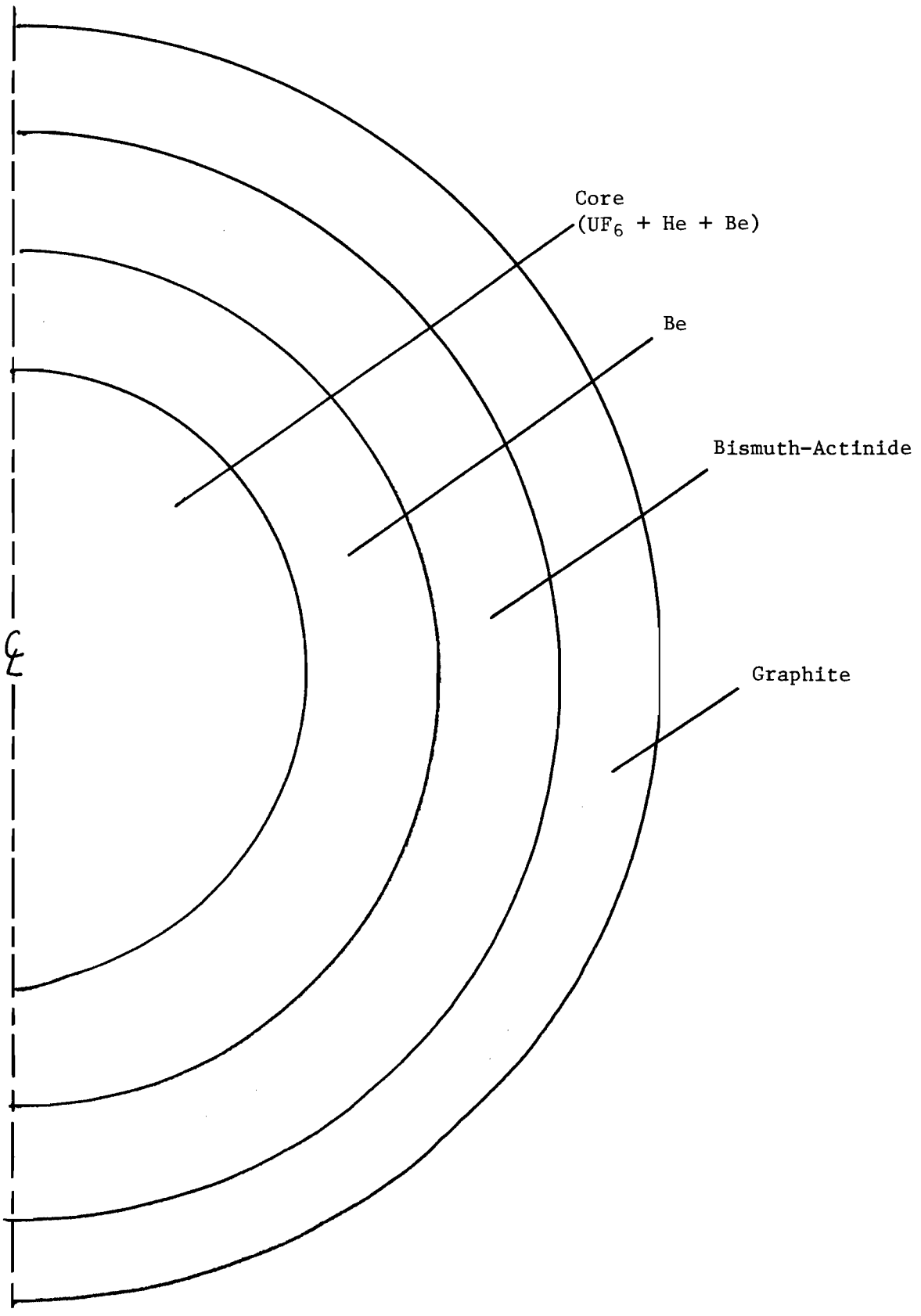

Fig. 3.2. Reactor Configuration of UFATR

TABLE 3.2

Summary of Operating Characteristics of
Beginning of Life UFATR

Reactor Type: Thermal

Geometry : Spherical

Region I:

Fuel: UF_6, He gas mixture
Enrichment: 100% U^{233}
Radius: 133 cm
Core pressure: 101 atm.
UF_6 partial pressure: 1.9 atm
He partial pressure: 99.1 atm
Core power: 2000 MWt
Power density: 203 Watts/cc
Mean core temperature: 783°K(510°C, 950°F)
U^{233} critical mass: 7.05 kg
Peak to avg. power density ratio: 1.002
Avg. thermal flux: 1.16×10^{16} n/cm^2-sec

Region II:

Reflector-Moderator: Be solid
Thickness: 35 cm
Mean temperature: 783°K(510°C, 950°F)
Be mass: 18.3 MT

Region III:

Blanket material: liquid Bi and actinides
Composition: 93 wt% Bi
7 wt% Actinides
Thickness: 20 cm
Mean temperature: 723°K(450°C, 842°F)
Actinide mass: 6.0 MT
Bi mass: 78.5 MT

Avg. thermal flux: 4.11×10^{13} n/cm^2-sec
Power: 239 MWt
Maximum design power: 1600 MWt
Maximum design power density: 200 Watts/cc

Region IV:

Reflector material: solid graphite
Thickness: 100 cm
Mean temperature: 723°K(450°C, 842°F)
Graphite mass: 116 MT

The maximum core power is set at 2000 MWt. The core dimension is chosen such that a reasonable volumetric heat generation rate of 200 watts/cc is obtained. No detailed thermal-hydraulic calculations are performed. Knowledge of the fission density distribution in the core is required for such calculations. However, no major difficulties are anticipated in this area.

The limiting materials problem in a UF_6 core reactor is the corrosion of the core containment vessel. Since the maximum temperature of the UF_6 in the core is rather low (> 800°K), Ni, Al, Mg, and Zr metals all have excellent F_2 corrosion resistance.[9] These metals can be used as a thin liner or clad. Even if the Be is exposed to F_2 through cracks, pinholes, etc., the BeF_2 that forms when Be reacts with F_2 is reported[10] to passivate the surface.

Reflector Moderator Design Considerations

Because Be has a high scattering cross section, a high atomic density, and the lowest absorption cross section of all metals, it is chosen as the reflector-moderator for the core.

Two conflicting considerations enter into the choice of reflector thickness. In order to have an abundant supply of core neutrons for transmutation, a thin beryllium region is desirable. However, too thin a reflector makes the core very sensitive to changes in the blanket region. Figure 3.3 is a plot of U^{233} concentration as a function of beryllium reflector thickness. The steep slope of the curve for a Be thickness less than 20 cm indicates the gas core is extremely sensitive to external moderation. For thicknesses greater than 50 cm, the core is close to an infinitely reflected assembly. Figure 3.4 shows the neutron leakage from the beryllium reflector. A Be thickness of

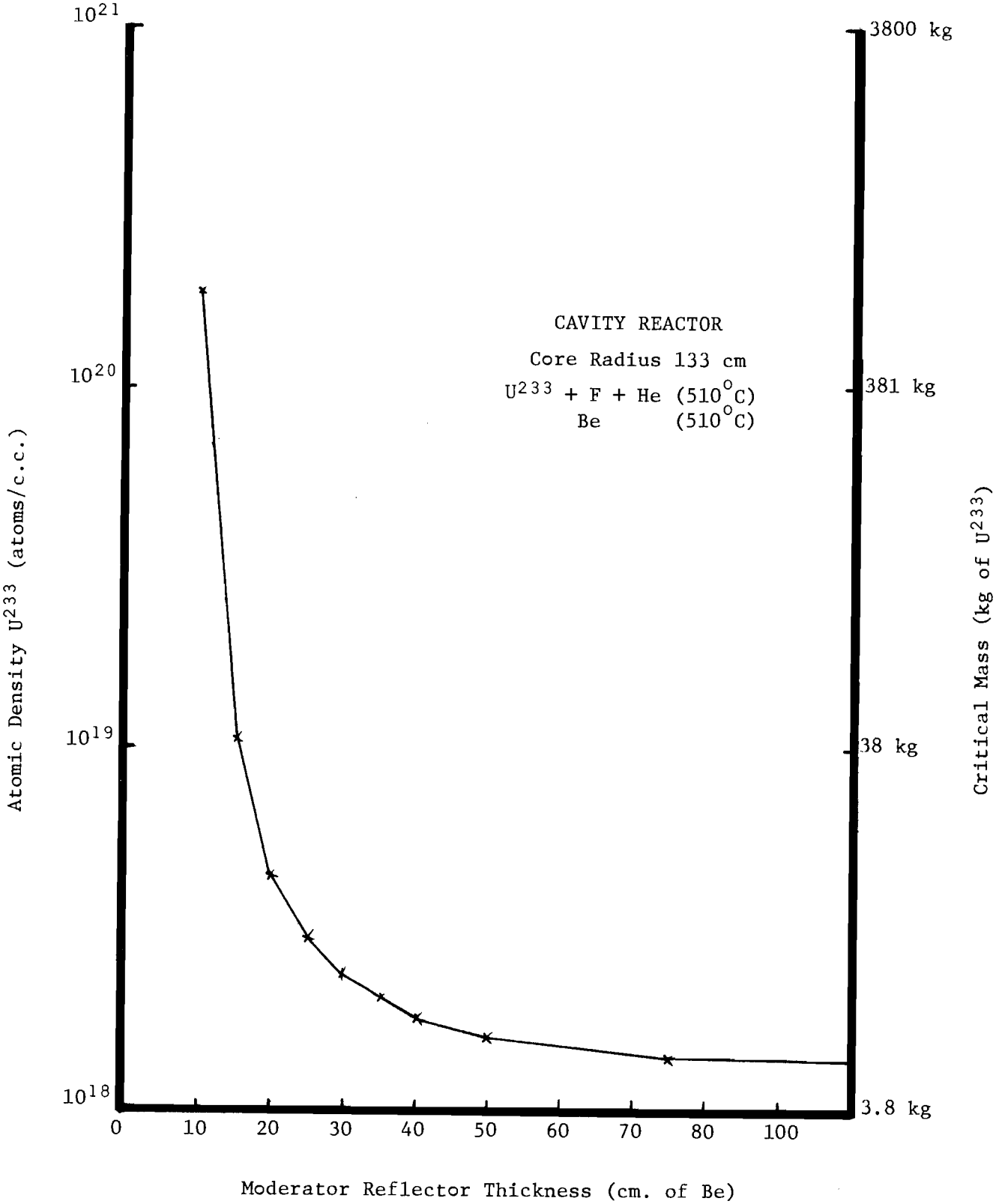

Fig. 3.3. Critical U^{233} Density and Mass vs Be Thickness

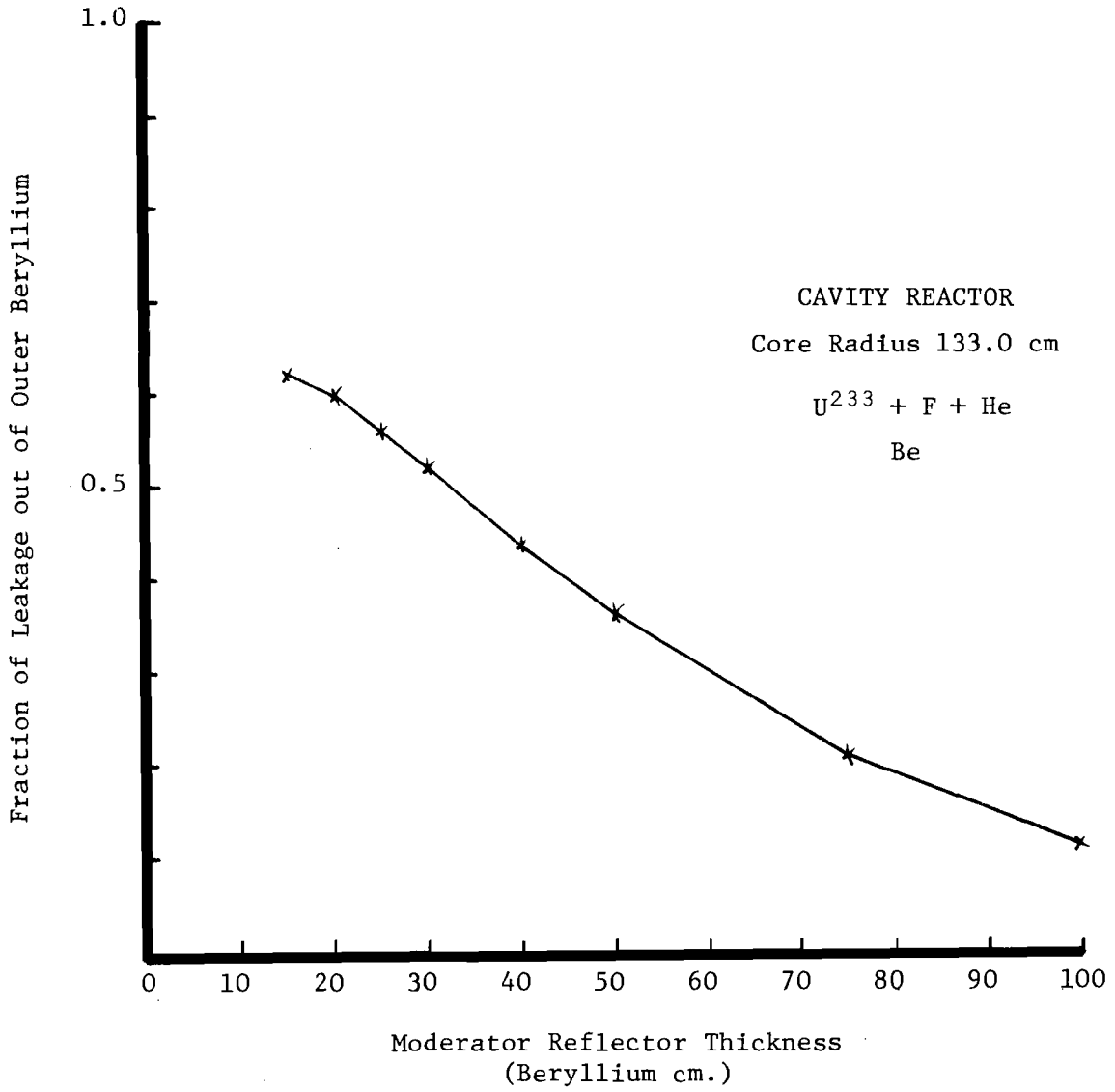

Fig. 3.4. Neutron Leakage Fraction as a Function of Be Thickness

35 cm is chosen as the optimum reflector thickness. For such dimensions, there is sufficient moderation and reflection of neutrons that the core is not sensitive to changes in the actinide blanket region. The fraction of neutrons leaked from the beryllium is 0.48, and 99.6% of these neutrons are thermalized. For a core power of 2000 MWt, 1.56×10^{20} neutrons/sec leave the core and are available for transmutation use. As pointed out by Safonov,[11] gas core reactors are ideal irradiators because they provide an abundant supply of neutrons for transmutation.

An interesting characteristic of externally moderated reactors is that the effective neutron temperature of the thermal flux is determined by the temperature of the external moderator. Hence, by controlling the temperature of the beryllium reflector, reactivity control of the core can be affected.

Actinide Blanket Design Considerations

Liquid metal fuel reactor systems have been studied extensively.[12] The present liquid bismuth-actinide blanket design relied substantially on information gathered in these early works.

In this design, the blanket consists of 93 wt% liquid bismuth and 7 wt% actinides. Since solubilities of actinide metals in liquid bismuth are not well established, the blanket may take the form of a homogeneous solution or that of an actinide-bismuth slurry. For the case of a slurry, the actinides are present as small particles dispersed uniformly throughout the bismuth. Additional attention will have to be directed towards the problems of concentration control, stability, and erosion.

The use of a liquid bismuth-actinide blanket has many advantages. Continuous reprocessing of fission product poisons can be carried out to ensure maximum utlization of neutrons for transmutation. Continuous refueling of the blanket leads to great flexibility in actinide fuel management. Since the fluid fuel can be cooled in an external heat exchanger separate from the reactor core, the nuclear requirements (of the core) and heat flow requirements (of the exchanger) need not both be satisfied at the same place. This may allow design for very high specific power. Furthermore, liquid bismuth can be operated at high temperatures without high pressures, is free from radiation damage, and has better heat transfer properties than water.

Bismuth is quite corrosive to most metals and alloys,[13] but its corrosiveness can be reduced (particularly with respect to steel) by the addition to the bismuth of zirconium or titanium in conjunction with magnesium. The zirconium (or titanium) is believed to react with nitrogen and/or carbon in the steel to form a protective layer of ZrN or ZrC which provides a barrier between the bismuth and the ferrous alloy substrate.[14,15] The role of magnesium in conjunction with zirconium or titanium is to getter oxygen from the system, thereby preventing any oxidation of the latter two elements which would destroy their effectiveness.[16] The materials that can be used to contain bismuth-uranium fuels are graphite, beryllium, carbon steels, low chromium steels, molybdenum, tantalum, tungsten, and some high alloy steels.[16]

A 20 cm thickness of blanket is chosen. Assuming a maximum volumetric heat generation rate of 200 watts/cc, the maximum blanket power is about 1600 MWt. No detailed analysis of heat transfer and fluid flow of the

TABLE 3.3

Core Neutronic Parameters for Different Blanket Composition

Core power = 2000 MWt

Bi = U = 93 = 7 Wt%

$\frac{U^{233}}{U^{238}}$ ratio	$\frac{0}{100}$	$\frac{0.0625}{99.9375}$	$\frac{0.125}{99.875}$	$\frac{0.25}{99.75}$
Blanket Power (MWt)	~ 0	180	370	790
Core peak-to-average power ratio	1.002	1.002	1.002	1.002
Core critical mass (kg of U^{233})	6.57	6.45	6.32	6.05

blanket was performed. However, no major difficulties are anticipated. An average blanket temperature of 723°K (450°C, 842°F) was assumed.

UFATR Core Neutronic Characteristics

Twenty five-group MACH-1 calculations are performed for the UFATR. Thermal neutrons induce fission in the gas core, leading to the production of 2.5 fast neutrons per fission. These fast neutrons quickly escape to the beryllium moderator and are thermalized. Some of them are returned to the core to maintain the self-sustaining reaction. A substantial portion (35%-50%) are trapped in the bismuth-actinide blanket leading to transmutation reactions. Figure 3.5 is a plot of neutron flux integrals in the core as a function of energy groups. Since a 25-group actinide cross section set was not available, their presence was simulated by a U^{233}- U^{238} mixture. The U^{233} fraction in the blanket was varied so that a blanket power from 0 to 800 MWt was produced. This would simulate the changing neutronic characteristics of the actinide blanket during irradiation. Table 3.3 shows some core parameters for different blanket compositions. Two desirable characteristics of the UFATR can be observed. The peak-to-average ratio of the core power is extremely close to unity. The core parameters are insensitive to changes in the actinide blanket composition.

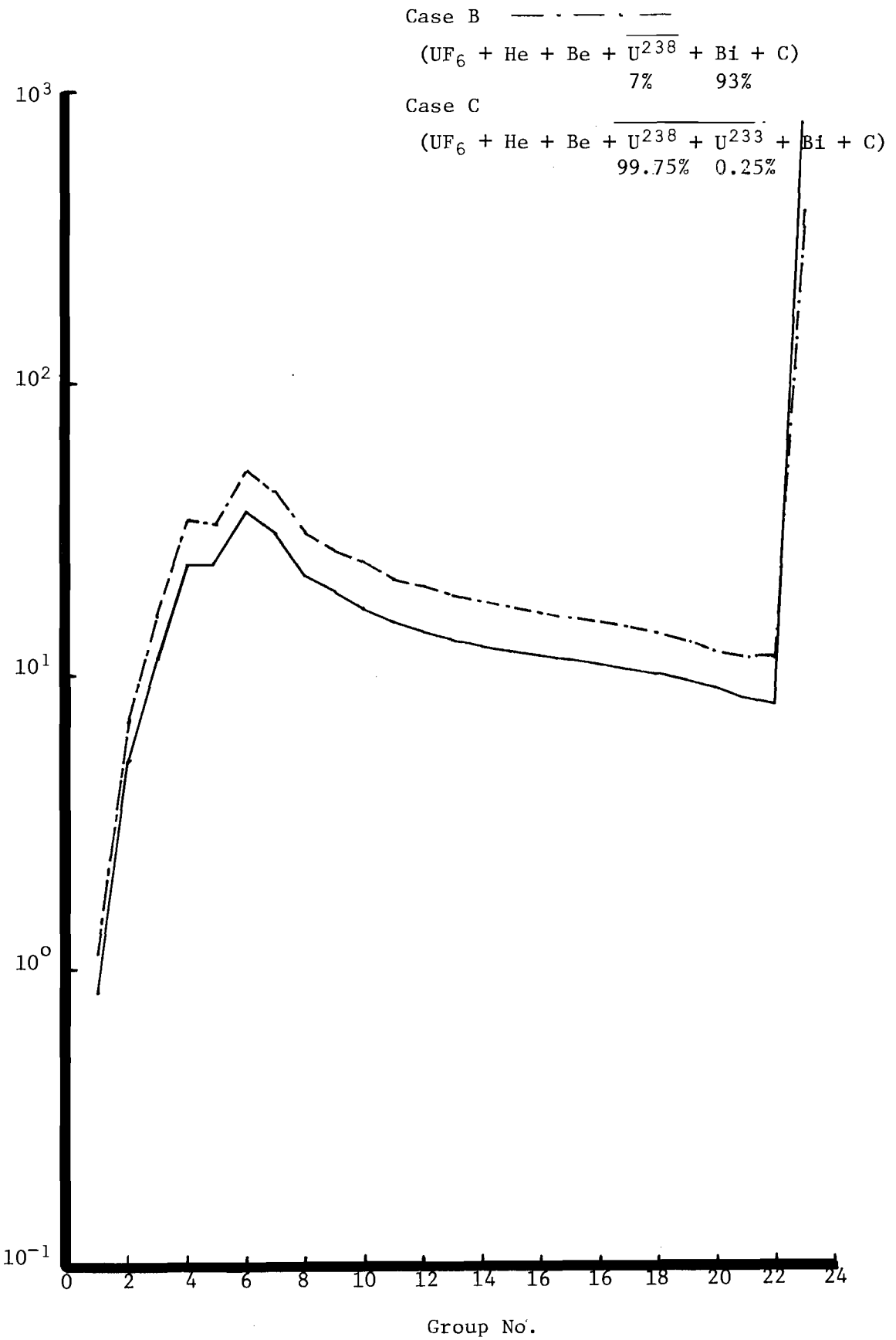

Fig. 3.5. Flux Integral vs Energy Group in UF_6 + HE Core Region

References for Chapter 3

1. Meneley, D. A., Kvitek, L. C. and O'Shea, D. M., "MACH-1, A One-Dimensional Diffusion-Theory Package," ANL - 7223 (June, 1966).

2. Abagyan, L. P., Bazazyants, N. O., Bondarenko, I. I. and Nikolaav, M. N., Group Constants for Nuclear Reactor Calculations, Consultants Bureau, New York (1964).

3. Mills, C. B., "Reactor Minimum Critical Dimensions," LA-3221-MS (April, 1965).

4. Mills, C. B., "Reflector Moderated Reactors," Nuclear Science and Engineering, 13, 301-305 (1962).

5. Westcott, C. H., "Effective Cross Section Values for Well-Moderated Thermal Reactor Spectra," CRRP-787 (August, 1958).

6. Garber, D. I. and Kinsey, R.R., "Neutron Cross Sections," 3rd Edition, Vol II, BNL-325 (January, 1976).

7. Hughes, D. J. and Schwartz, R. B., "Neutron Cross Sections," 2nd Edition, BNL-325 (July, 1958).

8. Clement, J. D. and Rust, J. H., "Gas Core Reactors for Actinide Transmutation and Breeder Applications," NASA Grant NSG-1288 (April, 1978).

9. Wagner, P., "Materials Considerations for UF_6 Gas-Core Reactor," LA-6776 - MS (April, 1977).

10. O'Donnell, P. M., "Kinetics of the Fluorination of Beryllium," J. Electrochem. Soc., 114, 1206-09 (1967).

11. Safonov, G., "Externally Moderated Reactors," Proc. Intern. Conf. Peaceful Uses of Atomic Energy, Geneva, 12, 705 (1958)

12. Lane, E. J. MacPherson, H. G. and Maslan, F., Ed., Fluid Fuel Reactors, Addison-Wesley Publisher Company, Inc. (September, 1958).

13. Berry, E. W., Corrosion in Nuclear Applications, John Wiley and Sons, Inc. (1971).

14. Romano, A. J., Klamut, C. J. and Gurinsky, D. H., "The Investigation of Container Materials for Bi and Pb Alloys, Part I, Thermal Convection Loops," BNL-811 (July, 1963).

15. Kammerer, O. F., Weeks, J. R., Sadofsky, J., Miller, W.E. and Gurinsky, D. H., "Zirconium and Titanium Inhibit Corrosion and Mass Transfer of Steels by Liquid Heavy Metals," Trans. Met. Soc. AIME, 212 (1), 20-25 (February, 1958).

16. Klamut, C. J., Schweitzer, D. G., Chow, J.G.Y., Meyer, R.A., Kammerer, O.F., Weeks, J. R. and Gurinsky, D. H., "Material and Fuel Technology for an LMFBR," Proceedings of the Second International Conference on the Peaceful Uses of Atomic Energy, Geneva, 7, 173-195 (September, 1958).

Chapter 4.

ANALYSIS OF ACTINIDE BURNUP IN UFATR

Actinide Cross Sections

The validity of actinide transmutation calculations are dependent upon the accuracy of actinide neutron cross sections. A large number of reactor concepts, including LWRs, LMFBRs, CTRs have been studied as transmutation candidates. Therefore, the range over which capture and fission cross sections of actinides need to be known extends from thermal to about 18 MeV of neutron energy.[1-6] There are 16 transactinium elements with 200 isotopes known to date. For many of these actinides, experimental data may not exist. This is due to short half lives, an inability to obtain samples of sufficient isotopic purity, and difficulty of obtaining higher energy (are 14 MeV) nonenergetic neutron sources for differential cross section measurement. Consequently, for many of these, the necessary data has been obtained by application of nuclear systematics and model calculations.[7] Generally, the main isotopes of Th, Pa, U, Np, and Pu have been evaluated extensively. There is an urgent need for evaluation of americium and curium isotopes cross sections, and to a lesser extent, those of berkelium and californium. For higher actinide isotopes, they usually are very short lived and exist in such minute quantities that they are insignificant for most applications. The thermal cross sections of the actinides have been found to yield computational results in agreement with experimental data from transplutonium production programs.[8-12] As one moves away from the thermal region into the fast energy region, greater uncertainty persists.

For the present calculation, a three-group actinide cross section set was generated as shown in Table 4.1. Only those nuclides which may

TABLE 4.1

Three Group Cross Section Set for the Actinides

Group # / Nuclide	1 (FAST)			2 (RESONANCE)			3 (THERMAL)		
	σ_a	$\nu\sigma_f$	ν	σ_a	$\nu\sigma_f$	ν	σ_a	$\nu\sigma_f$	ν
U^{232}	*2.63-3	0.0	0.0	42.0	70.1	3.13	2.63-3	0	0.0
U^{234}	1.93	5.06	2.62	44.1	0.0	0.0	54.56	0.0	0.0
U^{236}	1.62	4.31	2.66	25.55	0.0	0.0	2.83	0.0	0.0
U^{237}	1.88	5.19	2.76	84.0	0.0	0.0	205.85	0.0	0.0
Np^{237}	1.22	3.60	2.95	4.62	0.0	0.0	103.08	2.76-2	2.67
Np^{238}	0.0	0.0	0.0	61.6	17.06	2.77	1127.0	3123.0	2.77
Pu^{236}	0.0	0.0	0.0	0.0	0.0	0.0	88.2	244.4	2.77
Pu^{237}	0.0	0.0	0.0	0.0	0.0	0.0	154.0	440.4	2.86
Pu^{238}	2.63-3	0.0	0.0	13.23	5.07	2.895	313.8	27.27	2.895
Pu^{239}	2.06	6.4	3.2	35.07	21.07	2.87	1129.3	2080.7	2.87
Pu^{240}	1.23	3.825	3.11	560.9	0.0	0.0	185.2	8.37-2	2.79
Pu^{241}	7.90-3	0.0	0.0	51.24	116.67	2.924	1099.3	2369.4	2.924
Pu^{242}	7.40-3	0.0	0.0	89.58	0.925	2.81	10.44	0.0	0.0
Pu^{243}	1.29	4.22	3.27	56.42	110.4	2.91	14.56	285.25	2.91
Pu^{244}	0.0	0.0	0.0	2.975	0.0	0.0	0.926	0.0	0.0
Am^{241}	1.10	0.0	3.41	81.97	4.59	3.121	578.4	8.76	3.121
Am^{242}	1.85-2	0.0	0.0	0.0	0.0	0.0	1143.6	3636.7	3.18
Am^{242m}	1.83	6.44	3.52	109.9	358.7	3.264	5227.9	1.351+4	3.26
Am^{243}	0.0	0.0	0.0	135.1	0.7224	3.09	28.1	0.0	3.09
Cm^{242}	0.0	0.0	0.0	10.50	0.0	3.19	13.61	8.686	3.19
Cm^{243}	5.0-3	0.0	0.0	165.2	446.6	3.43	484.7	1.289+3	3.43
Cm^{244}	0.0	0.0	0.0	42.2	4.01	3.20	6.37	1.917	3.20
Cm^{245}	0.0	0.0	0.0	60.9	205.48	3.832	1.385+3	4.5096+3	3.832
Cm^{246}	0.0	0.0	0.0	8.886	2.644	3.80	0.8768	0.3518	3.80
Cm^{247}	0.0	0.0	0.0	88.3	202.4	3.80	70.96	149.2	3.79
Cm^{248}	0.0	0.0	0.0	18.59	4.013	3.90	1.759	0.7221	3.90

*read as 2.63×10^{-3}

have a significant effect on the blanket neutronics are included. Whenever possible, the more up-to-date data of Benjamin[11] is used to supplement the ORIGEN data library.[13] The cross sections are spectrum-averaged. The fast energy group extends from 10 MeV to 0.8 MeV. A fission neutron spectrum is assumed for this region. The resonance region extends from 0.8 MeV to 0.465 eV. A $\frac{1}{E}$ spectrum is assumed. The thermal region extends from 0 eV to 0.465 eV with a Maxwellian spectrum assumed. Cross sections of Np^{237}, Pu^{239}, Pu^{240}, Pu^{241}, Pu^{242}, Am^{241}, and Am^{243} are corrected with non-$1/v$ factors from Westcott.[14] For the other nuclides, $1/v$ behavior of cross sections is assumed. The downscattering cross sections for the actinides are appoximated by those of U^{238}. Since the actinides are heavy nuclides and present in low concentration, they should have little effect on the neutron transport characteristics of the liquid bismuth blanket.

Computational Strategy

Figure 4.1 illustrates the computational strategy used for analyzing the actinide blanket as a function of burnup. MACH-1 is used for neutronic analysis. The 26-group ABBN cross section set is collapsed to a 3-group cross section set for use in conjunction with the actinide cross sections generated previously. The code ORIGEN[13] is used to keep track of buildup and depletion of actinides during irradiation. The concentrations of actinides are inputed into MACH-1, which calculates the neutron flux distribution in the reactor. This information is used to generate the parameters, THERM, RES, FAST, and FLUX that are required for ORIGEN input. ORIGEN then calculates actinide concentrations at the end of the time step. This procedure is repeated.

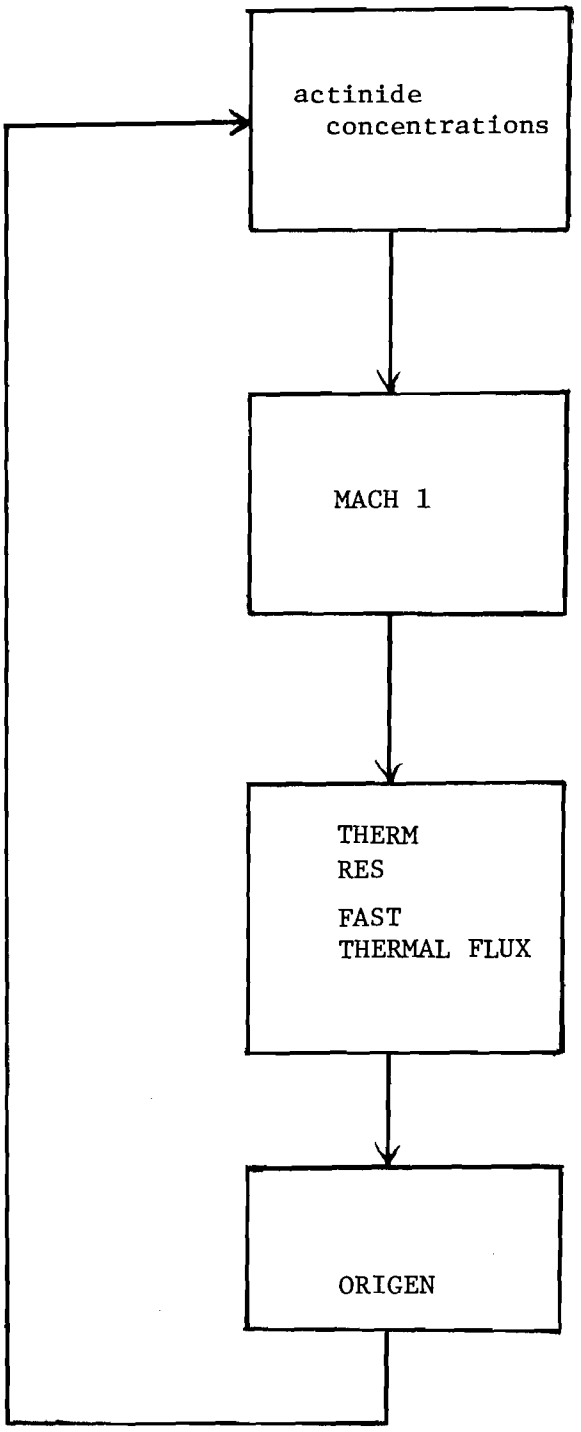

Fig. 4.1. Computational Strategy of UFATR.

Actinide Fuel Management During Burnup

Numerous actinides fuel management schemes are possible during irradiation of actinides. Detailed studies are required to choose a management scheme that will maximize the actinide burnup performance. For the present study, the following strategy is used. At the beginning of life, 6.0 metric tonnes of actinides is charged into the blanket. This quantity of actinides is equivalent to the amount produced from 300 LWR-years of operation. The reactor is operated with a core power of 2000 MWt. Since the blanket is very subcritical, only a small amount of power is produced. The liquid bismuth blanket is circulated to remove heat produced and for reprocessing of fission products. No refueling of actinides is carried out. As actinide nuclides are converted to more fissile isotopes, the blanket power rises. Eventually, it will reach 1600 MWt --- the maximum design power for the blanket. At this point in time, continuous refueling is introduced. The addition of the poor quality actinide feed makes the blanket become more subcritical. The blanket is operated at a constant power of 1600 MWt. The actinide refueling rate is set to match the depletion rate so the actinide inventory in the blanket is maintained constant. The blanket composition will change with time until equilibrium is reached.

Berwald[15] found a problem in the ORIGEN code when the continuous refueling option is chosen. His prescription for the correction of this error was adopted.

Analysis of Actinide Burnup Performance

Table 4.2 shows the core and blanket neutronic parameters as a function of burnup. It should be noted that core critical mass stays relatively constant for the 10 year irradiation period. For the first 4 years, the

TABLE 4.2

Core and Blanket Parameters as a Function of Burnup

	Time	0	1Y	2Y	3Y	4Y	5Y	6Y	7Y	8Y	10Y
Core	U^{233}mass (kg)	7.05	6.83	6.74	6.53	6.30	6.23	6.21	6.21	6.21	6.21
	flux	1.16+16	1.20+16	1.21+16	1.25+16	1.30+16	9.29+15	9.16+15	9.17+15	9.22+15	9.03+15
	power	2000	2000	2000	2000	2000	1410	1390	1390	1400	1370
Blanket	flux	4.11+13	5.67+13	5.16+13	5.41+13	4.88+13	4.78+13	4.82+13	4.90+13	4.98+13	5.02+13
	power	239	702	1109	1591	1600	1600	1600	1600	1600	1600

core power is set at 2000 MWt. During this time, the blanket is becoming more fissile and its power is rising rapidly. At the end of 4 years, the blanket power is approaching the design maximum of 1600 MWt. At this point, continuous refueling of actinides is carried out with the feed rate equalling the depletion rate. The blanket power is held constant at 1600 MWt; however, the core power is dropped to 1400 MWt. At the end of 10 years, the blanket is very close to equilibrium. Figure 4.2 shows the blanket power and flux as a function of burnup.

Table 4.3 shows the quantity of the more abundant actinides in the blanket during burnup. An initial load of 6 metric tonnes of actinides is charged. At the end of 4 years, the inventory is reduced to 3.9 metric tonnes. From 4 to 10 years, the blanket composition stabilizes very quickly, and is close to equilibrium after 10 years.

Table 4.4 shows the principal fissioning nuclides in the blanket as a function of time. At the beginning of life, the power is mostly coming from Am^{242m}, Cm^{245} and Np^{237}. As the irradiation proceeds, the blanket becomes more fissile due to the accumulation of plutonium isotopes. At the end of 10 years, the principal fissioning nuclides are Pu^{239}, Cm^{245}, and Pu^{241}. This change in blanket composition and criticality is reflected in changes in values of RES and FAST, as shown in Table 4.5. The parameters RES and FAST are proportional to the neutron flux in the resonance and fast regions, respectively, relative to the thermal flux. Figure 4.3 is a plot of the blanket fission densities as a function of radial distance for different burnup times.

To further evaluate the criticality of the blanket during burnup, MACH-1 analysis of the blanket is performed. The fissioning gas core is replaced by solid beryllium. The effective multiplication constant of the

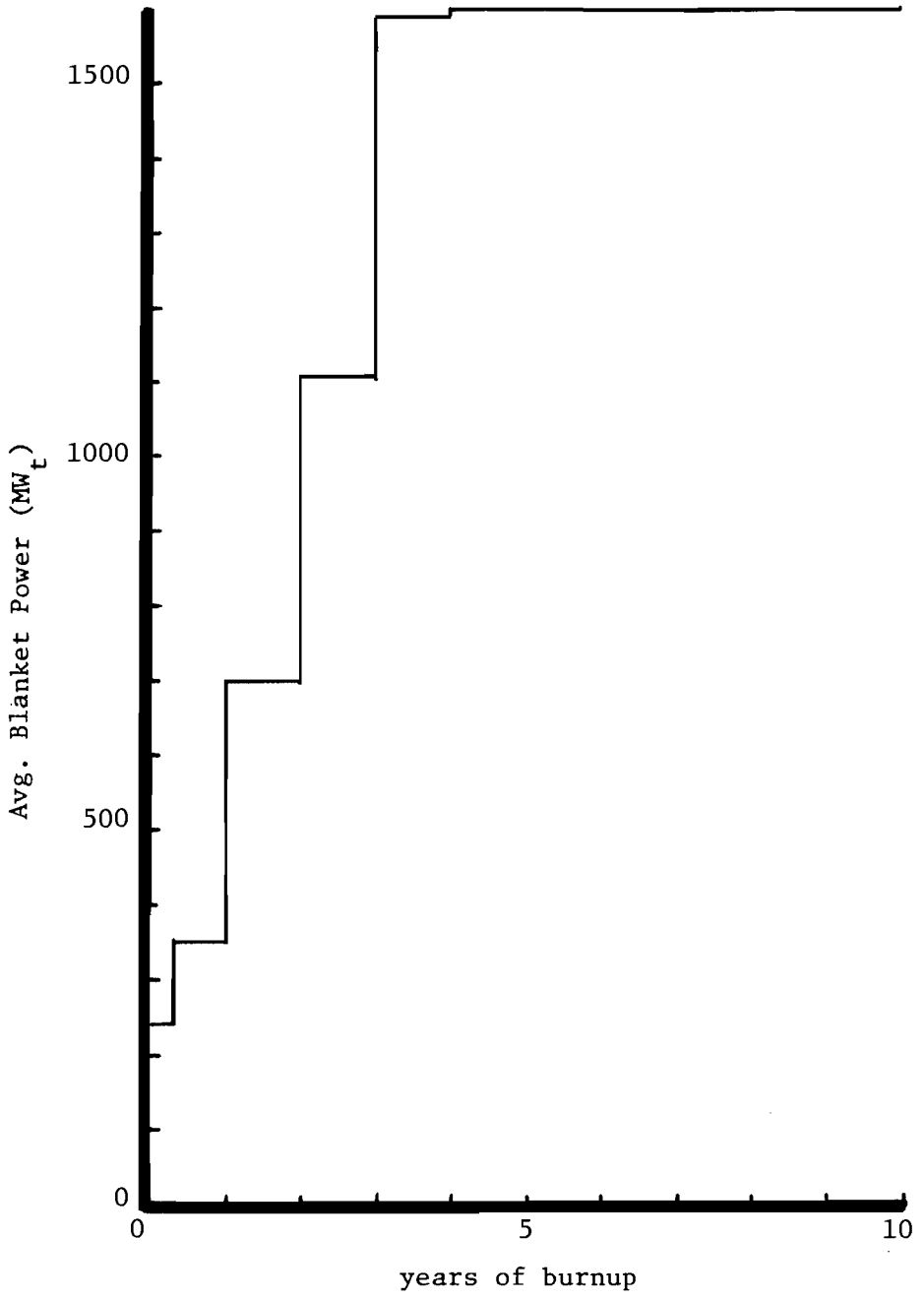

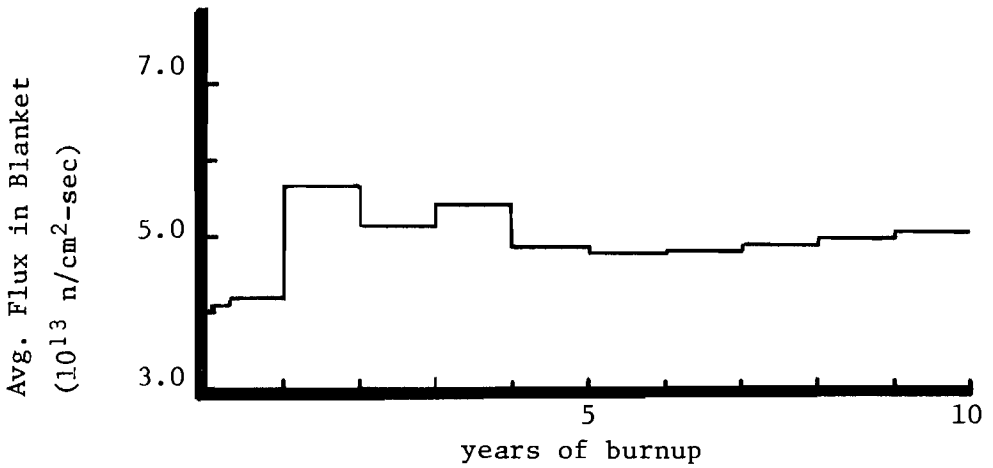

Fig. 4.2. Plot of Avg. Flux and Power in Blanket as a Function of Burnup Time

TABLE 4.3

Gm-Atoms of the Principal Actinides as a Function of Burnup

Nuclide	Charge	1Y	2Y	3Y	4Y	5Y	6Y	7Y	8Y	10Y
Np^{237}	1.85+4	1.52+4	1.13+4	8.23+3	5.56+3	5.39+3	5.29+3	5.21+3	5.15+3	5.04+3
Np^{238}		2.37+1	2.70+1	2.07+1	1.71+1	1.59+1	1.57+1	1.56+1	1.55+1	1.54+1
Pu^{238}		3.00+3	3.36+3	4.42+3	4.49+3	4.29+3	4.18+3	4.10+3	4.03+3	3.90+3
Pu^{239}		3.90+2	5.89+2	9.43+2	1.07+3	1.05+3	1.02+3	9.95+2	9.75+2	9.42+2
Pu^{240}		1.10+2	3.08+2	5.56+2	7.19+2	7.60+2	7.61+2	7.53+2	7.46+2	7.32+2
Pu^{241}		1.21+1	6.69+1	1.54+2	2.64+2	3.24+2	3.39+2	3.38+2	3.32+2	3.23+2
Pu^{242}		1.52+2	2.09+2	2.30+2	2.68+2	3.26+2	3.85+2	4.31+2	4.63+2	4.97+2
Am^{241}	1.75+3	7.05+2	1.96+2	5.72+1	1.83+1	1.09+2	1.32+2	1.37+2	1.37+2	1.35+2
Am^{242}	4.22-4	1.34+0	5.49-1	1.60-1	5.98-2	3.37-1	4.08-1	4.27-1	4.31-1	4.31-1
Am^{242m}	3.52+1	1.90+1	5.93+0	1.91+0	6.47-1	3.88+0	4.85+0	5.05+0	5.03+0	4.91+0
Am^{243}	3.53+3	2.92+3	2.12+3	1.49+3	9.61+2	9.51+2	9.67+2	9.92+2	1.02+3	1.05+3
Cm^{242}	4.09+1	3.27+2	2.13+2	8.52+1	3.17+1	4.95+1	7.28+1	8.28+1	8.62+1	8.72+1
Cm^{243}	2.93+0	5.92+0	6.65+0	4.03+0	1.69+0	1.13+0	1.36+0	1.62+0	1.77+0	1.87+0
Cm^{244}	1.06+3	1.60+3	2.17+3	2.45+3	2.49+3	2.50+3	2.51+3	2.53+3	2.56+3	2.63+3
Cm^{245}	7.17+1	5.55+1	9.51+1	1.45+2	1.97+2	2.25+2	2.32+2	2.33+2	2.32+2	2.35+2
Cm^{246}	8.18+0	2.41+1	5.16+1	9.24+1	1.54+2	2.20+2	2.87+2	3.53+2	4.17+2	5.42+2
Totals	2.50+4	2.46+4	2.07+4	1.90+4	1.64+4	1.63+4	1.64+4	1.63+4	1.63+4	1.64+4

TABLE 4.4

Percentage of Blanket Power from Actinides as a Function of Burnup

Nuclide	0 days	1Y	2Y	3Y	4Y	5Y	6Y	7Y	8Y	10Y
Np^{237}	12.7	9.3	7.0	5.0	3.4	3.3	3.3	3.2	3.2	3.2
Np^{238}	2.4	5.1	4.2	2.2	1.5	1.3	1.3	1.3	1.3	1.3
Pu^{238}		3.9	5.3	4.9	4.3	3.9	3.8	3.7	3.7	3.7
Pu^{239}		51.6	55.6	58.7	55.2	51.0	49.5	48.9	48.8	48.2
Pu^{241}		1.9	7.5	11.5	16.4	19.0	19.8	20.0	20.0	19.9
Am^{242m}	52.6	14.5	3.3			1.1	1.4	1.5	1.5	1.5
Cm^{245}	30.9	12.2	15.3	15.6	17.7	19.0	19.6	19.9	20.1	20.8

TABLE 4.5

Parameters RES and FAST as a Function of Burnup

Time	0 days	1Y	2Y	3Y	4Y	5Y	6Y	7Y	8Y	10Y
RES	0.0533	0.0888	0.121	0.163	0.186	0.189	0.188	0.185	0.182	0.178
FAST	2.29	4.04	5.79	8.82	10.79	11.52	11.56	11.42	11.24	11.01

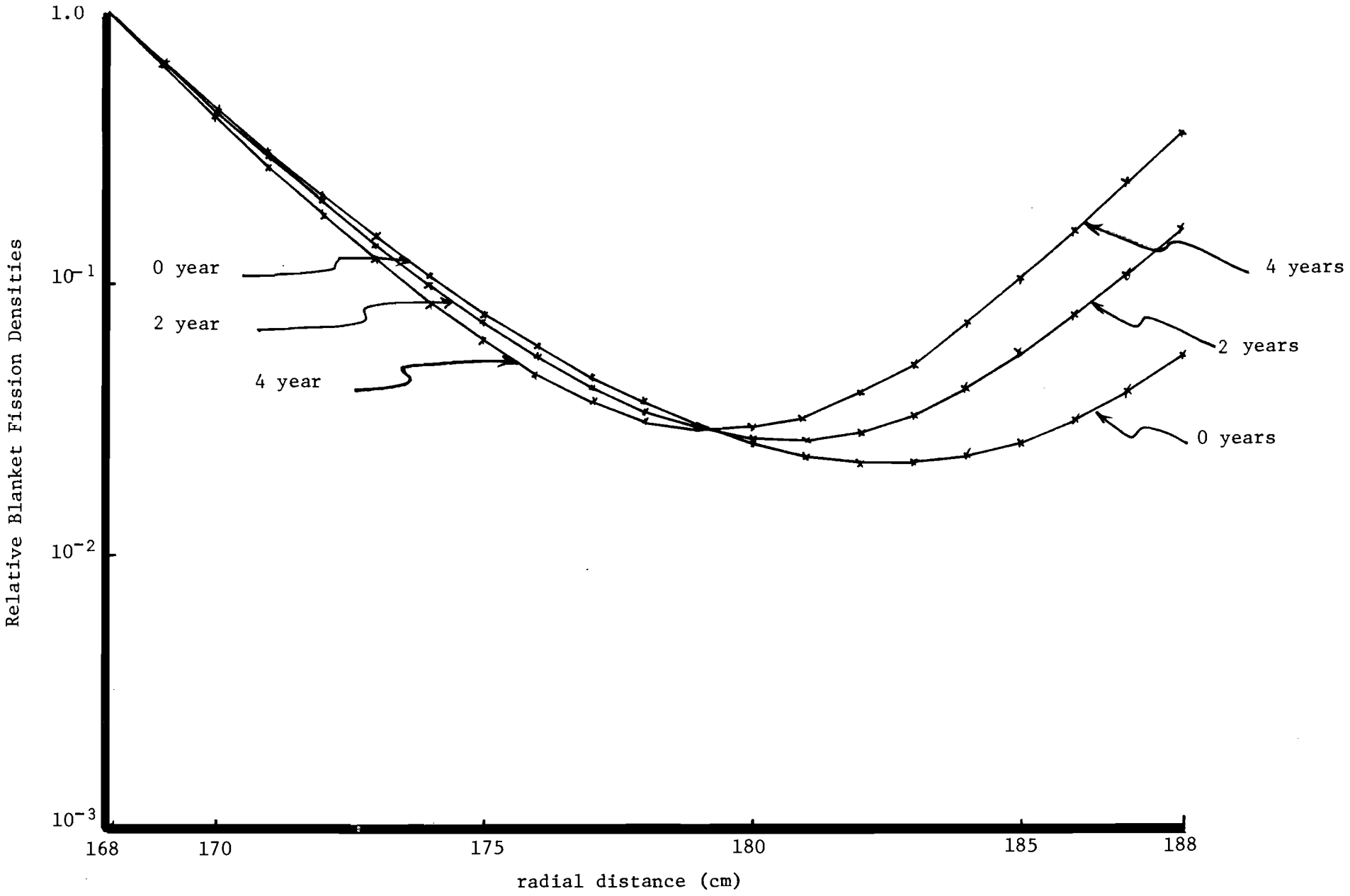

Fig. 4.3. Relative Blanket Fission Densities as a Function of Radial Distance at Different Times

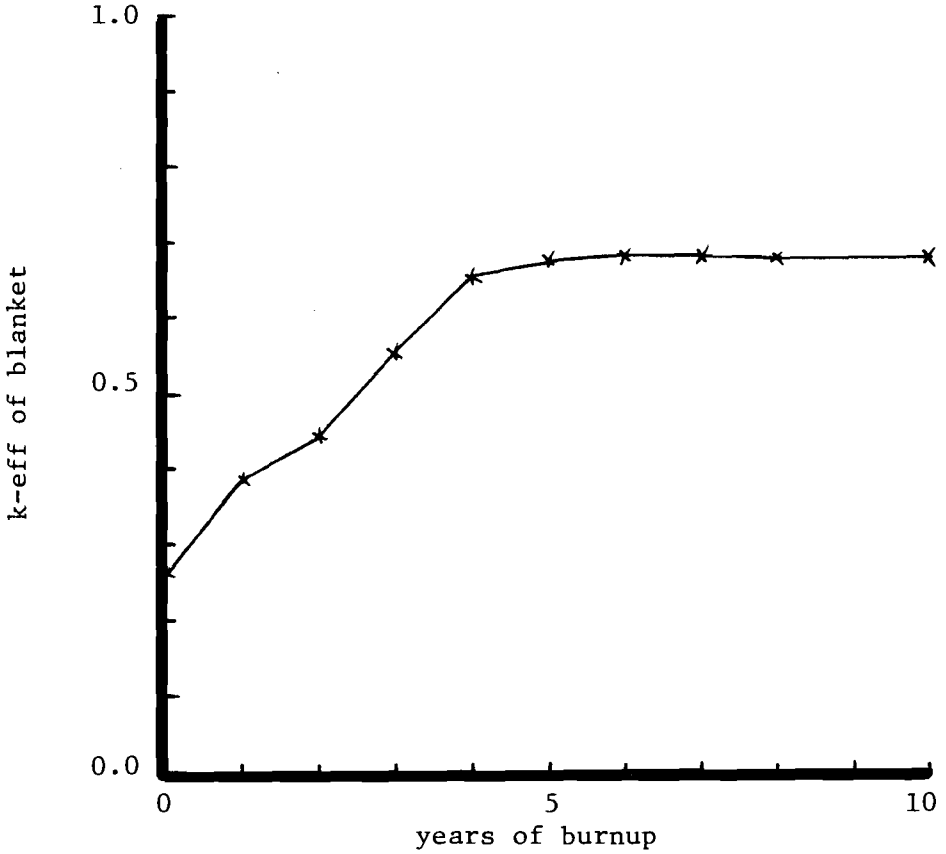

Fig. 4.4. Effective Multiplication of Blanket as a Function of Burnup Time.

blanket is calculated by MACH-1. Figure 4.4 is a plot of k_{eff} as a function of burnup time. At the beginning of life, the blanket is grossly subcritical with an effective multiplication constant of 0.26. At 5 years, the effective multiplication constant has risen to 0.68. At this point, blanket power is 1600 MWt and blanket criticality is suppressed by the addition of poor quality fresh actinide feed. It is conceivable that the blanket may become critical by itself.

Actinide Production in Core

A basic requirement of all transmutation schemes is that the quantity of actinides produced by the transmutation system must be less than the quantity of actinides that are destroyed. For the gas core reactor systems, actinides are produced by the capture reaction of U^{233}. Table 4.6 shows the capture-to-fission ratio as a function burnup. Taking a maximum capture-to-fission ratio of 0.013, and a core power of 2000 MWt, actinides production rate is 8.11×10^{17} atoms/sec. To take care of this quantity of actinides, assuming 200 MeV per fission, a power of 26 MWt is required. That is, the blanket power must be greater than 26 MWt in order for the reactor system to destroy actinides at a rate higher than their production rate in the core. For the UFATR, this requirement is met with little difficulty.

TABLE 4.6

Alpha (capture-to-fission ratio) of U^{233} as a Function of Actinide Burnup.

Time	0 Y	1 Y	2 Y	3 Y	4 Y	5 Y	6 Y	7 Y	8 Y	10 Y
Alpha	0.013	0.012	0.012	0.012	0.012	0.011	0.011	0.011	0.011	0.011

References for Chapter 4

1. Mann, F. M. and Schenter, R. E., "Actinide Cross-Section Calculations and Evaluations," Trans. Am. Nucl. Soc., 23, 546-547 (1976).

2. Morrison, G. W., Burns, T. J. and Weisbin," Actinide Transmutation: Cross Sections Methods, and Reactor Sensitivity Analysis," Trans. Am. Nucl. Soc., 23, 552 (1976),

3. Raman, S., "General Survey of Applications Which Require Actinide Nuclear Data," Proc. IAEA Advisory Group Mtg. Transactinium Isotope Nuclear Data, CONF - 751104 - 4, Review Paper A1 (1975).

4. Kusters, H. and Lalovic, M., "Review of Transactinium Isotope Build-Up and Decay in Reactor Fuel and Related Sensitivities to Cross-Section Changes and Results and Main Conclusions of the IAEA - Advisory Group Mfg. on Transactinium Nuclear Data Held at Karlsruhe, November, 1975," KFK-2283 (1976).

5. Yiftah, S., Gur, Y. and Caner, M., "Status of Transactinium Isotope Evaluated Nuclear Data in the Energy Range 10^{-3} eV to 15 MeV," IAEA-186, 165-194 (1976).

6. Dabbs, J. W. T., "The Nuclear Fuel Cycle and Actinide Wastes: Cross Section Needs and Recent Measurements," ORNL/TM - 5530 (1976).

7. Mann, F. M. and Schenter, R. E., "Actinide Cross Section Calculations and Evaluations," HEDL-SA-814 (1976).

8. Graves, W. E. and Benjamin, R. W., "Predicting Production Rates of Heavy Actinides," CONF-720901, 97-107 (1972).

9. Hennelly, E. J., "The Heavy Actinide Cross Section Story," CONF-710301, 2, 494-501.

10. Benjamin, R. W., McCrosson, F. J., Gorrell, T. C. and Vandervelde, V. D., "A Consistent Set of Heavy Actinide Multigroup Cross Sections," DP-1394 (1975).

11. Benjamin, R. W., "Status of Measured Neutron Cross sections of Transactinium Isotopes for Thermal Reactors," DP-MS-75-87 (1975).

12. Hennelley, E. J., "Nuclear Data for Actinide Recycle," Natl. Bur. Stands. Spec. Publ., CONF-750303-P1 (Oct., 1975).

13. Bell, M. J., "ORIGEN - The ORNL Isotope Generations and Depletion Code," ORNL-4628 (May, 1973).

14. Westcott, C. H., "Effective Cross Section Values for Well-Moderated Thermal Reactor Spectra," CRRP-787 (August, 1958).

15. Berwald, D. H., "Preliminary Design and Neutronic Analysis of a Laser Fusion Driven Actinide Waste Burning Hybrid Reactor," Ph. D. Thesis, Dept. of Nuclear Engineering, U. of Michigan (1977).

CONCLUSIONS AND RECOMMENDATIONS

Preliminary design and analysis of a uranium hexafluoride actinide transmutation reactor (UFATR) is performed. The purpose of this reactor is to convert long-lived actinide wastes to shorter-lived fission product wastes.

It is demonstrated that externally moderated gas core reactors are ideal irradiators. They provide an abundant supply of thermal neutrons and are insensitive to composition changes in the blanket.

For the present UFATR, an initial load of 6 metric tonnes of actinides is loaded. This is equivalent to the quantity produced by 300 LWR-years of operation. Initially, the core produces 2000 MWt and the blanket 239 MWt. After 4 years of irradiation, the actinide mass is reduced to 3.9 metric tonnes. With continuous actinide refueling, the actinide inventory is held constant and equilibrium essentially achieved at the end of 8 years. At equilibrium, the core produces about 1400 MWt and the blanket 1600 MWt. At this power level, the actinide destruction rate is equal to the production rate from 32 LWRs.

Recommendations

To further evaluate the UFATR, more design and research work is required in several areas. To be able to transmute actinides effectively, they must be extracted from bulk waste at high efficiencies. Research work on the chemical reprocessing of actinides is needed. The accuracy of actinide depletion calculations is strongly dependent on the precision of actinide cross sections. In particular, the americium and curium cross sections are very significant in determining blanket neutronic

characteristics. Detailed differential cross section measurements are required. The actinide fuel management strategy adopted for the present study is one of many possible ones. Future work should concentrate on defining a strategy that will optimize actinide burnup performance. For the present design, a maximum blanket effective multiplication constant of 0.68 is attained. It is conceivable that the blanket can become critical by itself. To complete the system design of the UFATR, more work is required in the areas of heat transfer and fluid flow of the UF_6-He fuel and liquid bismuth-actinide solution (or slurry). Additional work is required in the continuous reprocessing and refueling of the UF_6-He fuel and liquid bismuth-actinide solution (or slurry).

Appendix A Reprocessing Systems

No quantitative analysis was made of the reprocessing systems for the UF_6 breeder and actinide transmutation reactors. However, since the reprocessing systems are important to the operation of the power plants, a qualitative discussion is included in this study which is based on proposed systems given in Refs. 1 and 2. Although these studies were preliminary in nature, they did not encounter major obstacles.

There are two major reprocessing systems to be considered. The first is the cleanup of fission products in the UF_6-helium mixture. The second is the extraction of the actinides from other waste products to be used in the actinide transmutation reactor. These systems will be described in the following sections.

A.1 Fission Product Cleanup

Fission products must be removed from the UF_6-helium mixture continuously to avoid buildup of reactor poisons and condensation of volatiles. Fortunately, the technology for UF_6 separation and purification is available from the Molten Salt Breeder Reactor Program at Oak Ridge National Laboratory and helium purification technology is available from the High Temperature Gas Cooled Reactor developed by General Atomics.

It is expected that some UF_6 will dissociate in the core and that the fluorine formed will combine with metallic fission products to form fluorides. According to Ref. 1, the fluorides and gases in Table A.1 will be formed. The fluorides are divided into volatile, mobile, intermediate and refractory fluorides according to their boiling points. The mole fractions of the fission product gases, volatile fluorides, and mobile fluorides are on the order of 10^{-5} less than the mole fraction

TABLE A.1

Gaseous and Fluoride Fission Products[1]

Gases	Volatile Fluorides	Mobile Fluorides	Intermediate Fluorides	Refractory Fluorides
Kr	SeF_6 (236°K)*	SbF_5 (423°K)	Cs F (1524°K)	RaF_2 (2410°K)
Xe	MoF_6 (308°K)	NbF_5 (509°K)	Rb F (1663°K)	YF_3 (2500°K)
I	TeF_6 (309°K)	RuF_5 (523°K)		CeF_3 (2573°K)
Br		ZrF_5 (873°K)		NdF_3 (2573°K)
		SuF_4 (978°K)		PrF_4 (2600°K)
				LaF_3 (2600°K)
				SrF_2 (2762°K)

*numbers in parantheses are the boiling points of the various fluorides

of helium while the mole fractions of the intermediate and refractory fluorides are 10^{-3} less than the other fluorides.

Due to their low boiling points, the volatile and some of the mobile fluorides will remain in the UF_6-helium circulating gas loop until they are removed for reprocessing. The other fluorides will be deposited in the heat exchangers and piping. The problem is further complicated by radioactive decay of various species, resulting in a change of their chemical nature and the relocation of their deposition sites.

Reference 1 suggests that replaceable getter pads made of nickel wire be placed in the reactor outlet piping to capture the intermediate and refractory fluorides.

Lowry[1] of the Los Alamos Scientific Laboratory proposed the fission product cleanup system shown in Fig. A.1. A small amount of UF_6-helium gas mixture is bled from the circulating loop and is reduced in pressure to 1.5 atmospheres. The mixture then passes into a high temperature bed of NaF pellets at $500^{o}K$ where most of the volatile fluorides are absorbed and is cooled to $300^{o}K$ before entering a low temperature bed of NaF pellets. The low temperature bed absorbs the UF_6 and remaining metal fluorides while the helium containing xenon, krypton, bromine, iodine and other gases pass through the filter to the helium purification system.

Two low temperature beds are utilized. When one bed becomes loaded with UF_6, the flow into this bed is valved out and the fresh bed is placed in service. The bed loaded with UF_6 is then heated to $700^{o}K$ which drives off UF_6 as a gas along with small amounts of TeF_6. A helium purge gas is used to help remove the UF_6. Finally, the UF_6 passes through a

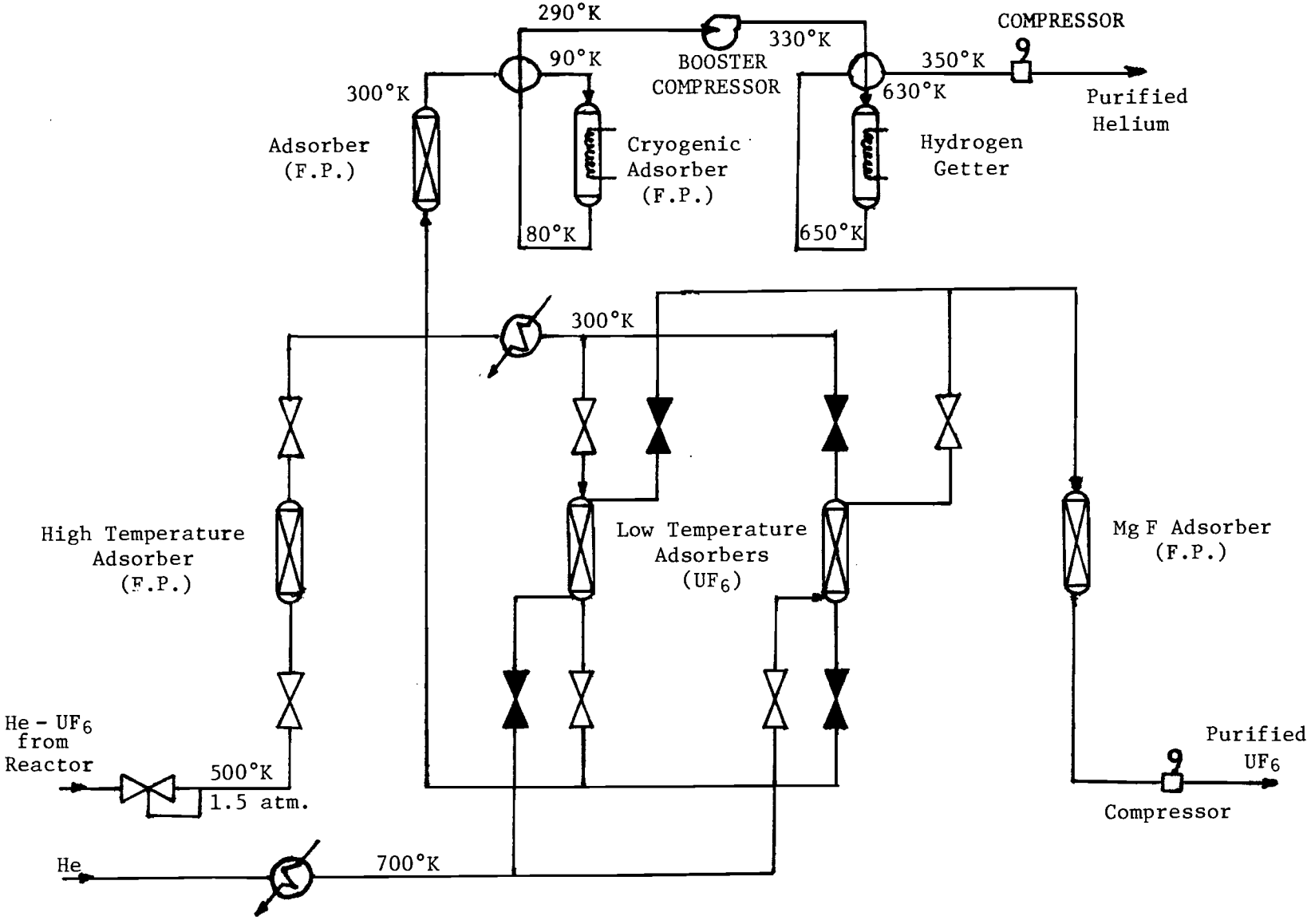

Fig. A.1 Fission Product Removal System[1]

bed of MgF_2 to remove the TeF_6 before being filtered, pressurized, and cooled to produce a purified liquid which is recycled to the reactor. The NaF and MgF_2 beds containing fission products are either stored or sent to a waste treatment plant.

Helium at 300°K flows into one of two parallel systems consisting of high and low temperature charcoal absorbers. The high temperature absorber contains activated charcoal impregnated with potassium. The charcoal removes the condensable metallic fission products while the potassium removes iodine by chemisorption.

The helium is then cooled to 90°K in a helium regenerator and passes through the low temperature absorber which removes krypton, xenon, nitrogen, and some hydrogen and tritium. Helium is cooled in the absorber to 80°K by liquid nitrogen. The purified helium then enters the cold side of the regenerator where it is heated to 290°K and is filtered to remove dust before being compressed and sent to the hydrogen removal section.

Helium leaving the compressor enters another regenerator before passing through one of two parallel hydrogen getters consisting of titanium sponges to remove hydrogen and tritium. Helium enters the getters at 630°K and is heated by the electrically heated sponges to 650°K. The helium then reenters the regenerator and is cooled to 350°K, filtered and recompressed.

The uranium inventory in the reprocessing system is not a function of reactor power but of regeneration frequency and volume of the NaF bed.

Distillation[1] is an alternative method for fission product removal especially if a large part of the primary stream must be cleaned up. The bled stream enters a distillation column where most of the fluorides are

removed as a concentrate at the bottom of the column. An aqueous wash removes the fluorides from the concentrate and residual UF_6 is returned to the column for further purification. The UF_6 and volatile fluorides are condensed and fed to a second column which produces pure UF_6 at the bottom of the column.

Another method for UF_6 purification is a combination of a cold trap process and fluoride volatility process proposed by Rust and Clement.[2]

Clearly, there are several possible methods for UF_6 purification. The method that will be selected should be based on consideration of economics, minimum uranium inventory, effectiveness in keeping the system as clean as possible, and compatibility with power plant operation.

A.2 Actinide Reprocessing System

Because of the hazardous radionuclides present in high-level wastes from present day reactors, schemes are needed which provide waste management programs of one million years or longer.

One alternative to this would be to remove the long-lived actinides which require long term surveillance. If this could be achieved, the remaining fission products and wastes would require a waste management program on the order of 1000 years. The actinides would then be transmuted in a fission or other type reactor to reduce the long half-lives to short ones, and thus reduce the radioactive hazard. The main problem to be overcome is separation of actinides from the rest of the waste products.

With the assumption that this separation can be done, an investigation was made to determine the necessary separation factors. The study indicated

that separations beyond certain limits may not yield enough to substantiate such separation factors. The separations of 99.99% for plutonium, 99.9% for uranium, americium and curium, and 99% for neptunium will reduce the hazard potential to about five percent of that for natural uranium.[3] After 99.9% removal of iodine, it will then be the long-lived remaining fission products which control the waste hazard. Higher removal factors for the actinides do not appear to be warranted unless long-lived fission products are also removed, especially Tc-99.

As means of recovering actinides from the spent waste, several schemes are available. Several schemes can be ruled out mainly due to expense and complexity. For example, a centrifuge is too "dirty" because of associated alpha emitters from the actinides.[4] This would require tight contamination control, and hence much shielding. Other processes require a gaseous form, but there are no gaseous forms of americium or curium.

Present feasibility studies indicate that separations based on solvent extraction, ion exchange, and scavenging precipitation have greatest possibilities. Solvent extraction by itself has not been shown to achieve desired results; however, multi-step solvent extraction processes have a greater probability of success.[5] If particular waste stream recycles solved, processes based on cation exchange may be a viable method for partitioning the actinides. Another method with potential in waste partitioning may be precipitation.

Figure A.2 illustrates the reprocessing scheme for fission products and actinides generated from Light Water Reactors. Spent fuel from LWRs

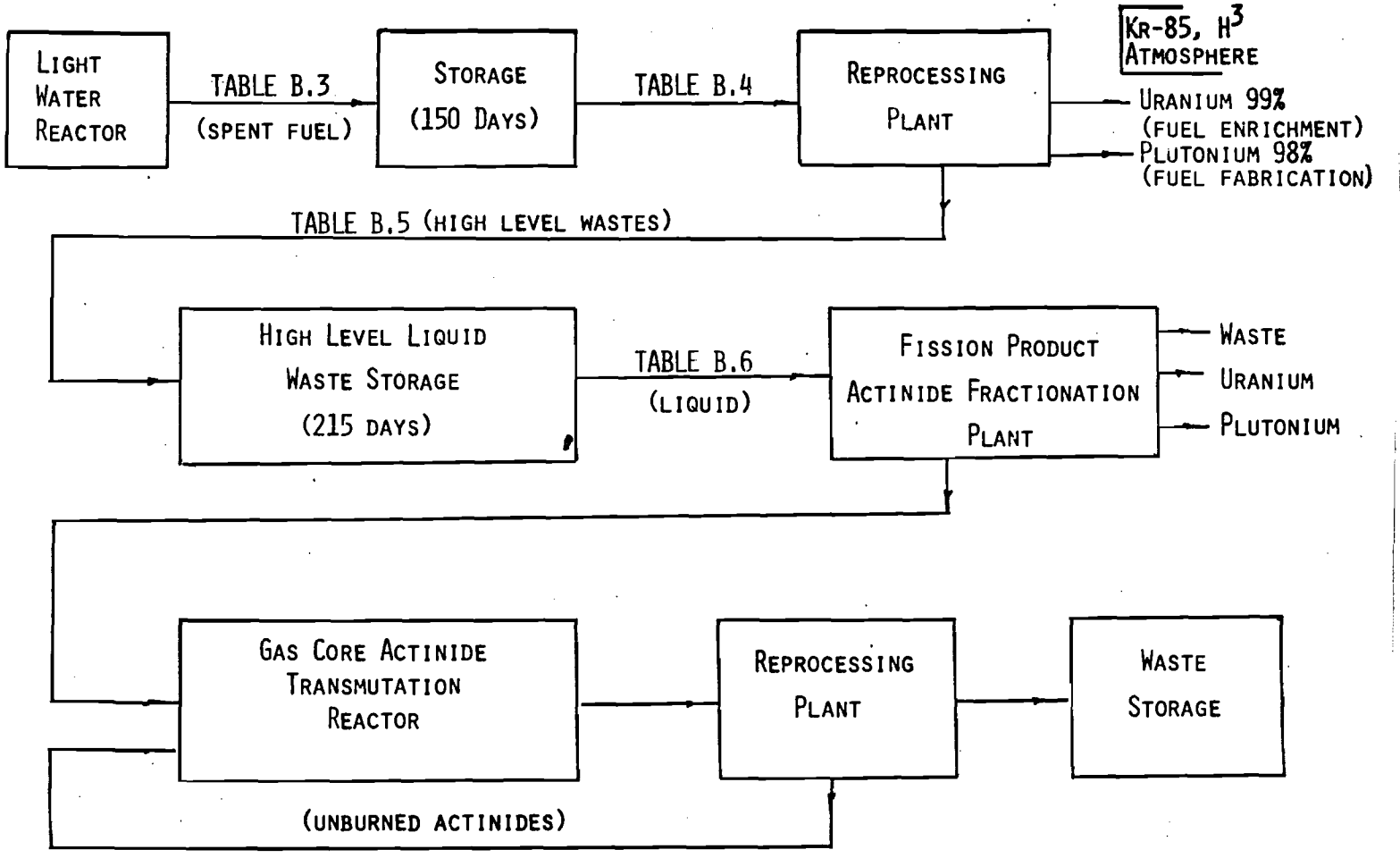

Fig. A.2 Actinide Reprocessing Scheme

containing fission products and actinides listed in Table A.2 is sent to storage for about 150 days. The wastes from storage, which is listed in Table A.3, is then sent to a reprocessing plant. This plant discharges Kr-85 and tritium to the air. Ninety nine percent of the uranium is removed from the waste and sent for enrichment and 98 percent of the plutonium is separated for further fuel fabrication.

The rest of the high-level waste goes to a high-level liquid waste storage for about 215 days. These high-level wastes are listed in Table A.4. After further storage these wastes (listed in Table A.5) go to a fission product/actinide fractionation plant.

Fractionation Schemes

Studies to date indicate that the best methods for removing actinides from wastes will be obtained by improving present state-of-the-art methods.[6] One of the present schemes is shown in the Fig. A.3. In this scheme, neptunium, uranium, and plutonium, are recovered in the primary PUREX plant. Various exhaustive extractions or further PUREX processes are used to accomplish complete removal of the neptunium, plutonium, and uranium. Through the PUREX plant process, a recovery rate of 95-99% for neptunium and improvements in uranium and plutonium recovery to 99.5% or better are expected.[7]

The interim waste storage is for the purpose of reducing the radiation hazard from the remaining high level wastes during subsequent processing. The radiation hazard will be high unless the fission product yttrium and rare earths, which are associated with americium and curium, are allowed to

TABLE A.2

FISSION PRODUCT AND ACTINIDE CONCENTRATIONS LEAVING A LWR

PWR FUEL CYCLE - DECAY TIMES OF FUEL DURING COOLING PERIOD
POWER= 30.00MW, BURNUP= 33000.MWD, FLUX= 2.92E+13N/CM**2-SEC
NUCLIDE INGESTION HAZARD, M**3 OF WATER AT RCG
BASIS = PER METRIC TONNE OF U LOADED IN REAC

Actinides

	DISCHARGE
PB212	7.50E+01
BI212	3.75E+00
RA223	1.27E+00
RA224	7.50E+02
TH228	2.13E+02
TH230	8.88E+00
TH231	3.36E+03
TH234	1.57E+04
PA231	2.71E+01
PA233	3.24E+03
PA234M	1.60E+01
PA234	6.52E+01
U232	2.00E+02
U233	1.52E+00
U234	2.55E+04
U235	5.70E+02
U236	9.61E+03
U237	8.65E+19
U238	7.85E+03
NP237	1.11E+05
NP239	1.85E+11
PU236	1.17E+04
PU238	6.34E+08
PU239	9.36E+07
PU240	9.55E+07
PU241	3.25E+08
PU242	2.76E+05
AM241	2.15E+07
AM242M	2.29E+06
AM242	6.34E+08
AM243	4.54E+06
CM242	1.67E+09
CM243	7.42E+05
CM244	3.49E+08
CM245	8.34E+04
CM246	1.71E+04
CM248	1.98E+00
BK249	8.96E+00
CF250	3.78E+00
CF252	2.55E+00
SUBTOT	1.93E+11
TOTALS	2.16E+11

Fission Products

	DISCHARGE
H 3	2.36E+05
KR 85	1.13E+04
RB 86	2.47E+07
SR 89	2.39E+11
SR 90	2.59E+11
Y 90	4.03E+09
Y 91	3.13E+10
ZR 93	2.36E+03
NB 93M	5.61E+02
ZR 95	2.29E+10
NB 95M	2.80E+04
NB 95	1.38E+10
MO 99	3.81E+10
TC 99	7.14E+04
RU103	1.52E+10
RH103M	1.22E+08
RU106	5.45E+10
RH106	7.40E+05
PD107	1.10E+02
AG110M	1.23E+08
AG111	1.59E+05
AG112	9.90E+08
CD113M	1.05E+01
IN114M	7.75E+04
CD115M	1.84E+07
SN119M	1.64E+01
SN123	8.88E+03
SB124	2.03E+07
SN125	6.76E+08
SB125	8.70E+07
TE125M	3.11E+07
TE127M	3.07E+08
TE127	3.60E+08
TE129M	2.86E+09
TE129	4.21E+08
I129	6.18E+05
I131	2.87E+12
XE131M	6.39E+03
TE132	5.92E+10
I132	1.53E+11
XE133	1.61E+06
CS134	2.74E+10
CS135	2.86E+03
CS136	1.01E+09
CS137	5.39E+09
BA137M	1.01E+05
BA140	7.27E+10
LA140	7.50E+10
CE141	1.54E+10
PR143	2.41E+10
CE144	1.11E+11
PR144	1.12E+06
ND147	9.81E+09
PM147	5.12E+08
PM148M	3.89E+04
PM148	1.99E+05
SM151	3.12E+06
EU152	1.57E+05
GD153	1.78E+05
EU154	3.49E+08
EU155	3.74E+07
EU156	6.26E+05
TB160	3.21E+07
SUBTOT	4.11E+12
TOTALS	6.40E+12

TABLE A.3

FISSION PRODUCT AND ACTINIDE CONCENTRATIONS AFTER 150 DAYS STORAGE

PWR FUEL CYCLE - DECAY TIMES OF FUEL DURING COOLING PERIOD
POWER= 30.00MW, BURNUP= 33000.MWD, FLUX= 2.92E+13N/CM**2-SEC
NUCLIDE INGESTION HAZARD, M**3 OF WATER AT RCG
BASIS = PER METRIC TONNE OF U LOADED IN REAC

Actinides

	150. D
PB212	1.10E+02
BI212	5.49E+00
RA223	1.70E+00
RA224	1.10E+03
TH223	3.18E+02
TH230	1.02E+01
TH231	8.55E+01
TH234	1.57E+04
PA231	2.74E+01
PA233	3.40E+03
PA234M	1.57E+01
PA234	6.14E+00
U232	5.46E+02
U233	1.54E+00
U234	2.52E+04
U235	6.70E+02
U236	9.61E+03
U237	2.03E+04
U238	7.85E+03
NP237	1.13E+05
NP239	1.92E+05
PU236	1.06E+04
PU238	5.04E+08
PU239	6.46E+07
PU240	9.53E+07
PU241	5.15E+08
PU242	2.75E+05
AM241	3.85E+07
AM242M	2.29E+06
AM242	9.13E+04
AM243	4.34E+06
CM242	8.38E+08
CM243	7.66E+05
CM244	3.44E+08
CM245	8.54E+04
CM246	1.71E+04
CM248	1.98E+00
BK249	6.54E+00
CF250	3.03E+00
CF252	2.06E+00
SUBTOT	2.52E+09
TOTALS	2.52E+09

Fission Products

	150. D
H 3	2.31E+05
KR 85	1.10E+04
RB 86	9.49E+04
SR 89	3.24E+10
SR 90	2.56E+11
Y 90	3.84E+09
Y 91	5.37E+09
ZR 93	2.36E+03
NB 93M	4.52E+02
ZR 95	4.62E+09
NB 95M	3.88E+03
NB 95	5.29E+04
MO 99	2.55E-06
TC 99	7.17E+04
RU103	1.10E+09
RH103M	8.83E+06
RU106	4.10E+10
RH106	4.10E+05
PD107	1.10E+02
AG110M	3.14E+07
AG110	3.17E+02
AG111	3.47E+02
CD113M	1.03E+01
IN114M	9.69E+03
CD115M	1.04E+06
SN119M	1.08E+01
SN123	3.86E+03
SB124	3.59E+05
SN125	1.06E+04
SB125	7.95E+07
TE125M	3.29E+07
TE127M	1.25E+08
TE127	3.04E+07
TE129M	1.65E+08
TE129	3.17E+06
I129	6.23E+05
I131	7.28E+05
XE131M	3.19E+00
TE132	7.97E-04
I132	1.95E-03
XE133	5.35E-03
CS134	2.58E+10
CS135	2.36E+03
CS136	3.41E+05
CS137	5.04E+09
BA137M	9.99E+04
BA140	2.16E+07
LA140	2.48E+07
CE141	6.27E+08
PR143	1.36E+07
CE144	7.71E+10
PR144	7.71E+05
ND147	8.39E+05
PM147	4.30E+08
PM148M	3.27E+07
PM148	2.63E+06
SM151	3.42E+05
EU152	1.93E+05
GD153	1.11E+05
EU154	5.43E+08
EU155	5.20E+07
EU156	2.01E+02
TB160	7.58E+06
SUBTOT	4.58E+11
TOTALS	4.58E+11

TABLE A.4

FISSION PRODUCT AND ACTINIDE CONCENTRATIONS EXITING FROM THE REPROCESSING PLANT

PWR FUEL CYCLE DECAY TIMES OF FUEL AFTER 1ST PROCESSING
POWER= 30.00MW, BURNUP= 33000.MWD, FLUX= 2.92E+13N/CM**-SEC
NUCLIDE INGESTION HAZARD, M**3 OF WATER AT RCG
BASIS = PER METRIC TONNE OF U LOADED IN REAC

Actinides

	DISCHARGE
PB212	1.10E+02
BI212	5.49E+00
RA223	1.70E+00
RA224	1.10E+03
TH228	3.18E+02
TH230	1.02E+01
TH234	1.57E+04
PA231	2.74E+01
PA233	3.40E+03
U232	2.46E+00
U234	2.52E+02
U235	5.70E+00
U236	9.61E+01
U237	2.65E+02
U238	7.85E+01
NP237	1.13E+05
NP239	1.82E+05
PU236	2.12E+02
PU238	1.13E+07
PU239	1.29E+06
PU240	1.91E+06
PU241	1.03E+07
PU242	5.52E+03
AM241	3.85E+07
AM242M	2.29E+06
AM242	9.15E+04
AM243	4.54E+06
CM242	8.88E+08
CM243	7.36E+05
CM244	3.44E+08
CM245	8.54E+04
CM246	1.71E+04
CM248	1.98E+00
BK249	6.44E+00
CF249	8.96E-01
CF251	3.69E+00
CF252	2.26E+00
SUBTOT	1.30E+09
TOTALS	1.30E+09

Fission Products

	DISCHARGE
H 3	2.31E+05
KR 85	1.10E+04
RB 86	9.49E+04
SR 89	8.24E+10
SR 90	2.56E+11
Y 90	3.84E+09
Y 91	5.37E+09
ZR 93	2.36E+03
NB 93M	4.52E+02
ZR 95	4.62E+09
NB 95M	5.88E+03
NB 95	5.20E+09
TC 99	7.17E+04
RU103	1.10E+09
RH103M	8.83E+06
RU106	4.10E+10
RH106	4.10E+05
PD107	1.10E+02
AG110M	8.14E+07
AG110	8.17E+02
CD113M	1.43E+01
IN114M	9.59E+03
CD115M	1.64E+06
SN119M	1.08E+01
SN123	5.36E+03
SB124	3.59E+06
SB125	7.95E+07
TE125M	3.20E+07
TE127M	1.23E+08
TE127	5.04E+07
TE129M	1.35E+08
TE129	2.17E+06
I129	6.23E+05
I131	7.28E+06
CS134	2.08E+10
CS135	2.69E+03
CS136	3.41E+05
CS137	5.34E+09
BA137M	9.99E+04
BA140	2.16E+07
LA140	2.48E+07
CE141	6.27E+08
PR143	1.36E+07
CE144	7.71E+10
PR144	7.71E+05
ND147	8.09E+05
PM147	4.90E+08
PM148M	3.07E+03
PM148	2.63E+02
SM151	3.12E+06
EU152	1.53E+05
GD153	1.16E+05
EU154	3.43E+08
EU155	3.20E+07
TB160	7.93E+06
SUBTOT	4.58E+11
TOTALS	4.58E+11

TABLE A.5

FISSION PRODUCT AND ACTINIDE CONCENTRATIONS AFTER 215 DAYS
STORAGE IN HIGH LEVEL LIQUID WASTE STORAGE FACILITY

PWR FUEL CYCLE DECAY TIMES OF FUEL AFTER 1ST PROCESSING
POWER= 30.00MW, BURNUP= 33000.MWD, FLUX= 2.92E+13N/CM**2-SEC
NUCLIDE INGESTION HAZARD, M**3 OF WATER AT RCG
BASIS = PER METRIC TONNE OF U LOADED IN REAC

Actinides

	CHARGE	215. D
PB212	0.	9.11E+01
BI212	0.	4.55E+00
RA223	0.	2.33E+00
RA224	0.	9.11E+02
TH228	0.	2.59E+02
TH230	0.	1.02E+01
TH234	0.	1.89E+02
PA231	0.	2.74E+01
PA233	0.	3.40E+03
U232	0.	3.56E+00
U234	5.45E+04	2.56E+02
U235	2.36E+03	5.70E+00
U236	0.	9.61E+01
U237	0.	4.81E+02
U238	8.05E+03	7.85E+01
NP237	0.	1.13E+05
NP239	0.	1.82E+05
PU236	0.	1.84E+02
PU238	0.	2.19E+07
PU239	0.	1.29E+06
PU240	0.	1.94E+06
PU241	0.	1.00E+07
PU242	0.	5.52E+03
AM241	0.	3.90E+07
AM242M	0.	2.28E+06
AM242	0.	9.12E+04
AM243	0.	4.54E+06
CM242	0.	3.56E+08
CM243	0.	7.26E+05
CM244	0.	3.36E+08
CM245	0.	8.54E+04
CM246	0.	1.71E+04
CM248	0.	1.98E+00
BK249	0.	4.01E+00
CF249	0.	1.49E+00
CF250	0.	3.58E+00
CF252	0.	1.94E+00
SUBTOT	6.50E+04	7.74E+08
TOTALS	6.50E+04	7.74E+08

Fission Products

	215. D
H 3	2.23E+05
KR 85	1.06E+04
RB 86	3.28E+01
SR 89	1.84E+09
SR 90	2.52E+11
Y 90	3.79E+09
Y 91	4.26E+08
ZR 93	2.36E+03
NB 93M	5.78E+02
ZR 95	4.67E+08
NB 95M	5.94E+02
NB 95	5.96E+08
TC 99	7.17E+04
RU103	2.56E+07
RH103M	2.05E+05
RU106	2.73E+10
RH106	2.73E+05
PD107	1.10E+02
AG110M	4.51E+07
AG110	1.76E+02
CD113M	9.99E+00
IN114M	4.92E+02
CD115M	5.11E+04
SN119M	5.96E+00
SN123	1.17E+03
SB124	2.99E+05
SB125	6.83E+07
TE125M	2.83E+07
TE127M	3.13E+07
TE127	7.74E+06
TE129M	1.69E+06
TE129	2.71E+04
I129	6.24E+05
I131	6.64E-02
CS134	1.95E+10
CS135	2.86E+03
CS136	3.58E+00
CS137	5.27E+09
BA137M	9.85E+04
BA140	1.89E+02
LA140	2.18E+02
CE141	6.31E+06
PR143	2.56E+02
CE144	4.56E+10
PR144	4.56E+05
ND147	1.24E+00
PM147	4.19E+08
PM148M	9.40E+01
PM148	7.55E+00
SM151	3.11E+06
EU152	1.48E+05
GD153	6.25E+04
EU154	3.35E+08
EU155	2.55E+07
TB160	9.60E+05
SUBTOT	3.56E+11
TOTALS	3.56E+11

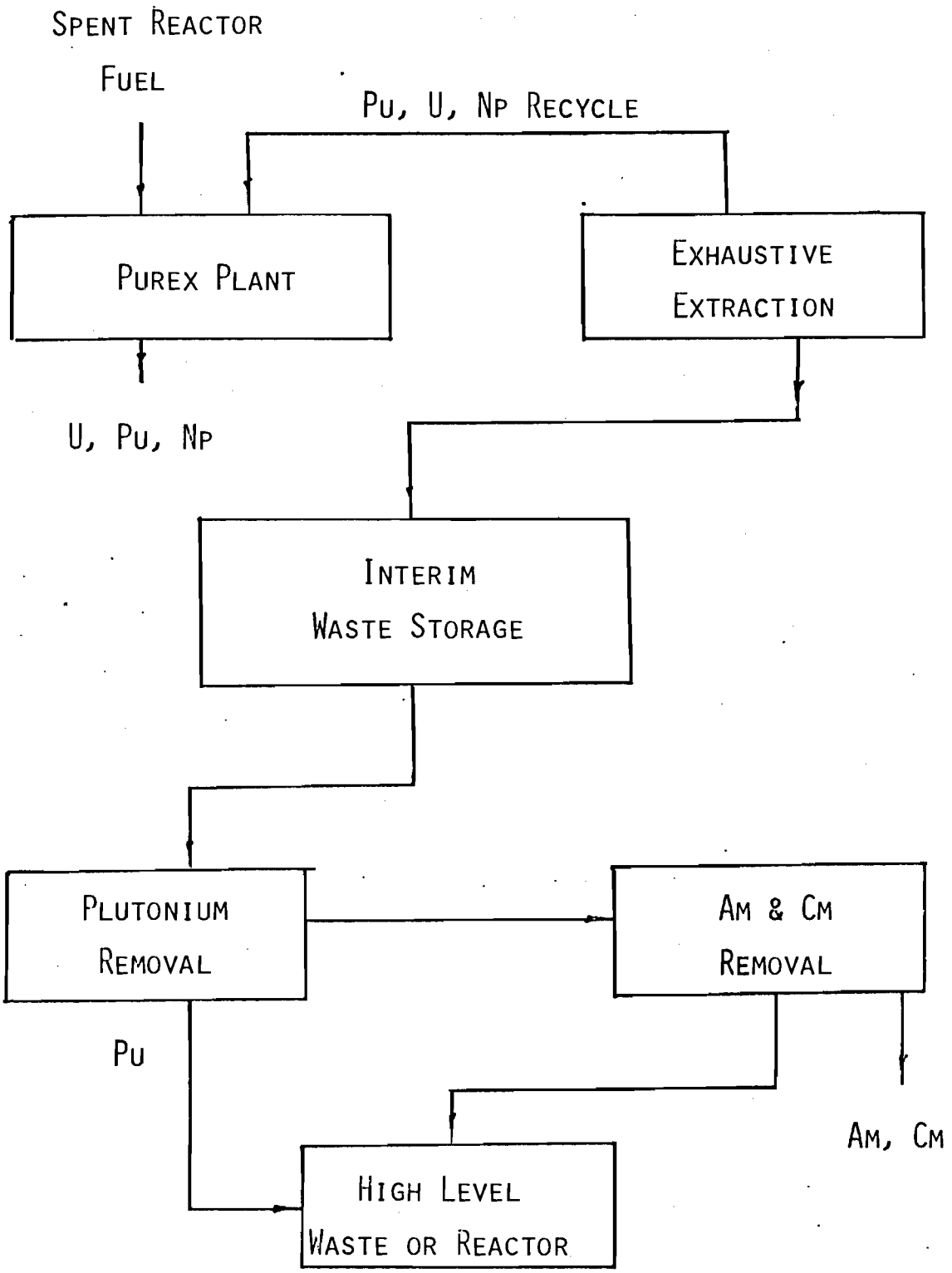

Fig. A.3 Present Processing Sequence for the Removal of Actinides

decay to less hazardous levels.[7] By considering the most important decay times, storage times of ten years would significantly reduce the hazards. Current NRC regulations require that wastes be solidified within five years. However, because of difficulties in working with a solid waste, it will be assumed that the americium and curium are removed from the liquid wastes after a five year period.

One disadvantage of interim waste storage is that the amount of plutonium in the waste grows by curium decay. Therefore, plutonium removal from the stored waste is necessary after several years of interim storage. The process showing most potential for recovering the plutonium is an all ion-exchange process.[8]

After removal of plutonium, the americium and curium are isolated from the rest of the waste. The problems associated with americium and curium removal are centered around finding a suitable chemical separation process for commercial high level wastes. Recovery of americium and curium has been done at the Oak Ridge National Laboratory and Savannah River Laboratory on a multigram basis using a Tramex process.[7] This process has problems with corrosive solutions that require processing equipment constructed of special and expensive materials. Because of these reasons, the process is not recommended. However, there is some possibility that the Tramex processing equipment can be constructed so as to allow safe working of both corrosive solution in the process and toxic radionuclides at little additional cost.

Other processes that have been developed and claim to give high americium and curium separation are Cation Exchange Chromatography (CEC)

and Trivalent Actinide-Lanthanide Separation by Phosphorous Reagent Extraction from Aqueous Complexes (TALSPEAK).[7] Cation Exchange Chromatography was developed at the Savannah River Laboratory and successfully used to separate about twenty-five percent of the necessary amounts of americium, curium, and rare earths in one metric ton of Light Water Reactor fuel.[7] A schematic flowsheet of CEC is shown in Fig. A.4. The TALSPEAK process, shown in Fig. A.5, has been developed only to the point of tracer-level laboratory studies at Karlsruhe for americium and curium removal.[7]

As means of separating Am and Cm from other wastes, the Tramex, CEC, and TALSPEAK processes require considerable developmental work and data gathering to determine their applicability to the commercial (high volume) extraction of actinides from high-level wastes.

Proposed Schemes

Present proposals for actinide partitioning are based on a sequence of separation processes using solvent extraction, ion exchange, and precipitation. These techniques have not yet been developed.[6] A multistep solvent extraction process combined with other processes, such as cation exchange, may work well in the removal of uranium, neptunium, and plutonium, as well as separations of americium and curium from other wastes.

Tributylphosphate (TBP) may be used as the solvent in the solvent extraction method.[6,9] As demonstrated in the PUREX process, TBP achieved highly efficient recovery of uranium, plutonium, and neptunium.[3]

As a means of separating americium and curium from the rest of fission products and wastes, two steps of cation exchange is quite promising. The potential here appears to be 99.9 percent or better.[6] In the first step

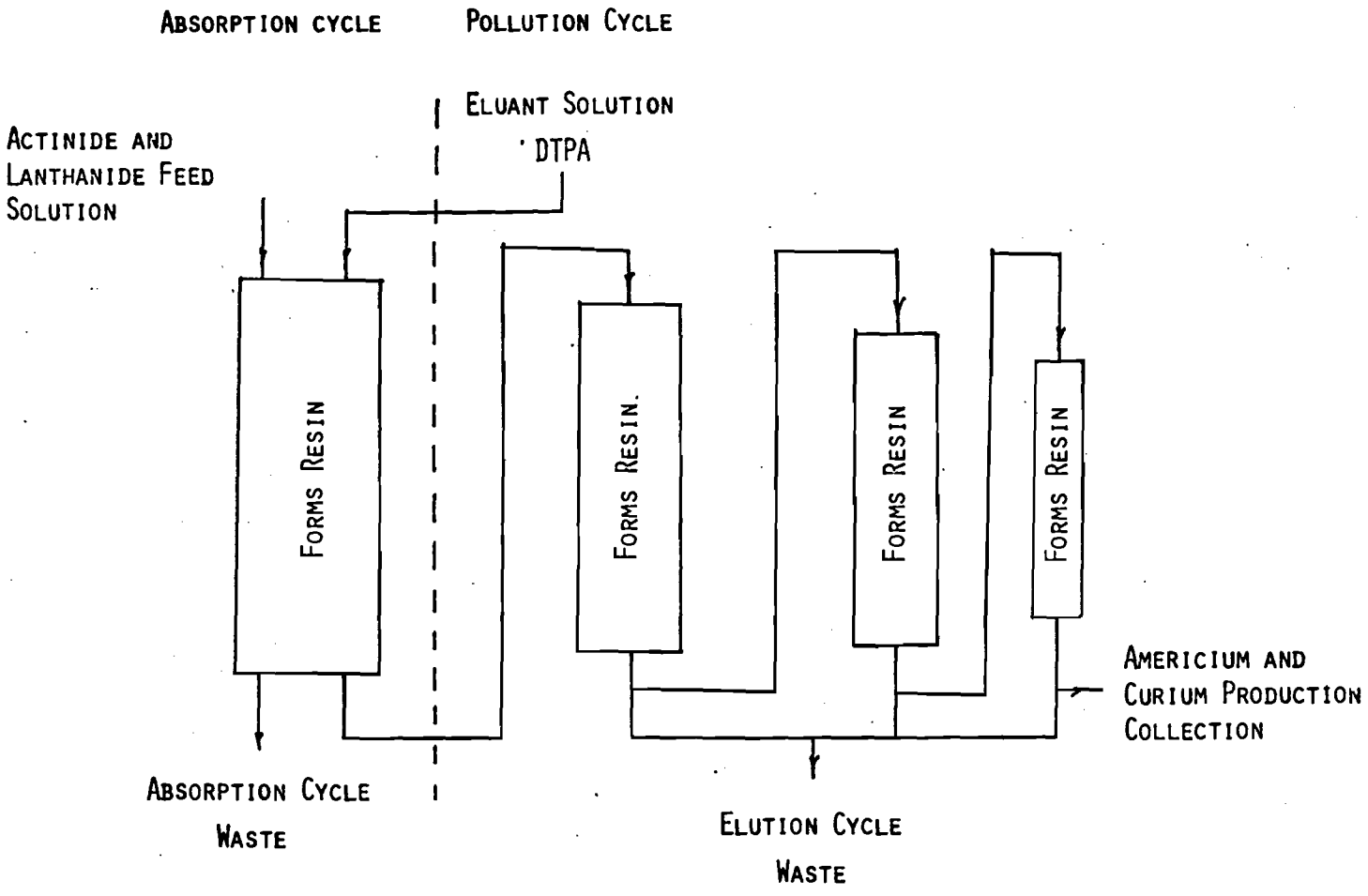

Fig. A.4 Schematic Flowsheet of Cation Exchange Chromatographic Process for Recovery of Americium and Curium[15]

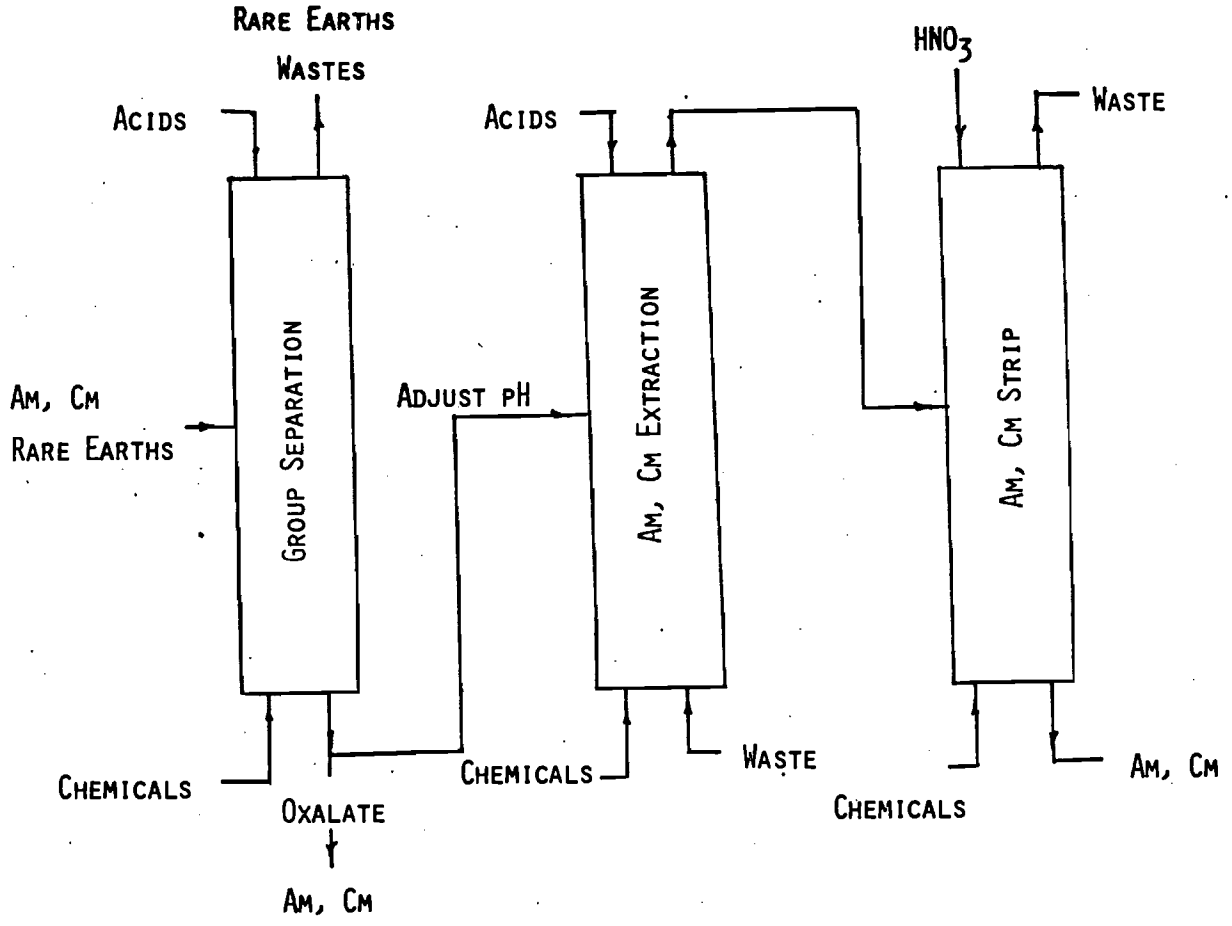

Fig. A.5 Conceptual Flow Sheet for Recovery of Americium and Curium by a TALSPEAK

the lanthanides and actinides are absorbed on a cation exchange resin column and eluted with nitric acid. In the following step the lanthanides and actinides are separated by cation exchange chromatography. Problems to be solved with this process are in converting the spent ion exchange resin to acceptable levels for waste generated in the chromatographic separation.

Precipitation methods combined with ion exchange and/or solvent extraction may be another possible method for partitioning actinides. Even though solid waste handling is unavoidable, ways are now under study for obtaining crude concentrations of plutonium, americium, curium, and fission products. These actinides would then be separated from the lanthanides in further ion exchange or solvent extraction steps. Oak Ridge National Laboratory is studying the use of oxalate[8] precipitation together with ion exchange to isolate the lanthanides and actinides.[6,11] A removal factor of 0.95 is achieved by precipitation while the remaining is removed in the cation exchange column.[7] Tracer-level studies indicate removal of 0.999 for americium and curium.[7] Almost complete removal has been demonstrated for americium and curium by use of multiple oxalate precipitation stages.[6] Further work in this area is still needed to determine the effect of the handling problems.

Technical feasibility, resultant benefits, and costs of partitioning actinides from high-level wastes are yet to be established. It must be decided if the net benefits will justify the use of partitioning. It must also be kept in mind that the separation schemes do not solve the long-term actinide problem. In order to justify this, the actinides

must somehow be transmuted to shorter-lived radionuclides or disposed of from our environment. These and many more problems still need research and investigation before a feasible actinide-separation-transmutation process can be substantiated.

From research done to date, it is concluded that much research and development is still needed in the area of actinide partitioning. Work being performed at the Oak Ridge National Laboratory may show encouraging results in the near future. Present state-of-the-art methods will not yield the results needed to establish a practical, economically feasible operating partitioning plant. It is believed that research in the area of combined methods of solvent extraction and ion exchange will yield the necessary separations factors.

References for Appendix A

1. Lowry, L. L., "Gas Core Reactor Power Plants Designed for Low Proliferation Potentials," LA-6900-MS (September, 1977).

2. Clement, J. D. and Rust, J. H., "Analysis of the Gas Core Actinide Transmutation Reactor (GCATR)," Annual Report, Georgia Institute of Technology, NASA Grant NSG-1288 (February, 1977).

3. Claiborne, H. C., "Effect of Actinide Removal on the Long Term Hazard of High-Level Waste," ORNL-TM-4724 (January, 1975).

4. Schneider, A., Georgia Institute of Technology, Personal consultation (April, 1976).

5. Bocola, W., Frittelli, L., Gera, F., Grossi, G., Moccia, A., and Tondinelli, L., "Considerations on Nuclear Transmutation for the Elimination of Actinides," IAEA-SM-207/86.

6. Blomeke, J. O., "Technical Alternatives Documents," ORNL, Prepublication Paper (1976).

7. Bond, W. D., and Leuze, R. E., "Feasibility Studies of the Partition of Commercial High-Level Wastes Generated in Spent Nuclear Fuel Processing: Annual Progress Report for FY-1974-1974," ORNL-5012 January, 1975).

8. Bond, W. D., Claiborne, H. C., and Leuze, R. E., "Methods for Removal of Actinides from High-Level Wastes," Nuclear Technology, 24, 367 (1974).

9. LaRiviere, J. R., et al., "The Hanford Isotopes Production Plant Engineering Study," HW-77770, Hanford Atomic Products Operation (July, 1963).

10. Rupp, A. F., "A Radioisotope-Oriented View of Nuclear Waste Management," ORNL-4776 (May, 1972).

11. Ferguson, D. W., et al., "Chemical Technology Division Annual Progress Report for Period Ending March 31, 1975," ORNL-5050, 6-11, 30-31 (October, 1975).

FINAL

E-26-621

FEDERAL CASH TRANSACTIONS REPORT

See instructions on the back. If report is for more than one grant or assistance agreement, attach completed Standard Form 272-A.)

Approved by Office of Management and Budget, No. 80-R0182

1. Federal sponsoring agency and organizational element to which this report is submitted: NASA-Langley Research Center

2. RECIPIENT ORGANIZATION

Name: Georgia Institute of Technology

Number and Street:

City, State and ZIP Code: Atlanta, Georgia 30332

3. FEDERAL EMPLOYER IDENTIFICATION NO.: 58-6002023

4. Federal grant or other identification number: NSG-1288

5. Recipient's account number or identifying number: E-26-621

6. Letter of credit number: 80-00-2314

7. Last payment voucher number:

Give total number for this period

8. Payment Vouchers credited to your account:

9. Treasury checks received (*whether or not deposited*):

10. PERIOD COVERED BY THIS REPORT

FROM (*month, day, year*): 3/1/76

TO (*month, day year*): 2/28/79

11. STATUS OF FEDERAL CASH (*See specific instructions on the back*)

a. Cash on hand beginning of reporting period	$ -0-
b. Letter of credit withdrawals	137,360.00
c. Treasury check payments	-0-
d. Total receipts (*Sum of lines b and c*)	137,360.00
e. Total cash available (*Sum of lines a and d*)	137,360.00
f. Gross disbursements	137,365.00
g. Federal share of program income	-0-
h. Net disbursements (*Line f minus line g*)	137,365.00
i. Adjustments of prior periods	-0-
j. Cash on hand end of period	$ (5.00) *

12. THE AMOUNT SHOWN ON LINE 11J, ABOVE, REPRESENTS CASH REQUIREMENTS FOR THE ENSUING N/A *Days*

13. OTHER INFORMATION

a. Interest income	$ -0-
b. Advances to subgrantees or subcontractors	$ -0-

REMARKS (*Attach additional sheets of plain paper, if more space is required*)

* To be drawn on next Letter of Credit request

CERTIFICATION

I certify to the best of my knowledge and belief that this report is true in all respects and that all disbursements have been made for the purpose and conditions of the grant or agreement

AUTHORIZED CERTIFYING OFFICIAL

SIGNATURE: <

DATE REPORT SUBMITTED: 6/5/79

TYPED OR PRINTED NAME AND TITLE: David V. Welch, Manager, Grants & Contracts Accounting

TELEPHONE (*Area Code*) 404 (*Number*) 894 (*Extension*) 4624

SPACE FOR AGENCY USE

STANDARD FORM 272 (7-76)
Prescribed by Office of Management and Budget
Cir. No. A-110

E-26-621

GEORGIA INSTITUTE OF TECHNOLOGY

FINAL FISCAL REPORT
(GRANTS)

GRANT NO.
NSG-1288

1. Cumulative Award	$ 137,396.00
2. Cumulative Costs	$ 137,365.00
(a) Balance	$ 31.00
3. Cost Sharing	$ 7,238.77

CERTIFICATION

I certify that all expenditures reported *(or payments requested)* are for appropriate purposes and in accordance with the agreements set forth in the application and award documents.

AUTHORIZED OFFICIAL OF THE UNIVERSITY *(Signature)*

David V. Welch, Manager, Grants & Contracts Accounting

DATE
6/5/79

REMARKS/COMMENTS

Dr. J. D. Clement, Professor — 5/31/79 Date

Dr. J. H. Rust, Professor — 5/31/79 Date